

# The beneficial effects of the Lab4 probiotic consortium in atherosclerosis

Victoria O'Morain BSc (Hons)



Primary Supervisor Professor Dipak P. Ramji

A dissertation presented for the degree of Doctor of Philosophy

2019

Cardiff School of Biosciences

Cardiff University

Museum Avenue

Cardiff CF10 3AX



# Declaration

---

This work has not been submitted in substance for any other degree or award at this or any other university or place of learning, nor is being submitted concurrently in candidature for any degree or other award.

Signed.......... (Candidate) Date.....09/08/2019.....

## STATEMENT 1

This thesis is being submitted in partial fulfilment of the requirements for the degree of Doctor of Philosophy.

Signed.......... (Candidate) Date.....09/08/2019.....


## STATEMENT 2

This thesis is the result of my own independent work/investigation, except where otherwise stated. Other sources are acknowledged by explicit references. The views expressed are my own.

Signed.......... (Candidate) Date.....09/08/2019.....

## STATEMENT 3

I hereby give consent for my thesis, if accepted, to be available for photocopying and for inter-library loan, and for the title and summary to be made available to outside organisations.

Signed.......... (Candidate) Date.....09/08/2019.....

# List of contents

---

Declaration	i
List of contents	ii
List of figures	vii
List of tables	xi
Abstract	xii
Acknowledgements	xiii
Abbreviations	xiv
<b>CHAPTER 1 –General Introduction</b>	<b>1</b>
1.1 Atherosclerosis - prevalence and aetiology	2
1.2 Pathophysiology	4
1.2.1 Initiation	5
1.2.2 Foam cell formation	8
1.2.3 Disease progression	12
1.3 Current and emerging therapies	14
1.4 Probiotics in atherosclerosis	17
1.4.1 The effect of probiotics on key atherosclerosis associated risk factors	19
1.5 The Lab4 probiotic consortium	26
1.6 Project aims	30
<b>CHAPTER 2 - Materials and Methods</b>	<b>33</b>
2.1 Materials	34
2.2 Production of bacterial conditioned media	36
2.2.1 Production	36
2.2.2 Processing and storage	36
2.3 Cell culture techniques	37
2.3.1 Maintenance of cell lines and cultures	37
2.3.2 Establishment and storage of cell lines	39
2.3.3 Cell counting	39
2.4 Cell based assays	39
2.4.1 Cell viability	39
2.4.2 Proliferation	40
2.4.3 Measurement of reactive oxygen species	42
2.4.4 Monocyte migration	43
2.4.5 Vascular smooth muscle cell invasion	44
2.4.6 Mitochondrial bioenergetic profile	45
2.4.7 Phagocytosis	46
2.5 Molecular techniques	47

2.5.1 RNA extraction	47
2.5.2 Agarose gel electrophoresis	48
2.5.3 Reverse transcriptase polymerase chain reaction (RT-PCR)	48
2.5.4 Real time quantitative PCR (qPCR)	49
2.6 Protein methods	52
2.6.1 Protein extraction	52
2.6.2 Protein quantification	52
2.6.3 Enzyme linked immunosorbent assay (ELISA)	53
2.7 Lipid methods	54
2.7.1 Oxidised LDL uptake	54
2.7.2 Macropinocytosis	54
2.7.3 Cholesterol efflux	55
2.7.4 Cholesterol metabolism	55
2.8 In vivo methods	57
2.8.1 Animals and feeding	57
2.8.2 Blood and tissue collection	57
2.8.3 Plasma lipid quantification	58
2.8.4 Immunophenotyping of bone marrow cell populations	60
2.8.5 Plaque morphometric analysis	64
2.8.6 Liver gene expression	66
2.9 Statistical analysis	67
CHAPTER 3 – <i>The effect of probiotic on CM key processes in atherosclerosis</i>	68
3.1 Introduction	69
3.1.1 Normalisation of probiotic CM batches	70
3.1.2 Cell viability	70
3.1.3 Key processes in atherosclerosis	71
3.1.4 Anti-inflammatory effects in atherosclerosis	77
3.2 Experimental design	79
3.3 Results	82
3.3.1 Normalisation of probiotic CM to total protein concentration	82
3.3.2 Probiotic CM has no detrimental effect on the viability of cell culture model systems used for in vitro studies	83
3.3.3 Monocyte migration is reduced in the presence of probiotic CM	84
3.3.4 Probiotic CM exerts varying effects on the production of ROS by THP-1 monocytes and macrophages	87
3.3.5 Macropinocytosis was attenuated in the presence of several different concentrations of probiotic CM	92
3.3.6 Probiotic CM has a strain specific effect on mitochondrial function	94
3.3.7 Phagocytic activity of THP-1 macrophages was enhanced in the presence of probiotic CM	96
3.3.8 Probiotic CM can attenuate proliferation of key cell types involved in atherogenesis	97

3.3.9 Probiotic CM displays a strain specific effect on the invasion of HASMCs	103
3.3.10 Activation of the NLRP3 inflammasome was enhanced in the presence of probiotic CM	104
3.3.11 Probiotic CM displays a number of strain specific effects on inflammatory gene expression in cytokine stimulated macrophages	105
3.4 Discussion	108
3.4.1 Probiotic CM attenuates MCP-1-stimulated migration of monocytes	108
3.4.2 Measurement of ROS as an indicator of antioxidant capacity	108
3.4.3 Uptake of modified LDL in macrophages via macropinocytosis	109
3.4.4 The effect of probiotic CM on mitochondrial function	110
3.4.5 Phagocytic activity of macrophages was enhanced in the presence of probiotic CM	110
3.4.6 Differential effects of probiotic CM on the proliferation of cell types involved in atherosclerosis	111
3.4.7 Invasion of SMCs	112
3.4.8 The effects of probiotic CM on common inflammatory markers	113
3.4.9 Future directions	114
CHAPTER 4 - <i>The effects of probiotic CM on foam cell formation</i>	115
4.1 Introduction	116
4.1.1 Uptake of modified LDL	117
4.1.2 Cholesterol efflux	118
4.1.3 Intracellular cholesterol metabolism	120
4.2 Experimental aims	121
4.3 Results	125
4.3.1 Probiotic CM attenuates receptor-mediated uptake of modified LDL in human macrophages	125
4.3.2 Expression of macrophage scavenger receptors was attenuated following treatment with probiotic CM	127
4.3.3 Probiotic CM enhances the efflux of cholesterol from human macrophage foam cells	130
4.3.4 Probiotic CM has strain specific effects on the expression of key genes involved in cholesterol efflux	132
4.3.5 Cholesterol metabolism	134
4.3.6 Probiotic CM has strain specific effects on the expression of genes involved in intracellular cholesterol metabolism	136
4.4 Discussion	138
4.4.1 Modified LDL uptake	138
4.4.2 Cholesterol efflux	139
4.4.3 Intracellular cholesterol metabolism	141
4.4.4 Summary and future work	143
CHAPTER 5 – <i>The effects of Lab4 and CUL66 combination in vivo</i>	145
5.1 Introduction	146
5.1.1 Study design	146

5.2 Experimental aim	147
5.3 Results	149
5.3.1 <i>Lab4/CUL66 supplementation had no effect on the body weight of LDLr<sup>-/-</sup> mice fed a high fat diet</i>	149
5.3.2 <i>The effect of Lab4/CUL66 supplementation on mouse body fat and organ weight</i>	150
5.3.3 <i>The effect of Lab4/CUL66 supplementation on plasma cholesterol levels in mice fed a high fat diet</i>	151
5.3.4 <i>Triglycerides were increased in the plasma of probiotic mice compared to the control</i>	154
5.3.5 <i>Plaque area and lipid content was reduced with Lab4/CUL66 supplementation</i>	154
5.3.6 <i>The effects of Lab4/CUL66 supplementation on macrophage, SMC and T cell content of plaques</i>	157
5.4 Discussion	162
5.4.1 <i>The effect of Lab4/CUL66 supplementation on mouse body and organ weights</i>	162
5.4.2 <i>Lab4/CUL66 supplementation has beneficial effects on plasma lipid composition</i>	163
5.4.3 <i>Lab4/CUL66 supplementation reduces plaque size and lipid content in LDLr<sup>-/-</sup> mice</i>	167
5.4.4 <i>The effect of Lab4/CUL66 supplementation on plaque composition</i>	168
5.4.5 <i>Summary and future work</i>	171
CHAPTER 6 – <i>Mechanisms underlying the effect of Lab4/CUL66 supplementation in atherosclerosis</i>	173
6.1 Introduction	174
6.2 Experimental aim	176
6.3 Results	179
6.3.1 <i>The effects of Lab4/CUL66 supplementation on the expression of key genes involved in atherosclerosis disease</i>	179
6.3.2 <i>The effect of Lab4/CUL66 supplementation on key bone marrow cell populations</i>	189
6.4 Discussion	194
6.4.1 <i>Lab4/CUL66 supplementation significantly attenuated the expression of key genes involved in cell adhesion</i>	194
6.4.2 <i>The effect of Lab4/CUL66 supplementation on the expression of genes involved in the regulation of extracellular matrix</i>	196
6.4.3 <i>Lipid transport and metabolism</i>	198
6.4.4 <i>Lab4/CUL66 supplementation attenuates gene expression of key pro-inflammatory cytokines</i>	199
6.4.5 <i>The effect of Lab4/CUL66 supplementation on key cell populations in the bone marrow of LDLr<sup>-/-</sup> mice</i>	201
6.4.6 <i>Summary</i>	204
CHAPTER 7 – <i>General discussion</i>	206

7.1 Introduction	207
7.2 Summary of key findings	208
7.3 Mechanisms of action	213
7.3.1 <i>Plasma lipid modulation</i>	214
7.3.2 <i>Foam cell formation</i>	215
7.3.3 <i>Monocyte recruitment</i>	217
7.3.4 <i>Additional mechanisms of action</i>	218
7.4 Further work and future perspective	220
7.5 Conclusions	223
<b>APPENDIX</b>	<b>225</b>
<b>REFERENCES</b>	<b>227</b>



# List of figures

---

Figure 1.1 - Overview of atherosclerosis disease development .....	5
Figure 1.2 – Recruitment of monocytes across the activated endothelium .....	7
Figure 1.3 - Schematic representation of processes involved in macrophage foam cell formation .....	9
Figure 1.4 - Overview of reverse cholesterol transport from peripheral tissues to the liver for excretion.....	11
Figure 1.5 - Probiotics beneficially modulate a number of atherosclerosis-associated cardiovascular risk factors.....	19
Figure 1.6 - Overview of the project aims.....	32
Figure 2.1 – Illustration of the modified Boyden chamber experimental set up used in the investigation of monocyte migration .....	43
Figure 2.2 - Illustration of the modified Boyden chamber experimental set up used for the investigation of SMC invasion .....	45
Figure 2.3 - Example of quality of RNA by size-fractionation .....	48
Figure 2.4 - Illustration of fractions obtained for the quantification of total cholesterol, free cholesterol, HDL and LDL/VLDL using the Abcam HDL and LDL/VLDL Cholesterol Assay Kit .....	59
Figure 3.1 – Illustration of the ETC components specifically targeted by respiratory modulators in the Seahorse Mito Stress Test .....	75
Figure 3.2 – Seahorse XFp Cell Mito Stress Test profile showing key parameters of mitochondrial respiration .....	75
Figure 3.3 - Experimental strategy for the investigation of the effects of probiotic CM on key cellular processes in atherosclerosis .....	80
Figure 3.4 - Experimental strategy for the investigation of the effect of probiotic CM on the proliferation of key cell types in atherosclerosis .....	81
Figure 3.5 - Experimental strategy for the investigation of the anti-inflammatory effects of probiotic CM .....	81
Figure 3.6 - Viability of THP-1 macrophages assessed using the LDH Assay Kit .....	83
Figure 3.7 - Probiotic CM has no detrimental effect on the viability of cell culture model systems utilised in the study .....	84
Figure 3.8 - Migration of THP-1 monocytes in response to MCP-1 was attenuated by various concentrations of probiotic CM.....	86
Figure 3.9 - Migration of monocytes in response to MCP-1 was attenuated in the presence of probiotic CM. ....	87
Figure 3.10 – The effect of probiotic CM on TBHP-induced ROS production in THP-1 monocytes.....	89
Figure 3.11 - Probiotic CM increases TBHP-induced ROS production in THP-1 macrophages .....	90
Figure 3.12 – The effect of probiotic CM on TBHP-induced ROS production in THP-1 monocytes.....	91
Figure 3.13 - Probiotic CM increases TBHP-induced ROS production in THP-1 macrophages .....	92

Figure 3.14 - Probiotic CM attenuates macropinocytosis in PMA-differentiated macrophages. ....	93
Figure 3.15 - Probiotic CM attenuates macropinocytosis in THP-1 macrophages.....	94
Figure 3.16 - Oxygen consumption rate measured following the serial injection of respiration modulators .....	95
Figure 3.17 - Probiotic CM has strain specific effects on mitochondrial function.....	96
Figure 3.18 - Probiotic CM increases phagocytosis in THP-1 macrophages .....	97
Figure 3.19 - Probiotic CM reduces the proliferation of THP-1 monocytes over a 7-day period .....	99
Figure 3.20 - Probiotic CM reduces the proliferation of THP-1 monocytes over a 7-day period.....	99
Figure 3.21 - Proliferation of macrophages was reduced in the presence of probiotic CM .....	100
Figure 3.22 - Probiotic CM has a strain-specific effect on the proliferation rate of THP-1 macrophages .....	101
Figure 3.23 - Probiotic CM reduces the proliferation of HASMCs over a 7-day period .....	102
Figure 3.24 - Probiotic CM has a strain-specific effect on the proliferation rate of HASMCs .....	103
Figure 3.25 - Invasion of HASMCs was attenuated in the presence of probiotic CM in a strain- specific manner.....	104
Figure 3.26 - Inflammasome activation was significantly increased in the presence of probiotic CM .....	105
Figure 3.27 - Probiotic CM has strain specific effects on inflammatory gene expression in cytokine stimulated macrophages .....	107
Figure 4.1 - Schematic representation of processes involved in macrophage foam cell formation .....	116
Figure 4.2 - Experimental strategy for the investigation of the effect of probiotic CM on the expression of key genes in foam cell formation. ....	122
Figure 4.3 – Experimental strategy for the investigation of the effect of probiotic CM on the uptake of oxLDL. ....	122
Figure 4.4 – Experimental strategy for the investigation of the effect of probiotic CM on cholesterol efflux from macrophage foam cells. ....	123
Figure 4.5 – Experimental strategy for the investigation of the effect of probiotic CM on macrophage intracellular cholesterol metabolism. ....	124
Figure 4.6 - Receptor-mediated uptake of modified lipoproteins was attenuated in the presence of probiotic CM .....	126
Figure 4.7 - Probiotic CM inhibits the uptake of modified lipoproteins in primary human macrophages .....	126
Figure 4.8 – Gene expression of macrophage scavenger receptors was inhibited by probiotic CM treatment .....	128
Figure 4.9 - Probiotic CM attenuates the expression of scavenger receptor genes in primary human macrophages .....	129
Figure 4.10 - Treatment with probiotic CM enhances efflux of cholesterol from THP-1 macrophages .....	131

Figure 4.11 - Probiotic CM has a strain specific effect on cholesterol efflux in primary human macrophages .....	131
Figure 4.12 - Probiotic CM has strain specific effects on the expression of key genes involved cholesterol efflux .....	133
Figure 4.13 - Probiotic CM increases the expression of key genes involved in cholesterol efflux from primary human macrophage foam cells .....	134
Figure 4.14 - The effect of probiotic CM on the incorporation of [ <sup>14</sup> C] acetate into major lipid classes.....	135
Figure 4.15 – Probiotic CM has strain specific effects on the expression of key genes involved in cholesterol metabolism .....	137
Figure 5.1 - Experimental strategy used to assess the effect of probiotic treatment on plaque formation and lipid profile <i>in vivo</i> .....	148
Figure 5.2 - Probiotics have no effect on mouse body weights compared to the control group.....	149
Figure 5.3 – Mouse fat and organ weight recorded at study end.....	150
Figure 5.4 - Increased HDL and decreased LDL cholesterol levels in probiotic mice compared to the control .....	152
Figure 5.5 – Probiotic treatment has beneficial effects on cholesterol ratios compared to the control .....	153
Figure 5.6 - Plasma triglyceride levels were increased in the probiotic compared to the control group .....	154
Figure 5.7 - H&E and Oil Red O staining of the aortic sinus in the control and probiotic groups .....	155
Figure 5.8 - Plaque area was significantly reduced in probiotic mice compared to the control.....	156
Figure 5.9 – Lipid content was significantly reduced in the aortic sinus of probiotic mice compared to the control .....	156
Figure 5.10 - Immunofluorescent staining of macrophages present in sections of the aortic sinus.....	158
Figure 5.11 - Immunofluorescent staining of T cells present in sections of the aortic sinus .....	159
Figure 5.12 - Immunofluorescent staining of SMCs present in sections of the aortic sinus .....	160
Figure 5.13 – Macrophage, SMC and T cell content was significantly reduced in the aortic sinus of probiotic mice compared to the control.....	161
Figure 6.1 - Simplified representation of bone marrow cell populations .....	175
Figure 6.2 - Experimental strategy for the analysis of liver gene expression and bone marrow cell populations. ....	177
Figure 6.3 – Representative flow plots outlining the gating strategy utilised in the analysis of haematopoietic cell populations by flow cytometry .....	178
Figure 6.4 - Volcano plot showing changes in gene expression with Lab4/CUL66 supplementation compared to control .....	185
Figure 6.5 – Heatmaps showing a visual representation of fold-change in gene expression with Lab4/CUL66 supplementation.....	187

<b>Figure 6.6 – Related genes show significant change in expression with Lab4/CUL66 supplementation compared to the control .....</b>	<b>188</b>
<b>Figure 6.7 – Treatment with Lab4/CUL66 had no significant effect on white blood cell counts in the bone marrow .....</b>	<b>191</b>
<b>Figure 6.8 – The effect of Lab4/CUL66 supplementation on bone marrow stem cell populations .....</b>	<b>191</b>
<b>Figure 6.9 - The effect of Lab4/CUL66 supplementation on bone marrow CLP progenitor cell populations.....</b>	<b>192</b>
<b>Figure 6.10 - The effect of Lab4/CUL66 supplementation on bone marrow lineage differentiated cell populations .....</b>	<b>193</b>
<b>Figure 6.11 - Bone marrow cell populations showing significant changes with probiotic supplementation .....</b>	<b>202</b>
<b>Figure 7.1 - Key anti-atherosclerotic effects of Lab4, Lab4b, CUL66 and Lab4/CUL66. ....</b>	<b>209</b>
<b>Figure 7.2 - Probiotics exert effects in a number of key stages in atherosclerosis development.....</b>	<b>213</b>

# List of tables

---

Table 1.1 – The athero-protective effects of probiotic bacteria .....	20
Table 1.2 – The composition of Lab4 and Lab4b probiotic consortia .....	27
Table 1.3 - Completed trials of Lab4 and Lab4b probiotic consortia .....	29
Table 2.1 - Materials and reagents used during the course of the study.....	34
Table 2.2 – Concentrations of compounds used in the Seahorse Cell Mito Stress Test .....	46
Table 2.3 - Composition of cDNA master mix used in the reverse transcription process .....	49
Table 2.4 - Intron-spanning primer sequences used in qPCR .....	51
Table 2.5 - Composition of 1X master mix used in qPCR and microarray reactions.....	51
Table 2.6 - Amplification steps for qPCR and microarray reactions .....	52
Table 2.7 - Composition of antibody cocktails used in the immunophenotyping of bone marrow cell populations .....	62
Table 2.8 - Markers used in the immunophenotyping of bone marrow cell populations .....	63
Table 2.9 - Antibodies used for immunofluorescent staining of sections.....	66
Table 5.1 - Bacteria species included in the Lab4/CUL66 probiotic supplement .....	147
Table 6.1 - Change in expression of each gene tested using the Atherosclerosis RT <sup>2</sup> Profiler PCR Arrays .....	181
Table 6.2 – Atherosclerosis-associated genes showing significant changes in expression. ....	184
Table 6.3 - Further genes showing significant changes in expression and their role in atherosclerosis.....	201
Table 7.1 - Summary of key findings from <i>in vitro</i> investigations of the effects of Lab4, Lab4b and CUL66 on key processes in atherosclerosis.....	212
Table 7.2 - Summary of key findings from <i>in vivo</i> investigation of the effect of Lab4/CUL66 supplementation in LDLr <sup>-/-</sup> mice. ....	212
Appendix 1 - Full list of genes included in the RT <sup>2</sup> Atherosclerosis Array .....	225

# Abstract

---

## *Background*

Cardiovascular disease (CVD) is currently the leading cause of mortality world-wide, responsible for approximately one-third of all global deaths. Atherosclerosis, the primary cause of CVD, is a chronic inflammatory disease characterised by lipid accumulation in the arterial wall. Despite the success of current therapies, the incidence of CVD continues to rise and the search continues for alternative therapeutic agents. The Lab4, Lab4b and CUL66 probiotic consortia have been shown to possess lipid-lowering and immunomodulatory capabilities, highlighting their anti-atherogenic potential. The aim of this project was to assess the anti-atherogenic effects of Lab4, Lab4b and CUL66 probiotic consortia using *in vitro* and *in vivo* model systems.

## *Results*

Experiments using *in vitro* model systems demonstrated probiotic-induced attenuation of macrophage foam cell formation at the cellular and molecular levels. In addition, probiotics reduced monocyte migration, increased phagocytosis, and reduced proliferation of key atherosclerosis-associated cell types. Mice supplemented with a live combination of Lab4 and CUL66 demonstrated reduced atherosclerotic plaque formation, and an improved plasma lipid profile compared to the control. In addition, numbers of macrophages and T-cells were reduced in both the plaque and the bone marrow of probiotic-treated mice. Liver gene expression analysis revealed probiotic-induced attenuation of several key pro-atherogenic genes.

## *Conclusion*

Findings from this study demonstrate many anti-atherogenic effects of Lab4, Lab4b and CUL66 probiotic consortia in both *in vitro* and *in vivo* model systems, and highlight their potential as candidates for inclusion in clinical trials and future atherosclerosis intervention strategies. Underlying mechanisms of action have also been investigated and proposed, thereby contributing to the understanding of probiotic action.

# Acknowledgements

---

Firstly, I would like to thank my supervisor Prof. Dipak Ramji for the fantastic opportunity to complete this PhD in his lab. His patience, advice and guidance over the past three years has proven invaluable in the success of this project. From him I have learned how good robust scientific research should be conducted, for which I will be forever grateful.

I would like to thank Dr. Daryn Michael, Dr. Irina Guschina and Dr. Timothy Hughes who have provided valuable guidance throughout this project. I also give a special thank you to Dr. Jessica Williams and Miss Yee Chan, who have provided much appreciated assistance, and who's friendship has made this project such an enjoyable experience. And to all of my lab mates, past and present, thank you for what has been a truly unforgettable research experience.

Last but not least, I would like to thank all of my family and friends for their continuous support. Thank you to my children, Ethan and Evan, who have been a constant source of encouragement. And most of all I thank my husband Chris, who's tireless support during the last three years has made completion of this PhD possible.



*Knowledge Economy Skills Scholarships (KESS) is a pan-Wales higher level skills initiative led by Bangor University on behalf of the HE sector in Wales. It is part funded by the Welsh Government's European Social Fund (ESF) convergence programme for West Wales and the Valleys.*

# Abbreviations

---

Abbreviation	Full name
ABC	ATP-binding cassette
ACAT1	Acyl-CoA acyltransferase 1
ACE	Angiotensin-converting enzyme
AcLDL	Acetylated LDL
AF	Alexa Fluor
ANOVA	One-way analysis of variance
ANSA	8-anilino-4-naphthosulphonic acid
Apo	Apolipoprotein
ATP	Adenosine triphosphate
BMDMs	Bone marrow derived macrophages
BrdU	5-Bromo-2'-deoxy-uridine
BSA	Bovine serum albumin
BSH	Bile salt hydrolase
CAD	Coronary artery disease
CCL2	C-C motif chemokine ligand 2
CCR2	C-C motif chemokine receptor 2
CE	Cholesterol esters
CETP	Cholesterol ester transfer protein
CFLAR	CASP8 And FADD like apoptosis regulator
CFU	Colony forming units
CHD	Coronary heart disease
CLP	Common lymphoid progenitor
CM	Conditioned media
CMP	Common myeloid progenitor
CVD	Cardiovascular disease
DCFDA	2'7'-dichlorofluorescein diacetate
DGLA	Dihomo- $\gamma$ -linolenic acid
DHA	Docosahexaenoic acid
ECM	Extracellular matrix
ECs	Endothelial cells
ELISA	Enzyme-linked immunosorbent assay
eNOS	Endothelial nitric oxide synthase
EPA	Eicosapentaenoic acid
ER	Endoplasmic reticulum
ERK	Extracellular signal-regulated kinase
ETC	Electron transport chain
FACS	Flow assisted cell sorting
FAD	Fatty acid desaturase
FC	Free cholesterol
FCCP	Carbonyl cyanide-4 (trifluoromethoxy) phenylhydrazine
FFA	Free fatty acid



Abbreviation	Full name
FH	Familial hypercholesterolaemia
FITC	Fluorescein isothiocyanate
GAPDH	Glyceraldehyde 3-phosphate dehydrogenase
GDC	Genomic DNA control
GMP	Granulocyte-macrophage progenitor
H&E	Haematoxylin & eosin
HASMCs	Human aortic smooth muscle cells
HBEGF	Heparin-binding EGF-like growth factor
HDL	High density lipoprotein
HFD	High fat diet
HI-FCS	Heat-inactivated foetal calf serum
HMDM	Human monocyte-derived macrophages
HMG CoA reductase	3-hydroxy-3-methylglutaryl-CoA reductase
HPC II	Haematopoietic progenitor cells II
HPF	High power fields
HRP	Horseradish-peroxidase
HSC	Haematopoietic stem cell
HSPCs	Haematopoietic stem/progenitor cells
ICAM	Intercellular adhesion molecule
IDL	Intermediate density lipoproteins
IFN	Interferon
IL	Interleukin
JNK	Janus kinase
LAL	Lysosomal acid lipase
LCAT	Lecithin cholesterol acyltransferase
LDH	Lactate dehydrogenase
LDL	Low density lipoprotein
LDLr	LDL receptor
LK	Lin- c-Kit+
LPA	Lysophosphatidic acid
LPC	Lysophosphatidylcholine
LPL	Lipoprotein lipase
LPS	Lipopolysaccharide
LXR	Liver X receptor
LY	Lucifer yellow CH dilithium salt
LYPLA1	Lysophospholipase A1
Mac-1	Macrophage-1-antigen
MCP	Monocyte chemotactic protein
M-CSF	Macrophage colony-stimulating factor
MDSC	Myeloid derived suppressor cells
MEP	Megakaryocyte-erythroid progenitor
MMLV	Moloney murine leukaemia virus
MMP	Matrix metalloproteinase
MPP	Multipotent progenitor cells
NCEH	Neutral cholesterol ester hydrolase
NF-κB	Nuclear factor-kappa B

Abbreviation	Full name
NLRP3	NACHT, LRR and PYD domains-containing protein 3
NPC1L1	Niemann-Pick C1-like protein
OCR	Oxygen consumption rate
OxLDL	Oxidised LDL
PAI-1	Plasminogen activator inhibitor 1
PAMPs	Pathogen-associated molecular patterns
PBS	Phosphate buffered saline
PC	Phosphorylcholine
PCSK9	Proprotein convertase subtilisin/kexin type 9
PDGF	Platelet-derived growth factor
PDGFR	Platelet-derived growth factor receptor
PE	Phycoerythrin
PFA	Paraformaldehyde
PMA	Phorbol-12-myristate-13-acetate
PPAR	Peroxisome proliferator-activated receptor
PPC	Positive PCR control
PRR	Pattern recognition receptor
PSGL-1	P-selectin glycoprotein ligand-1
qPCR	Quantitative polymerase chain reaction
RCT	Reverse cholesterol transport
ROS	Reactive oxygen species
RTC	Reverse transcription control
SCFA	Short chain fatty acids
SELE	E-selectin
SLAM	Signalling lymphocytic activation molecule
SLpA	S-layer protein A
SR	Scavenger receptor
TBE	Tris/borate/EDTA
TBHP	Tert-butyl hydroperoxide
TC	Total cholesterol
TD	Tangier disease
TIMP	Tissue inhibitors of MMP
TG	Triacylglycerol
TGF	Transforming growth factor
TLC	Thin layer chromatography
TLRs	Toll-like receptors
TMAO	Trimethylamine <i>N</i> -oxide
TNF	Tumour necrosis factor
Tregs	Regulatory T cells
VCAM	Vascular cell adhesion molecule
VEGF	Vascular endothelial growth factor
VLDL	Very low density lipoproteins
VSMC	Vascular smooth muscle cells
WHO	World Health Organisation

# CHAPTER 1

*General Introduction*

---

## 1.1 Atherosclerosis - prevalence and aetiology

Cardiovascular disease (CVD) is a class of diseases involving the heart and the circulatory system including coronary artery diseases (CAD), stroke and peripheral artery disease. Together CVD is the leading cause of mortality worldwide with one in three deaths attributed to the disease (World Health Organization, 2018). In 2016, the total number of global deaths due to CVD was estimated to be 17.9 million, representing 31% of all global deaths (World Health Organization, 2018). Furthermore, the prevalence of CVD presents a tremendous financial burden, costing the UK economy an estimated 19 billion annually (BHF, 2018).

Atherosclerosis is the primary cause underlying CVD-related morbidity and mortality. Atherosclerosis is a chronic inflammatory disease featuring slow onset, and the prevalence of atherosclerosis-associated CVD in people under 50 years of age is reported to be less than 1%. However, this figure rises to 25% between the ages of 70 and 79, and 40% above the age of 80 (Hinton *et al.*, 2018). Risk of atherosclerosis disease progression is largely determined by common modifiable cardiovascular risk factors including dyslipidaemia, tobacco smoking (Lubin *et al.*, 2017), hypertension (Petruski-Ivleva *et al.*, 2016), diabetes and obesity (Groh *et al.*, 2018; Lee *et al.*, 2017). One of the most important causal agents of atherosclerosis is apolipoprotein-B (apoB)-containing lipoproteins, which include chylomicron remnants, very low density lipoproteins (VLDL), low density lipoproteins (LDL) and intermediate density lipoproteins (IDL) (Shapiro and Fazio, 2017). These apoB-containing lipoproteins are highly atherogenic and LDL cholesterol (LDL-C) in particular has long been regarded as the principle driver in the initiation and progression of the atherosclerotic plaque (Tabas *et al.*, 2007). LDL is the most abundant atherogenic lipoprotein in fasting blood, and while most lipoproteins are capable of promoting plaque formation, LDL is the most prominent driver of circulating cholesterol accumulation in the arterial wall (Shapiro and Fazio, 2017) where an inflammatory response is initiated (Linton *et al.*, 2000). In fact, in a recent evaluation of evidence from a variety of meta-analyses of genetic, epidemiological and clinical studies, authors reported an unequivocal causality between LDL cholesterol and atherosclerosis-associated CVD (Ference *et al.*, 2017).

In addition to modifiable lifestyle factors, individual risk of developing atherosclerosis also depends on unmodifiable factors including age above 50 (Nanayakkara *et al.*, 2018), male gender (Kouvari *et al.*, 2018), ethnicity and familial predisposition (Gijbberds *et al.*, 2015). A number of genetic defects are known to result in a predisposition to early onset atherosclerosis and CVD including a group of disorders known as primary dyslipidaemias. Primary or familial hypercholesterolaemias (FH) are dyslipidaemias caused by mutations in genes involved in the hepatic uptake of low density lipoprotein (LDL), resulting in elevated LDL cholesterol and high risk of premature atherosclerosis disease (Averna *et al.*, 2017). Advances in genetic testing has enabled the screening and diagnosis of many mutations known to cause FH, with early intervention improving prognosis for these patients. However, many dyslipidaemias remain largely undiagnosed and untreated (Averna *et al.*, 2017). Tangier disease is a rare autosomal recessive disease characterised by severely low levels of high density lipoprotein (HDL) cholesterol (HDL-C), resulting from mutations in the ATP-binding cassette transporter A1 (ABCA1) gene involved in cholesterol transport. ABCA1 is a transmembrane protein involved in cholesterol efflux and reverse cholesterol transport (RCT), a process by which cholesterol is transported from the vessel wall back to the liver for biliary excretion (discussed later) (Yin *et al.*, 2010). Tangier disease is rare, however extremely low HDL-C is a strong risk factor for atherosclerosis and CVD, and patients with TD suffer a predisposition to early onset of CVD and clinical complications (Hovingh *et al.*, 2004).

Genetic mutations in genes involved in lipid homeostasis, as in FH and TD, have provided valuable insight into the aetiology and pathophysiology of atherosclerosis. Additionally, mouse models commonly used in atherosclerosis research have also significantly improved our understanding of the pathology of atherosclerosis. Wild-type mice lack the cholesterol ester transfer protein (CETP) which promotes the transfer of cholesterol esters from HDL to LDL/VLDL, and consequently carry the majority of cholesterol via HDL particles (Oppi *et al.*, 2019). This high level of HDL-C together with low levels of LDL-C confers a natural resistance to atherosclerosis in wild-type mice, and current atherosclerosis models are based on alteration of lipid metabolism via dietary or genetic manipulation (Zadelaar *et al.*, 2007). The most commonly used models are the apolipoprotein E (apoE)-deficient mice (ApoE<sup>-/-</sup>) and the LDL receptor-deficient mice (LDLR<sup>-/-</sup>). ApoE, which is secreted by the liver and macrophages, is a major component of

plasma lipoproteins and functions to promote the uptake of atherogenic lipoproteins from the circulation (Greenow *et al.*, 2005). Homozygous deletion of the *APOE* gene therefore results in a deleterious increase in plasma LDL/VLDL levels, and spontaneous development of atherosclerotic lesions resembling those found in humans (Zadelaar *et al.*, 2007). The LDL receptor is a widely expressed membrane protein involved in the clearance of both apoB and apoE-containing lipoproteins. Similar to ApoE<sup>-/-</sup> mice, those lacking the *LDLR* gene exhibit elevated plasma cholesterol levels in comparison to wild-type mice even on a standard chow diet. However, due to a relatively mild increase in atherosclerotic lipoproteins compared to the ApoE<sup>-/-</sup> model, this model does not spontaneously develop atherosclerotic lesions and is most often utilised in combination with a high-fat, high-cholesterol 'western' type diet (Getz and Reardon, 2015). Upon feeding with high fat diet (HFD) LDLr<sup>-/-</sup> mice show highly elevated plasma cholesterol levels and rapid development of atherosclerotic lesions (Zadelaar *et al.*, 2007).

In addition to the traditional risk factors associated with atherosclerosis and CVD, clonal haematopoiesis of indeterminate potential (CHIP) is an emerging age-related risk factor, reported to correlate with atherosclerotic cardiovascular disease (Jaiswal *et al.*, 2017). Over time, haematopoietic stem cells in the bone marrow accumulate mutations, some of which may confer a survival advantage. Clonal expansion of these mutant stem cells is considered premalignant, and can be detected in peripheral blood. CHIP is the presence of these clonal haematopoietic cells exceeding >2% of peripheral blood cells count. (Libby and Ebert, 2018) Recently, Jaiswal and colleagues reported a significant association between the presence of CHIP and cardiovascular risk in human participants, supporting the hypothesis that somatic mutations in haematopoietic stem cells may contribute to the development of atherosclerosis (Jaiswal *et al.*, 2017).

## 1.2 Pathophysiology

Atherosclerosis is a disease of the medium and large arteries occurring predominantly at sites of low shear stress and disturbed lamina flow (Groh *et al.*, 2018), and is characterised by chronic low-grade inflammation. Atherosclerosis involves a complex interplay of lipids, inflammatory responses and cell signalling molecules to orchestrate

initiation, development and progression of the disease. Figure 1.1 shows an overview of each stage of atherosclerosis development.

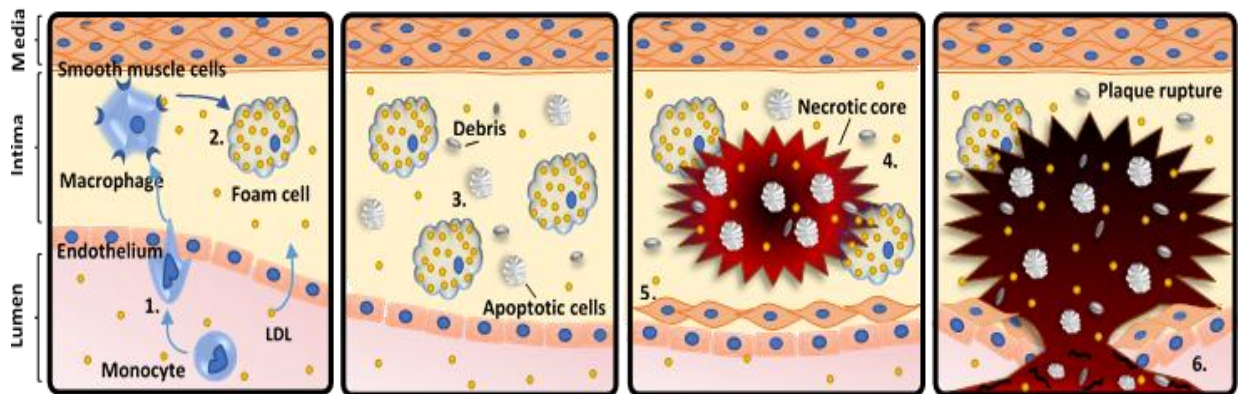


**Figure 1.1 - Overview of atherosclerosis disease development.** 1. Circulating LDL that has become trapped in the arterial intima triggers an inflammatory response and activation of the endothelium. Activated endothelial cells express a variety of adhesion molecules and chemokines which aid in the recruitment of circulating monocytes to the site. Through a process of adherence and rolling, monocytes transmigrate into the intima, where they differentiate into macrophages. 2. Uptake of LDL via the LDL receptor is regulated via a negative feedback mechanism. However, uptake of modified LDL via macrophage scavenger receptors occurs autonomously in an unregulated manner, which when coupled with ineffective metabolism and efflux of cholesterol, results in the formation of lipid-laden foam cells – the hallmark of atherosclerosis. 3. Cholesterol-induced cytotoxicity results in increased apoptotic and necrotic cell death, which in addition to reduced efferocytosis, leads to the accumulation of apoptotic cells and necrotic debris. 4. As the atherosclerotic plaque advances, a sustained inflammatory response together with continuous accumulation of apoptotic cells and debris, pro-atherogenic lipoproteins and lipoprotein remnants, leads to secondary necrosis and the formation of a lipid-rich necrotic core. 5. VSMCs migrate from the media to the intima and contribute to extracellular matrix (ECM) remodelling and formation of a protective fibrous cap between the necrotic core and the lumen, which functions to stabilise the plaque. 6. In advanced disease and under an enhanced inflammatory setting, protease action degrades the ECM, compromising the integrity of the protective cap. Plaque vulnerability and eventual rupture results in the release of plaque contents into the lumen, thrombosis and subsequent clinical complications.

### 1.2.1 Initiation

Initial stages of atherosclerosis disease involve endothelial cell activation or dysfunction in response to environmental insult and vascular injury. Activation of the endothelium leads to the recruitment, attachment and migration of monocytes into the arterial intima. Monocytes differentiate into macrophages which via aberrant uptake of modified lipoproteins develop into lipid laden foam cells, which accumulate resulting in the formation of a fatty streak – the hallmark of early atherosclerosis (Crowther, 2005).

Endothelial cells are sensitive and susceptible to shear stress induced by laminar blood flow, particularly at sites of arterial branching and curvature where disturbed flow

contributes to subendothelial accumulation of apoB-containing lipoproteins and lesion initiation (McLaren *et al.*, 2011a; Mestas and Ley, 2008). Hypertension and hyperlipidaemia increase the risk of atherosclerosis where increased shear stress or greater levels of circulating LDL may lead to increased accumulation at susceptible sites. Accumulation of LDL in the vessel wall induces endothelial cell activation and triggers a chronic inflammatory response, resulting in the expression of a large variety of pro-inflammatory molecules and recruitment of circulating immune cells to the site of activation (McLaren *et al.*, 2011a).

Monocyte recruitment represents one of the earliest events in atherosclerosis lesion formation. Vascular injury and activation of endothelial cells results in the upregulation of the expression of chemokines and cell adhesion molecules involved in the recruitment of circulating monocytes (Mestas and Ley, 2008). A simplified depiction of monocyte recruitment is shown in Figure 1.2. Monocytes initially roll and adhere to surface molecules expressed by activated endothelial cells such as E- and P-selectins, which mediate tethering and rolling through binding to P-selectin glycoprotein ligand-1 (PSGL-1) expressed on all monocytes (Gerhardt and Ley, 2015). Selectins signal through PSGL-1 to activate integrins; heterodimeric cell surface receptors that further support rolling and adhesion of monocytes via association with additional adhesion molecules, including vascular cell adhesion molecule-1 (VCAM-1) and intercellular adhesion molecule-1 (ICAM-1). VCAM-1 and ICAM-1 are members of a superfamily of cell adhesion molecules, expressed on the surface of cytokine-stimulated endothelium. While VCAM-1 mediates the firm adhesion of monocytes, ICAM-1 is believed to be involved in adhesion, thereby strengthening transendothelial migration (Mestas and Ley, 2008). In addition to adhesion molecules, activated endothelial cells express many cytokines and chemokines that participate in the recruitment and transendothelial migration of monocytes, including macrophage colony-stimulating factor (M-CSF), interleukin-8 (IL-8), tumour necrosis factor- $\alpha$  (TNF- $\alpha$ ) and junctional adhesion molecules (JAMs) (McLaren *et al.*, 2011a; Weber *et al.*, 2007). One of the most characterised is the chemokine monocyte chemoattract protein-1 (MCP-1), also known as CC chemokine ligand-2 (CCL2), and its cognate receptor CCR2 which are known to play a key role in monocyte recruitment. Studies in atherosclerosis mouse models deficient in MCP-1 or its receptor have demonstrated decreased subendothelial monocyte accumulation and



protection against lesion development (Combadière *et al.*, 2008; Mestas and Ley, 2008; Raghu *et al.*, 2017). Following slow rolling and arrest, the monocytes spread, polarise and undergo intraluminal ‘crawling’ to the nearest junction where migration takes place (Gerhardt and Ley, 2015). Intraluminal crawling is dependent upon endothelial adhesion molecules ICAM-1 and ICAM-2 as well as macrophage-1-antigen (Mac-1), and blocking of these molecules has been shown to disrupt crawling and therefore disable transmigration (Schenkel *et al.*, 2004).

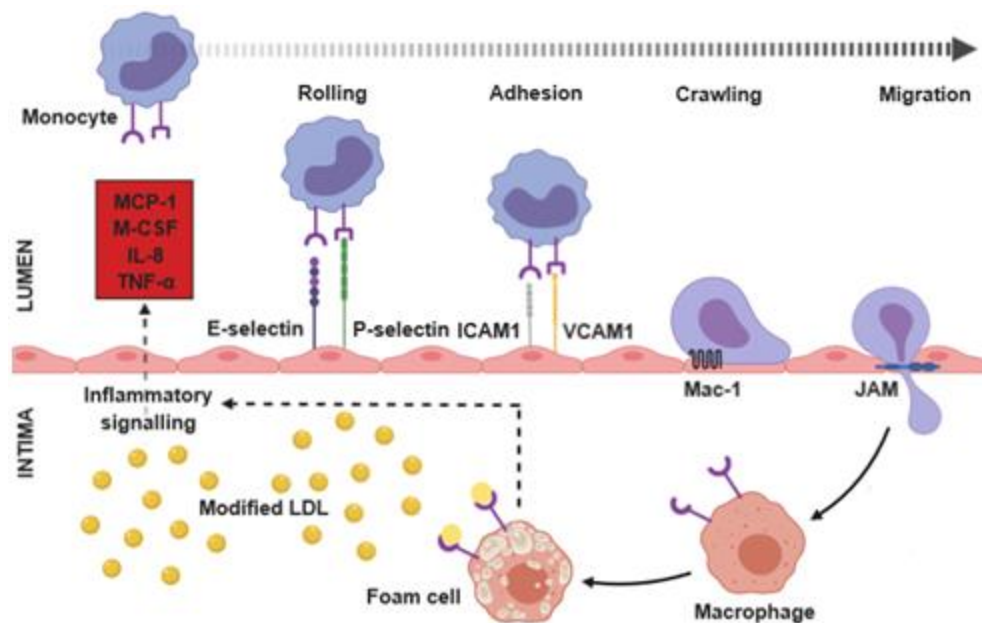


**Figure 1.2 – Recruitment of monocytes across the activated endothelium.** Activated endothelial cells express a number of cell adhesion molecules in addition to cytokines and chemokines including MCP-1, M-CSF, IL-8 and TNF- $\alpha$ , that participate in the recruitment and transendothelial migration of monocytes. Circulating monocytes initially roll and adhere to surface molecules present on activated endothelial cells including E- and P- selectins. Further binding via ICAM1 and VCAM1 mediates firm adhesion. Monocytes then undergo intraluminal crawling to the nearest junction, a process mediated by ICAM1 and Mac-1. JAMs then mediate transmigration of monocytes across the endothelium to the arterial intima where they differentiate into macrophages. Uptake of modified LDL by monocyte-differentiated and resident macrophages occurs in an unregulated manner leading to the formation lipid-laden foam cells. Macrophage foam cells lead to the production of further pro-inflammatory cytokines and chemokines such as MCP-1 and TNF- $\alpha$ , thereby sustaining the recruitment of monocytes from the lumen into the arterial intima. Abbreviations: ICAM1, intercellular adhesion molecule 1; VCAM1, vascular cell adhesion molecule 1; Mac-1, macrophage-1-antigen; JAM, junctional adhesion molecule; MCP-1, monocyte chemotactic protein 1; M-CSF, macrophage colony stimulating factor; IL-8, interleukin 8; TNF- $\alpha$ , tumour necrosis factor alpha.

Once across the endothelium, monocytes differentiate into macrophages which undergo differential polarisation into a wide spectrum of macrophage phenotypes (Shaikh *et al.*, 2012). The process of macrophage polarisation is subject to the influence of the intimal micro-environment resulting a heterogenous range of macrophage subsets, characterised at the extremes by either M1 or M2 polarised phenotypes (Colin *et al.*, 2014). M1, or classically activated macrophages, are phenotypically different to

M2 macrophages where the M1 phenotype is considered pro-inflammatory, and the M2 phenotype is considered anti-inflammatory (Nagenborg *et al.*, 2017). M1 macrophages, which correlate with atherosclerosis progression, are associated with an elevated level of cytokines and chemokines, including MCP-1 and TNF- $\alpha$ , which further promote monocyte recruitment to the site (Bai *et al.*, 2017) and contribute to an increased and sustained inflammatory response (Colin *et al.*, 2014). At the opposite end of the macrophage spectrum, M2 'alternatively' activated macrophages are associated with tissue repair, phagocytosis, fibrosis and angiogenesis and are considered anti-inflammatory and anti-atherogenic (Colin *et al.*, 2014; Nagenborg *et al.*, 2017). Under atherosclerotic conditions, monocyte-derived macrophages exhibit many morphological changes, including increased expression of surface proteins and enhanced sensitivity to cell signalling molecules (Bobryshev *et al.*, 2016). Furthermore, macrophages residing in atherosclerotic lesions exhibit decreased ability to migrate, a feature which contributes to the failure of inflammation resolution and to plaque progression (Randolph, 2014). M1 polarised pro-inflammatory macrophages represent the most abundant immune cells residing in atherosclerotic plaques, originating either from local proliferation or from transmigration and differentiation of circulating monocytes (Groh *et al.*, 2018). Monocyte-derived macrophages represent a large portion of the macrophage population present in atherosclerotic lesions. However, local proliferation of resident macrophages contributes significantly to lesional macrophage accumulation (Robbins *et al.*, 2013), and recent studies have now demonstrated the direct involvement of local macrophage proliferation in the formation and progression of atherosclerotic plaques (Sukhovshin *et al.*, 2016; Yamada *et al.*, 2018).

### 1.2.2 Foam cell formation

A small proportion of foam cells originate from ECs with a significant proportion originating from vascular smooth muscle cells (VSMCs) (Sun *et al.*, 2016), however the majority are believed to originate from macrophages (Chistiakov *et al.*, 2017). The formation of foam cells occurs as a result of a disruption of the normal homeostatic mechanisms governing macrophage cholesterol metabolism, which results in the excessive uptake of modified lipoproteins, particularly oxidised LDL (oxLDL; see below), together with decreased efflux of cholesterol and the accumulation of intracellular

cholesterol esters (Chistiakov *et al.*, 2017). A simplified depiction of macrophage foam cell formation is shown in Figure 1.3. Foam cells contribute to the progression of the atherosclerotic plaque via a variety of mechanisms, including the secretion of high levels of pro-inflammatory cytokines and chemokines, as well as matrix metalloproteinases (MMPs) which contribute to plaque destabilisation, and by driving disease progression and necrotic core formation (Groh *et al.*, 2018).

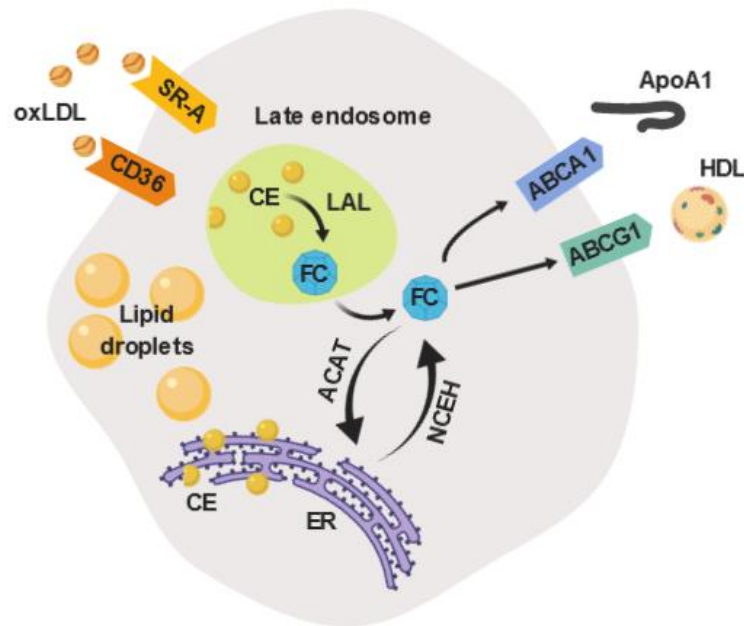


**Figure 1.3 - Schematic representation of processes involved in macrophage foam cell formation.** OxLDL is internalised and trafficked to the endosome where the cholesterol ester (CE) portion is converted to free cholesterol (FC) via lysosomal acid lipase (LAL). FC is then either transported out of the cell via ABC cassette transporters to apoA1 or HDL, or trafficked to the ER and re-esterified via ACAT enzymes. This re-esterified cholesterol is then either stored within the cytoplasm as lipid droplets, or hydrolysed to FC by NCEH enzymes and transported from the cell. Image created using BioRender. Abbreviations: OxLDL, oxidised LDL; SR-A, scavenger receptor-A; ACAT, acyl-CoA cholesterol acyltransferase; NCEH, neutral cholesterol ester hydrolase; ER, endoplasmic reticulum; ABCA1/G1, ATP-binding cassette transporter A1/G1.

Once trapped in the subendothelial space, LDL undergoes enzymatic modification by processes such as glycation, acetylation, aggregation or oxidation. Oxidation represents one of the most common modifications leading to the formation of oxLDL, a highly pro-inflammatory and pro-atherogenic molecule (Bobryshev *et al.*, 2016) and a key instigator of atherogenesis. During the oxidation of LDL, oxidation-specific neoepitopes are generated which are not only immunogenic but prominent targets of pattern recognition receptors (PRRs) (Chou *et al.*, 2008). Macrophage scavenger receptors are classic PRRs which readily recognise these oxidation-specific epitopes on oxLDL particles (Chou *et al.*, 2008). Macrophages ingest native LDL via LDL receptors in a process which

is negatively regulated by an increase in intracellular cholesterol levels (McLaren *et al.*, 2011a). In contrast, the ingestion of modified LDL, namely oxLDL, via macrophage scavenger receptors is unregulated, rapid and excessive (Di Pietro *et al.*, 2016). Receptor-mediated uptake and degradation of modified LDL by macrophages is mediated primarily via CD36 and SR-A (Jiang *et al.*, 2012), two of the most characterised scavenger receptors since their discovery in the 1970s (Goldstein *et al.*, 1979). OxLDL represents the major form of modified LDL internalised via scavenger receptors (Plüddemann *et al.*, 2007). Absence of CD36 and/or SR-A has been shown to prevent foam cell formation and protect against atherosclerosis in a number of studies using ApoE<sup>-/-</sup> hyperlipidaemic mice (Febbraio *et al.*, 2004; Kuchibhotla *et al.*, 2008; Mäkinen *et al.*, 2010). Scavenger receptor-mediated uptake represents the most characterised mode of modified lipoprotein uptake by macrophages (Michael *et al.*, 2013). However, uptake via receptor-independent processes including macropinocytosis, a form of fluid-phase endocytosis, has also been shown to contribute significantly to foam cell formation (Kruth *et al.*, 2002; Michael *et al.*, 2013).

Further to the aberrant uptake of modified lipoproteins, mechanisms governing cholesterol efflux are also disrupted in atherosclerosis, leading to reduced efflux and subsequently the accumulation of excess intracellular cholesterol. Under normal conditions, the efflux machinery functions to transport excess intracellular cholesterol out of the cell either by HDL-mediated passive diffusion, or to extracellular lipid acceptors for hepatic removal via RCT. RCT is a process responsible for the removal of excess cholesterol from peripheral tissues, where it may be reused or transported to the liver and intestine for excretion (Litvinov *et al.*, 2016). An overview of RCT is shown in Figure 1.4. In the initial stages, free cholesterol is transferred out of the cell to lipid-free apoA1, forming nascent HDL. Free cholesterol is esterified on the surface of HDL particles by lecithin cholesterol acyltransferase (LCAT), and as further cholesterol is acquired, mature HDL particles are formed. HDL cholesterol may then be delivered to the liver directly via SR-B1, where it is prepared for excretion. Alternatively, HDL cholesterol may be delivered to the liver indirectly via CETP-mediated transfer. During this process, CEs are transferred to apoB-containing LDL/VLDL particles in exchange for triglycerides, and are subsequently delivered to the liver via LDL receptors. (Tosheska Trajkovska and Topuzovska, 2017)

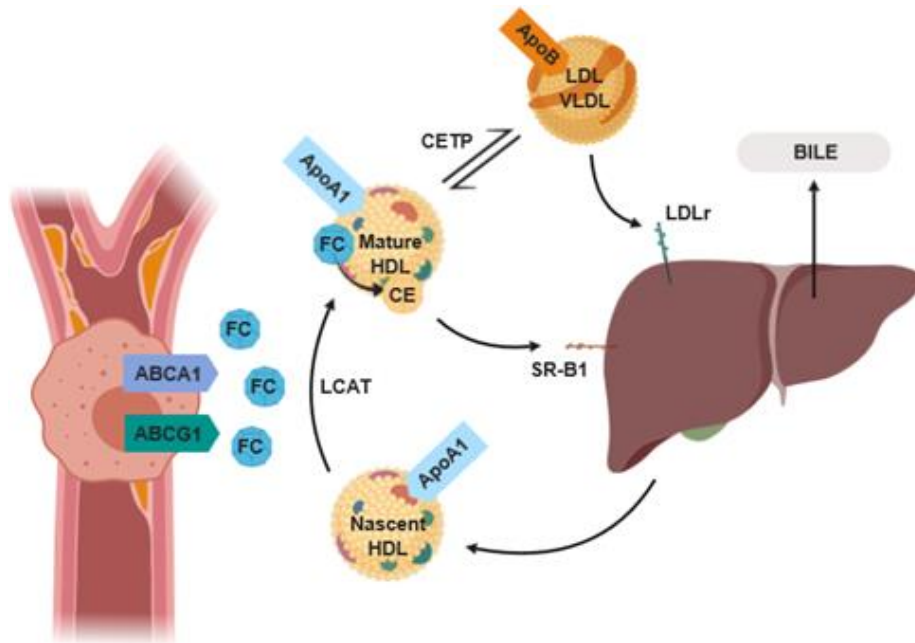


**Figure 1.4 - Overview of reverse cholesterol transport from peripheral tissues to the liver for excretion.** Excess intracellular cholesterol is transported out of the cell via cholesterol efflux machinery including ABCA1/G1. Lipid-free apoA1 binds FC to form nascent HDL particles. FC is then esterified to CE on the surface of HDL particles via the enzyme LCAT, and as further FC is acquired nascent HDL particles become larger and mature. CE may also be exchanged for triglycerides via CETP-mediated transfer to LDL/VLDL. HDL cholesterol may be transported directly to the liver for excretion via SR-B1, or indirectly transported via LDL/VLDL particles and transferred to the liver through LDLr. Abbreviations: ABCA1/G1, ABC cassette transporter A1/G1; FC, free cholesterol; CE, cholesterol esters; HDL, high density lipoprotein; ApoA1, apolipoprotein A1; SR-B1, scavenger receptor class B type 1; LDLr, LDL receptor; LCAT, lecithin cholesterol acyltransferase; CETP, cholesteryl ester transfer protein.

The ATP-binding cassette transporters ABCA1 and ABCG1 are integral membrane proteins that mediate ATP-dependent transport of cholesterol across the membrane to apoA1 or HDL cholesterol respectively (Favari *et al.*, 2015). ABCA1 and similarly ABCG1 are localised both at the plasma membrane and at intracellular compartments, cycling between locations and thereby promoting the flow of intracellular cholesterol to the plasma membrane (Favari *et al.*, 2015). ABCA1 and ABCG1 are key transporters involved in cholesterol efflux and their expression is upregulated primarily in response to cholesterol enrichment via liver X receptors (LXRs), which sense intracellular cholesterol accumulation (Bobryshev *et al.*, 2016). Although additional cholesterol-responsive ABC transporters have been described, their relevance in atherogenic foam cell formation and RCT requires further investigation (Favari *et al.*, 2015; Fu *et al.*, 2013). ApoE is a lipoprotein component synthesised by many cell types, including macrophages in atherosclerotic lesions, in response to stimuli such as cytokines and lipid enrichment (Favari *et al.*, 2015). ApoE secreted from cholesterol-rich macrophages is known to promote cholesterol efflux in the absence of cholesterol acceptors (Huang *et al.*, 2001). Furthermore, genetic deficiency of apoE in mice leads to the development of

atherosclerosis, while re-expression of the protein reduces the severity of the disease (Greenow *et al.*, 2005). As discussed previously the ApoE<sup>-/-</sup> mouse is commonly utilised as a model for atherosclerosis study *in vivo*. Additionally the class B scavenger receptor, SR-B1, contributes to cholesterol efflux; however, it also internalises modified LDL and its role in atherosclerosis is complex (Huang *et al.*, 2019; Yancey *et al.*, 2003).

An imbalance between cholesterol uptake and efflux is largely responsible for the formation of macrophage foam cells in atherosclerotic lesions; however, aberrant intracellular cholesterol metabolism has also been shown to play a role. Under normal conditions, lipoproteins are internalised and degraded in lysosome compartments. Cholesterol esters are hydrolysed via neutral cholesteryl ester hydrolase 1 (NCEH1) and lysosomal acid lipase (LAL) to form free cholesterol and fatty acids (Chistiakov *et al.*, 2017). Free cholesterol may then be either transported out of the cell or trafficked to the ER where it is re-esterified via the acetyl-coenzyme A cholesterol acetyltransferase 1 (ACAT1) enzyme (Chistiakov *et al.*, 2016). Cholesterol esters then coalesce to form membrane-bound cytoplasmic lipid droplets (Tabas, 2009). Under atherosclerotic conditions, cholesterol efflux may be ineffective due to compromised efflux machinery, increased esterification via ACAT1 and/or decreased hydrolysis via NCEH1, leading to increased esterification and the accumulation of large numbers of lipid droplets. This accumulation of lipid droplets is responsible for the foamy appearance of foam cells when observed under the microscope. Furthermore, the excessive accumulation of cholesterol esters in the ER membrane leads to cholesterol-induced cytotoxicity and apoptosis in macrophages (Feng *et al.*, 2003), which when coupled with ineffective clearance of these apoptotic cells propagates disease progression.

### 1.2.3 Disease progression

Efferocytosis is the clearance of apoptotic cells by phagocytes, including macrophages, which are the predominant phagocytes in the atherosclerotic lesion (Tabas, 2009). Under normal conditions apoptosis occurs at a very high rate, and apoptotic cells are rapidly cleared via efferocytosis. In early lesions, the numbers of apoptotic macrophages balance with effective efferocytosis leading to reduced plaque cellularity. However, in advanced lesions efferocytosis is ineffective, resulting in an accumulation of apoptotic

and necrotic cells and debris and subsequently leading to secondary necrosis. The contents of dying macrophages are released and a large accumulation of lipids, together with apoptotic cells and debris, leads to the formation of a lipid-rich necrotic core (Tabas, 2009). Via increased apoptotic cell death coupled with impaired efferocytosis, dead and dying macrophages are largely responsible for necrotic core formation, which is characteristic of advanced atherosclerotic plaques (Bobryshev *et al.*, 2016).

A further essential process in disease progression involves growth factor-induced migration of VSMCs from the media into the arterial intima, where they secrete a variety of extracellular matrix molecules (ECMs) (Fernández-Hernando *et al.*, 2009). ECM proteins contribute to plaque progression, plaque stabilisation and to the formation of a protective fibrous cap (Vassiliadis *et al.*, 2013). In the healthy artery, VSMCs reside in a largely quiescent state within the medial layer of the vessel wall. However, under atherosclerotic conditions, stimulated cells migrate through to the intima where they function to remodel the ECM. As a result of this remodelling, a dense protective cap of collagenous tissue is deposited between the endothelium and the lipid-rich necrotic core (Rohwedder *et al.*, 2012) providing a protective barrier between thrombogenic plaque and the bloodstream. The maintenance of a thick fibrous cap is achieved through a balance between the generation and degradation of ECM components, and is a key determinant of long-term disease prognosis (Rohwedder *et al.*, 2012). When degradation exceeds the generation of ECM proteins, the fibrous cap is compromised and the plaque becomes unstable and vulnerable to rupture, leading to thrombus formation and subsequent clinical complications. The exact mechanisms of fibrous cap thinning remain unclear; however, a number of factors including increased production of MMPs, have been implicated in the degradation and loss of ECM proteins. Macrophage foam cells are an abundant source of serine proteases and MMPs (Johnson and Newby, 2009) that actively degrade ECM components, including collagens, elastins and ECM glycoproteins (Newby *et al.*, 2009). Additionally, the expansion of the necrotic core is associated with increased VSMC death and reduced production of ECM proteins. According to the plaque disruption theory, only a minority of plaques become unstable and rupture, and this process is associated more with the size of the necrotic core than the size of the plaque itself (Tabas, 2009).

### 1.3 Current and emerging therapies

Cost effective interventions identified by the World Health Organisation include a number of possible population-wide and individual interventions. Population-wide interventions include tobacco control, taxation of foods high in fat or sugar, building walking and cycling paths to encourage physical activity and providing healthy school meals for children (World Health Organization, 2018). At an individual level, primary intervention aims to prevent first cardiovascular events in individuals at increased risk of CVD, while secondary prevention strategies in those with established disease involve pharmacological intervention (World Health Organization, 2018). Angiotensin-converting enzyme (ACE) inhibitors, statins and calcium channel blockers were recently reported to be the most commonly prescribed pharmaceutical agents (Hinton *et al.*, 2018).

Statins represent first-line lipid-lowering therapy in global treatment guidelines (Khunti *et al.*, 2018). Statins belong to a class of cholesterol-lowering pharmaceutical agents and are known for their ability to inhibit 3-hydroxy-3-methylglutaryl-CoA (HMG CoA) reductase, an enzyme involved in the rate limiting step of cholesterol biosynthesis. Inhibition of HMG CoA reductase results in a reduction of circulating LDL-C, subsequently lowering cardiovascular risk. In addition to these LDL-C-dependent effects, statins have also been reported to exert LDL-C-independent (pleiotropic) effects including anti-inflammatory effects (Oesterle *et al.*, 2017). However, owing to the overshadowing effect of cholesterol reduction on cardiovascular risk, the clinical significance of these pleiotropic effects remains controversial (Oesterle *et al.*, 2017). The maximum reduction in cardiovascular mortality that can be attributed to statin therapy is approximately 22% per 1 mmol/L reduction in LDL cholesterol (Bohula *et al.*, 2017), and a substantial residual cardiovascular risk is associated with statin therapy as reported by a large number of studies (Bertrand and Tardif, 2017; Cannon *et al.*, 2015; Sampson *et al.*, 2012; Wong *et al.*, 2017). Furthermore, of those patients receiving statins a small subset are unable to achieve target plasma cholesterol levels even at the highest possible dose, while further subsets suffer intolerable statin-associated side effects such as statin-associated myopathy (Whayne, 2013). Due to the limitations of statin therapy, a number of statin co-therapies with non-statin agents have been developed. One co-



therapy involves statins in combination with the non-statin lipid-lowering agent ezetimibe, designed to reduce cholesterol absorption in the intestine (Cannon *et al.*, 2015). In IMPROVE-IT (Improved Reduction of Outcomes: Vytorin Efficacy International Trial), the addition of ezetimibe to statin therapy in the long-term treatment of patients following acute coronary syndrome led to a significant reduction in cardiovascular events (Cannon *et al.*, 2015). Furthermore, a recent comparative meta-analysis reported that statin-ezetimibe co-therapy was more effective in reducing the incidence of CVD in comparison to statin monotherapy (Miao *et al.*, 2019). Proprotein convertase subtilisin/kexin type 9 (PCSK9)-inhibitors have also shown potential as efficient lipid-lowering agents (Saborowski *et al.*, 2018). PCSK9 is a serine protease which binds to the LDL receptor, inducing intracellular degradation and thereby reducing clearance of LDL cholesterol. Monoclonal antibodies targeting PCSK9, namely alirocumab and evolocumab, have shown success in lowering LDL cholesterol and are currently approved for use in hypercholesterolaemic patients who otherwise fail to respond to statin therapy (Preiss and Baigent, 2017; Saborowski *et al.*, 2018). However, due to the high expense of these treatments, they are restricted to high risk patients such as those with homo or heterozygous FH (Weintraub and Gidding, 2016).

In addition to lipid-lowering agents, a number of alternative therapies have been investigated, including HDL elevating agents and anti-inflammatory agents. Low levels of HDL-C are known to be associated with high cardiovascular risk as demonstrated in patients with Tangier disease, while increasing levels of HDL-C is known to lower the risk of CVD (Mahdy Ali *et al.*, 2012; Singh and Rohatgi, 2018). The beneficial effects of HDL and its negative correlation with CVD is thought to be due to its role in RCT of excess cholesterol from macrophages to the liver for biliary excretion (Farrer, 2018). In prospective epidemiologic studies, every 1 mg/dL increase in HDL was associated with a 2-3% decrease in cardiovascular risk, independent of LDL-C and TG levels (Farrer, 2018; Lloyd-Jones, 2014). HDL-C represents a promising target for pharmacological intervention; however, studies report conflicting results. Niacin has been shown to reduce CVD risk by both lowering LDL and elevating HDL cholesterol (Farrer, 2018). However, in the trial Heart Protection Study 2—Treatment of HDL to Reduce the Incidence of Vascular Events (HPS2-THRIVE), niacin treatment did not significantly reduce major vascular events and was associated with adverse events (McCarthy, 2014).

Given the inflammatory nature of atherosclerosis disease, anti-inflammatory agents represent a promising therapeutic strategy for the reduction of cardiovascular risk; however many promising candidates have failed clinical trials. In patients with high levels of the inflammatory marker C-reactive protein (CRP), treatment with canakinumab, a monoclonal antibody that inhibits inflammation by blocking IL-1 $\beta$ , resulted in significantly reduced incidence of atherosclerotic events than placebo in the CANTOS (Canakinumab Anti-inflammatory Thrombosis Outcomes Study) trial (Dolgin, 2017). However, patients also became prone to infection and so treatment may be restricted to high risk patients. Despite the promising success of IL-1 $\beta$  blockers to date, trials of alternative anti-inflammatory agents have reported fewer encouraging outcomes. For example, one potential anti-inflammatory which is currently used in the treatment of rheumatoid arthritis is methotrexate. However, the CIRT (Cardiovascular Inflammation Reduction Trial) trial of methotrexate failed to reduce the incidence of cardiovascular events in patients with hyperglycaemia and high levels of CRP (Mullard, 2018; Ridker *et al.*, 2019). Additionally, the highly anticipated lipoprotein-associated phospholipase A2 (Lp-PLA2) inhibitor darapladib, developed by pharmaceutical giant GlaxoSmithKline, failed to reduce cardiovascular risk in two separate clinical trials; STABILITY (Stabilisation of Atherosclerotic Plaque by Initiation of Darapladib Therapy) and SOLID-TIMI 52 (The Stabilisation Of pLaques usIng Darapladib-Thrombolysis In Myocardial Infarction 52) (Mullard, 2014). The potential of anti-inflammatory agents to reduce the incidence of CVD remains the subject of investigation as the search continues for effective anti-inflammatory therapies.

An alternative strategy for atherosclerosis intervention involves the use of nutraceuticals, defined as foods or dietary supplements with health benefits beyond their basic nutritional value. A number of nutraceuticals have demonstrated anti-atherogenic effects in preclinical and human trials and are reviewed in detail in Moss and Ramji, 2016. Unlike pharmaceuticals, nutraceuticals are derived from natural compounds and are therefore considered safe for use over an extended period of time. Among the most studied in human trials are omega-3 polyunsaturated fatty acids (PUFAs), hydroxytyrosol, flavanols, phytosterols, butyrate and vitamin C and E (Moss and Ramji, 2016). One nutraceutical that has shown particular promise is hydroxytyrosol, a polyphenol compound found in olive oil, which is known to have anti-

inflammatory properties (Moss and Ramji, 2016). A large number of clinical trials have reported anti-atherogenic benefits of hydroxytyrosol, including reduced serum oxLDL levels, increased HDL-C levels, reduced expression of inflammatory markers and improved endothelial function (Fitó *et al.*, 2005, 2008; Gimeno *et al.*, 2007; Valls *et al.*, 2015). Overall, clinical studies have been successful in highlighting hydroxytyrosol as a promising anti-atherosclerotic nutraceutical. Similarly flavanols, plant metabolites commonly found in fruits and vegetables, have also been shown to have anti-atherogenic properties with a number of human studies reporting reduced LDL-C, reduced expression of pro-inflammatory markers and enhanced endothelial function (Hsu *et al.*, 2007; Matsuyama *et al.*, 2008; Sansone *et al.*, 2015). Omega-3 PUFAs have also been held in high regard in previous decades for their beneficial effects, where their dietary supplementation has been shown to reduce the number of cardiovascular events in several preclinical and human trials (Moss and Ramji, 2016; Yokoyama *et al.*, 2007); however, additional studies have reported no change in the number of cardiovascular events or overall mortality rate (Enns *et al.*, 2014; Hooper *et al.*, 2006; Myung *et al.*, 2012; Rizos *et al.*, 2012). Recently, the clinical trial The Reduction of Cardiovascular Events with Icosapent Ethyl–Intervention Trial (REDUCE-IT), which was designed to address residual cardiovascular risk in statin-treated patients with elevated triglycerides, demonstrated success in further reducing cardiovascular risk (Bhatt, 2019). In this study icosapent ethyl, a highly purified ethyl ester of eicosapentaenoic acid (EPA) omega-3 PUFA, was found to significantly reduce the risk of major adverse cardiovascular events by 25% (Bhatt, 2019). In addition to these nutraceuticals, recent studies have revealed an association between atherosclerosis-associated CVD and gut microbial dysbiosis, and probiotic bacteria have been highlighted as potential candidates for atherosclerosis intervention (Lau *et al.*, 2017). The role of probiotics in atherosclerosis is discussed in the next section.

#### 1.4 Probiotics in atherosclerosis

Composed of approximately  $1 \times 10^{14}$  bacteria (Lubomski *et al.*, 2019), the gut microbiota is an essential mediator in health and disease and can be influenced by many factors, including host genetics, diet, stress and disease state (Feng *et al.*, 2018). The intestinal barrier is an epithelial monolayer which forms a primary interface preventing the

diffusion of potentially injurious factors from the intestinal lumen into the tissue and systemic circulation (Rao and Samak, 2013). Dysbiosis in the gut compromises intestinal barrier function leading to the leakage of lipopolysaccharide (LPS) and other bacterial components into the circulation, triggering an inflammatory response. Toll-like receptors (TLRs) are a family of recognition receptors for pathogen associated molecular patterns (PAMPs), activated in response to bacterial components (Chan *et al.*, 2016b). Upon activation of TLRs, an inflammatory response is orchestrated via the expression of a variety of pro-inflammatory cytokines and chemokines. Furthermore, microbiota-derived metabolites, including atherogenic molecules such as choline and trimethylamine *N*-oxide (TMAO) (Li and Tang, 2017) link the gut microbiome to disease. Dysbiosis in the host gut has causative links to atherosclerosis, and microbial immunogens originating from the gut have been implicated as instigators of chronic inflammation which drives atherosclerosis (Chan *et al.*, 2016b; Lau *et al.*, 2017).

Probiotics are defined as microorganisms that when ingested in adequate amounts, confer a health benefit to the host. Probiotics are 'good' bacteria that may be exploited for their ability to combat dysbiosis and promote gut health. Probiotic bacteria have beneficial effects on the host by producing vitamins K and B2, together with short chain fatty acids (SCFA) such as acetate or propionate, which are used as fuel by intestinal flora and colonocytes (Moludi *et al.*, 2018). Importantly, probiotics are known to improve gut barrier function via strengthening of the epithelial tight junctions (Rao and Samak, 2013). By reducing gut leakage, probiotic bacteria strengthen immunological and non-immunological gut barrier function, and reducing the translocation of microbial immunogens (Mennigen and Bruewer, 2009). The implication of host gut microbiota in disease and the ability of probiotics to promote overall gut health has led to an explosion of research showing therapeutic benefits in a vast range of disease states. Indeed, probiotics are currently used in clinics for the treatment and prevention of inflammatory bowel diseases, irritable bowel syndrome, gluten intolerance, gastroenteritis and antibiotic-associated diarrhoea (Rao and Samak, 2013). More recent data implicates the gut microbiota in a diverse range of diseases via the gut-brain axis (Dinan and Cryan, 2017; Kennedy *et al.*, 2017; Mehrian-Shai *et al.*, 2019; Niemarkt *et al.*, 2019), gut-lung axis (Dang and Marsland, 2019; Dumas *et al.*, 2018; Liu *et al.*, 2019), gut-liver axis (Bajaj

and Hays, 2019; Denny *et al.*, 2019; Ohtani and Kawada, 2019) and gut-vascular axis (Bu and Wang, 2018; Li *et al.*, 2017) among others (Feng *et al.*, 2018).

### 1.4.1 The effect of probiotics on key atherosclerosis associated risk factors

Probiotic supplementation has been shown to beneficially modify a number of major atherosclerosis-associated cardiovascular risk factors, including hypercholesterolaemia, dyslipidaemia, hypertension and chronic inflammation (Figure 1.5). The anti-atherogenic effects of several different probiotic strains as reported by human and animal studies are summarised in Table 1.1.

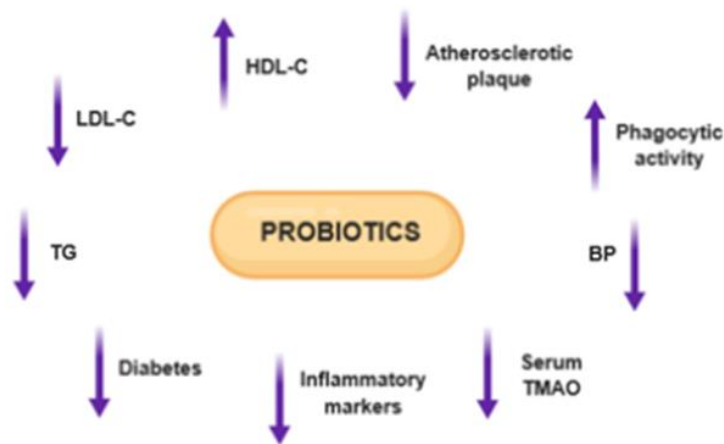


**Figure 1.5 - Probiotics beneficially modulate a number of atherosclerosis-associated cardiovascular risk factors.** Abbreviations: HDL-C, HDL cholesterol; BP, blood pressure; TMAO, trimethylamine *N*-oxide; TG, triglycerides; LDL-C, LDL cholesterol.

**Table 1.1 – The athero-protective effects of probiotic bacteria**

Probiotic	Anti-atherogenic effects	Study group	References
VSL#3	Reduced lesion development; reduced vascular inflammation	ApoE <sup>-/-</sup> mice	(Chan <i>et al.</i> , 2016b)
<i>L. rhamnosus</i> GG	Reduced lesion development; reduced plasma cholesterol, E-selectin, ICAM-1, VCAM-1 and endotoxin	ApoE <sup>-/-</sup> mice	(Chan <i>et al.</i> , 2016a)
<i>E. faecium</i> CRL183	Increased HDL-C; reduced triglycerides; no change in plaque size	Hypercholesterolemic rabbits	(Cavallini <i>et al.</i> , 2009)
<i>Pediococcus acidilactici</i> R037	Reduced lesion development; reduced production of pro-inflammatory cytokines and CD4+ T cells	ApoE <sup>-/-</sup> mice	(Mizoguchi <i>et al.</i> , 2017)
<i>L. acidophilus</i> 145 and <i>B. longum</i> 913	Increased HDL cholesterol; reduced LDL/HDL ratio	Human	(Kiessling <i>et al.</i> , 2002)
<i>L. acidophilus</i> ATCC 4356	Reduced lesion development; reduced plasma cholesterol; reduced serum oxLDL and TNF- $\alpha$ , increased serum IL-10	ApoE <sup>-/-</sup> mice	(Chen <i>et al.</i> , 2013; Huang <i>et al.</i> , 2014)
<i>L. plantarum</i> ZDY04	Reduced TMAO-induced lesion development; reduced serum TMAO	ApoE <sup>-/-</sup> mice	(Qiu <i>et al.</i> , 2018)
<i>L. acidophilus</i> and <i>B. bifidum</i>	Reduced TC, HDL-C and LDL-C	Human	(Rerksuppaphol and Rerksuppaphol, 2015)
VSL#3	Reduced TC, LDL-C, TG, hsCRP; increased HDL-C; increased insulin sensitivity	Human	(Rajkumar <i>et al.</i> , 2014)
<i>S. thermophiles</i> , <i>L. bulgaricus</i> , <i>L. acidophilus</i> LA5, <i>B. lactis</i> BB12	Reduced TC, LDL-C; reduced insulin resistance; reduced postprandial blood glucose; reduced fasting insulin	Human	(Madjd <i>et al.</i> , 2016)
<i>L. plantarum</i> LRCC 5273	Reduced TC and LDL-C; upregulation of LXR- $\alpha$ expression	C57BL/6 mice	(Heo <i>et al.</i> , 2018)
<i>S. cerevisiae</i> ARDMC1	Reduced TC, LDL-C, TG	Wister rats	(Saikia <i>et al.</i> , 2018)
<i>L. plantarum</i> ECGC 13110402	Reduced TC, LDL-C, TG; increased HDL-C	Human	(Costabile <i>et al.</i> , 2017)

Probiotic	Anti-atherogenic effects	Study group	References
<i>B. lactis</i> HN019	Reduced TC and LDL-C; reduced BMI; reduced TNF- $\alpha$ and IL-6	Human	(Bernini <i>et al.</i> , 2016)
<i>L. casei</i> W8	Reduced TG	Human	(Bjerg <i>et al.</i> , 2015)
<i>L. acidophilus</i> 74-2 and <i>B. animalis subsp lactis</i> DGCC 420	Reduced TG; increased phagocytic activity of granulocytes and monocytes	Human	(Klein <i>et al.</i> , 2008)
BSH-active <i>L. reuteri</i> NCIMB 30242	Reduced TC, LDL-C; reduced apoB-100	Human	(Jones <i>et al.</i> , 2012)
Probiotic yogurt and <i>Cucurbita ficifolia</i>	Reduced TG; increased HDL-C; Reduced blood glucose, HbA1c, hsCRP; reduced systolic and diastolic blood pressure	Human	(Bayat <i>et al.</i> , 2016)
<i>L. acidophilus</i> La5 and <i>B. lactis</i> Bb12	Reduced TC, LDL-C; reduced TC/HDL-C and LDL-C/HDL-C ratios	Human	(Ejtahed <i>et al.</i> , 2011)
<i>L. acidophilus</i> , <i>L. casei</i> , <i>L. lactis</i> , <i>B. bifidum</i> , <i>B. longum</i> and <i>B. infantis</i>	Reduced fasting insulin; reduced HbA1c	Human	(Firouzi <i>et al.</i> , 2017)
<i>L. acidophilus</i> (LA-5) and <i>B. animalis subsp. Lactis</i> (BB-12)	Reduced TC, TG, oxLDL; reduced blood glucose	Hamster	(Stancu <i>et al.</i> , 2014)

Human and animal studies showing the beneficial effects of probiotic supplementation on common atherogenic risk factors. VSL#3 is composed of *Bifidobacterium longum*, *Bifidobacterium infantis*, *Bifidobacterium breve*, *Lactobacillus acidophilus*, *Lactobacillus casei*, *Lactobacillus delbrueckii subsp. bulgaricus*, *Lactobacillus plantarum*, and *Streptococcus salivarius subsp. Thermophilus*. Abbreviations: TC, total cholesterol; LDL-C, low density lipoprotein cholesterol, HDL-C, high density lipoprotein cholesterol; ICAM-1, intercellular adhesion molecule-1; VCAM-1, vascular cell adhesion molecule-1; oxLDL, oxidised LDL; IL-10, interleukin-10; TMAO, trimethylamine-N-oxide; hsCRP, high sensitivity C-reactive protein; BMI, body mass index; HbA1c, haemoglobin A1c.

### 1.4.1.1 Lesion formation

Few studies have investigated the effect of probiotic supplementation on atherosclerotic plaque formation. VSL#3 is a consortium of 8 lyophilised lactic acid bacterial strains (*Bifidobacterium longum*, *Bifidobacterium infantis*, *Bifidobacterium breve*, *Lactobacillus acidophilus*, *Lactobacillus casei*, *Lactobacillus delbrueckii subsp. bulgaricus*, *Lactobacillus plantarum*, and *Streptococcus salivarius subsp. thermophilus*) (Corthésy *et al.*, 2007). Chan and colleagues have demonstrated significantly reduced high fat diet (HFD)-induced lesion development in ApoE<sup>-/-</sup> mice supplemented with the VSL#3 consortium, in addition to reduced vascular inflammation and significant reductions in the levels of serum ICAM-1, VCAM-1, E-selectin and MCP-1 (Chan, 2012; Chan *et al.*, 2016b). A previous study investigated the effect of two *Lactobacillus* strains (*L. acidophilus* ATCC 4356 and 4962) on atherosclerosis development in ApoE<sup>-/-</sup> mice (Huang *et al.*, 2014). Authors reported a dramatic reduction in atherosclerotic lesion area in the L.4356 group; however, no significant effect was observed in the L.4962 group. In the same study, serum levels of TC and non-HDL-C were significantly reduced and a significant reduction in cholesterol absorption was achieved. In a separate study, *L. acidophilus* ATCC 4356 was again shown to reduce atherosclerosis lesion development in ApoE<sup>-/-</sup> mice, in addition to reduced serum oxLDL and TNF- $\alpha$  levels, and increased serum IL-10 indicating a beneficial effect on inflammatory markers (Chen *et al.*, 2013).

### 1.4.1.2 Dyslipidaemia

The beneficial effects of probiotic supplementation on plasma lipids is well documented and a large number of meta-analyses concur that probiotics are associated with a significant reduction in TC and LDL-C. One meta-analysis of the effects of probiotic supplementation on lipid profiles of normal and hypercholesterolaemic individuals included 26 clinical studies utilising fermented milk products and probiotic supplements (Shimizu *et al.*, 2015). Probiotic supplementation resulted in a significant reduction in TC and LDL-C, with no change in HDL-C or triglycerides. Subgroup analysis revealed a statistically greater reduction in TC and LDL-C with long-term (>4 weeks) probiotic intervention. Authors highlighted *L. acidophilus* as the strain most effective in reducing TC and LDL-C. A further meta-analysis included 15 clinical studies with 788 participants



(Sun and Buys, 2015). Significant pooled effects of probiotics were achieved for the reduction of TC, LDL-C, body mass index (BMI) and inflammatory markers. Subgroup analysis revealed statistically greater reductions in TC and LDL-C with long-term (>8 weeks) intervention, and with multiple versus single probiotic strains. Again *L. acidophilus* was highlighted as the most effective strain in reducing LDL-C (Sun and Buys, 2015). A more recent meta-analysis of 32 clinical trials and 1971 patients also reported a significant reduction in TC with probiotic supplementation (Wang *et al.*, 2018). Subgroup analysis suggested that a difference in baseline TC as well as the duration of intervention may significantly impact results; however, the probiotic strain and the dose were found to have no significant influence. There is a confounding body of evidence that probiotic bacteria are able to influence host lipid profiles, however the exact mechanisms of action remain to be ascertained.

#### ***1.4.1.3 Inflammation***

Probiotics are known to modify host immune responses (Li *et al.*, 2019). However, interactions between probiotic bacteria, the gut and the host immune systems is highly complex and despite increasingly growing clinical evidence, remains poorly understood (Moludi *et al.*, 2018). In a recent study, a reduction in atherosclerotic lesion development was accompanied by the suppression of IFN- $\gamma$ -producing CD4<sup>+</sup> T cells and pro-inflammatory cytokine production in *Pediococcus acidilactici* R037-treated mice (Mizoguchi *et al.*, 2017). In addition to a reduction in pro-inflammatory T cells, probiotic bacteria have been shown to reduce inflammation via an increase in regulatory T cells (Tregs) (Karimi *et al.*, 2009; Shah *et al.*, 2012; Smits *et al.*, 2005). DNA from the VSL#3 consortium has been shown to limit epithelial proinflammatory responses *in vivo* and *in vitro*, and to attenuate systemic release of TNF- $\alpha$  in response to *Escherichia coli* DNA injection (Jijon *et al.*, 2004). In a separate study, VSL#3 DNA was shown to exert anti-inflammatory effects via TLR9 signalling (Rachmilewitz *et al.*, 2004); interestingly, the authors concluded that the protective anti-inflammatory effects of probiotics are mediated via their own DNA rather than metabolites, and that TLR9 signalling is essential in mediating this effect.

#### 1.4.1.4 Hypertension and hyperglycaemia

In a meta-analysis of the effect of probiotics on hypertension, the authors reported a significant reduction in systolic and diastolic blood pressure (BP), particularly with a baseline blood pressure of >130/85 mmHg (Khalesi *et al.*, 2014). Subgroup analysis revealed a greater reduction achieved with long-term treatment duration (>8 weeks), where durations of <8 weeks showed no significant reduction. Additionally, the inclusion of multiple compared to single strains, and daily consumption of doses >10<sup>11</sup> CFU, were associated with significant reductions in both systolic and diastolic BP. Furthermore, a recent meta-analysis of 11 clinical studies also reported beneficial effects of probiotic supplementation on both hypertension and dyslipidaemia in diabetic patients (Hendijani and Akbari, 2018). Pooled data demonstrated significantly reduced systolic and diastolic BP in addition to serum LDL-C, TC and TG. Similarly, studies investigating probiotic supplementation in relation to type 2 diabetes and insulin resistance have shown success (Gijsbers *et al.*, 2016; Rad *et al.*, 2017; Rezaei *et al.*, 2017). In a meta-analysis of 22 cohort studies and 579,832 patients, total dairy consumption was inversely associated with type 2 diabetes risk, where yogurt consumption was reported to be particularly effective (Gijsbers *et al.*, 2016). A separate meta-analysis of 10 clinical trials reported significantly reduced fasting blood glucose in addition to reduced systolic and diastolic BP, reduced serum TC, LDL-C and TG in type 2 diabetic patients with probiotic supplementation (He *et al.*, 2017). Further studies have demonstrated probiotic-associated reduction in blood glucose levels and/or insulin resistance with various strains of *Lactobacillus*, *Bifidobacterium* and *Streptococcus* (Firouzi *et al.*, 2017; Madjd *et al.*, 2016; Rajkumar *et al.*, 2014). However, the association between probiotic treatment and diabetes is less clear with a small number of studies showing no such association (Bernini *et al.*, 2016; Sabico *et al.*, 2017). In a recent clinical trial, type 2 diabetic patients receiving a consortium of 8 different probiotic strains exhibited significantly higher median glucose levels, in addition to higher circulating TC and LDL-C (Sabico *et al.*, 2017). Several additional studies have similarly reported no beneficial effect of probiotic supplementation on blood glucose levels (Bernini *et al.*, 2016; Hütt *et al.*, 2015).

#### 1.4.1.5 TMAO

In addition to their effects on atherogenic risk factors, probiotic bacteria have been shown to affect the production of potentially atherogenic metabolites. One metabolite currently receiving attention for its strong association with atherosclerosis is TMAO. The bacterial metabolite TMA is produced by gut microbiota from dietary choline, then oxidised to TMAO in the liver and released into the circulation (Ufnal *et al.*, 2015). It has been suggested that TMAO contributes to atherosclerosis in part by promoting macrophage foam cell formation in atherosclerotic lesions as well as ineffective RCT (Bennett *et al.*, 2013; Moludi *et al.*, 2018) and disruption of lipid homeostasis (Ufnal *et al.*, 2015). Probiotic treatment has been shown to reduce levels of TMAO in correlation with reduced atherosclerosis development (Martin *et al.*, 2008); however, this effect is strain specific. A recent study investigated potential TMAO-lowering property of five different probiotic strains (Qiu *et al.*, 2018). Only *L. plantarum* ZDY04 was able to significantly reduce serum TMAO, and it was suggested that this effect was achieved via the remodelling of the gut microbiota. Furthermore, *L. plantarum* ZDY04 significantly attenuated the development of TMAO-induced atherosclerosis in ApoE<sup>-/-</sup> choline-fed mice (Qiu *et al.*, 2018). In a similar study, serum TMAO was significantly reduced in choline-fed mice treated with *Enterobacter aerogenes* ZDY01, and a similar remodelling of gut microbiota was demonstrated (Qiu *et al.*, 2017). However, the beneficial effect of probiotic bacteria on TMAO production is strain specific and a separate study investigating *Streptococcus thermophilus* (KB19), *Lactobacillus acidophilus* (KB27), and *Bifidobacteria longum* (KB31), reported no change in TMAO levels (Borges *et al.*, 2018).

A large body of evidence suggests a beneficial role for probiotic bacteria in the management of many atherogenic risk factors. *L. acidophilus* in particular has shown promise in many human and animal studies where a variety of strains have had significant beneficial effects on atherosclerotic plaque development, plasma lipid profile, pro-inflammatory markers, and even insulin resistance and blood glucose levels (Bubnov *et al.*, 2017; Chen *et al.*, 2013; Hong *et al.*, 2016; Huang *et al.*, 2010, 2014; Song *et al.*, 2015). However, these anti-atherogenic effects are subject to strain specific variation and a number of further studies have shown no effect, or even pro-atherogenic effects of probiotic treatment (Hove *et al.*, 2015; Hütt *et al.*, 2015; Sabico *et al.*, 2017).

Moreover, little is understood about the mechanisms underlying the observed effects of probiotics on host health. The cholesterol-lowering effect of certain probiotics is thought to be a result of bile salt hydrolase (BSH) activity and its interaction with the enterohepatic circulation (Michael *et al.*, 2017). BSHs deconjugate conjugated bile acids (CBAs) forming deconjugated bile salts, which are less soluble and are less efficiently reabsorbed from the intestine. Deconjugated bile salts are therefore excreted in the faeces, which creates greater demand for the *de novo* synthesis of bile acids to replace those lost in the faeces (Ishimwe *et al.*, 2015). As cholesterol is a precursor of bile salts, this deconjugation and loss of bile acids results in a cholesterol-lowering effect. Deconjugated bile acids are also less efficient in the solubilisation and absorption of lipids in the gut leading to reduced absorption of cholesterol from the intestinal lumen (Kumar *et al.*, 2012).

Mechanisms of immunomodulation have also been investigated and thought to be achieved via changes in cytokine production and modulation of signalling pathways in intestinal epithelial and immune cells (Cambeiro-Pérez *et al.*, 2018; Hemarajata and Versalovic, 2013). This has been demonstrated via probiotic release of bioactive metabolites and immunomodulatory factors; for example, histamine derived from *L. reuteri*. It has previously been shown that *L. reuteri*-derived histamine suppresses pro-inflammatory TNF production via transcriptional regulation through protein kinase A (PKA) and extracellular signal-regulated kinase (ERK) signalling (Thomas *et al.*, 2012). Additionally, S-layer protein A (SlpA) produced by the probiotic *L. acidophilus* NCFM has been shown to bind to the intestinal dendritic cell surface receptor DC-specific ICAM-3-grabbing nonintegrin (DC-SIGN), inducing the production of anti-inflammatory IL-10 in a dose-dependent manner (Konstantinov *et al.*, 2008).

## 1.5 The Lab4 probiotic consortium

The Lab4 probiotic consortium developed by Cultech Ltd (Port Talbot, UK) is composed of distinct populations of *Lactobacillus* spp. and *Bifidobacterium* spp. In addition to Lab4, Lab4b is a similar consortium also developed by Cultech Ltd featuring alternative *Lactobacillus* spp. The exact composition of Lab4 and Lab4b consortia is given in Table 1.2.

**Table 1.2 – The composition of Lab4 and Lab4b probiotic consortia**

Lab4	Lab4b
<i>Lactobacillus acidophilus</i> CUL21 (NCIMB 30156)	<i>Lactobacillus salivarius</i> CUL61 (NCIMB 30211)
<i>Lactobacillus acidophilus</i> CUL60 (NCIMB 30157)	<i>Lactobacillus paracasei</i> CUL08 (NCIMB 30154)
<i>Bifidobacterium bifidum</i> CUL20 (NCIMB 30153)	<i>Bifidobacterium bifidum</i> CUL20 (NCIMB 30153)
<i>Bifidobacterium animalis subsp.</i> <i>lactis</i> CUL34 (NCIMB 30172)	<i>Bifidobacterium animalis subsp.</i> <i>lactis</i> CUL34 (NCIMB 30172)

Species of lactic acid bacteria (*Lactobacillus*, *Lactococcus*, *Streptococcus*), as well as *Bifidobacterium*, have a long history of safe use as probiotics. *Lactobacillus*, as included in Lab4 and Lab4b consortia, are rod-shaped gram-positive bacteria with a low guanine-cytosine (G+C) content. Similarly, *Bifidobacterium* are also gram-positive rods, with a high G+C content (de Melo Pereira *et al.*, 2018). In line with selection criteria guidelines from the Food and Agriculture Organization of the United Nations (FAO)/WHO (Araya *et al.*, 2002), a potential probiotic strain is subject to a systematic series of tests. Stress tolerance, to survive the stresses of the human digestive tract; adhesion ability, to colonise the gastrointestinal tract; anti-pathogenic activity, through the production of antimicrobial components, competition for nutrients, coaggregation or immune system activation; safety assessment, to confirm absence of virulence, infectivity, toxicity and transferable antibiotic resistance genes (de Melo Pereira *et al.*, 2018).

Over the previous 15 years, clinical studies have shown the benefit of Lab4 and Lab4b consortia in a variety of functions, including digestive health, immune health, mood and cognition, in adults, children and babies (Table 1.3). The Sheffield Irritable Bowel Syndrome (IBS) Trial investigated the effect of Lab4 supplementation on symptoms of IBS, reporting significant improvement in symptoms compared to the placebo (Williams *et al.*, 2009). In 2013, The Adult Immune Response Study examined the effects of Lab4 on *ex-vivo* pro-inflammatory and anti-inflammatory cytokine production by peripheral blood mononuclear cells extracted from healthy volunteers (Hepburn *et al.*, 2013). A significant increase in the production of the anti-inflammatory cytokines IL-10 and TGF-

$\beta$  was observed over a 12 week period. Furthermore, in the presence of pro-inflammatory bacterial toxin, the production of pro-inflammatory cytokines IL-6 and IL-1 $\beta$  was significantly reduced, highlighting the potential immunomodulatory benefits of Lab4 probiotics (Hepburn *et al.*, 2013). The benefits of Lab4 supplementation also extends to children. The ProChild Study investigated the efficacy of Lab4 probiotics plus vitamin C in reducing symptoms of coughs and colds in a randomised, double-blind placebo controlled study involving 57 children aged 3-6 years (Garaiova *et al.*, 2015). Compared to placebo, children taking Lab4 with vitamin C exhibited a significant 49% reduction in the duration and a 33% reduction in the incidence of cough and cold symptoms. In addition, the study reported a 30% reduction in absenteeism from school, and a 43% reduction in GP visits. Details on completed trials of Lab4 and Lab4b consortia are listed in Table 1.3.

A further probiotic bacteria of interest to Cultech Ltd is *L. plantarum* CUL66 (NCIMB 30280). It has previously been demonstrated that CUL66 exhibits BSH activity and the ability to assimilate cholesterol from culture media (Michael *et al.*, 2016). Furthermore, Caco-2 epithelial cells treated with CUL66 exhibited significantly reduced uptake and efflux of cholesterol, and reduced expression of Niemann-Pick C1-Like 1 (NPC1L1). As discussed previously, NPC1L1 expressed on intestinal epithelial cells is not only critical for intestinal cholesterol absorption but is the target of cholesterol-lowering drug ezetimibe (Garcia-Calvo *et al.*, 2005). Together, these results highlight CUL66 as an effective cholesterol-lowering probiotic strain. These results are corroborated by additional studies reporting reduced cholesterol uptake via down-regulation of NPC1L1 in response to *L. plantarum* strains (Yoon *et al.*, 2013). Further to *in vitro* studies, the anti-cholesterolaemic effect of short-term Lab4/CUL66 feeding was investigated in C57BL/6J mice fed high fat diet (HFD) or HFD plus Lab4/CUL66 for a period of 2 weeks (Michael *et al.*, 2017). Lab4/CUL66 supplementation resulted in a significant reduction in TC, in addition to significant reduction in weight gain, and a significant increase in unconjugated bile salts present in the faeces. Results from these preliminary studies are promising and when considered in conjunction with previously demonstrated immunomodulatory effects, highlight the potential benefit of Lab4, Lab4b or CUL66 supplementation as potential athero-protective agents.

**Table 1.3 - Completed trials of Lab4 and Lab4b probiotic consortia**

Study	Study number	Outcomes	References
The Cambridge Clostridium difficile Study	138	Reduction in the incidence of <i>Clostridium difficile</i> diarrhoea in hospitalised patients; Reduction in the presence of the <i>Clostridium difficile</i> toxin	(Plummer <i>et al.</i> , 2004)
The Cambridge Probiotic/Antibiotic Trial 1	22	Reduction in the overgrowth of undesirable and potentially harmful bacteria both during and following antibiotic therapy	(Madden <i>et al.</i> , 2005)
The Cambridge Probiotic/Antibiotic Trial 2	155	Reduction in gut microbiota disruption; Reduction in the level of antibiotic resistance within the re-growth microbiota	(Plummer <i>et al.</i> , 2005)
The Sheffield IBS Trial	52	Improvement of total IBS symptoms	(Williams <i>et al.</i> , 2009)
The Safety in Newborns Study	454	Tolerance of Lab4b in late pregnancy and early infancy	(Allen <i>et al.</i> , 2010)
The Adult Immune Response Study	20	Significant enhancement of production of the anti-inflammatory cytokines IL-10 and TGF- $\beta$ ; Significant decrease in production of the pro-inflammatory cytokines IL-6 and IL-1 $\beta$	(Hepburn <i>et al.</i> , 2013)
The Cambridge IBS Study	12	Reduction in yeast overgrowth in IBS patients receiving antibiotic treatment	(Plummer <i>et al.</i> , 2013)
The Swansea Baby Study	308	Reduction in development of atopic eczema and atopic sensitisation	(Allen <i>et al.</i> , 2014)
The Keele Study	50	Reduction in anxiety over a 6 week period; Increased continuity of attention	(Owen <i>et al.</i> , 2014)
The ProChild Study	57	Reduction in duration and incidence of cough and cold symptoms	(Garaiova <i>et al.</i> , 2015)
The Hertfordshire Study	30	Reduction in gut symptom severity score during training; Reduction in endotoxin levels; Reduction in race finish times	(Roberts <i>et al.</i> , 2016)

## 1.6 Project aims

Despite the success of current therapies, CVD remains the leading cause of death worldwide and represents a major economic burden. Probiotics have been highlighted as potential anti-atherogenic agents owing to their demonstrated ability to influence a number of atherogenic risk factors, including cholesterol homeostasis, plasma lipid levels and the host immune response. Given the cholesterol-lowering and immunomodulatory effects of Lab4, Lab4b and CUL66, these specific consortia represent potential novel anti-atherogenic agents. Several clinical studies have demonstrated the beneficial effects of Lab4 and Lab4b consortia in a variety of conditions (Davies *et al.*, 2018; Garaiova *et al.*, 2015; Michael *et al.*, 2017, 2019); however, their role in atherosclerosis has not previously been investigated.

The overall aim of this project was to assess the anti-atherogenic effects of the Lab4 probiotic consortium on key processes in atherosclerosis development. Further work aimed to investigate the mechanisms underlying these effects, and to provide valuable insight into probiotic mechanisms of action. Initial investigations were carried out *in vitro* using CM from Lab4, Lab4b and CUL66 cultures, where the effect of probiotic CM on key atherogenic processes was investigated in human monocytes, macrophages and VSMCs. Key findings from *in vitro* investigations on monocyte/macrophage cell lines were then confirmed in primary human macrophages isolated from human buffy coats. The project then progressed to determine the anti-atherogenic effects of a Lab4/CUL66 combined live supplementation *in vivo* in an atherosclerosis mouse model. A schematic diagram of the project outline is shown in Figure 1.5, and the main project objectives are outlined below.

- Chapter 3 aimed to broadly investigate potential anti-atherosclerotic effects of Lab4, Lab4b and CUL66 across a number of key cellular processes in atherosclerosis initiation and progression, using *in vitro* model systems. Probiotic CM was first optimised and then used to assess the effects of each probiotic in human monocytes, macrophages and VSMCs. Key findings were confirmed in primary human macrophages isolated from human buffy coats.



- In Chapter 4, the effects of Lab4, Lab4b and CUL66 on macrophage foam cell formation was investigated *in vitro* at the cellular and molecular level, and key findings confirmed in primary human macrophages.
- Chapter 5 presents initial findings from the *in vivo* study of Lab4/CUL66 supplementation in the LDLr<sup>-/-</sup> mouse model. The effect of Lab4/CUL66 on plaque formation and plaque composition are presented in addition to changes in plasma lipid profiles.
- Chapter 6 continues the investigation of the *in vivo* effects with analysis of changes in atherosclerosis-associated gene expression and bone marrow cell populations, in an attempt to elucidate possible underlying mechanisms of observed anti-atherogenic effects.

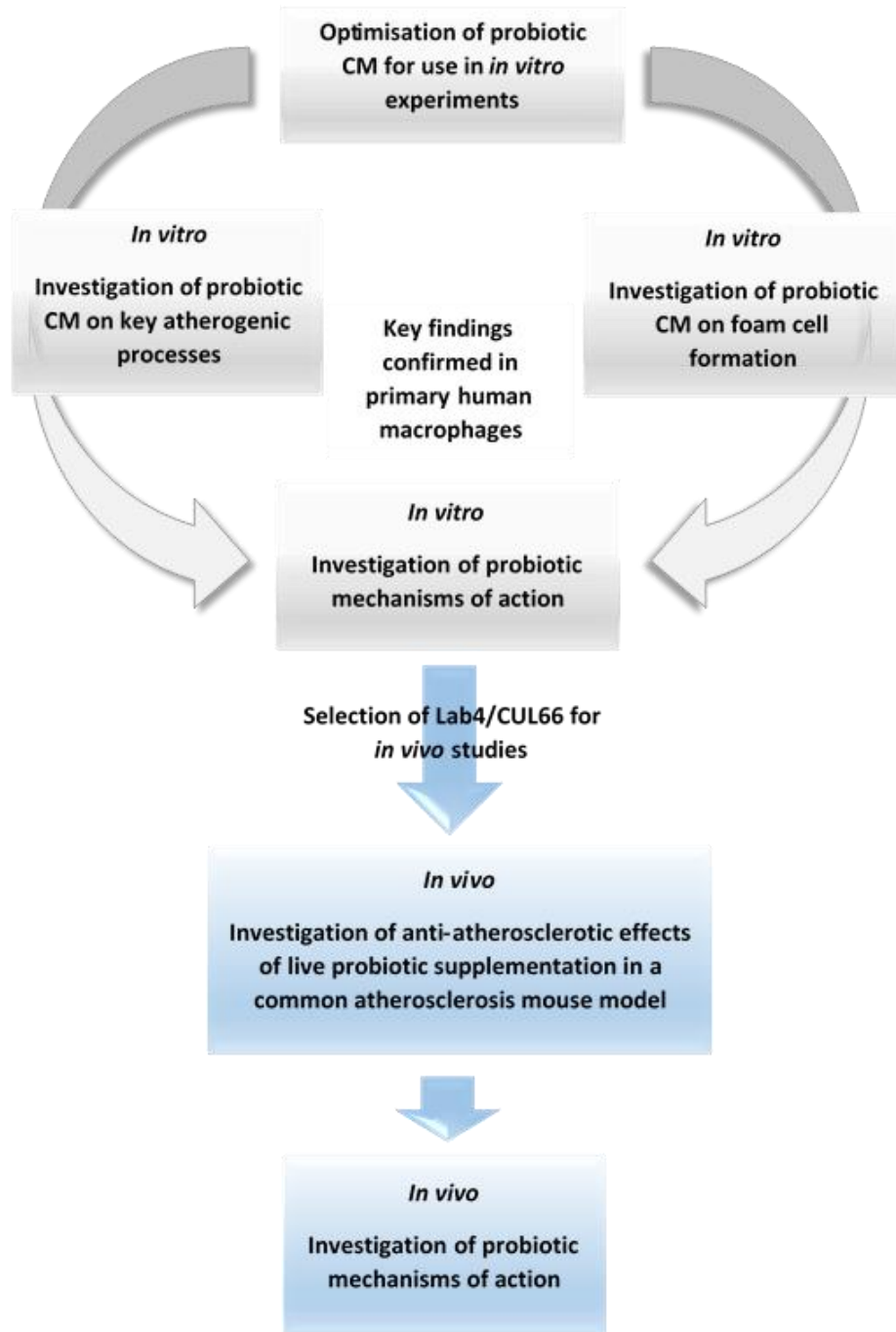


**Figure 1.6 - Overview of the project aims.** Details on the specific methods and the rationale for each investigation are described through Chapters 2 – 6.

# CHAPTER 2

## *Materials & Methods*

---

## 2.1 Materials

A list of materials and reagents used in this study is provided in Table 2.1.

**Table 2.1 - Materials and reagents used during the course of the study**

Supplier	Material or reagent
Abcam, UK	DCFDA Cellular ROS Detection Assay Kit; Eosin Y; HDL and LDL/VLDL Cholesterol Assay Kit; Haematoxylin; Oil Red O Staining Kit; Triglyceride Assay Kit
Agilent, UK	Seahorse cell culture microplates; Seahorse XF calibrant solution; Seahorse XF Cell Mito Stress Test Kit
Alfa Aesar, UK	Acetylated LDL, human; DiI-labelled oxidised LDL, human; Oxidised LDL, human
BD Bioscience, UK	FITC-conjugated anti-mouse CD34
Biolegend, USA	APC-conjugated anti-mouse c-Kit; PE-conjugated anti-mouse Sca-1; FITC-conjugated anti-mouse CD48; PE/Cy7-conjugated anti-mouse CD150; APC/Cy7-conjugated anti-mouse Sca-1; PE/Cy7-conjugated anti-mouse CD16/32; BV650-conjugated anti-mouse CD127
Cultech Limited, UK	Lab4, Lab4b, <i>Lactobacillus plantarum</i> CUL66
Fisher Scientific, UK	Agarose; MRS broth (Oxoid); Pierce Coomassie Plus Assay Kit
GE Health Care, UK	[4- <sup>14</sup> C] cholesterol
Helena Biosciences, UK	0.22 µM pore syringe filters; Cell scrapers
Jackson Laboratory, USA	LDLR <sup>-/-</sup> mice
Life Technologies, UK	Foetal calf serum (FCS)
Lonza, UK	Dulbecco's Modified Eagle Medium (DMEM); RPMI 1640 with L-Glutamine medium
Peprtech, UK	IFN-γ; IL-1β; MCP-1; M-CSF; PDGF-BB; TNF-α
Promega, UK	MMLV Reverse Transcriptase; MMLV RT 5x buffer; Random primers; RNasin ribonuclease inhibitor
Qiagen, UK	Atherosclerosis RT <sup>2</sup> Profiler PCR Arrays

Supplier	Material or reagent
R&D Systems, UK	Human IL-1 $\beta$ DuoSet ELISA
Sigma-Aldrich, UK	1, 2-Propanediol; 12/24/96-well plates; 10/25 mL strippets; 15/50 mL Falcon tubes; 25/75 cm <sup>2</sup> tissue culture flasks; 5-Bromo-2'-deoxy-uridine Labeling and Detection Kit III; Accuspin tubes; Acetic acid; Acetone; Apolipoprotein A-I; Bovine serum albumin (BSA); Carbonyl cyanide 4-(trifluoromethoxy)phenylhydrazone (FCCP); Chloroform; Crystal violet; DAPI nuclear stain; DPX Mountant; Donkey serum; Matrigel ECM gel; Ethanol; Ethidium bromide; Fluoroshield™ with DAPI; Hexane; Isopropanol; Lucifer yellow CH dipotassium salt (LY); Methanol; Oligomycin A; Penicillin-Streptomycin 10,000 U/mL; Phorbol-12-myristate-13-acetate (PMA); Phosphate buffered saline (PBS) tablets; Primers; Protease inhibitor cocktail; RIPA lysis buffer; Smooth Muscle Cell Growth Medium; SYBR Green Jumpstart Taq Readymix; Sodium hydroxide; Sudan black B; THP-1 human acute monocytic leukemia cell line; Tris-borate EDTA (TBE)
Special Diets Services, UK	High fat diet [21% (w/w) pork lard and 0.15% (w/w) cholesterol]
Starlabs, UK	96-well PCR plates for Roche® Lightcycler®; Polypropylene PCR sealing film strips; Reagent reservoirs
Stemcell Technologies, UK	Ammonium chloride solution; Lymphoprep™
Thermo Scientific, UK	Ambion™ nuclease-free water; Cryoprotected tissue freezing reagent (OCT); Cryomolds; Diethyl ether; Hank's Balanced Salt Solution (HBSS); Paraformaldehyde (PFA); Pierce™ Coomassie protein assay kit; Pierce™ LDH Cytotoxicity Assay Kit; RiboRuler high range RNA ladder; Ribozol; RNA loading dye (2X); Streptavidin; Trypsin-EDTA (0.05%); Vybrant® Phagocytosis Assay Kit; Xylene, Honeywell™
VWR Jencons, UK	Falcon® cell culture inserts (8 $\mu$ m pore size); Falcon® 12-well companion plates; Microscope slides

Abbreviations: DCFDA, 2'7'-dichlorofluorescein diacetate; ROS, reactive oxygen species; HDL, high density lipoprotein; LDL, low density lipoprotein; VLDL, very low density lipoprotein; APC, allophycocyanin; Cy7, cyanine7; FITC, fluorescein isothiocyanate; PE, phycoerythrin; LDLr, LDL receptor; IFN, interferon; IL, interleukin; MCP-1, monocyte chemotactic protein-1; M-CSF, macrophage colony-stimulating factor; PDGF, platelet-derived growth factor; TNF, tumour necrosis factor; MMLV, moloney murine leukaemia virus; LDH, lactate dehydrogenase.

## 2.2 Production of bacterial conditioned media

Lab4, Lab4b and CUL66 were provided by Cultech Limited as premixed, freeze dried stock and stored as aliquots at -80°C. Stock was removed as required and used in the production of probiotic conditioned media (CM).

### 2.2.1 Production

Probiotic stock was cultured in MRS broth (0.1 mg/mL) for 18 hours at 37°C under anaerobic and non-agitating conditions (80% N<sub>2</sub>, 10% CO<sub>2</sub>, 10% O<sub>2</sub>, v/v). Bacteria were then pelleted by centrifugation (10 minutes, 1,000 x g), washed in 1X PBS and resuspended in the same volume of cell culture media (RPMI-1640 or Dulbecco's Modified Eagle Media (DMEM)). Suspensions were incubated for a further 5 hours at 37°C under anaerobic and non-agitating conditions (80% N<sub>2</sub>, 10% CO<sub>2</sub>, 10% O<sub>2</sub>, v/v). The bacteria were pelleted by centrifugation (10 minutes, 1,000 x g) and the now conditioned cell culture media was transferred to new tubes for further processing.

### 2.2.2 Processing and storage

Probiotic CM was pH adjusted to 7.4 using 0.5 M sodium hydroxide (NaOH), then treated with Penicillin-Streptomycin (both 10,000 U/mL), and filter sterilised using 0.22 µm pore filters. Protein quantification was carried out on each batch of CM using the Pierce Coomassie Plus Assay Kit (Section 2.6.2) prior to the addition of either 10% (v/v) heat-activated (56°C for 30 minutes) foetal calf serum (HI-FCS), or 0.2% (w/v) bovine serum albumin (BSA) as required. CM was then aliquoted into 1.5 mL Eppendorf tubes and stored at -80°C until required. Once defrosted, CM was not subjected to any further freeze/thaw cycles. For quality control purposes, probiotic cultures were assessed for the presence of any microbial contamination. During CM production, 1 mL aliquots of bacterial suspension were transferred to Eppendorf tubes and stored in 20% (v/v) glycerol at -80°C until collected and cultured by Cultech Limited.

## 2.3 Cell culture techniques

### 2.3.1 Maintenance of cell lines and cultures

#### 2.3.1.1 THP-1

The THP-1 cell line is a non-adherent human monocytic leukemia cell line. Upon differentiation with phorbol 12-myristate 13-acetate (PMA), THP-1 cells become adherent and display many physiological and biochemical properties of human monocyte-derived macrophages (HMDMs). Furthermore, responses observed in THP-1 cells are conserved in primary cultures (McLaren *et al.*, 2010). It is therefore one of the most extensively utilised models for the *in vitro* investigation of monocytes and macrophages in the cardiovascular system and in atherogenesis (Chanput *et al.*, 2014; Qin, 2012).

Cells were cultured in RPMI-1640 medium with L-glutamine, supplemented with 10% (v/v) HI-FCS and Penicillin-Streptomycin (both 10,000 U/mL) and maintained in a humidified incubator at 37°C, 5% (v/v) CO<sub>2</sub>. Cell culture media was used supplemented unless otherwise stated. Cells were cultured in 75 cm<sup>3</sup> tissue culture flasks to a confluency of 60% before sub-culturing by pelleting cells (5 minutes, 250 x g), and resuspending in fresh culture media at a ratio of 1:3. Cells between passage 4 and 10 were used at a concentration of 1 x 10<sup>6</sup> cells per mL unless otherwise stated. THP-1 monocytes were differentiated into monocyte-derived macrophages by incubation with 0.16 µM PMA for 24 hours at 37°C, 5% (v/v) CO<sub>2</sub>. After 24 hours, the cells were observed under a microscope for typical changes in morphological features to ensure differentiation had occurred.

#### 2.3.1.2 Human aortic smooth muscle cells

Primary Human Aortic Smooth Muscle Cells (HASMCs) were utilised as a popular vascular SMC model commonly employed in the study of cardiovascular function and disease (Boehme *et al.*, 2018; Jiang *et al.*, 2009). Cells were cultured in Smooth Muscle Cell Growth Medium (Sigma-Aldrich). Sub-culturing was performed at 80% confluency.

To sub-culture, cells were washed with Hank's Balanced Salt Solution (HBSS), incubated briefly in 10 mL Trypsin-EDTA then resuspended by gently scraping. To inactivate the trypsin enzyme, 10 mL of fresh DMEM was added. The cells were then pelleted (5 minutes, 220 x g) and resuspended in fresh culture media at a ratio of 1:3. Cells between passage 4 and 10 were used at a concentration of  $1 \times 10^4$  cells per mL unless otherwise stated.

### 2.3.1.3 Human monocyte-derived macrophages

THP-1 monocyte-derived macrophages display properties of primary human macrophages, and experimental results are often conserved in primary human cells (McLaren *et al.*, 2010). However, to ensure that results were not due to the transformed nature of the cell line, key findings were confirmed in primary cultures of human monocyte-derived macrophages (HMDMs). HMDMs were isolated from human buffy coats provided by the National Blood Service Wales, using the protocol detailed below. Ethical approval was granted by the National Blood Service Wales for use in research.

The buffy coat was removed to 50 mL tubes and diluted 1:1 with Dulbecco's PBS at room temperature (RT). Buffy coat was then layered on top of Lymphoprep™ density gradient medium and centrifuged for 30 minutes at RT, 250 x g with no brake. The peripheral blood mononuclear cell (PBMC) layer was carefully collected and transferred to new tubes. To lyse red blood cell contamination, PBMCs were incubated for 3 minutes in 1 mL ammonium chloride and then pelleted by centrifugation for 7 minutes at 250 x g, 4°C. PBMCs were washed in cold PBS a further 6 – 8 times at 4°C to remove platelet contamination, and then plated at a concentration of  $2 \times 10^6$  cells per mL in supplemented RPMI-1640 media containing human macrophage colony stimulating factor (HM-CSF; 20 ng/mL). Plates were incubated in a humidified incubator at 37°C, 5% (v/v) CO<sub>2</sub> for 4 days to allow differentiation to occur. Once differentiated, HMDM cells were washed thoroughly in culture media and then utilised in experiments.



### 2.3.2 Establishment and storage of cell lines

Upon removal from storage, cells were defrosted and immediately added to 10 mL complete culture media. Cells were then pelleted (5 minutes, 250 x g), resuspended in 5 mL fresh complete culture media, transferred to a 25 cm<sup>3</sup> tissue culture flask and placed in a humidified incubator at 37°C, 5% (v/v) CO<sub>2</sub>. Culture media was changed regularly until the cell cultures were established, and then maintained and sub-cultured as described in Section 2.3.1.

For the generation of frozen stocks, cells of passage 3 or less were grown to 80% confluency, and then pelleted as described in Section 2.3.1 and resuspended in cell freezing medium-DMSO (ThermoFisher Scientific). Cells were then transferred to 1 mL cryotubes and stored in a Nalgene™ Cryo 1°C freezing container overnight at -80°C. Cell stocks were transferred to liquid nitrogen for long term storage.

### 2.3.3 Cell counting

To obtain the correct number of cells required for the experimental set up, the concentration of cells in suspension was calculated using a glass haemocytometer with a 5 x 5 grid (Helena Biosciences, UK). Cells were pelleted as described in Section 2.3.1 and resuspended in 5 mL fresh culture media. Then, 7.5 µL of cell suspension was placed on a haemocytometer and a cover slip applied. The average number of cells per square of the 5 x 5 grid was calculated and multiplied by 10<sup>4</sup> to obtain number of cells per mL.

## 2.4 Cell based assays

### 2.4.1 Cell viability

The Pierce LDH Cytotoxicity Assay Kit exploits LDH enzyme activity to create a simple colourimetric method of quantifying cytotoxicity in a 96-well format. LDH is an enzyme normally present in the cytosol, which upon damage to the plasma membrane is released into the cell culture media. LDH catalyses the conversion of lactate to pyruvate via the reduction of NAD<sup>+</sup> to NADH, which is subsequently used by an enzyme

diaphorase in the reduction of a tetrazolium salt 2-(4iodophenyl)-3-(4-nitrophenyl)-5-phenyl-2H-tetrazolium chloride (INT) to formazan; a red product that can be measured at 490 nm. The level of formazan produced by this coupled enzymatic reaction is directly proportional to the level of LDH released into the media, and hence a reliable measure of cytotoxic effect.

The effect of probiotic CM on cell viability was assessed for each cell system using the Pierce LDH Cytotoxicity Assay Kit according to manufacturer's guidelines. Cells were seeded in 96-well plates and treated with either vehicle control or probiotic CM for 24 hours at 37°C, 5% (v/v) CO<sub>2</sub>. A treatment time of 24 hours was chosen as the maximum length of time cells were treated during *in vitro* investigations. From this point the assay was carried out according to manufacturer's instructions. At 45 minutes prior to the assay start point, lysis buffer (provided in the kit) was added to the positive control wells (to lyse the cells) and the plate returned to the incubator until assay start. Then, 50 µL of supernatant from each well was transferred to a new 96-well plate and 50 µL of reaction mix (components provided in the kit) was added. The plate was returned to the incubator for a further 30 minutes before adding 50 µL of stop solution (provided in the kit) to each well. The absorbance was then read in a microplate reader at 490 nm.

## 2.4.2 Proliferation

The effect of probiotic CM on cell proliferation was assessed in THP-1 monocytes, THP-1 macrophages and HASMCs. Three different methods were used to assess proliferation including simple cell counting (THP-1 monocytes), crystal violet staining (THP-1 macrophages and HASMCs) and the 5-Bromo-2'-deoxy-uridine (BrdU) Labeling and Detection Kit III (THP-1 macrophages and HASMCs).

### 2.4.2.1 Cell counting

Cell counting is the most simple and reliable method for determining cell numbers over a period of time. To assess the effect of probiotic CM on proliferation of THP-1 monocytes, cells were seeded in 12-well plates at a concentration of 1 x 10<sup>6</sup> cells per mL

in either vehicle or CM. The plate was incubated for 7 days at 37°C, 5% (v/v) CO<sub>2</sub> and cells counted daily using a haemocytometer as described in section 2.3.3.

#### *2.4.2.2 Crystal violet staining*

Crystal violet is a potent DNA binding dye which freely enters cells, staining DNA purple. Upon cell lysis the stained DNA is released into solution, where the level of purple staining is proportional the amount of DNA and therefore cell number. Crystal violet staining is a reliable method for quantifying cell number which when measured over a period of time, also allows assessment of cell proliferation. THP-1 macrophages and HASMCs were treated with either vehicle or CM and total proliferation over a 7 day period determined by daily measurement of cell number using the crystal violet staining method. Cells were stained for 5 minutes with crystal violet (0.2% (w/v) crystal violet in 10% (v/v) ethanol), then washed thoroughly 3 times with 1X PBS. The cells were then lysed by rocking for 30 minutes in solubilisation buffer (0.1 M NaH<sub>2</sub>PO<sub>4</sub> in 50% (v/v) ethanol). The absorbance was then read in a microplate reader at 570 nm. Cell proliferation was assessed according to changes in cell number from day 0 to day 7. Cells were monitored for changes in viability using the LDH assay kit as described in Section 2.4.1.

#### *2.4.2.3 5-Bromo-2'-deoxyuridine labelling*

The rate of proliferation was assessed using the BrdU Labeling and Detection Kit III. 5-Bromo-2'-deoxyuridine is a synthetic nucleoside which is incorporated into cellular DNA during the DNA synthesis stage of replication, by substitution in place of a thymidine base. The greater the level of cell proliferation that occurs, the greater the incorporation of BrdU into cellular DNA. The BrdU Labelling Detection Kit uses a standard enzyme-linked immunosorbent assay (ELISA) protocol to quantify the level of BrdU incorporated into DNA. BrdU is specifically targeted using monoclonal anti-BrdU labelled with peroxidase, which following addition of substrate, catalyses the formation of a coloured reaction product detectable at 405 nm.

THP-1 macrophages and HASMCs were incubated at 37°C, 5% (v/v) CO<sub>2</sub> with vehicle control or probiotic CM for 24 hours (THP-1), or for 7 days (HASMCs) with fresh culture media added on days 2, 5 and 7 to maintain culture conditions. The rate of proliferation following this incubation period was then assessed using the BrdU Labeling and Detection Kit according to manufacturer's guidelines (Sigma-Aldrich). Unless otherwise stated, all reagents were provided in the kit and reconstituted according to these instructions. Cells were incubated with 10 µM bromouridine labelling solution for 3 hours at 37°C, 5% (v/v) CO<sub>2</sub> for incorporation to occur. Cells were then washed with culture media and fixed for 30 minutes at -20°C in ice cold fixative (0.5 M HCl in 70% (v/v) ethanol). Once fixed, the cells were washed a further 3 times with culture media and then incubated with nuclease solution for 30 minutes at 37°C in a non-CO<sub>2</sub> incubator. Cells were again washed in culture media and incubated with anti-BrdU Fab fragments solution for 30 minutes at 37°C, 5% (v/v) CO<sub>2</sub>. Finally, cells were washed with wash buffer and peroxidase substrate solution added for 30 minutes at RT in the dark. Colour product was then measured in a microplate reader at 405 nm with a reference wave-length at 490 nm.

### 2.4.3 Measurement of reactive oxygen species

The effect of probiotic CM on tert-butyl hydroperoxide (TBHP)-induced ROS production was assessed using the DCFDA Cellular ROS Detection Assay Kit according to manufacturer's guidelines (Abcam). The kit utilises a fluorogenic dye, 2',7'-dichlorofluorescein diacetate (DCFDA), which following diffusion into the cell is deacetylated by cellular esterases into a non-fluorescent compound. This compound is then oxidised by cellular ROS to form the highly fluorescent 2',7'-dichlorofluorescein (DCF), detectable by fluorescence spectroscopy at a level proportional to ROS generation in the cell. The ROS inducer TBHP (provided in the kit) was used to stimulate ROS production in the cells in order to assess the ability of probiotic CM to lower its production. THP-1 monocytes or THP-1 macrophages were stained with 20 µM DCFDA for 45 minutes at 37°C, 5% (v/v) CO<sub>2</sub>. Cells were then washed with 1X buffer and resuspended in either vehicle alone (negative control), vehicle with 55 µM TBHP (vehicle control) or probiotic CM with 55 µM TBHP. Cells were then seeded in 96-well plates and

incubated for 3 hours at 37°C, 5% (v/v) CO<sub>2</sub>. Fluorescence was measured in a microplate reader at excitation/emission (Ex/Em) 490/535 nm.

#### 2.4.4 Monocyte migration

The effect of probiotic CM on monocyte migration was investigated using a modified Boyden chamber method as previously used in the laboratory (Gallagher, 2016; Moss *et al.*, 2016), in which monocytes are allowed to migrate across a membrane mimicking the arterial endothelium as illustrated in Figure 2.1. For this, 8 µM pore Falcon® cell culture inserts were housed in Falcon® 12-well companion plates, where an 8 µM pore membrane represents the arterial endothelium. THP-1 monocytes were added to the inserts in either vehicle control (Negative and Vehicle controls) or probiotic CM. Then, 1 mL of culture media was added to the bottom well either alone (Negative control) or with the chemoattractant MCP-1 (20 ng/mL; Vehicle control and probiotic CM wells). Plates were then incubated for 3 hours at 37°C, 5% (v/v) CO<sub>2</sub> to allow the cells to migrate. Cells in the bottom layer were then counted using a haemocytometer as described in Section 2.3.3, and migration calculated as a percentage of cells added to the cell culture insert.

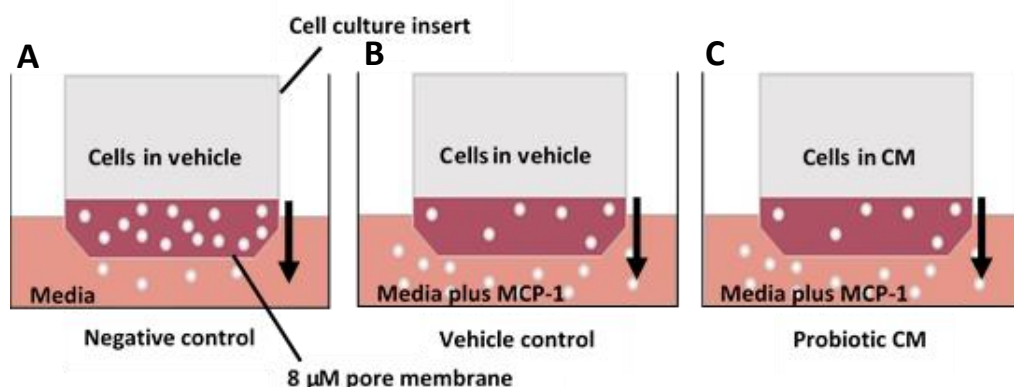


**Figure 2.1 – Illustration of the modified Boyden chamber experimental set up used in the investigation of monocyte migration.** THP-1 monocytes were suspended in either vehicle control or probiotic CM and added to the cell culture inserts (upper chamber). Cells are allowed to migrate through the 8 µM pore membrane to the bottom layer (lower chamber) in the presence of MCP-1. Migrated cells in the lower chamber were counted and percentage migration calculated. (A) Negative control representing physiological migration in the absence of chemoattractant stimulus, with cells plus vehicle in the upper chamber and media only in the lower chamber. (B) Vehicle control, with cells plus vehicle in the upper chamber and media plus MCP-1 in the lower chamber. (C) Treatment wells, with cells plus probiotic CM in the upper chamber and media plus MCP-1 in the lower chamber.

### 2.4.5 Vascular smooth muscle cell invasion

The effect of probiotic CM on the invasion of SMCs was investigated using HASMCs in a modified Boyden chamber set up similar to that used for monocyte migration in Section 2.4.4. The experimental set up is illustrated in Figure 2.2. In place of MCP-1 chemoattractant, HASMC invasion was stimulated using human platelet-derived growth factor-BB (PDGF-BB), a potent mitogen for SMCs in atherosclerotic conditions. To mimic invasion through the basement membrane, cell culture inserts were coated with Matrigel (Sigma-Aldrich) extracellular matrix (ECM) gel, forming an ECM layer on top of the insert membrane. Coating of the inserts was carried out at 4°C to prevent setting of the gel, then the plate was incubated at 37°C, 5% (v/v) CO<sub>2</sub> for 30 minutes to allow the gel to set. Once set, HASMCs were added to the insert at a concentration of  $1 \times 10^4$  cells per mL in 500 µL culture media and returned to the incubator for 24 hours to allow the cells to adhere. The culture media was then replaced with serum-free DMEM, and the plate returned to the incubator for a further 48 hours to allow the cells to become quiescent. After 48 hours, the serum-free DMEM was replaced with either vehicle control (Negative and Vehicle controls) or probiotic CM, and 1 mL culture media was added to the bottom wells either alone (Negative control) or with PDGF (20 ng/mL; Vehicle control and probiotic CM wells). The plate was incubated for a further 4 hours to allow invasion to occur. Supernatant was then removed from the inserts and loose cells removed from the topside with a cotton swab. Membranes were carefully removed and mounted on slides with Fluoroshield™ mountant containing DAPI. Cells were counted and an average taken over 5 high power fields (HPF) using an Olympus BX61 microscope with DAPI filter.

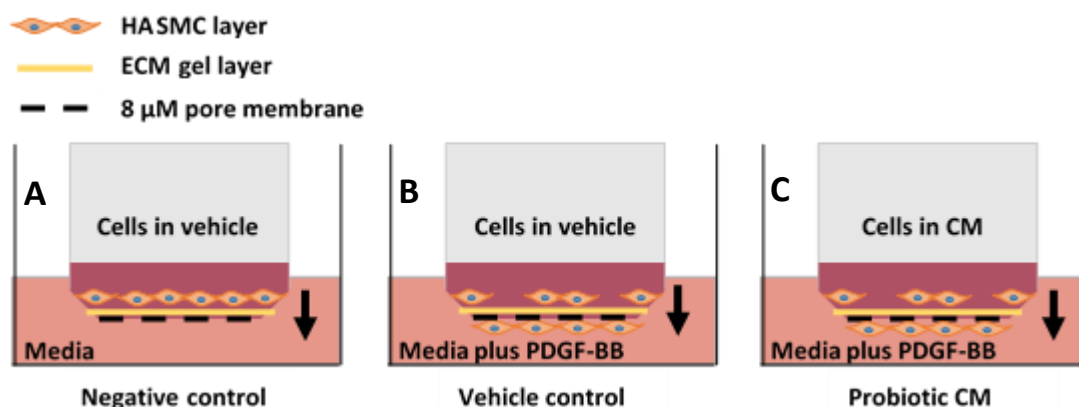


**Figure 2.2 - Illustration of the modified Boyden chamber experimental set up used for the investigation of SMC invasion.** HASMCs suspended in either vehicle or CM in cell culture inserts (upper chamber) invade through the ECM gel layer to the underside of the 8  $\mu$ M pore membrane (lower chamber), either in the absence of (Negative control) or the presence of PDGF-BB (Vehicle control and probiotic CM wells). Membranes were then removed and mounted on slides with Fluoroshield™ mountant containing DAPI. Cells were counted and an average taken over 5 high power fields (HPF) using an Olympus BX61 microscope with DAPI filter. (A) Negative control representing unstimulated invasion to the underside of the membrane, with cells plus vehicle in the upper chamber and media alone in the lower chamber. (B) Vehicle control, with cells plus vehicle in the upper chamber and media plus PDGF-BB in the lower chamber. (C) Treatment wells, with cells plus probiotic CM in the upper chamber, and media plus PDGF-BB in the lower chamber.

#### 2.4.6 Mitochondrial bioenergetic profile

To investigate the effect of probiotic CM on mitochondrial bioenergetic profile, the Agilent Seahorse XFp Cell Mito Stress Test was used. The Mito Stress Test directly measures oxygen consumption rate (OCR) in response to the serial injection of compounds involved in the modulation of components of the electron transport chain (ETC), revealing information on key parameters of mitochondrial function.

THP-1 monocytes were plated in Seahorse 96-well plates at a concentration of 250,000 cells/mL (cell number as previously optimised in the laboratory) and differentiated to macrophages using PMA as described previously (Section 2.3.1.1). Cells were then incubated with either vehicle or probiotic CM for a further 24 hours at 37°C, 5% (v/v) CO<sub>2</sub>. A Seahorse utility plate was hydrated with Seahorse calibrant (200  $\mu$ L per well) and incubated overnight at 37°C in a non-CO<sub>2</sub> incubator. The cells were then washed twice with pre-warmed Seahorse assay medium (serum-free RPMI-1640 supplemented with L-Glutamine (2 mM), sodium pyruvate (1 mM) and glucose (10 mM); pH 7.4 at 37°C), and then incubated in assay medium (175  $\mu$ L per well) for 1 hour at 37°C, in a non-CO<sub>2</sub> incubator. During this time, Stress Test compounds oligomycin, carbonyl cyanide-4 (trifluoromethoxy) phenylhydrazone (FCCP) and a mix of rotenone and antimycin A were

prepared in assay medium according to manufacturer's instructions (Agilent). The working concentration of each compound was previously optimised in the laboratory according to manufacturer's guidelines (Agilent). Stock and final working concentrations used for each compound are shown in Table 2.2. The compounds were then loaded into corresponding ports of the hydrated sensor cartridge (20  $\mu$ L per well).

**Table 2.2 – Concentrations of compounds used in the Seahorse Cell Mito Stress Test**

Compound	Stock ( $\mu$ M)	Working ( $\mu$ M)
Oligomycin	100	1
FCCP	100	4
Rotenone + Antimycin A	50	0.5

The Mito Stress Test was carried out on an Agilent Seahorse FX96 analyser according to the manufacturer's pre-loaded program. The prepared utility plate with sensor cartridge was loaded into the analyser to allow calibration of the instrument, after which the utility plate was removed and the Seahorse cell culture plate inserted. Assay data was exported to Microsoft Excel for analysis. Upon removal from the Seahorse FX96 analyser, total protein concentration of cells in each well was determined as outlined in Section 2.6.2 and used in the normalisation of OCR values.

### 2.4.7 Phagocytosis

The effect of probiotic CM on phagocytic capability of macrophages was assessed in THP-1 macrophages using the Vybrant® Phagocytosis Assay Kit according to manufacturer's instructions (Thermo Scientific). The assay utilises fluorescein-labelled inactivated *E-coli* (K-12 strain) which when internalised by cells can be detected in a microplate reader at Ex/Em 480/520 nm. THP-1 macrophages were incubated with either vehicle or probiotic CM for 3 hours at 37°C, 5% (v/v) CO<sub>2</sub>. Supernatant was then replaced with *E. coli* BioParticles® and the plate returned to the incubator for a further 2 hours. BioParticles were then removed and the cells stained for 1 minute with trypan blue to limit fluorescence from non-internalised BioParticles. Trypan blue was then removed, and the fluorescence read on a microplate reader at Ex/Em 480/520 nm. Phagocytosis was calculated as a percentage of the vehicle control after subtraction of background signal.



## 2.5 Molecular techniques

### 2.5.1 RNA extraction

RNA was extracted from both cells (THP-1 macrophages, HMDMs) and tissue (mouse liver) for the purpose of gene expression analysis, using methods adapted from those previously used in the laboratory (Moss, 2018). To minimise RNase activity, all steps were carried out on ice unless otherwise stated. Cells were washed with 1X PBS and then suspended in 1 mL RiboZol™ for 10 minutes for cell lysis to occur. Tissues were directly homogenised in RiboZol™ to minimise RNase activity. Following cell lysis/tissue homogenisation, suspensions were transferred to Eppendorf tubes and 200 µL chloroform added. Tubes were shaken vigorously for 15 seconds and then incubated at room temperature for 3 minutes. For phase separation, tubes were centrifuged for 15 minutes (12,000 x g at 4°C), creating a lower phenol-chloroform phase, a white interphase, and an upper aqueous phase containing the RNA. To minimise contamination approximately 80% of the aqueous phase was transferred to new RNase-free Eppendorf tubes ensuring that the interphase was not disturbed. The RNA was then precipitated by adding an equal volume of isopropanol and freezing for at least 1 hour (up to a maximum of 48 hours for low RNA yields) at -80°C. RNA was then pelleted (10 minutes, 12,000 x g, 4°C), washed in 75% (v/v) ethanol and pelleted again (5 minutes, 7,500 x g, 4°C). The pellet was washed a minimum of 3 times and then left to air dry before resuspending in nuclease-free water, and heating for 10 minutes at 60°C to re-dissolve the RNA.

#### 2.5.1.1 RNA quality assessment

The quality and concentration of extracted RNA was determined using a NanoDrop™ ND2000 spectrophotometer. The absorbance ratios  $A_{260}/A_{280}$  and  $A_{230}/A_{260}$  were used to assess RNA purity where values of 1.8 – 2.0 were considered acceptable. To assess RNA integrity, an aliquot was size-fractionated by agarose gel electrophoresis as detailed below (Section 2.5.2). RNA of acceptable integrity was judged when distinct bands representing the 28S and 18S ribosomal subunits were visible. Additionally the 28S band was twice the intensity of the 18S, together with an absence of a high molecular weight

band indicative of genomic DNA contamination, or smearing indicative of RNA degradation. An example of quality RNA as determined by size-fractionation is shown in Figure 2.3.

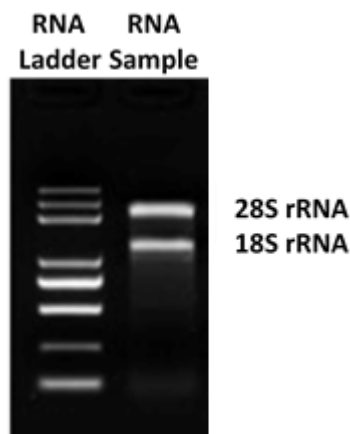


**Figure 2.3 - Example of quality of RNA by size-fractionation** showing the relative positions of 28S and 18S ribosomal subunits. The 28S band is twice the intensity of the 18S band and evidence of RNA degradation or genomic DNA contamination is absent.

## 2.5.2 Agarose gel electrophoresis

Agarose (final concentration of 1.5%, w/v) was dissolved in 1X Tris-borate-EDTA (TBE; 89 mM Tris-borate, 89 mM boric acid, 2 mM EDTA, pH 8.3) buffer by heating in a microwave until fully dissolved. For visualisation, the nucleic acid stain ethidium bromide (20  $\mu\text{M}/\text{mL}$ ) was added to the gel prior to setting. To prepare samples, 2X RNA loading dye (ThermoFisher Scientific) was added to RNA extracts in equal volumes and the samples denatured by heating for 10 minutes at 70°C and then placed on ice. Electrophoresis was carried out in a horizontal gel tank at 70 V for 60 minutes in 1X TBE. RiboRuler High Range RNA ladder was included to indicate the size of RNA products. The gel was then visualised under UV light using a Sygene Gel Documentation system.

## 2.5.3 Reverse transcriptase polymerase chain reaction (RT-PCR)

RNA was reverse transcribed into complementary DNA (cDNA) by the process of RT-PCR. Thus, 200 pmol of random primers were added to 1  $\mu\text{g}$  RNA and made up to a total volume of 14  $\mu\text{L}$  with nuclease-free water. The samples were incubated for 5 minutes at 70°C and placed on ice. cDNA master mix (Table 2.3) was then added to a final volume

of 20  $\mu\text{L}$  and the samples incubated for 60 minutes at 37°C. This was followed by a final incubation for 5 minutes at 90°C and then cooling to 4°C. To monitor for the presence of DNA contamination, a negative RT control was also included in the reaction.

**Table 2.3 - Composition of cDNA master mix used in the reverse transcription process**

Reagent	Master mix (X1) ( $\mu\text{L}$ )
100 mM dNTP mix (dATP, dGTP, dCTP, dTTP)	1.0
M-MLV buffer (5X)	4.0
RNase inhibitor (40 U/ $\mu\text{L}$ )	0.5
M-MLV reverse transcriptase (200 U/ $\mu\text{L}$ )	0.5

cDNA samples were made up to a concentration of 10 ng/ $\mu\text{L}$  with nuclease-free water and stored at -20°C for use in subsequent gene expression analysis.

#### 2.5.4 Real time quantitative PCR (qPCR)

Gene expression was quantified using real time quantitative PCR (qPCR) on a Roche light cycler, using the popular fluorescent DNA binding dye SYBR Green to quantify DNA product in real time. SYBR Green intercalates into double-stranded DNA and fluorescence is measured and recorded at the end of each cycle. Since the dye only fluoresces when bound to DNA, the strength of emission is proportional to the amount of cDNA template. Threshold ( $C_T$ ) values for the gene of interest are then compared to reference values using housekeeping genes of stable expression, and the relative gene expression calculated.

In this study qPCR was performed using gene-specific, intron-spanning primers (primer sequences shown in Table 2.4) or PCR microarray plates (Atherosclerosis RT<sup>2</sup> Profiler PCR Arrays from Qiagen). All primer sequences were designed by members of the laboratory to be intron spanning for the purpose of detecting any genomic DNA contamination if present, where the amplified genomic DNA products are larger due to the presence of the intron. Microarray plates contained a panel of 84 atherosclerosis-related genes, five different housekeeping genes plus positive, negative and genomic DNA controls. Due to the high expense of microarray plates, cDNA used in the microarray format was subjected to an additional pre-check using the housekeeping

gene  $\beta$ -actin to assess the efficacy of the reaction prior to running microarray plates. qPCR reaction mix and amplification conditions are shown in Tables 2.5 and 2.6 respectively. Standard qPCR involved a 3-step amplification process to include melting, annealing and extension over 40 cycles. However, for qPCR microarrays, the amplification process involved only 2 steps, melting and annealing, over 45 cycles.

Based on previous optimisation studies in the laboratory the housekeeping gene GAPDH was used as a reference gene for standard qPCR (Gallagher, 2016). For qPCR microarrays, an average of five stable housekeeping genes was used (*Actb* (actin, beta), *B2m* (beta-2 microglobulin), *Gapdh*, *Gusb* (glucuronidase, beta), and *Hsp90ab1* (heat shock protein 90 alpha, class B member 1)). Following amplification, melting curve analysis was carried out on individual samples where a single peak representing amplification of a single product was acceptable. Relative gene expression was then calculated using the  $\Delta\Delta C_T$  method (Rao *et al.*, 2013).

**Table 2.4 - Intron-spanning primer sequences used in qPCR**

Target gene	Forward Sequence (5'-3')	Reverse Sequence (5'-3')
<b>GAPDH</b>	CTTTTGCCTCGCCAGCCGAG	GCCCAATACGACCAAATCCGTTGACT
<b>MCP-1</b>	CGCTCAGCCAGATGCAATCAATG	TGGTCTTGAAGATCACAGCTTCTTTGG
<b>ICAM-1</b>	GACCAGAGGTTGAACCCAC	GCGCCGGAAAGCTGTAGAT
<b>SR-A</b>	GTCCAATAGGTCCTCCGGGT	CCCACCGACCAGTCGAAC
<b>CD36</b>	AGCCATTTTAAAGATAGCTTTCC	AAGCTCTGGTCTTATTACACA
<b>LPL</b>	GAGATTTCTCTGTATGGCACC	CTGCAAATGAGACACTTTCTC
<b>ACAT1</b>	ATACTCAGCCCTCTGCGACC	TCTTATTTCTGCACCAGCCT
<b>NCEH1</b>	CTGGTCACCTTCAGATGAAAT	TTGTGGCCCGTACAACATCA
<b>LXR-<math>\alpha</math></b>	CCTTCAGAACCCACAGAGATCC	ACGCTGCATAGCTCGTTCC
<b>LXR-<math>\beta</math></b>	GCTAACAGCGGCTCAAGAACT	GGAGCGTTTGTGCACTGC
<b>ABCA1</b>	AGTGGAAACAGTTAATGACCAG	GCAGCTGACATGTTTGTCTTC
<b>ABCG1</b>	GGTGGACGAAGAAAGGATACAAGACC	ATGCCCGTCTCCCTGTATCCA
<b>APOE</b>	CAGGAGCCGACTGGCCAATC	ACCTTGGCCTGGCATCCTG

Abbreviations: GAPDH, glyceraldehyde 3-phosphate dehydrogenase; MCP-1, monocyte chemotactic protein-1; ICAM-1, intercellular adhesion molecule-1; SR-A, scavenger receptor-A; LPL, lipoprotein lipase; ACAT1, acetyl-CoA acetyltransferase 1; NCEH1, neutral cholesterol ester hydrolase 1; LXR, liver X receptor; ABCA1, ATP-binding cassette transporter A1; ABCG1, ATP-binding cassette transporter G1; APOE, apolipoprotein E.

**Table 2.5 - Composition of 1X master mix used in qPCR and microarray reactions**

Reagent	qPCR volume ( $\mu$ L)	Microarray volume ( $\mu$ L)
SYBR Green Jumpstart™ Taq Readymix™	12.5	12.5
Forward primer (2.5 $\mu$ M)	0.5	-
Reverse primer (2.5 $\mu$ M)	0.5	-
cDNA (10 ng/ $\mu$ L)	1	1
Nuclease-free H <sub>2</sub> O	10.5	11.5
TOTAL	25	25

**Table 2.6 - Amplification steps for qPCR and microarray reactions**

PCR step	qPCR		qPCR microarray		
	Temp (°C)	Time (s)	Temp (°C)	Time (s)	
Preincubation	94	120	95	600	
Melting	95	30	95	15	] X45
Annealing	60	60	60	60	
Extension	72	60			

## 2.6 Protein methods

### 2.6.1 Protein extraction

To extract proteins, the cells were washed with 1X PBS and then lysed by incubating for 3 minutes with RIPA lysis buffer (Sigma-Aldrich) supplemented with protease inhibitor cocktail (X1; Sigma-Aldrich). The suspension was transferred to Eppendorf tubes and pelleted for 3 minutes (10,000 x g, 4°C). The supernatant was then transferred to clean tubes and stored at -20°C.

### 2.6.2 Protein quantification

Total protein was quantified using the Pierce™ Coomassie Protein Assay Kit according to manufacturer's instructions. Coomassie is a brown dye which binds to proteins causing an immediate shift from brown to a blue colour with absorbance at 595nm. Protein concentration was determined by reference to a range of BSA protein standards (1 – 50 µg/mL). In this study, protein quantification of either cell extracts or aliquots of probiotic CM was carried out in a 96-well plate, where 150 µL of Coomassie dye was added to 100 µL of sample or BSA protein standards. The plate was then incubated for 10 minutes at RT and the absorbance read at 595nm in a microplate reader. Absorbance values for the BSA protein standards were used to construct a standard curve from which the concentration of the samples was determined.

### 2.6.3 Enzyme linked immunosorbent assay (ELISA)

Activation of the NLRP3 inflammasome in response to a pro-inflammatory stimulus may be assessed according to the level of IL-1 $\beta$  production, measurable by standard ELISA methods (Moss, 2018). Activation of the inflammasome *in vitro* requires priming followed by a second stimulus using lipopolysaccharide (LPS), followed by cholesterol crystals. However, in the current study the use of PMA to differentiate THP-1 monocytes to macrophages acts as the first stimulus, and therefore LPS was not required. To determine the effect of probiotic CM on inflammasome activation, THP-1 macrophages treated with either vehicle or probiotic CM were stimulated with cholesterol crystals (1 mg/mL) for 24 hours at 37°C, 5% (v/v) CO<sub>2</sub>. Supernatant was then transferred to Eppendorf tubes and the cholesterol crystals removed by centrifugation at 9,000 x g for 5 minutes. The concentration of IL-1 $\beta$  was then determined using a standard ELISA protocol according to manufacturer's instructions (R&D Systems).

All materials and reagents were provided in the kit unless otherwise stated. ELISA plates were coated with human IL-1 $\beta$  capture antibody (4  $\mu$ g/mL) and incubated overnight at RT. The next day, the plates were washed 3 times in wash buffer and incubated for 2 hours with reagent diluent. Plates were washed a further 3 times. Samples and a series of IL-1 $\beta$  standards (1 – 250 pg/mL) were prepared using reagent diluent and added to the plate. The plate was incubated for 2 hours, wash steps repeated and then incubated for a further 2 hours with biotinylated IL-1 $\beta$  antibody (200 ng/mL). Wash steps were repeated, Streptavidin-HRP added for 20 minutes and then the plate washed again. The substrate solution was then added and the incubation continued for an additional 20 minutes. Finally, stop solution was added and the absorbance read on a microplate reader at 450 nm with reference values at 540 nm. Absorbance values of the IL-1 $\beta$  standards were used to prepare a standard curve from which the IL-1 $\beta$  concentration of the samples was determined.

## 2.7 Lipid methods

### 2.7.1 Oxidised LDL uptake

Dil-conjugated oxidised low density lipoprotein (Dil-oxLDL) is a fluorescently labelled human oxLDL that can be taken up by macrophages in an unregulated manner via cell surface receptors (scavenger receptor-mediated uptake). The level of oxLDL uptake can then be determined by flow cytometry following a similar method to that described by Moss, 2018. The effect of probiotic CM on the uptake of Dil-oxLDL was assessed in THP-1 macrophages. In this and subsequent studies involving analysis of lipid homeostasis, the culture media was supplemented with 0.2% (w/v) fatty acid free BSA in place of HI-FCS due to the ability of serum to enhance efflux of cholesterol (Gallagher, 2016). The cells were treated with either vehicle or probiotic CM plus Dil-oxLDL (10 µg/mL) and incubated for 24 hours at 37°C, 5% (v/v) CO<sub>2</sub>. After 24 hours, the supernatant was discarded and the cells detached following 30 minutes incubation with Trypsin-EDTA (0.05%; Sigma-Aldrich). The cell suspension was transferred to Eppendorf tubes and pelleted at 9,000 x g for 5 minutes. The supernatant was discarded and the cells resuspended in 2% (w/v) paraformaldehyde (PFA). Dil-oxLDL uptake was then measured by flow cytometry using a BD FACS Canto Flow Cytometer where 10,000 events were recorded for each sample.

### 2.7.2 Macropinocytosis

Lucifer yellow CH dilithium salt (LY) is a highly fluorescent dye taken up by macrophages via macropinocytosis, a form of fluid-phase endocytosis (McLaren *et al.*, 2010). The effect of probiotic CM on macropinocytosis was assessed in THP-1 macrophages. THP-1 macrophages were treated with either vehicle or probiotic CM plus LY (100 µg/mL) and incubated for 24 hours at 37°C, 5% (v/v) CO<sub>2</sub>. The supernatant was then discarded and the cells detached following 30 minutes incubation with Trypsin-EDTA (0.05%; Sigma-Aldrich). The cell suspension was then transferred to Eppendorf tubes and pelleted at 9,000 x g for 5 minutes. The supernatant was discarded and the cells resuspended in 2% (w/v) PFA. LY incorporation was then measured by flow cytometry using a BD FACS Canto Flow Cytometer where 10,000 events were recorded for each sample.



### 2.7.3 Cholesterol efflux

Cholesterol efflux from THP-1 macrophages or HMDMs was assessed using a traditional method previously utilised within the laboratory (Gallagher, 2016; McLaren *et al.*, 2010; Moss, 2018). Cholesterol efflux from macrophages can be measured following transformation into foam cells using acLDL, in the presence of radioactively labelled [4-<sup>14</sup>C] cholesterol, which is incorporated into the cells. Efflux of cholesterol is then stimulated by apolipoprotein A1 (apoA1), a component of HDL particles, and the radioactivity measured in both cells and supernatant by scintillation counting. Cells were cultured in 12-well plates for 24 hours with cell culture media (BSA) containing acLDL (25 µg/mL) and 0.5 µCi/mL [4-<sup>14</sup>C] cholesterol at 37°C, 5% (v/v) CO<sub>2</sub>. The cells were then washed and incubated for a further 24 hours in vehicle alone (negative control), with vehicle plus apoA1 (10 µg/mL; vehicle control), or probiotic CM plus apoA1 (10 µg/mL). After 24 hours, 500 µL of supernatant was transferred to polyethylene scintillation vials with 10 mL OptiFluor® scintillation fluid. The cells were then washed and solubilised by shaking in 0.2% (w/v) NaOH for 30 minutes, and 500 µL cell suspension transferred to scintillation vials with 10 mL OptiFluor®. Both supernatant and cellular fractions were then analysed on a liquid scintillation counter (TriCarb 2800TR, Perkin Elmer), and radioactivity recorded as the number of disintegrations per minute (dpm). Cholesterol efflux was calculated as the percentage of radioactivity present in the supernatant versus total radioactivity (supernatant plus cellular fractions).

### 2.7.4 Cholesterol metabolism

The effect of probiotic CM on intracellular metabolism of cholesterol was assessed in THP-1 macrophage foam cells by measuring the incorporation of [<sup>14</sup>C] acetate (1 µCi/mL) into major lipid classes, using a method adapted from Gallagher, 2016. Cells were seeded in 6-well plates at a concentration of 2 x 10<sup>6</sup> cells per mL, and incubated for 24 hours at 37°C, 5% (v/v) CO<sub>2</sub> to allow cells to adhere. The cells were then incubated for a further 24 hours with either vehicle plus [<sup>14</sup>C] acetate (1 µCi/mL; negative control), vehicle plus [<sup>14</sup>C] acetate (1 µCi/mL) and 25 µg/mL acLDL (vehicle control) or probiotic CM plus [<sup>14</sup>C] acetate (1 µCi/mL) and 25 µg/mL acLDL. Lipids were then extracted (Section 2.7.4.1) and separated into major lipid classes by TLC (Section 2.7.4.2). The

incorporation of [ $^{14}\text{C}$ ] acetate into individual fractions was measured by liquid scintillation counting as described in Section 2.7.3.

#### 2.7.4.1 Lipid extraction

Lipids were extracted following a procedure similar to Folch's method (Folch *et al.*, 1957). Cells were washed with 1X PBS, scraped and transferred to Eppendorf tubes. The cells were then pelleted (5 minutes, 9,000 x g) and the supernatant discarded. Cells were transferred to glass tubes with 2 mL of chloroform: methanol (2: 1) solution and incubated for 15 minutes at RT. Then, 1 mL chloroform and 2 mL Garbus solution (2 M potassium chloride (KCl) in 0.5 M potassium phosphate buffer, pH 7.6) (Garbus *et al.*, 1963) was added, vortexed and separation of layers achieved by centrifugation for 3 minutes at 220 x g. The chloroform layer containing the lipids was then transferred to clean glass tubes, evaporated under nitrogen gas and reconstituted in 50  $\mu\text{L}$  chloroform. Samples were used immediately for separation of lipids or stored at  $-20^{\circ}\text{C}$ .

#### 2.7.4.2 Thin layer chromatography (TLC)

Separation of lipid classes was achieved by one-dimensional TLC, where the following lipid classes were obtained: total polar lipids (TPL), triglycerides (TG), free fatty acids (FFA) and cholesterol esters (CE). Lipid extracts were applied to 10 x 10 cm silica gel plates (Merck) housed vertically in a glass tank containing hexane: diethyl ether: acetic acid (80:20:1, v/v/v). Chromatography was carried out until the solvent front reached approximately 1 mm from the top of the plates. The plates were then removed and allowed to air dry. The lipids were visualised under UV light by spraying plates with a 0.05% (v/v) solution of 8-anilino-4-naphthosulphonic acid (ANSA) in methanol. Separated lipid fractions were identified, marked on the plate, and then scraped into scintillation vials for quantification of radioactivity present in each separated lipid fraction using a liquid scintillation counter as described in Section 2.7.3.

## 2.8 *In vivo* methods

### 2.8.1 Animals and feeding

Investigation of the effect of probiotic supplementation *in vivo* was carried out using LDLr<sup>-/-</sup> mice homozygous for the LDLr<sup>tm1Her</sup> mutation and backcrossed to the C57BL/6J strain (Jackson Laboratory). All studies and protocols were approved by the Cardiff University Institutional Ethics Review Committee and the United Kingdom Home Office, and experiments were performed in accordance with the Guide for the Care and Use of Laboratory Animals (NIH Publication No. 85–23, revised 1996; Experimental licence 30/3365).

Male-8 week-old LDLr<sup>-/-</sup> mice were housed in a ventilated cabinet (Scantainer) in a light and temperature-controlled facility (12-hour light/dark cycle, 22°C) with free access to water and food. The mice (30) were randomly distributed between two groups (15 per group based on previous studies in the laboratory) and fed high fat diet (HFD) [21 % (w/w) pork lard and 0.15 % (w/w) cholesterol] or HFD supplemented with probiotic bacteria (1 x 10<sup>8</sup> CFU/g; 100 billion CFU/day equivalent human dose as decided by Cultech Ltd), for a period of 12 weeks. For both the control and probiotic groups, food was prepared in advance by Cultech Ltd and stored at 4°C until required for feeding. To maintain viability of the probiotic bacteria, mice were fed approximately every 2 days for the duration of the study. Mouse body weight was measured using an electronic scale and recorded at each feeding. The weight of food remaining together with food supplied was also recorded for the purpose of monitoring of approximate food consumed per mouse per day. At the end of the study, all mice were sacrificed by increasing the levels of CO<sub>2</sub> and death confirmed by an absence of a pulse.

### 2.8.2 Blood and tissue collection

Whole blood from cardiac puncture was collected into Eppendorf tubes containing heparin (5000 U/mL) to prevent clotting, and the heart flushed with PBS. Plasma was obtained by centrifugation for 5 minutes at 12,000 x g. Subcutaneous fat, gonadal fat, spleen, thymus and liver were dissected, weighed, snap frozen in dry ice and stored at -

80°C. The heart, brachiocephalic artery and a section of the liver were removed and stored in cryomolds with optimum cutting temperature formulation (OCT) at -80°C. The descending aorta was also isolated from the aortic arch to the subclavian arteries and stored in 1X PBS at 4°C. Rear legs were removed and stored in 1X PBS supplemented with 2% (v/v) HI-FCS for subsequent analysis of cell populations in the bone marrow.

### 2.8.3 Plasma lipid quantification

The effect of probiotic treatment on plasma lipids was assessed using cholesterol and triglyceride kits according to manufacturer's instructions (Abcam).

#### *2.8.3.1 Plasma cholesterol*

The concentration of cholesterol in mouse plasma samples was determined using the Abcam HDL and LDL/VLDL Cholesterol Assay Kit. Following the separation of lipoprotein fractions (HDL, LDL, VLDL), the enzyme cholesterol oxidase produces a product from free cholesterol which on addition of a probe, reacts to produce colour detectable at 570 nm. In addition, the kit uses cholesterol esterase to hydrolyse cholesterol esters into free cholesterol, allowing the differential detection of both free cholesterol and cholesterol esters. The concentration of different cholesterol fractions is then determined by reference to a range of cholesterol standards. Preparation of all fractions for cholesterol quantification is illustrated in Figure 2.4. All reagents were provided in the kit and prepared according to manufacturer's instructions unless otherwise stated. For total cholesterol and free cholesterol fractions no additional preparation of mouse plasma was required. To separate the HDL and LDL/VLDL fractions, the plasma was first mixed with precipitation buffer and incubated for 10 minutes at RT. Separation was achieved by centrifugation for 10 minutes at 2,000 x g. The upper supernatant containing the HDL fraction was transferred to clean tubes, and the lower fraction containing LDL/VLDL resuspended in 1X PBS. Total cholesterol (including cholesterol esterase) and free cholesterol (no cholesterol esterase) reaction mixes were prepared according to manufacturer's instructions. Total cholesterol reaction mix was added to all of the standards and HDL, LDL/VLDL, and total cholesterol fractions. Free cholesterol reaction mix was added to the free cholesterol fractions only. The plate was incubated

for 60 minutes at 37°C to allow colour to develop, and the absorbance read in a microplate reader at 570 nm. Absorbance values for the cholesterol standards were used to construct a standard curve from which the concentration of cholesterol in all the samples was determined.

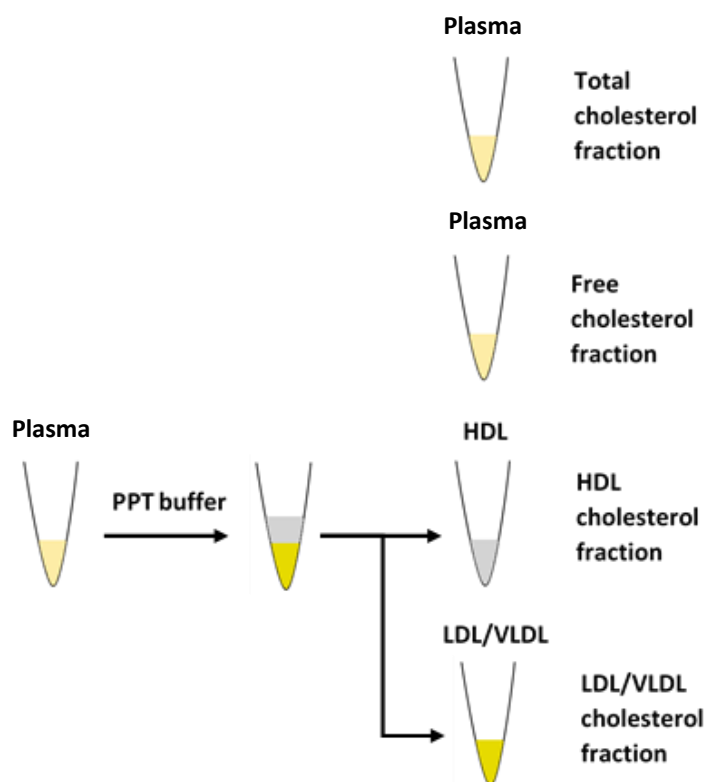


**Figure 2.4 - Illustration of fractions obtained for the quantification of total cholesterol, free cholesterol, HDL and LDL/VLDL using the Abcam HDL and LDL/VLDL Cholesterol Assay Kit.** Plasma was used directly for total and free cholesterol fractions. For HDL and LDL/VLDL fractions the plasma was mixed with the precipitation buffer (PPT buffer) and separated by centrifugation for 10 minutes at 2,000 x g. The HDL fraction was then transferred to a new tube and the remaining LDL/VLDL fraction resuspended in 1X PBS.

### 2.8.3.2 Plasma triglyceride levels

TG levels in mouse plasma were quantified using the Abcam Triglyceride Quantification Assay Kit according to manufacturer's instructions. During the assay, triglycerides are converted to free fatty acids and glycerol. The glycerol is then oxidised to a product, which on addition of a probe reacts to produce a colour detectable at 570 nm. TG concentration was then determined by reference to a range of standards. All reagents were provided in the kit and prepared according to manufacturer's instructions unless otherwise stated. TG standards were prepared (0 – 10 nmol) and the samples diluted within range of the standards as determined from initial pilot experiments. Each

standard and sample were then incubated with the lipase enzyme for 20 minutes at RT. A master mix of TG probe, enzyme and assay buffer was prepared according to manufacturer's instructions and added to all standards/samples for 1 hour at RT to allow the colour to develop. The absorbance was then read on a microplate reader at 570 nm. Absorbance values for the TG standards were used to construct a standard curve from which the concentration of the samples were determined.

#### 2.8.4 Immunophenotyping of bone marrow cell populations

Analysis of bone marrow cell populations was carried out using a method adapted from that previously used in the laboratory (Moss, 2018). As soon as possible following the collection of rear legs, the tibia and fibia were crushed in a pestle and mortar in 1X PBS supplemented with 2% HI-FCS (v/v), referred to as 2% PBS-FCS from here on. Homogenised marrow was then passed through a sterile 70  $\mu$ M filter into a Falcon tube and made up to a volume of 30 mL with 2% PBS-FCS. Then, 1 mL of cell suspension was transferred to a separate tube and pelleted for 5 minutes at 220 x g. Red blood cells were lysed by resuspending in 500  $\mu$ L ammonium chloride and incubating for 5 minutes before pelleting the cells again and resuspending in 1 mL 2% PBS-FCS for counting. Cell counting was carried out as described in Section 2.3.3.

To analyse the signalling lymphocytic activation molecule (SLAM) and progenitor cell populations, 10 or 8 million cells respectively were transferred from the cell suspension to new tubes, and the cells pelleted for 5 minutes at 5,000 x g, 4°C. All centrifugation steps were carried out on this setting unless otherwise stated. Cells were then resuspended in a mix of lineage marker fluorochrome-conjugated antibodies present within the SLAM and progenitor populations as detailed in Table 2.7, and incubated for 30 minutes at 4°C. Cells were then washed with 2% PBS-FCS, pelleted and resuspended in PerCP-Cy5.5 conjugated streptavidin (2%; v/v) for a further 15 minutes at 4°C. Cells were again washed in 2% PBS-FCS, pelleted and resuspended in fresh 2% PBS-FCS ready for FACS analysis.

For the preparation of lineage cell populations, 1 mL of cell suspension was transferred to a clean tube. Cells were pelleted and resuspended in lineage marker antibodies as

detailed in Table 2.7, then incubated for 20 minutes at 4°C. Cells were then washed in 2% PBS-FCS, pelleted, and resuspended in fresh 2% PBS-FCS for FACS analysis. Samples incubated with a single lineage marker antibody representing each fluorochrome (plus DAPI and unstained controls) were prepared simultaneously alongside lineage cell populations, to be used in the calibration of fluorochromes during FACS analysis.

Once all of SLAM, progenitor, lineage and single cell fluorochrome preparations were complete, samples were filtered into FACS tubes using sterile 40 µM pore filters and stored at 4°C. Samples were analysed on a BD FACS Tosseta flow cytometer. Immediately prior to analysis, 0.5 µg/mL DAPI nuclear stain was added to identify viable cells (SLAM, progenitor, lineage and DAPI control only), and the cells vortexed. For SLAM and progenitor populations, samples were analysed for 5 minutes or until no cells remained. Lineage samples were analysed for 1 minute, and single cell stains were analysed until 10,000 counts were reached. In order to avoid cross-over between fluorochromes, compensation was performed for each sample using single cell fluorochrome stains. Gating of cell populations was then carried out according to cell specific markers as detailed in Table 2.8. To ensure the accuracy of gating a backgating strategy was applied, in which final gated populations were overlay with preceding parent populations. Analysis of cell populations was carried out using FlowJo v.10 software. A schematic representation of the gating strategy employed is shown in Figure 6.3, and full details on population-specific gating is provided in Chapter 6.

**Table 2.7 - Composition of antibody cocktails used in the immunophenotyping of bone marrow cell populations**

Class	Antibody	Fluorochrome
SLAM	Ly-6A/E (Sca-1)	PE
	CD48	FITC
	CD150	PE/Cy7
	CD117 (c-Kit)	APC
	Lineage cocktail	
	2% PBS-FCS	
Progenitor	Ly-6A/E (Sca-1)	APC/Cy7
	CD127	PE
	CD117 (c-Kit)	APC
	Lineage cocktail	
	2% PBS-FCS	
Lineage	Ly-6G/Ly-6C (Gr-1)	PE/Cy7
	CD11b (Mac-1)	PE
	CD45R/B220	APC
	CD3	FITC
	TER-119	APC/Cy7
	2% PBS-FCS	
Lineage cocktail	Biotin CD3	
	Biotin CD4	
	Biotin CD8a	
	Biotin Ly-6G/Ly-6C (Gr-1)	
	Biotin CD11b	
	Biotin CD45R/B220	
	Biotin TER-119	

Abbreviations: PE, phycoerythrin; Cy7, cyanine7; APC, allophycocyanin; Sca-1, stem cell antigen-1; FITC, fluorescein isothiocyanate



**Table 2.8 - Markers used in the immunophenotyping of bone marrow cell populations**

Class	Cell type	Identifier
SLAM	Lineage -	
	LSK	Lin <sup>-</sup> Sca-1 <sup>+</sup> c-Kit <sup>+</sup>
	HSC	CD150 <sup>+</sup> CD48 <sup>-</sup>
	MPP	CD150 <sup>-</sup> CD48 <sup>-</sup>
	HPC I	CD150 <sup>-</sup> CD48 <sup>+</sup>
	HPC II	CD150 <sup>+</sup> CD48 <sup>+</sup>
Progenitor	Lineage -	
	CLP	CD127 <sup>+</sup>
Lineage	Lineage +	
	Granulocyte	GR1 <sup>+</sup> Mac1 <sup>-</sup>
	MDSC	GR1 <sup>+</sup> Mac1 <sup>+</sup>
	Macrophages	GR1 <sup>-</sup> Mac1 <sup>+</sup>
	B-Cell	B220 <sup>+</sup>
	T-Cell	CD3 <sup>+</sup>

Abbreviations: SLAM, signalling lymphocyte activation molecule; HSC, haematopoietic stem cell; MPP, multipotent progenitors; HPC, hematopoietic progenitor cell; CLP, common lymphoid progenitor; MDSC, myeloid-derived suppressor cells.

## 2.8.5 Plaque morphometric analysis

### 2.8.5.1 Sectioning

Cryosections of OCT-embedded aortic roots were obtained by microtome-cryostat sectioning at -20°C, where 10 µM sections were cut serially from the aortic root site such that all three leaflets of the aortic valves were visible. Sections were collected onto poly-L-lysine coated slides and air-dried for 1 hour before storage at -80°C.

### 2.8.5.2 Haematoxylin & Eosin

Haematoxylin and eosin (H&E) staining is a standard histological staining technique used to impart contrast to tissues for microscopy. Haematoxylin is a dark blue/purple stain, which due to its basic nature stains basophilic structures such as DNA in the nuclei, resulting in blue/purple stained nuclei. The red stain eosin, used as a counterstain, is acidic in nature resulting in the staining of positive structures such as cytoplasmic proteins in a contrasting red colour.

Thawed sections were rinsed in distilled water for 5 minutes and then stained in 5% (w/v) Gill's haematoxylin (0.1% (w/v) haematoxylin, 0.02% (v/v) sodium iodate and 2% (v/v) glacial acetic acid) for 5 minutes. Slides were then rinsed in running tap water until clear (approximately 10 minutes). Slides were counterstained in Eosin for 10 minutes, then dehydrated by passing through 80%, 95% and 100% ethanol for 5 minutes each. Finally, the slides were incubated in xylene for 5 minutes and then mounted using DPX mountant. Images were captured using a Leica DMRB brightfield microscope with ProgRes® CapturePro 2.8.8 software at X40 magnification (X4 objective).

### 2.8.5.3 Oil Red O

Oil Red O is a red lipid soluble dye used in the visualisation of lipids in tissue sections. In atherosclerosis, analysis of red pigment in stained sections allows quantification of plaque area and lipid content. Thawed sections were fixed in 4% (w/v) PFA for 15 minutes and then washed 3 times in distilled water and counterstained in Gill's

haematoxylin for 3 minutes. Slides were rinsed under running tap water. To dispel water, slides were placed in absolute propylene glycol before staining in Oil red O for 15 minutes at 60°C. Slides were then regressed in 85% propylene glycol for 5 minutes, washed three times in distilled water and mounted using DPX mountant. Images were captured using a Leica DMRB brightfield microscope with ProgRes® CapturePro 2.8.8 software at X40 magnification (X4 objective). Oil red O stained sections were analysed and plaque area and lipid content measured using ImageJ software.

#### *2.8.5.4 Immunohistochemistry*

Immunofluorescent (IF) staining of sections was carried out using cell surface marker antibodies to detect macrophages (anti-mouse MOMA-2), SMCs (anti-mouse  $\alpha$ SMA) and T cells (anti-mouse CD3), which were then photographed by fluorescent microscopy and analysed using ImageJ software. Details of antibodies used, stock concentrations and working dilutions are shown in Table 2.9. Antibodies were used in accordance with previous optimisation in the laboratory and diluted in 0.1% (w/v) BSA in PBS. Thawed sections were first fixed in acetone for 15 minutes and then washed twice in PBS. Sections were marked using a hydrophobic pen and then blocked for 30 minutes with 5% (v/v) serum in 5% (w/v) BSA/PBS. Blocking serum was chosen in accordance with the species of secondary antibody used in order to limit non-specific binding. Primary antibodies were then applied to sections and the slides incubated overnight at 4°C. The isotype controls (rabbit IgG or rat IgG) were included to monitor specificity and control for background staining. Following overnight incubation in primary antibody, the slides were washed twice in PBS and the corresponding secondary antibodies applied for 1 hour in the dark. Slides were then washed a further twice and counterstained for 20 minutes in 0.3% (w/v) Sudan Black in order to limit auto fluorescence of the sections. Slides were finally washed three times in PBS and mounted in Fluoroshield™ with DAPI nuclear stain.

**Table 2.9 - Antibodies used for immunofluorescent staining of sections**

Antibody	Species	Stock (mg/mL)	Working dilution
Anti- $\alpha$ SMA	Rabbit	0.2	1/100
Anti-CD3	Rabbit	0.2	1/100
Anti-MOMA-2	Rat	0.5	1/100
Rabbit IgG	Rabbit	0.5	1/100
Rat IgG	Rat	0.5	1/100
Chicken anti-rat IgG AF-594	Chicken	2	1/500
Donkey anti-rabbit IgG AF-488	Donkey	2	1/500

All antibodies were purchased from Abcam, UK. Abbreviations: MOMA-2, monocyte and macrophage antibody;  $\alpha$ SMA, alpha smooth muscle Actin; AF, Alexa Fluor®

Images were captured using an Olympus BX61 microscope with analySIS v3.2 software at X40 magnification (X4/0.13 objective). DAPI, FITC and AF-488 filters were applied for imaging of DAPI, AF-594 and AF-488 fluorophores respectively. All images were captured using consistent exposure, intensity and contrast settings for comparable downstream analyses. Regions of staining were quantified using ImageJ software.

### 2.8.6 Liver gene expression

Liver gene expression was analysed using the Qiagen Atherosclerosis RT<sup>2</sup> Profiler PCR Arrays. The PCR array plates contain a panel of 84 atherosclerosis-related genes which are listed in Appendix 1. Liver samples (50 mg) were homogenised directly in 1 mL RiboZol™ with a pestle and mortar. Homogenate was transferred to RNase-free Eppendorf tubes and RNA extraction continued as described in Section 2.5.1. RNA quality and integrity was examined (Section 2.5.1.1) and RNA reverse transcribed to cDNA (Section 2.5.3). As an additional check, qPCR was performed for each cDNA sample using the housekeeping gene *Gapdh*, and analysis of C<sub>T</sub> values and melting curves performed to ensure good amplification efficiency prior to the processing of Atherosclerosis RT<sup>2</sup> Profiler PCR Arrays as outlined in Section 2.5.4.

## 2.9 Statistical analysis

For all data sets, values outside of 2 standard deviations of the mean were removed as outliers prior to statistical analysis. Data sets were tested for normality using Q-Q plots in addition to Shapiro-Wilk test and histograms. To compare the means of two data sets, either a Student's t-test (where data displays normal distribution) or Mann Whitney U test (where normality could not be achieved) was performed. For the comparison of means between three or more data sets, a One-way analysis of variants (ANOVA) was performed. Homogeneity of variances was tested using Levene's statistic and post-hoc tests selected according to whether equal variances were observed. The Dunnett 2-sided post-hoc test was performed where equal variances were present, or Dunnett T3 in the case of unequal variances. All statistical analysis was performed using IBM SPSS Statistics 23 software unless otherwise stated. Significance was defined as  $p \leq 0.05$ .

## CHAPTER 3

*The effect of probiotics on  
key processes in  
atherosclerosis*

---

### 3.1 Introduction

Supplementation with a variety of probiotic strains has been shown to beneficially modify a number of atherosclerosis risk factors including hypercholesterolaemia (Bernini *et al.*, 2016), dyslipidaemia (Rerksuppaphol and Rerksuppaphol, 2015), hypertension (Bayat *et al.*, 2016) and chronic inflammation (Mizoguchi *et al.*, 2017). Indeed, select strains of probiotic bacteria have been shown to inhibit atherosclerotic plaque formation in ApoE<sup>-/-</sup> mice (Chan *et al.*, 2016b, 2016a). Clinical trials have reported beneficial effects of Lab4 and Lab4b supplementation in a number of conditions, including antibiotic-associated diarrhoea (Madden *et al.*, 2005), irritable bowel syndrome (IBS) (Williams *et al.*, 2009), atopic sensitisation in infants (Allen *et al.*, 2014), and the severity and incidence of coughs and colds in children (Garaiova *et al.*, 2015). Furthermore, CUL66 has been shown to exert cholesterol-lowering effects *in vitro* (Michael *et al.*, 2016), and *in vivo* in combination with the Lab4 consortium (Michael *et al.*, 2017). In addition to their cholesterol-lowering potential, Lab4 and Lab4b have also demonstrated immunomodulatory effects. The Adult Immune Study carried out by Cultech Ltd reported a significant reduction in the pro-inflammatory cytokines IL-6 and IL-1 $\beta$ , with a significant increase in production of the anti-inflammatory cytokines IL-10 and TGF- $\beta$  (Hepburn *et al.*, 2013). Together, results from previous studies have highlighted potential anti-atherogenic effects of Lab4, Lab4b and CUL66; however, the effects of these consortia have not previously been investigated in relation to atherosclerosis.

The overall aim of studies presented in this chapter was to investigate the effects of Lab4, Lab4b and CUL66 treatment across a range of key processes in atherosclerosis development, thereby providing an initial assessment of the potential anti-atherosclerotic effects of these probiotic consortia. Initial investigations were carried out *in vitro* using human monocytes, macrophages and SMCs treated with probiotic CM. Initially, probiotic CM was normalised to total protein concentration, then the concentration was optimised for use in further experiments. Investigations then continued to assess the effect of each probiotic CM on monocyte migration, ROS production, lipoprotein uptake via macropinocytosis, VSMC invasion, phagocytosis, proliferation of key cell types and inflammatory processes.

### 3.1.1 Normalisation of probiotic CM batches

Batch effects may be introduced by technical sources of variation during processing. While it's not possible to completely eliminate batch effects, the production of CM batches was optimised in order to minimise variation and to ensure a robust protocol and production of consistent, reproducible results. However, due to the use of live bacteria in this study, additional batch effects in the form of biological variation had to be considered. Biological variation was reduced by ensuring that the probiotic bacteria were thoroughly mixed (Lab4 or Lab4b) and accurately weighed before culturing. A simple measure of CFU is often used for normalisation. However, further variation created during bacterial culturing is unavoidable, particularly with regards to Lab4 and Lab4b where metabolic interaction between the different bacteria strains can occur (Kort *et al.*, 2015). Therefore, it was considered necessary for greater confidence of results, to control for batch effects by normalising probiotic CM treatment to a measurable parameter. Owing to ease of measurement, high reproducibility and low assay cost, total protein concentration was selected as the most suitable parameter for this purpose. For each probiotic CM, cell viability was assessed using a range of protein concentrations. The optimal concentration was then determined as the highest protein concentration at which cells maintain >85% viability.

### 3.1.2 Cell viability

Prior to the start of *in vitro* investigations, the effect of each CM on the viability of cells was assessed for each individual cell culture model system utilised in the study. This was carried out to ensure that results were not influenced by cell death and that firm conclusions were made. Cell viability was assessed using the Pierce LDH Cytotoxicity Assay Kit as described in Section 2.4.1. Damage to the cell membrane results in the release of the cytosolic enzyme LDH into the culture media where it catalyses the conversion of lactate to pyruvate via the reduction of NAD<sup>+</sup> to NADH, which is subsequently used by the enzyme diaphorase in the reduction of a tetrazolium salt 2-(4iodophenyl)-3-94-nitrophenyl)-5-phenyl-2H-tetrazolium chloride (INT) to formazan; a red coloured product that can be measured at 490 nm. The level of formazan produced



by this coupled enzymatic reaction is directly proportional to the level of LDH released into the culture media.

Following cell viability assays, initial *in vitro* investigations were performed in a dose-dependent manner in order to test the effectiveness of probiotic CM at a range of concentrations, with the aim of selecting a single optimal concentration of each probiotic CM for use in the remainder of *in vitro* studies.

### 3.1.3 Key processes in atherosclerosis

#### 3.1.3.1 Monocyte recruitment and migration

One of the key initiating processes in atherosclerosis is the recruitment and migration of circulating monocytes from the lumen into the arterial wall. Activated endothelial cells express a number of chemokines and adhesion molecules involved in the capture and immobilisation of monocytes followed by their transmigration across the endothelium in response to a range of chemoattractants (Ramji and Davies, 2015). MCP-1 (also known as CCL2) is a key pro-inflammatory chemokine fundamental in the regulation of monocyte recruitment and migration (Deshmane *et al.*, 2009) and a potent monocyte chemotactic factor implicated in the development of atherosclerosis (Aiello *et al.*, 1999). Studies in ApoE knockout mice have shown MCP-1 deficiency to result in smaller, less extensive lesion development (Gosling *et al.*, 1999), while increased expression of MCP-1 by leukocytes has been shown to increase atherosclerosis lesion development (Aiello *et al.*, 1999). Attenuation of MCP-1 stimulated monocyte migration by probiotic CM would therefore represent a potential anti-atherogenic effect. A previous study has demonstrated the ability of probiotic *Enterococcus faecalis* to significantly downregulate the expression of MCP-1 in C57BL/6 mice (Chen *et al.*, 2017). However, this is the first study to investigate the effects of probiotics, or CM derived from them, on monocyte migration in atherosclerosis. In this study, a modified Boyden chamber method was used to assess the effect of probiotic CM treatment on migration of monocytes through an 8 µM pore membrane, towards a chemoattractant (MCP-1) stimulus, where the membrane mimics the arterial endothelial layer.

### 3.1.3.2 Modification of lipoproteins by ROS

ROS are a group of small highly reactive oxygen derivatives such as hydrogen peroxide ( $\text{H}_2\text{O}_2$ ) and the superoxide anion ( $\text{O}_2^-$ ), involved in the normal functioning of biological processes and cellular metabolic control (Goncharov *et al.*, 2015). While ROS are critical for healthy vascular homeostasis, excess production results in a state of imbalance known as oxidative stress (Kattoor *et al.*, 2017). ROS production and oxidative stress is increased in many conditions known to be risk factors for atherosclerosis including diabetes, hypertension, smoking and lipid dysregulation (Giacco and Brownlee, 2010; Kattoor *et al.*, 2017; Steffen *et al.*, 2012). ROS are considered to be pro-atherogenic factors integral in the pathogenesis of atherosclerosis (Goncharov *et al.*, 2015). In fact, the oxidation hypothesis suggests that oxidised LDL is a major factor driving the development of atherosclerosis (Choi *et al.*, 2017). Oxidative modification of LDL to form oxLDL induces the expression of adhesion molecules that enhance leukocyte recruitment and their migration into the arterial wall (Goncharov *et al.*, 2015). Differentiated macrophages express scavenger receptors which internalise these modified forms of LDL resulting in the formation of macrophage foam cells, the hallmark of atherosclerosis. Additionally, foam cells release proinflammatory cytokines further promoting ROS production (Kattoor *et al.*, 2017). In conjunction with growth factors, ROS stimulate the migration of VSMCs, the expression of VSMC scavenger receptors and subsequent formation of VSMC-derived foam cells (Kattoor *et al.*, 2017). Furthermore in advanced atherosclerosis, the production of MMPs induced by ROS contributes to the degradation of the fibrous cap and to plaque instability (Kattoor *et al.*, 2017). A number of pharmacological agents have been shown to have beneficial effects on atherogenesis by modulating oxidative stress, including ACE inhibitors and angiotensin II receptor type 1 (AT1 receptor) blockers (ARBs) (Saso *et al.*, 2017). In this study, probiotic CM was tested for its effect on cellular ROS production in the presence of potent ROS stimulant  $\text{H}_2\text{O}_2$ , using the Abcam Cellular ROS Detection Assay Kit.

### 3.1.3.3 Macropinocytosis

The unregulated uptake of excessive amounts of modified LDL by macrophages is a key event in the formation of macrophage foam cells, and essential to atherosclerosis

development. Uptake of modified LDL by macrophages is regarded as being largely receptor-mediated; however, a significant portion is taken up by a non-receptor-mediated process of fluid-phase endocytosis known as macropinocytosis (Kruth *et al.*, 2002). During this process, actin-dependent ruffling of the plasma membrane is followed by fusion of the membrane to itself, leading to the internalisation of the surrounding contents in fluid-filled intracellular vacuoles (Michael *et al.*, 2013). This process has been shown to contribute substantially to the uptake of both unmodified and modified LDL and to the formation of macrophage foam cells (Michael *et al.*, 2013). While the effect of probiotics on macropinocytosis hasn't yet been studied, previous studies have shown that inhibiting macropinocytosis in macrophages decreases foam cell formation (Gallagher, 2016; Yao *et al.*, 2009). In this study, the effect of probiotic CM on macropinocytosis was assessed in macrophages using the fluorescent molecule luciferase yellow LY as described in Section 2.7.2. LY is a popular dye that has been successfully utilised for the measurement of macropinocytosis in macrophages in previous studies (McLaren *et al.*, 2011b; Michael *et al.*, 2013; Swanson, 1989).

#### ***3.1.3.4 Mitochondrial function***

Mitochondria are well known as the energy producing powerhouse of the cell, though the role of mitochondria goes beyond their energy producing capacity. As mentioned previously, mitochondrial ROS production is a popular target for the reduction of oxidative stress (Kattoor *et al.*, 2017) and mitochondrial dysfunction, and mitochondrial oxidative stress (mitoOS) has been shown to strongly correlate with atherosclerotic lesion progression (Wang *et al.*, 2017d). Mitochondrial respiratory function is routinely assessed by Agilent Seahorse technology, where the OCR is measured in response to the serial injection of respiratory modulators (Hujber *et al.*, 2018; Tan *et al.*, 2015) targeting specific components of the electron transport chain (Figure 3.1). The effect of probiotic bacteria on mitochondrial function has not yet been studied, therefore this study aims to investigate the effect of probiotic CM on mitochondrial function using the Seahorse Mito Stress Test as described in Section 2.4.6.

The Seahorse Mito Stress Test measures OCR following serial injection of oligomycin at 15 minutes, FCCP at 34 minutes and rotenone/antimycin A at 54 minutes as illustrated

in Figure 3.2. Initial OCR measurements represent basal respiration prior to the injection of compounds, i.e. the energy demands of the cell under baseline conditions. Oligomycin inhibits ATP synthase (Figure 3.1) and so the decrease in OCR following injection at 15 minutes correlates to ATP production (Figure 3.2). FCCP is an uncoupling agent which targets the inner mitochondrial membrane, causing disruption of the mitochondrial membrane potential and uninhibited flow of electrons through the ETC (Figure 3.1). The peak in OCR following the injection of FCCP therefore represents the maximum respiration achievable where the ETC is operating at full capacity, and by deduction of basal respiration allows calculation of spare respiratory capacity (Figure 3.1). Spare respiratory capacity is an essential parameter giving a measure of the cells capacity to deal with increased energy demand and a sign of cellular health. The final injection is a mix of rotenone and antimycin, which together inhibits the remaining ETC complexes leading to complete cessation of mitochondrial respiration (Figure 3.1). The remaining OCR therefore represents non-mitochondrial respiration (Figure 3.2). Finally, the OCR following the cessation of respiration is deducted from the OCR following oligomycin injection to provide a measure of proton leak (Figure 3.2). Proton leak is the remaining basal respiration that is not coupled to ATP production, and is a sign of mitochondrial damage. In this study, mitochondrial function was assessed in THP-1 macrophages treated with either vehicle or probiotic CM by measurement of basal respiration, maximal respiration, spare respiratory capacity, ATP production, non-mitochondrial respiration and proton leak.

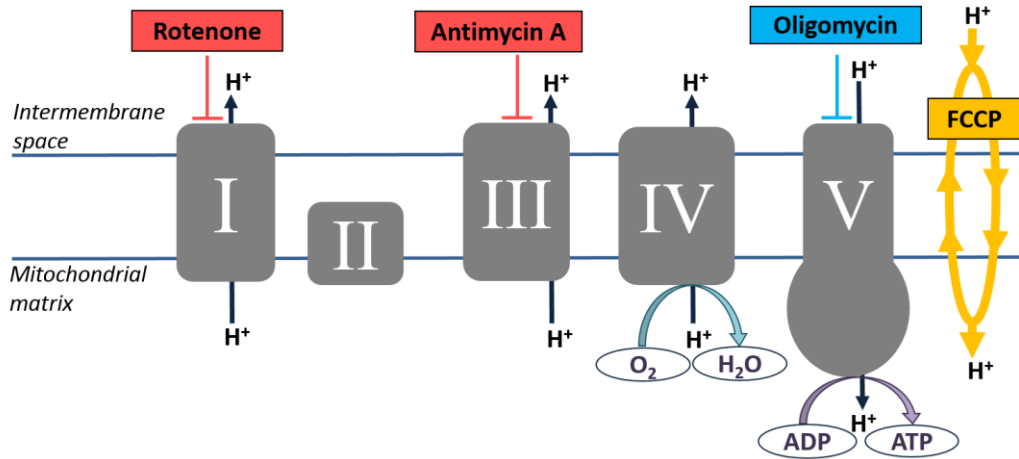


**Figure 3.1 – Illustration of the ETC components targeted by respiratory modulators in the Seahorse Mito Stress Test.** Oligomycin targets ATP synthase (complex V), inhibiting cellular ATP production. FCCP is an uncoupling agent that targets the inner mitochondrial membrane, causing collapse of the proton gradient and uninhibited flow of electrons through the ETC. As a result oxygen is maximally consumed by complex IV. Rotenone/antimycin shuts down mitochondrial respiration via the inhibition of complexes I and III respectively. Image taken from the Agilent Seahorse Cell Mito Stress Test User Guide (Agilent Technologies, 2019).

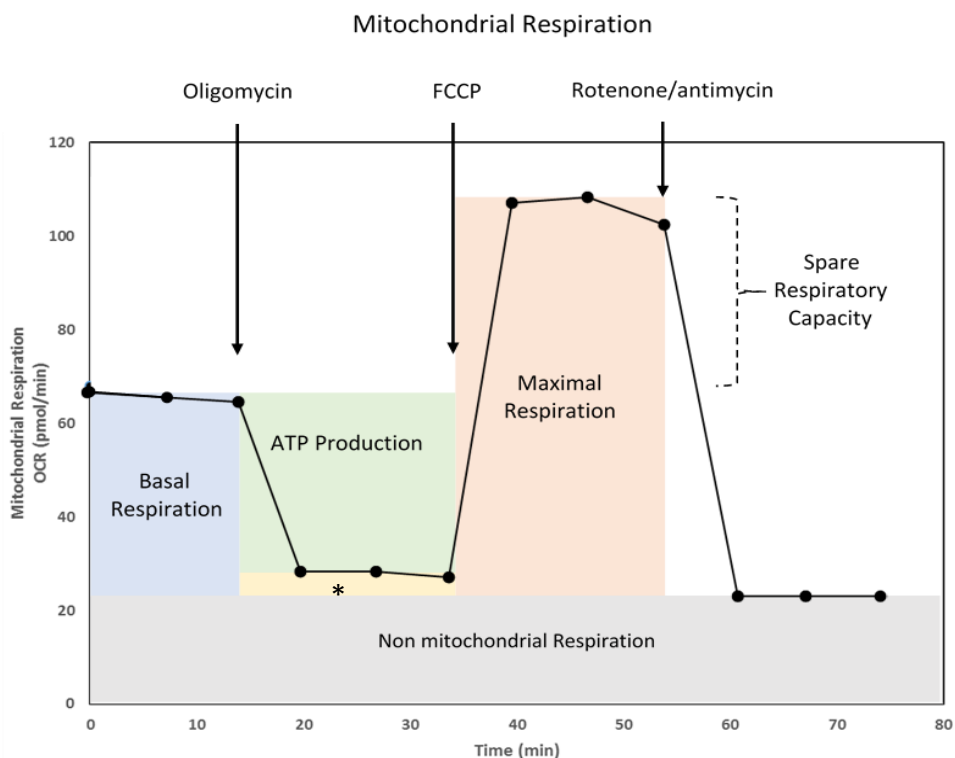


**Figure 3.2 – Seahorse XFP Cell Mito Stress Test profile showing key parameters of mitochondrial respiration.** OCR is measured during serial injection of respiratory modulators oligomycin, FCCP and rotenone/antimycin, thereby allowing the determination of basal respiration, ATP production, maximal respiration, spare respiratory capacity, proton leak and non-mitochondrial respiration. \*, proton leak. Abbreviations: OCR, oxygen consumption rate; FCCP, carbonyl cyanide-4 (trifluoromethoxy) phenylhydrazone.

### 3.1.3.5 Phagocytosis

In addition to the uptake of oxLDL, macrophages play an important role in phagocytosis of apoptotic cells and cellular debris which would otherwise accumulate, contributing to the formation of a necrotic core (Schrijvers, 2005) and advanced plaque progression. Phagocytosis by macrophages is known to be reduced in human atherosclerotic plaques (Kojima *et al.*, 2016). Recent studies have demonstrated that reduced macrophage phagocytosis is associated with increased uptake of oxLDL and increased plaque formation, while increased phagocytosis is associated with the opposite effect (Laguna-Fernandez *et al.*, 2018). The effect of probiotics on macrophage phagocytic activity has not yet been investigated. This study aims to elucidate the effect of probiotic CM on phagocytosis in human macrophages using the Vybrant Phagocytosis Assay Kit as described in Section 2.4.7.

### 3.1.3.6 Proliferation of key cell types involved in atherosclerosis

Macrophage proliferation is a key aspect involved in the progression of atherosclerosis, believed to be more relevant to lesion advancement than monocyte recruitment, and has been identified as a potential therapeutic target for disease intervention (Robbins *et al.*, 2013). A study in ApoE<sup>-/-</sup> mice has demonstrated a reduction in macrophage proliferation corresponding to a reduction in lesion size irrespective of the level of monocyte recruitment (Robbins *et al.*, 2013). Another study involving the disruption of cell cycle regulators at the genetic level, demonstrated increased arterial macrophage and VSMC proliferation with corresponding acceleration of atherosclerosis in ApoE<sup>-/-</sup> mice (Diez-Juan *et al.*, 2004). This study aims to investigate the effect of probiotic treatment on the proliferation of human macrophages using crystal violet staining and a BrdU ELISA method as described in Section 2.4.2.2. Briefly, proliferation was initially assessed periodically over a 7-day period using crystal violet staining in conjunction with cell viability testing to ensure results were not influenced by cell death. Additionally, the rate of proliferation was assessed at 48 hours using the BrdU Labeling and Detection Kit. Further to macrophages, the proliferation of VSMCs was also assessed in a similar manner using HASMCs treated with either vehicle or probiotic CM. The proliferation of monocytes was also assessed by simple cell counting over a 7-day period with

concurrent assessment of cell viability. This allows for a more complete picture of the effect of probiotics on the proliferation of key cell types involved in atherosclerosis.

### 3.1.3.7 VSMC invasion

Following on from VSMC proliferation, this study investigates the effect of probiotic CM on VSMC invasion. VSMCs migrate from the media towards the arterial intima in response to vascular injury, a complex process driven by many cytokines, chemokines and growth factors (Kim *et al.*, 2014), including platelet-derived growth factor (PDGF). PDGF is a potent mitogen and chemoattractant for SMCs (Sano *et al.*, 2001) and inducer of VSMC proliferation and migration (Ricci and Ferri, 2015). When physiological migration of VSMCs becomes dysregulated, it becomes pathological and is often referred to as VSMC invasion, an important factor in atherogenesis (Louis and Zahradka, 2010). As described in Chapter 1, migrated SMCs together with their secreted ECM proteins form a protective cap surrounded by a collagen-rich matrix, which functions to provide plaque stability (Louis and Zahradka, 2010). However, the proliferation and invasion of SMCs remains closely associated with atherosclerosis progression and has been shown to play a key role in neointima formation (Chen *et al.*, 2018; Zhang, 2009). To investigate the effect of probiotic CM on VSMC invasion, this study uses a modified Boyden chamber method as described in Section 2.4.5, where HASMCs treated with either vehicle or CM were allowed to migrate towards a PDGF stimulus.

### 3.1.4 Anti-inflammatory effects in atherosclerosis

Atherosclerosis is now widely regarded as an inflammatory disorder with anti-inflammatory agents receiving much attention in the search for anti-atherosclerotic therapeutics. More recently probiotics, including many different *Lactobacilli* strains, have been shown to have beneficial anti-inflammatory actions in atherosclerosis, with a large range of strains investigated in the literature (Ding *et al.*, 2017). However, this effect is highly strain specific with as many strains showing no effect or even pro-inflammatory actions (Ding *et al.*, 2017). In a strain-specific manner, probiotics have been shown to exert many immunomodulatory effects including the promotion of anti-inflammatory M2 macrophage polarisation (Ukibe *et al.*, 2015), reduction of T-

lymphocyte helper 1 (Th1) cell numbers and pro-inflammatory cytokine production (Smelt *et al.*, 2013), and an increase in regulatory T cells (Tregs) (Ding *et al.*, 2017; Smits *et al.*, 2005). This study aims to investigate the potential anti-inflammatory effects of probiotic CM treatment on the inflammatory response of human macrophages to pro-inflammatory cytokine stimulation.

#### *3.1.4.1 Activation of the NLRP3 inflammasome*

The inflammasome is a multi-protein complex formed by the activation of an innate immune system pattern recognition receptors (PRR). NLRP3 is the most well defined inflammasome responsible for the maturation of proinflammatory IL-1 family cytokines; IL-1 $\beta$  and IL-18 (Jo *et al.*, 2016) and has been implicated in a variety of inflammatory diseases including atherosclerosis (Ozaki *et al.*, 2015). Activation of NLRP3 in response to a pro-inflammatory stimulus can be assessed by the level of IL-1 $\beta$  production, measurable by standard ELISA methods. This study investigates the effect of probiotic CM on the activation of the NLRP3 inflammasome by IL-1 $\beta$  ELISA as described in Section 2.6.3.

#### *3.1.4.2 Inflammatory gene expression*

Many classes of cytokines are present in atherosclerotic plaques with all atherosclerosis-associated cell types capable of secreting and responding to them (Ramji and Davies, 2015). Key cytokines are very highly expressed in atherosclerotic regions including the pro-inflammatory IL-1 $\beta$ , IFN- $\gamma$  and TNF- $\alpha$ . Of these, IFN- $\gamma$  is considered a master regulator of atherosclerosis; highly involved in many stages of disease progression and a popular target for anti-atherosclerotic therapies (McLaren and Ramji, 2009). One study demonstrated that the attenuation of IFN- $\gamma$  action by administration of an inhibitory protein prevented plaque progression in ApoE<sup>-/-</sup> mice, in addition to the downregulation of pro-inflammatory cytokine expression (Koga *et al.*, 2007). Further studies, including the previously mentioned CANTOS trial (Dolgin, 2017) have demonstrated that the inhibition or blocking of IL-1 $\beta$  leads to a corresponding suppression of atherosclerosis progression in ApoE<sup>-/-</sup> mice (Bhaskar *et al.*, 2011; Ramji and Davies, 2015), while TNF- $\alpha$  knockout significantly reduced fatty streak formation with corresponding



downregulation in expression of pro-inflammatory factors (Xiao *et al.*, 2009). The effect of various probiotic bacteria on cytokine production has been investigated with conflicting results. Many studies show beneficial effects with specific strains attenuating the production of pro-inflammatory cytokines, including those mentioned above, while inducing the production of anti-inflammatory cytokines such as IL-10 (Kekkonen *et al.*, 2008; Singh *et al.*, 2018; Štofilová *et al.*, 2017). However, the exact effects are highly strain-specific with some strains having no effect or even a pro-inflammatory influence (Meyer *et al.*, 2007). MCP-1 and ICAM1 are both robust markers of inflammation and play an essential role in the continued migration of monocytes across the endothelium. Their expression is known to be induced by a range of pro-inflammatory cytokines, including IFN- $\gamma$  (Moss *et al.*, 2016), IL-1 $\beta$  (Lappas, 2017) and TNF- $\alpha$  (Jiang *et al.*, 2015), thereby making these genes strong markers for the investigation of cytokine-induced inflammatory effects. This study therefore investigates the effect of probiotic CM treatment on cytokine-induced expression of inflammatory markers MCP-1 and ICAM1 in human macrophages stimulated with either IFN- $\gamma$ , IL-1 $\beta$  or TNF- $\alpha$ .

### 3.2 Experimental design

Prior to the start of *in vitro* investigations, probiotic CM batches were normalised to total protein concentration and confirmed to have no detrimental effects on cell viability. Initial assays were performed in a dose response format to determine an optimal concentration of the probiotic CM for further studies. Following optimisation, Lab4, Lab4b and CUL66 CM was used at concentrations of 8, 1.5 and 5  $\mu\text{g}/\text{mL}$  respectively. Experiments then continued to investigate the effect of probiotic CM on key processes associated with atherosclerosis development as outlined in Figures 3.3 – 3.5. Specific methods for each experimental aim are detailed in Chapter 2.

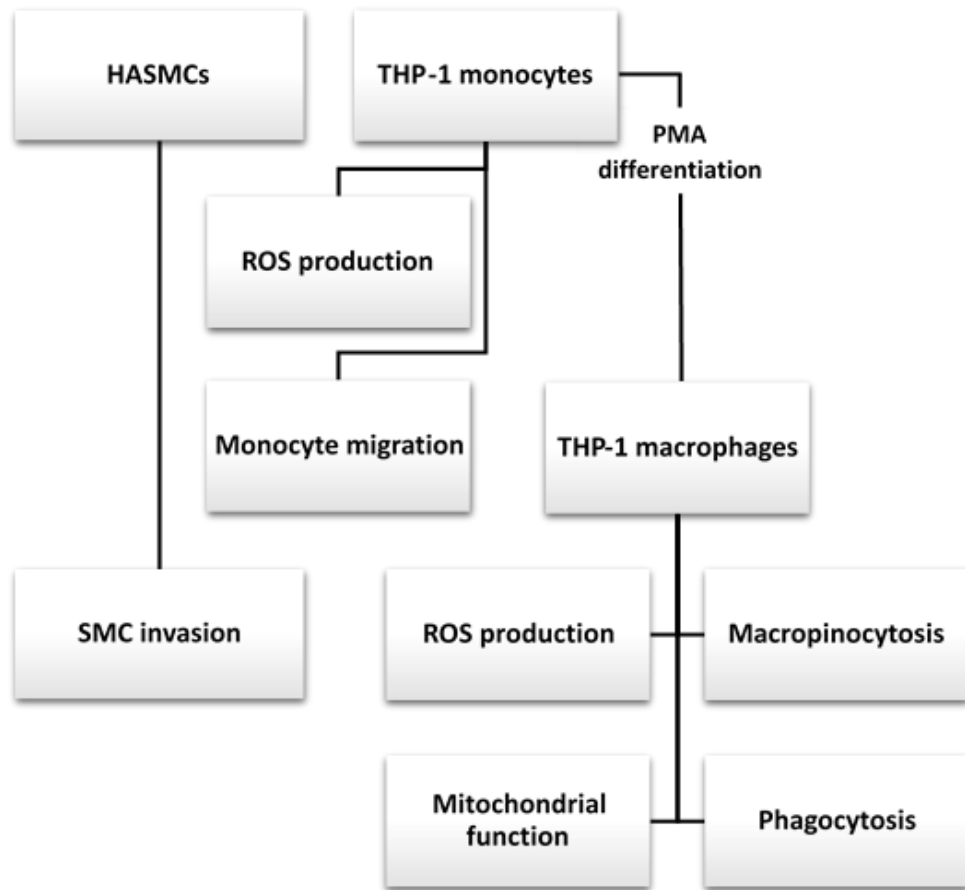


**Figure 3.3 - Experimental strategy for the investigation of the effects of probiotic CM on key cellular processes in atherosclerosis.** Abbreviations: HASMCs, human aortic smooth muscle cells; SMC, smooth muscle cells; ROS, reactive oxygen species.

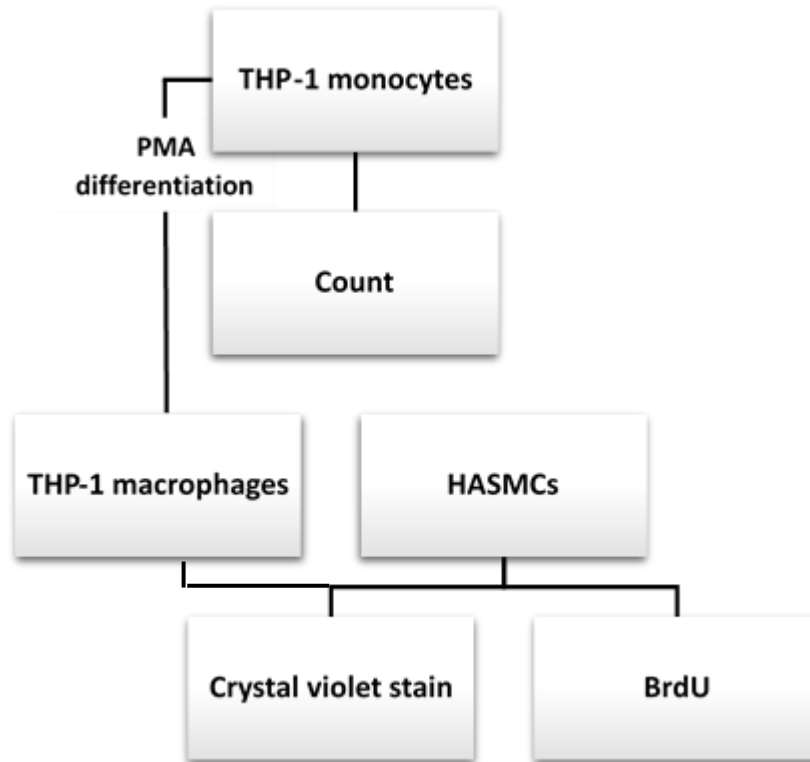


Figure 3.4 - Experimental strategy for the investigation of the effect of probiotic CM on the proliferation of key cell types in atherosclerosis. Abbreviations: HASMCs, human aortic smooth muscle cells; BrdU, 5-Bromo-2'-deoxy-uridine

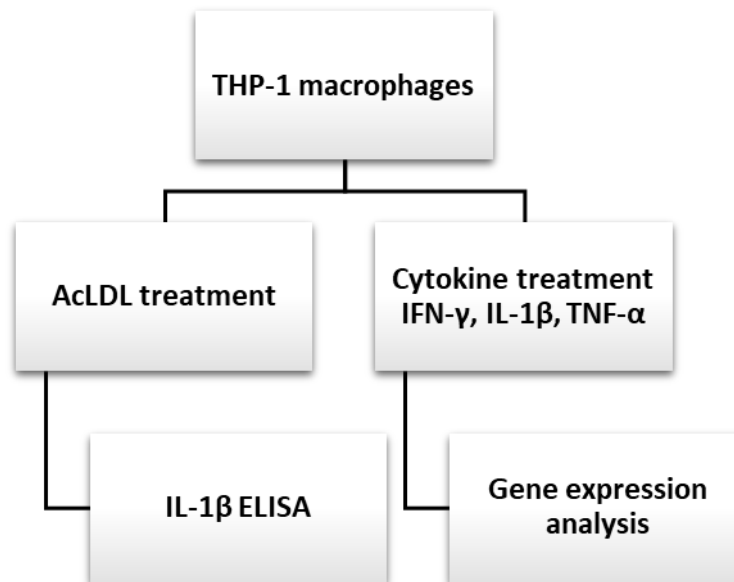


Figure 3.5 - Experimental strategy for the investigation of the anti-inflammatory effects of probiotic CM. Abbreviations: AcLDL, acetylated LDL; ELISA, enzyme-linked immunosorbent assay.

### 3.3 Results

#### 3.3.1 Normalisation of probiotic CM to total protein concentration

To control for batch effects, each probiotic CM was normalised according to the total protein concentration, and the optimal concentration estimated as the maximum concentration at which the cells remain viable. Probiotic CM was prepared and the total protein quantified as described in Sections 2.2 and 2.6.2 respectively. Cell viability was then assessed using the LDH Assay Kit (Section 2.4.1), using a range of known protein concentrations for each CM at 100% then approximately 80%, 60% and 40% dilution. For Lab4 CM, the protein concentrations of 21, 17, 13 and 8  $\mu\text{g}/\text{mL}$  were tested where 21  $\mu\text{g}/\text{mL}$  represents 100% CM. Similarly for Lab4b and CUL66, concentrations of 3, 2.5, 1.5 and 1  $\mu\text{g}/\text{mL}$  (Lab4b) and 5, 4, 3 and 2  $\mu\text{g}/\text{mL}$  (CUL66) were tested where 3  $\mu\text{g}/\text{mL}$  and 5  $\mu\text{g}/\text{mL}$  represent 100% CM respectively. THP-1 macrophages were treated for 24 hours with either vehicle or probiotic CM at the range of concentrations detailed above. Cell viability was determined as a percentage of the vehicle control, and a cell viability of 85% or over was considered acceptable.

For Lab4 CM, higher concentrations of 21 and 17  $\mu\text{g}/\text{mL}$  led to reductions in cell viability below 85% (Figure 3.6A), indicating a detrimental effect and so were considered unsuitable for use in experiments. All other tested concentrations of Lab4 displayed less than 15% reduction in cell viability and were therefore considered suitable for use in experiments. For some batches of Lab4 CM, total protein concentration was measured at a maximum of 8  $\mu\text{g}/\text{mL}$ , therefore this concentration was selected as the optimal concentration for use in experiments. For Lab4b, cell viability remained at or above 85% following treatment with all tested concentrations (Figure 3.6B). However, as with Lab4, a concentration of 1.5  $\mu\text{g}/\text{mL}$  was selected to reflect the minimum protein concentration measured in any batch of Lab4b CM. Similarly, all tested concentrations of CUL66 resulted in greater than 85% cell viability (Figure 3.6C) and so the maximum concentration of 5  $\mu\text{g}/\text{mL}$  was selected for use in future experiments.

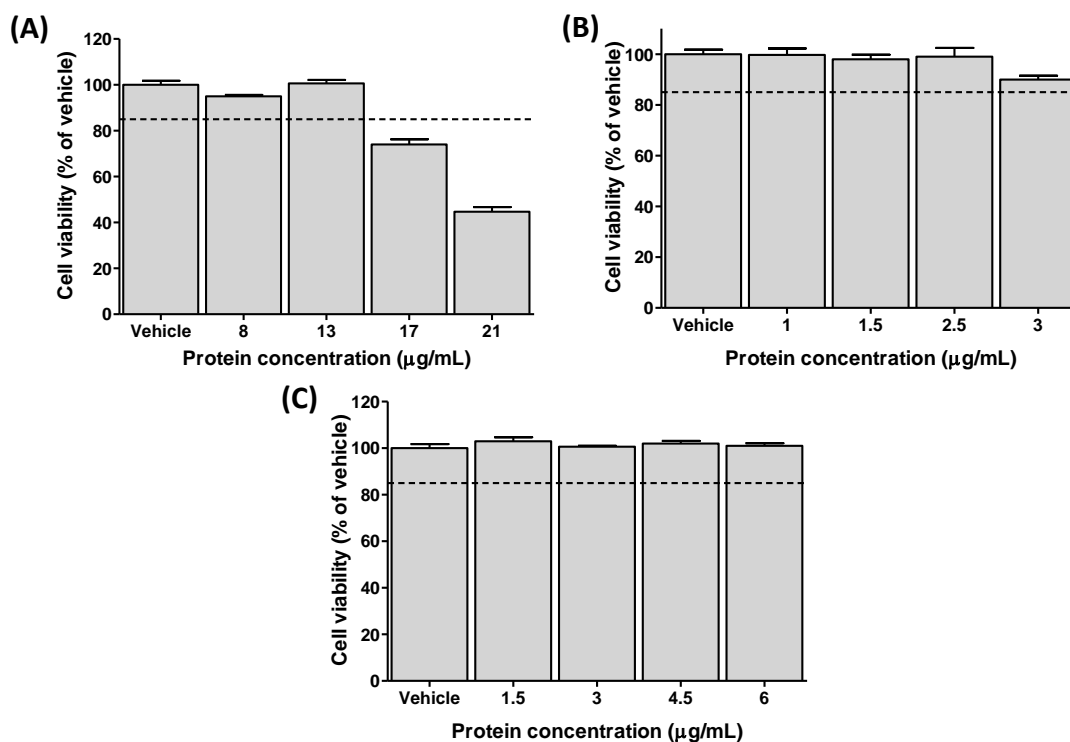


**Figure 3.6 - Viability of THP-1 macrophages assessed using the LDH Assay Kit.** THP-1 macrophages were treated with either the vehicle control or probiotic CM at a range of known protein concentrations. LDH assays were performed and cell viability determined as a percentage of the vehicle control which was set to 100%. Dashed line denotes acceptable level of viability at 85% and above. (A) Cells treated with Lab4 CM of 21, 17, 13 and 8 µg/mL protein concentration. (B) Cells treated with Lab4b CM of 3, 2.5, 1.5 and 1 µg/mL protein concentration. (C) Cells treated with CUL66 CM of 5, 4, 3 and 2 µg/mL protein concentration. The data are presented as mean ± SEM from three independent experiments.

### 3.3.2 Probiotic CM has no detrimental effect on the viability of cell culture model systems used for *in vitro* studies

The effect of each probiotic CM on cell viability was then assessed for each cell culture model system to be utilised in the study. Cells were incubated for 24 hours with vehicle or probiotic CM and cell viability assessed using the LDH Assay Kit (Section 2.4.1). Results are shown in Figure 3.7. Treatment with probiotic CM resulted in a significant increase in the viability of cells, but no detrimental effect on the viability of THP-1 macrophages, HASMCs or HMDMs.

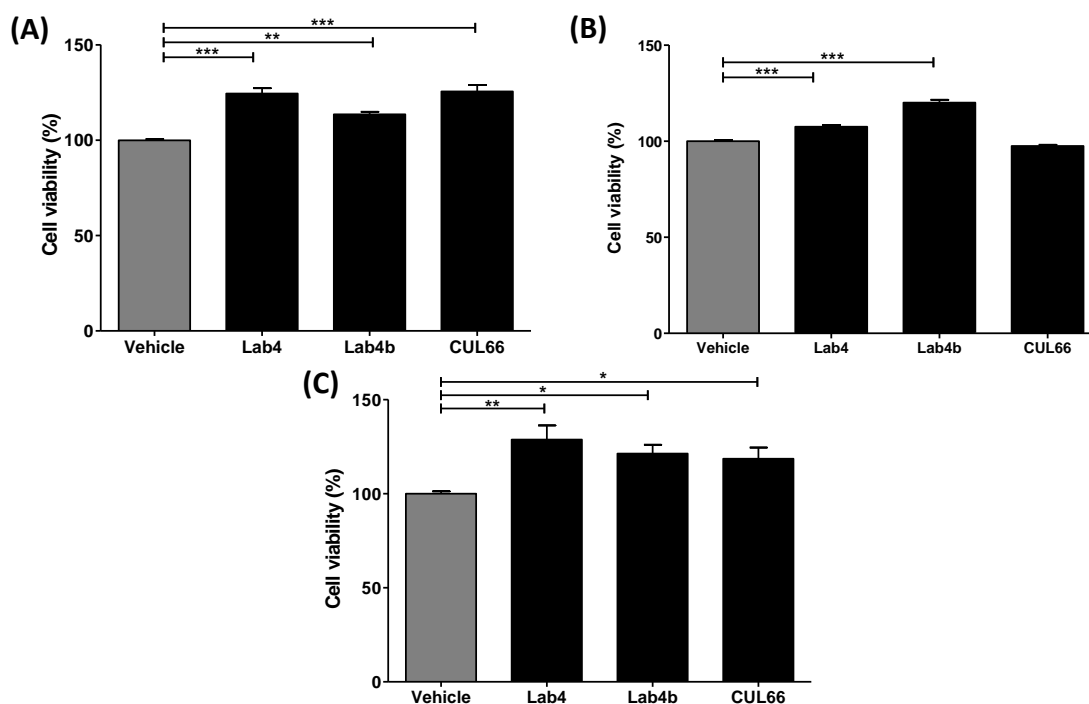


**Figure 3.7 - Probiotic CM has no detrimental effect on the viability of cell culture model systems utilised in the study.** (A) THP-1 macrophages, (B) HASMCs and (C) HMDMs were treated for 24 hours with the vehicle control or Lab4 (8  $\mu\text{g}/\text{mL}$ ), Lab4b (1.5  $\mu\text{g}/\text{mL}$ ) or CUL66 (5  $\mu\text{g}/\text{mL}$ ) CM, and cell viability assessed using the LDH Assay Kit. Cell viability was determined as a percentage relative to the vehicle control which was set to 100%. Data are presented as mean  $\pm$  SEM from three independent experiments. Statistical analysis was performed using a One-way ANOVA with Dunnett T3 post-hoc test where \* $p < 0.05$ , \*\* $p < 0.01$  and \*\*\* $p < 0.001$ .

### 3.3.3 Monocyte migration was reduced in the presence of probiotic CM

Monocyte migration was assessed using a modified Boyden chamber method (Section 2.4.4). Initially, the assay was performed in a concentration dependent manner using protein concentrations of 8, 6 and 4  $\mu\text{g}/\text{mL}$  for Lab4 CM; 1.5, 1 and 0.5  $\mu\text{g}/\text{mL}$  for Lab4b CM; and 5, 4 and 3  $\mu\text{g}/\text{mL}$  for CUL66 CM. Results are shown in Figure 3.8. In all cases, the migration of monocytes was significantly increased ( $p < 0.001$ ) in the presence of MCP-1 compared to vehicle alone (no MCP-1 control). In the presence of Lab4 CM, the MCP-1-induced migration was attenuated by 0.58-fold ( $p < 0.001$ ), 0.73-fold ( $p = 0.002$ ) or 0.65-fold ( $p < 0.001$ ) with concentrations of 8, 6 or 4  $\mu\text{g}/\text{mL}$  respectively (Figure 3.8A). Similarly, with Lab4b treatment the MCP-1-induced migration was attenuated in a concentration dependent manner by 0.53-fold ( $p < 0.001$ ), 0.57-fold ( $p < 0.001$ ) or 0.68-fold ( $p < 0.001$ ) with concentrations of 1.5, 1 or 0.5  $\mu\text{g}/\text{mL}$  respectively. CUL66 treatment also attenuated MCP-1-driven migration in a concentration dependent manner showing

reductions of 0.73-fold ( $p = 0.004$ ), 0.7-fold ( $p = 0.002$ ) or 0.6-fold ( $p < 0.001$ ) with concentrations of 5, 4 or 3  $\mu\text{g}/\text{mL}$  respectively.

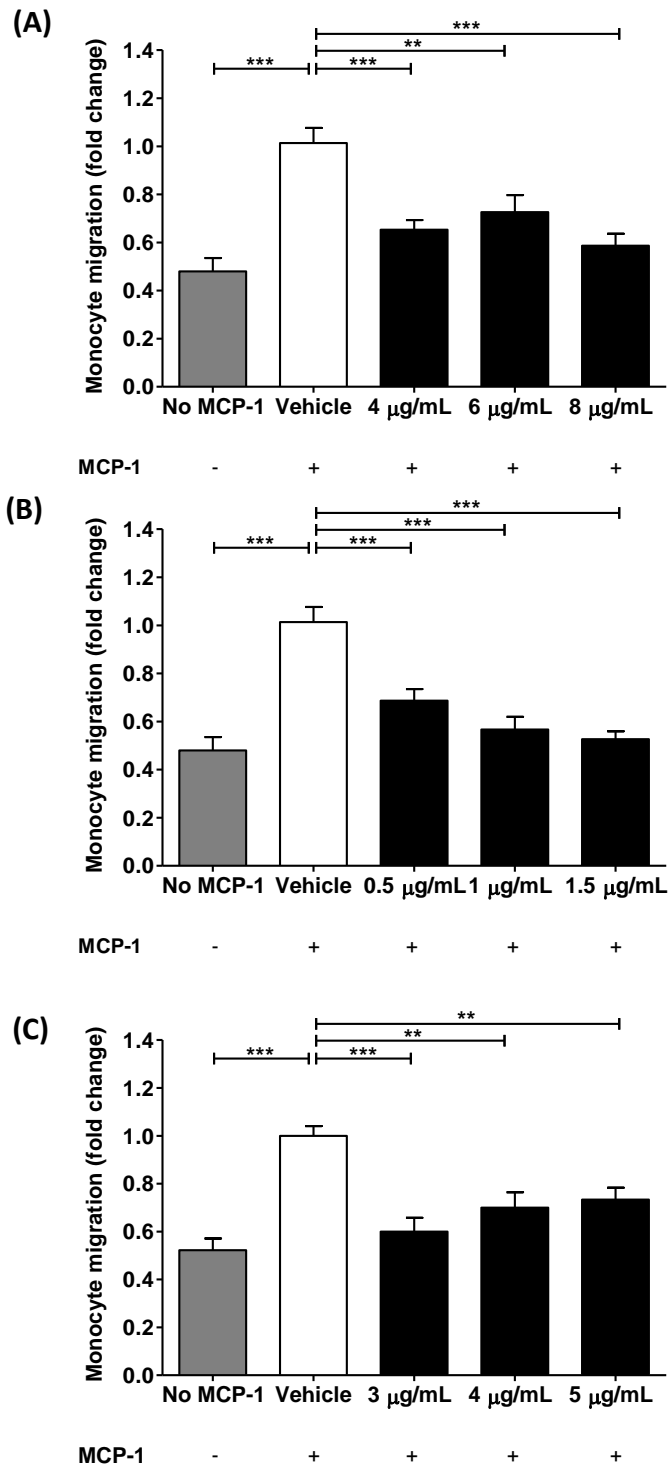


**Figure 3.8 - Migration of THP-1 monocytes in response to MCP-1 was attenuated by various concentrations of probiotic CM.** The effect of each probiotic CM on monocyte migration was assessed in a concentration dependent manner using the Boyden chamber method. THP-1 monocytes were allowed to migrate in the presence of MCP-1 and either vehicle (Vehicle control) or probiotic CM. Cells treated with vehicle but in the absence of MCP-1 were included for comparative purposes (No MCP-1). (A) Lab4 CM used at concentrations of 8, 6 and 4 µg/mL. (B) Lab4b CM used at concentrations of 1.5, 1 and 0.5 µg/mL (C) CUL66 CM used at concentrations of 5, 4 and 3 µg/mL. Migration was determined as a percentage of the total cells, and displayed as fold-change in migration relative to the Vehicle control which was arbitrarily set to 1. Data are presented as mean ± SEM from five (A and B), or three (C) independent experiments. Statistical analysis was performed using a One-way ANOVA with Dunnett (2-sided) post-hoc test where \*\*  $p < 0.01$  and \*\*\*  $p < 0.001$ .



Subsequently, once a protein concentration was selected to which to normalise all future CM, the assay was repeated for comparison of the activity of each probiotic CM. Again, migration was significantly increased in the presence of MCP-1 compared to vehicle alone ( $p < 0.001$ ). The MCP-1-induced migration was significantly attenuated by 0.66-fold ( $p = 0.006$ ), 0.55-fold ( $p < 0.001$ ) and 0.71-fold ( $p = 0.026$ ) in the presence of Lab4, Lab4b and CUL66 CM respectively (Figure 3.9).

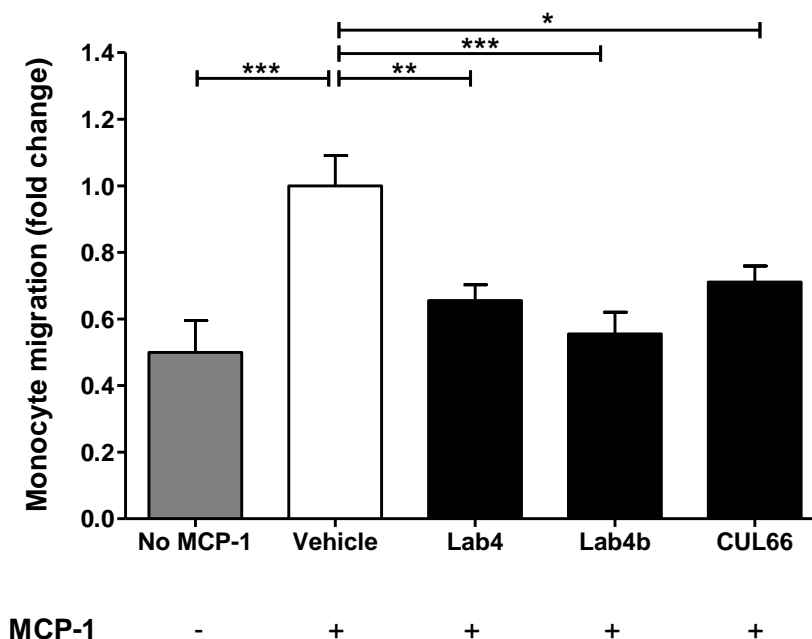


**Figure 3.9 - Migration of monocytes in response to MCP-1 was attenuated in the presence of probiotic CM.** The effect of each probiotic CM on monocyte migration was assessed using a modified Boyden chamber method. THP-1 monocytes were allowed to migrate in the presence of MCP-1 and either vehicle (Vehicle control) or Lab4 (8  $\mu\text{g}/\text{mL}$ ), Lab4b (1.5  $\mu\text{g}/\text{mL}$ ) or CUL66 (5  $\mu\text{g}/\text{mL}$ ) CM. Cells treated with vehicle but in the absence of MCP-1 were included for comparative purposes (No MCP-1). Migration was determined as a percentage of the total cells, and displayed as fold-change in migration relative to the Vehicle control which was arbitrarily set to 1. Data are presented as mean  $\pm$  SEM from five three independent experiments. Statistical analysis was performed using a One-way ANOVA with Dunnett (2-sided) post-hoc test where \* $p < 0.05$ , \*\* $p < 0.01$  and \*\*\* $p < 0.001$ .

### 3.3.4 Probiotic CM exerts varying effects on the production of ROS by THP-1 monocytes and macrophages

The effects of probiotic CM on TBHP-induced ROS production was assessed in THP-1 monocytes and macrophages using the DCFDA Cellular ROS Detection Assay Kit as described in Section 2.4.3. Initially the assay was performed in a concentration dependent manner using protein concentrations of 8, 6 and 4  $\mu\text{g}/\text{mL}$  for Lab4 CM; 1.5,

1 and 0.5  $\mu\text{g}/\text{mL}$  for Lab4b CM; and 5, 4 and 3  $\mu\text{g}/\text{mL}$  for CUL66 CM. Results of investigations in both THP-1 monocytes and macrophages are shown in Figures 3.10 and 3.11 respectively. TBHP significantly induced ROS production in both monocytes and macrophages compared to vehicle alone ( $p < 0.001$ ). In THP-1 monocytes, no significant change in TBHP-induced ROS production was observed with any probiotic CM at any tested concentration, with the exception of the lowest concentration of Lab4b (0.5  $\mu\text{g}/\text{mL}$ ) which produced a significant 1.3-fold ( $p = 0.003$ ) increase in ROS production (Figure 3.10B). Each probiotic CM at all tested concentrations increased the TBHP-induced ROS production in THP-1 macrophages (Figure 3.11). Thus, treatment with Lab4 CM resulted in a similar degree of increase in ROS production across all concentrations tested showing 1.5-fold ( $p = 0.003$ ), 1.46-fold ( $p = 0.010$ ) or 1.47-fold ( $p = 0.003$ ) increase with 8, 6 or 4  $\mu\text{g}/\text{mL}$  of protein respectively (Figure 3.11A). Similarly with Lab4b treatment ROS production was increased by 1.73-fold ( $p = 0.016$ ), 1.52-fold ( $p < 0.001$ ) and 1.81-fold ( $p < 0.001$ ) with 1.5, 1 or 0.5  $\mu\text{g}/\text{mL}$  of protein respectively (Figure 3.11B). In the presence of CUL66 CM, the TBHP-induced ROS production displayed an increase in a concentration dependent manner from 1.43-fold ( $p < 0.001$ ), to 1.52-fold ( $p = 0.002$ ) and 1.64-fold ( $p < 0.001$ ) with 5, 4 or 3  $\mu\text{g}/\text{mL}$  of protein respectively (Figure 3.11C).

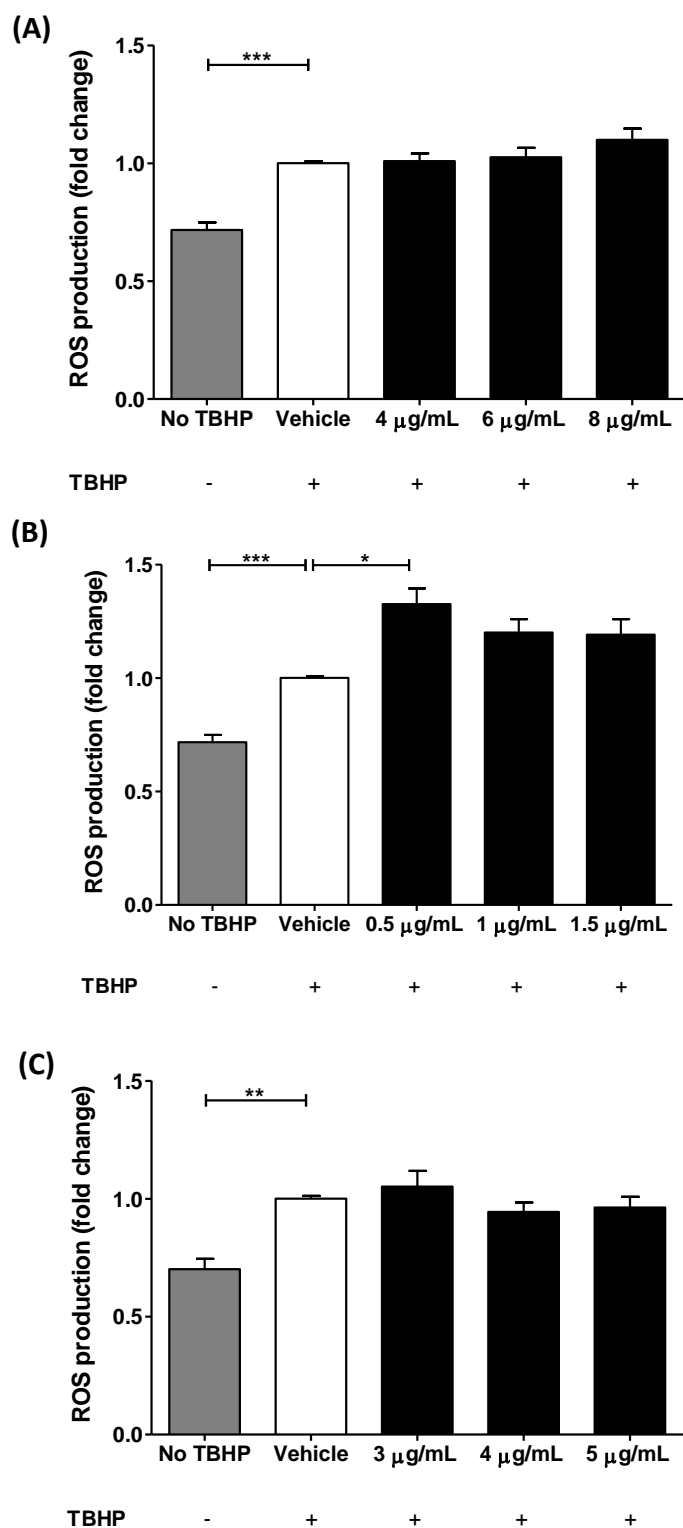


**Figure 3.10 – The effect of probiotic CM on TBHP-induced ROS production in THP-1 monocytes.** The effect of each probiotic CM on TBHP-induced ROS production was assessed in a concentration dependent manner using the DCFDA Cellular ROS Detection Assay Kit. THP-1 monocytes were treated with TBHP and either vehicle (Vehicle control) or the indicated concentration of probiotic CM. Cells treated with vehicle in the absence of TBHP were included for comparative purposes (No TBHP control). (A) Lab4 CM used at concentrations of 8, 6 and 4  $\mu\text{g/mL}$ . (B) Lab4b CM used at concentrations of 1.5, 1 and 0.5  $\mu\text{g/mL}$ . (C) CUL66 CM used at concentrations of 5, 4 and 3  $\mu\text{g/mL}$ . ROS production is displayed as fold-change to the Vehicle control which was arbitrarily set to 1. Data are presented as mean  $\pm$  SEM from five independent experiments. Statistical analysis was performed using a One-way ANOVA with Dunnett T3 post-hoc test where \*\*  $p < 0.01$ , \*\*\*  $p < 0.001$ .

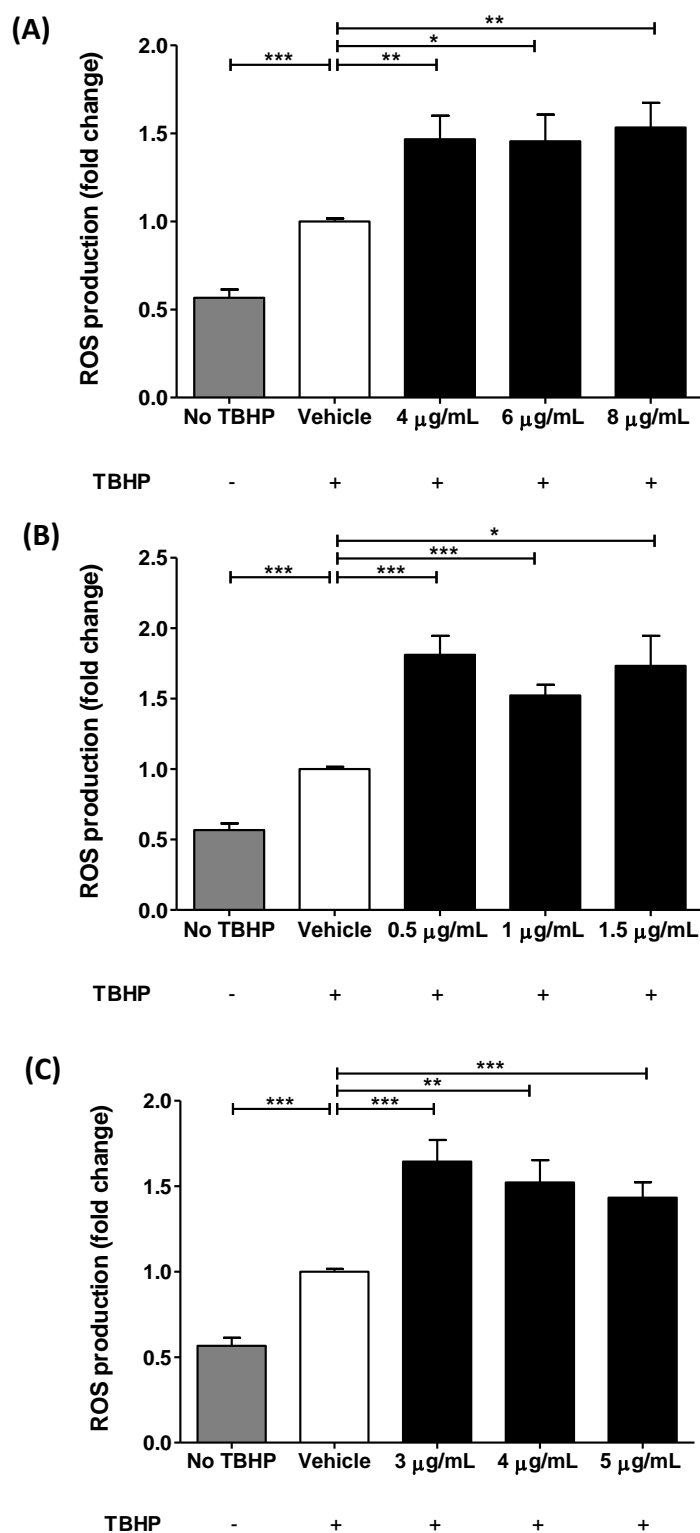


**Figure 3.11 - Probiotic CM increases TBHP-induced ROS production in THP-1 macrophages.** The effect of each probiotic CM on TBHP-induced ROS production was assessed in a concentration dependent manner using the DCFDA Cellular ROS Detection Assay Kit. THP-1 macrophages were treated with TBHP and either vehicle (Vehicle control) or the indicated concentration of probiotic CM. Cells treated with vehicle in the absence of TBHP were included for comparative purposes (No TBHP control). (A) Lab4 CM used at concentrations of 8, 6 and 4 µg/mL. (B) Lab4b CM used at concentrations of 1.5, 1 and 0.5 µg/mL. (C) CUL66 CM used at concentrations of 5, 4 and 3 µg/mL. ROS production is displayed as fold-change to the Vehicle control which was arbitrarily set to 1. Data are presented as mean  $\pm$  SEM from five independent experiments. Statistical analysis was performed using a One-way ANOVA with Dunnett T3 post-hoc test where \*  $p < 0.05$ , \*\*  $p < 0.01$  and \*\*\*  $p < 0.001$ .

Subsequently, once a protein concentration was selected to which to normalise all future CM, the assay was repeated for comparison of the activity of each CM. For both THP-1 monocytes and macrophages, ROS production was increased in the presence of TBHP compared to vehicle alone ( $p < 0.001$ ). In agreement with results obtained during the dose dependent investigations, no significant change in ROS production was observed in THP-1 monocytes (Figure 3.12), while ROS production was significantly increased in THP-1 macrophages with Lab4 (2.4-fold;  $p < 0.001$ ), Lab4b (1.66-fold;  $p < 0.001$ ) and CUL66 (2.5-fold;  $p = 0.028$ ) treatment (Figure 3.13).

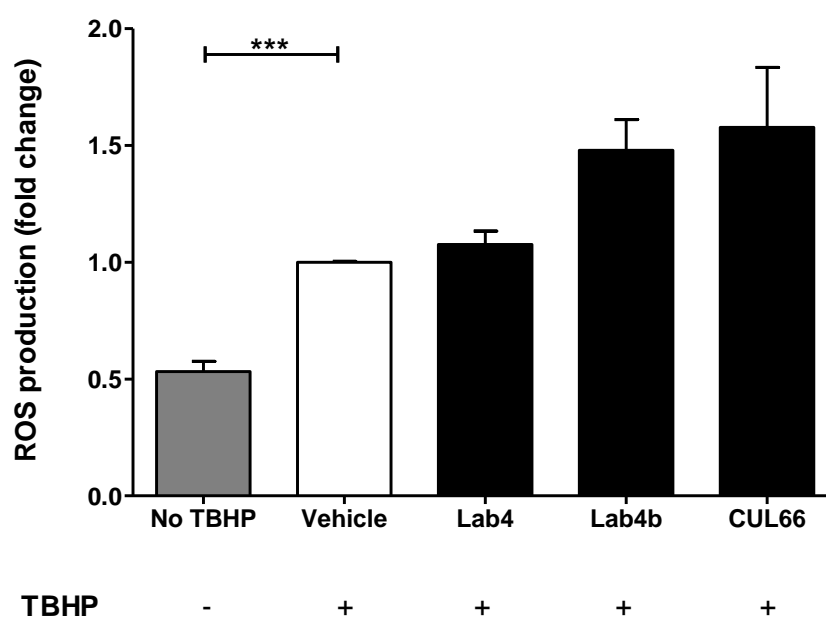


**Figure 3.12 – The effect of probiotic CM on TBHP-induced ROS production in THP-1 monocytes.** The effect of each probiotic CM on TBHP-induced ROS production was assessed using the DCFDA Cellular ROS Detection Assay Kit. THP-1 monocytes were treated with TBHP and either vehicle (Vehicle control) or Lab4 (8  $\mu\text{g}/\text{mL}$ ), Lab4b (1.5  $\mu\text{g}/\text{mL}$ ) or CUL66 (5  $\mu\text{g}/\text{mL}$ ) CM. Cells treated with vehicle in the absence of TBHP were included for comparative purposes (No TBHP control). ROS production is displayed as fold-change relative to the Vehicle control which was arbitrarily set to 1. Data are presented as mean  $\pm$  SEM from three independent experiments. Statistical analysis was performed using a One-way ANOVA with Dunnett T3 post-hoc test where \*\*\*  $p < 0.001$ .

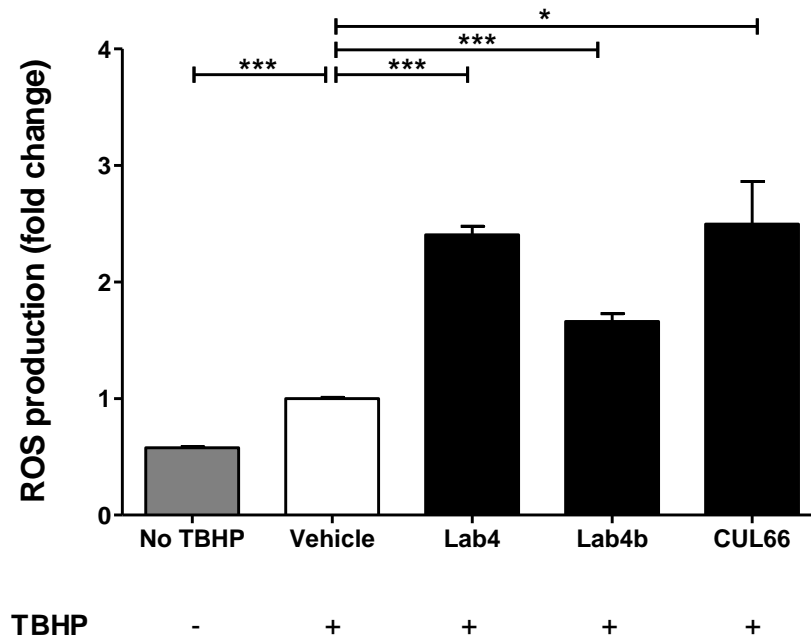


**Figure 3.13 - Probiotic CM increases TBHP-induced ROS production in THP-1 macrophages.** The effect of each probiotic CM on TBHP-induced ROS production was assessed using the DCFDA Cellular ROS Detection Assay Kit. THP-1 monocytes were treated with TBHP and either vehicle (Vehicle control) or Lab4 (8  $\mu\text{g}/\text{mL}$ ), Lab4b (1.5  $\mu\text{g}/\text{mL}$ ) or CUL66 (5  $\mu\text{g}/\text{mL}$ ) CM. Cells treated with vehicle in the absence of TBHP were included for comparative purposes (No TBHP control). ROS production is displayed as fold-change relative to the Vehicle control which was arbitrarily set to 1. Data are presented as mean  $\pm$  SEM from three independent experiments. Statistical analysis was performed using a One-way ANOVA with Dunnett T3 post-hoc test where \*\*\*  $p < 0.001$ , \*  $p < 0.05$ .

### 3.3.5 Macropinocytosis was attenuated in the presence of several different concentrations of probiotic CM

The effect of each probiotic CM on macropinocytosis was assessed using the fluorescent dye lucifer yellow as described in Section 2.7.2. Initially, the assay was performed in a dose dependent manner using protein concentrations of 8, 6 and 4  $\mu\text{g}/\text{mL}$  for Lab4 CM; 1.5, 1 and 0.5  $\mu\text{g}/\text{mL}$  for Lab4b CM; and 5, 4 and 3  $\mu\text{g}/\text{mL}$  for CUL66 CM. As shown in Figure 3.14, macropinocytosis was inhibited by each probiotic CM at all concentrations, with a greater effect generally obtained at the higher concentration. Treatment with Lab4 CM resulted in reductions of 78% ( $p < 0.001$ ), 76% ( $p < 0.001$ ) and 73% ( $p < 0.001$ ) with concentrations of 8, 6 or 4  $\mu\text{g}/\text{mL}$  respectively. Similarly, Lab4b treatment resulted in reductions of 83% ( $p < 0.001$ ), 73% ( $p < 0.001$ ) and 66% ( $p < 0.001$ ) with concentrations of 1.5, 1 or 0.5  $\mu\text{g}/\text{mL}$  respectively. In the presence of CUL66 CM, macropinocytosis was reduced by 76% ( $p < 0.001$ ), 72% ( $p < 0.001$ ) and 66% ( $p < 0.001$ ) with concentrations of 5, 4 or 3  $\mu\text{g}/\text{mL}$  respectively.

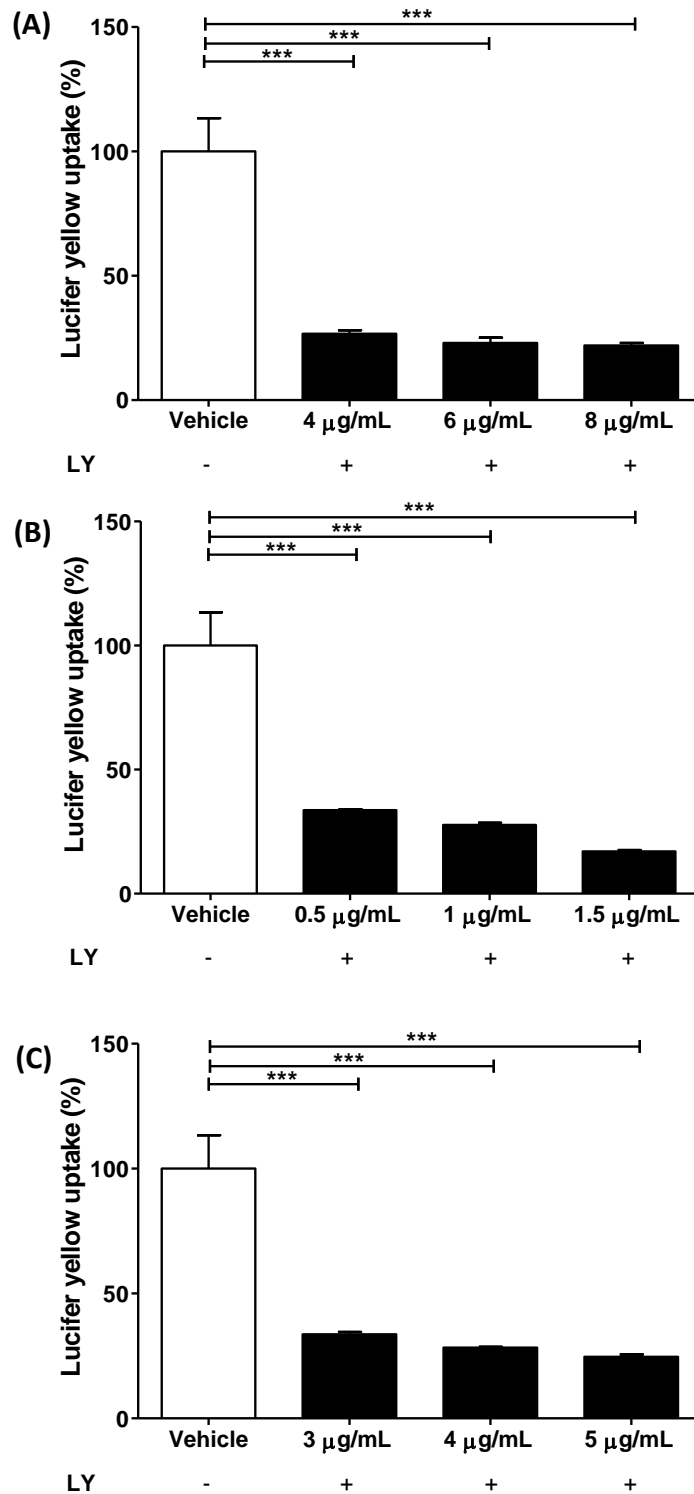


**Figure 3.14 - Probiotic CM attenuates macropinocytosis in THP-1 macrophages.** The effect of probiotic CM on macropinocytosis in macrophages was determined following incubation with LY and either vehicle (Vehicle control) or the indicated concentration of probiotic CM. (A) Lab4 CM used at concentrations of 8, 6 and 4 μg/mL; (B) Lab4b CM used at concentrations of 1.5, 1 and 0.5 μg/mL; and (C) CUL66 CM used at concentrations of 5, 4 and 3 μg/mL. Macropinocytosis was determined as a percentage relative to the vehicle control which was arbitrarily set to 100% following background subtraction. Data are presented as mean ± SEM from three independent experiments. Statistical analysis was performed using a One-way ANOVA with Dunnett 2-sided post-hoc test where \*\*\*  $p < 0.001$ .

Subsequently, once a protein concentration was selected to which to normalise all future CM, the assay was repeated for comparison of the activity of each probiotic CM. In agreement with results of dose dependent investigations, macropinocytosis was significantly attenuated in the presence of Lab4, Lab4b and CUL66 CM by 72% ( $p < 0.001$ ), 78% ( $p < 0.001$ ) and 71% ( $p < 0.001$ ) respectively (Figure 3.15).

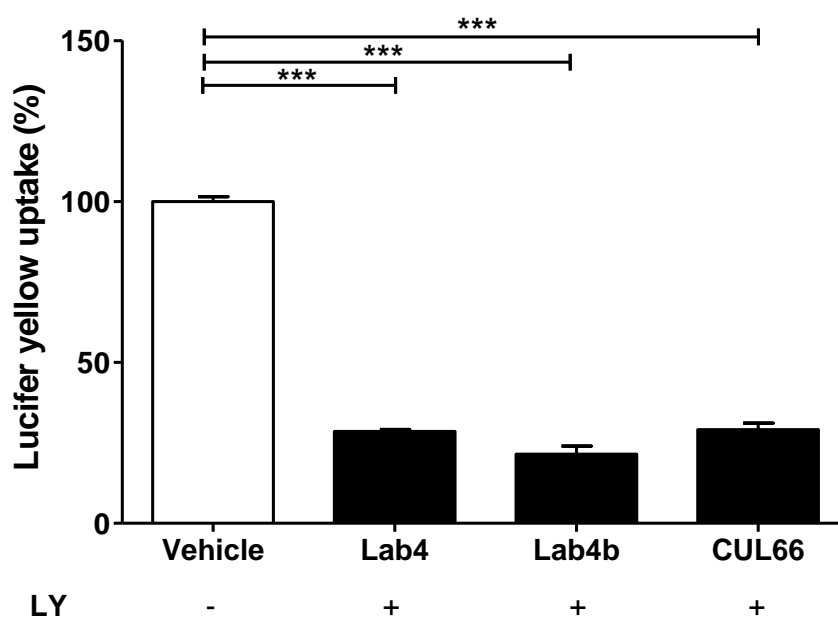


**Figure 3.15 - Probiotic CM attenuates macropinocytosis in THP-1 macrophages.** The effect of probiotic CM on macropinocytosis in THP-1 macrophages was determined following incubation with LY and either vehicle (Vehicle control) or Lab4 (8  $\mu\text{g}/\text{mL}$ ), Lab4b (1.5  $\mu\text{g}/\text{mL}$ ) or CUL66 (5  $\mu\text{g}/\text{mL}$ ) CM. Macropinocytosis was determined as a percentage relative to the Vehicle control which was arbitrarily set to 100% following background subtraction. Data are presented as mean  $\pm$  SEM from three independent experiments. Statistical analysis was performed using a One-way ANOVA with Dunnett 2-sided post-hoc test where \*\*\*  $p < 0.001$ .

### 3.3.6 Probiotic CM has a strain-specific effect on mitochondrial function

The effect of probiotic CM on mitochondrial function was assessed in THP-1 macrophages treated with vehicle or probiotic CM using the Agilent Seahorse Mito Stress Test (Section 2.4.6), where OCR was measured in response to the serial injection of oligomycin, FCCP and rotenone/antimycin (Rot/Ant) at 15, 34 and 54 minutes respectively (Figure 3.16). For each experiment a consistent protein concentration was confirmed across all samples. OCR values were then exported to Excel and used to determine the effect of probiotic CM on key parameters as follows (Figure 3.17):



- Basal respiration; significant increase with Lab4 ( $p = 0.042$ ) and CUL66 ( $p = 0.014$ ) CM, no significant change with Lab4b CM;
- ATP production; significant increase with CUL66 CM ( $p = 0.034$ ), no significant change with Lab4 or Lab4b CM;
- Maximal respiration; significant increase with Lab4 ( $p = 0.027$ ) and CUL66 ( $p = 0.003$ ) CM, no significant change with Lab4b CM;
- Spare respiratory capacity; significant increase with CUL66 CM ( $p = 0.002$ ), no significant change with Lab4 or Lab4b CM;
- Proton leak; no significant change with Lab4, Lab4b or CUL66 CM.
- Non-mitochondrial respiration; significant increase with Lab4 ( $p = 0.029$ ), no significant change with Lab4b or CUL66 CM.

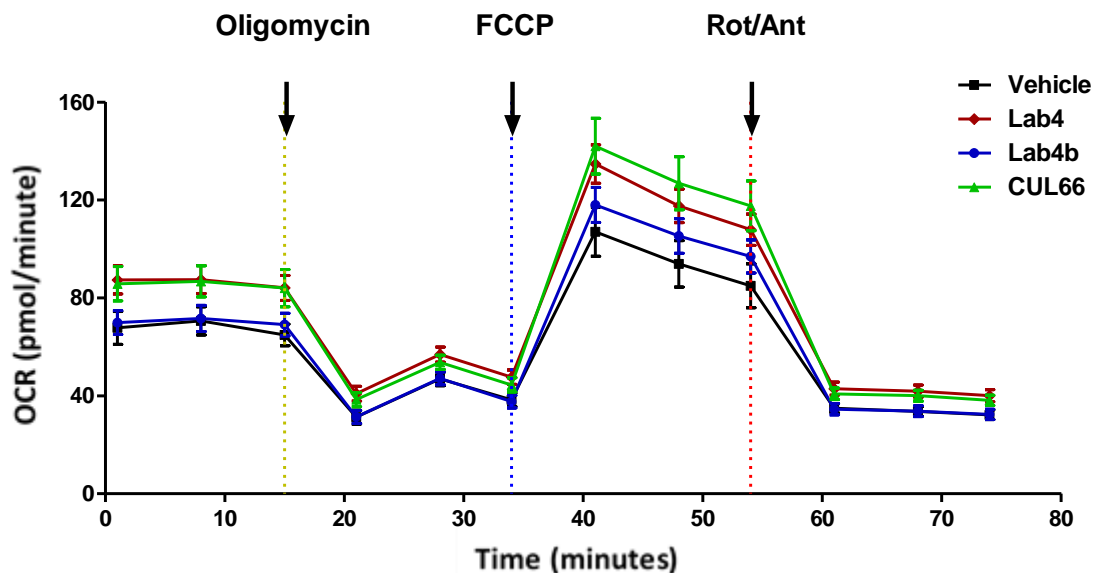


**Figure 3.16 - Oxygen consumption rate measured following the serial injection of respiration modulators.** THP-1 macrophages were treated with either vehicle control or probiotic CM and OCR measured at intervals following the injection of Oligomycin at 15 minutes, FCCP at 34 minutes and Rot/Ant at 54 minutes. Black square, Vehicle; red diamond, Lab4; blue circle, Lab4b; green triangle, CUL66. Data are presented as mean OCR  $\pm$  SEM from three independent experiments. Abbreviations: FCCP, carbonyl cyanide-4 (trifluoromethoxy) phenylhydrazone; Rot/Ant, Rotenone plus antimycin A.

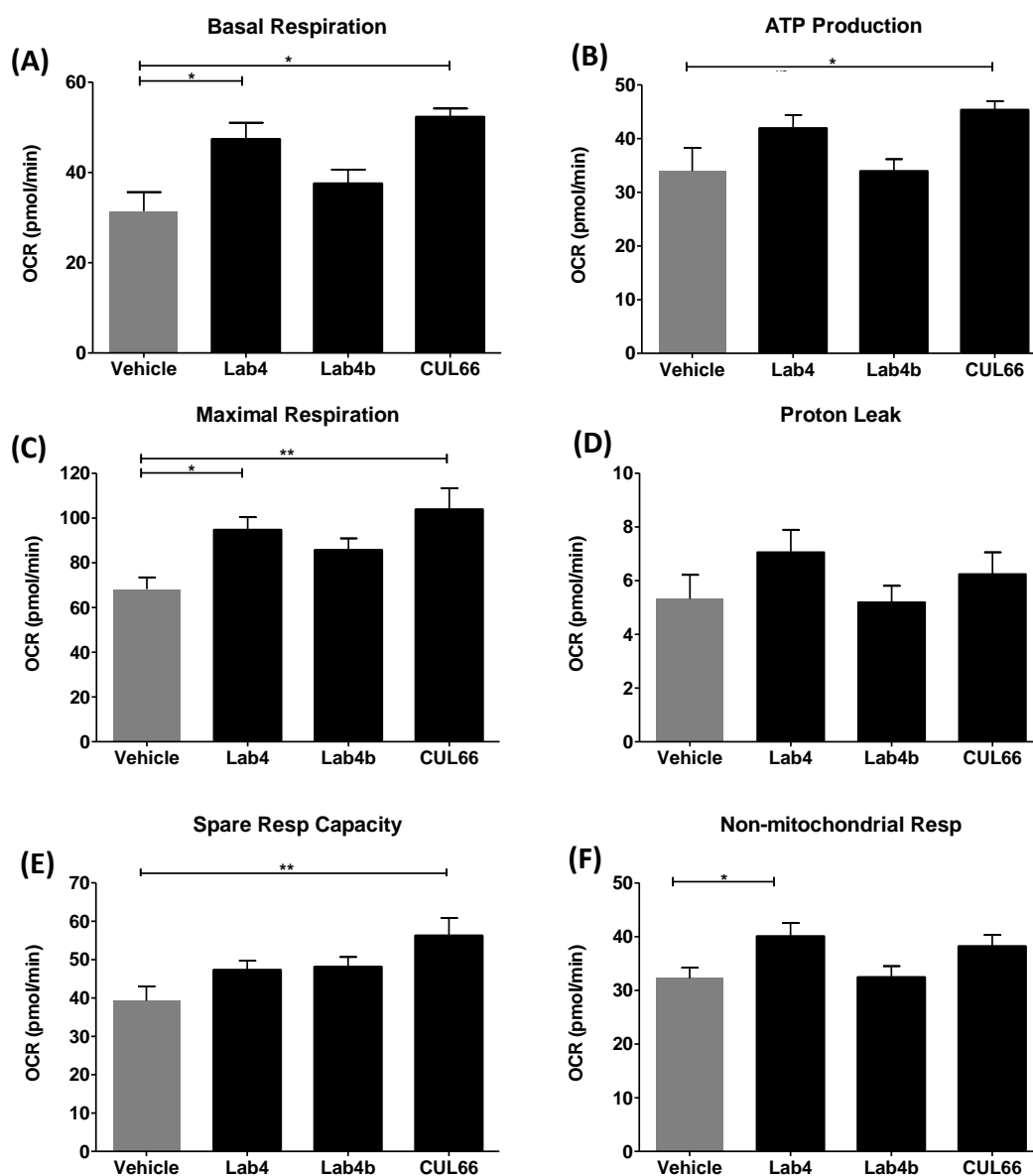


**Figure 3.17 - Probiotic CM has strain specific effects on mitochondrial function.** THP-1 macrophages were treated with either vehicle control, Lab4 (8  $\mu\text{g}/\text{mL}$ ), Lab4b (1.5  $\mu\text{g}/\text{mL}$ ) or CUL66 (5  $\mu\text{g}/\text{mL}$ ) CM and key parameters of respiration assessed using the Seahorse Cell Mito Stress Test. Data are presented as mean OCR  $\pm$  SEM from three independent experiments. Statistical analysis was performed using a One-way ANOVA and Dunnett T3 post-hoc test where \* $p$  < 0.05 and \*\* $p$  < 0.01.

### 3.3.7 Phagocytic activity of THP-1 macrophages was enhanced in the presence of probiotic CM

The effect of each probiotic CM on phagocytosis was assessed in THP-1 macrophages using the Vybrant Phagocytosis Assay Kit as described in Section 2.4.7. Phagocytosis was calculated as a percentage relative to the vehicle control which was set to 100% after background subtraction. Treatment with Lab4 CM resulted in a 1.4-fold increase ( $p$

<0.001) in phagocytosis, Lab4b in a 1.6-fold increase ( $p = 0.035$ ) and CUL66 in a 1.3-fold increase ( $p = 0.025$ ) relative to the vehicle control (Figure 3.18).

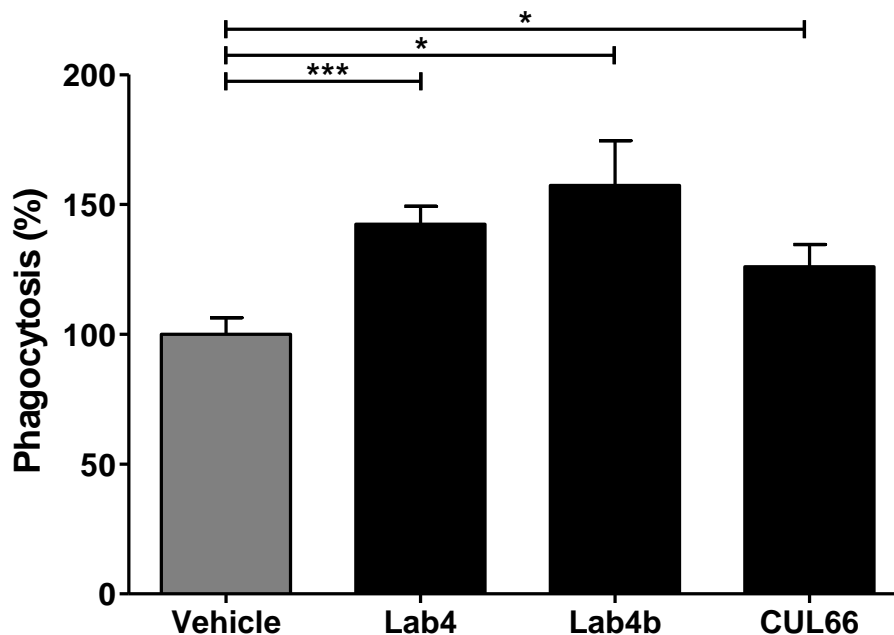


**Figure 3.18 - Probiotic CM increases phagocytosis in THP-1 macrophages.** The effect of CM on phagocytic activity was assessed in THP-1 macrophages treated with Vehicle or Lab4 (8  $\mu\text{g}/\text{mL}$ ), Lab4b (1.5  $\mu\text{g}/\text{mL}$ ) or CUL66 (5  $\mu\text{g}/\text{mL}$ ) CM, using the Vybrant Phagocytosis Assay Kit. Phagocytosis was calculated as a percentage of the vehicle control after background subtraction, and presented relative to Vehicle which was set to 100%. Data are presented as mean  $\pm$  SEM from three independent experiments. Statistical analysis was performed using a One-way ANOVA and Dunnett T3 post-hoc test where \*  $p < 0.05$  and \*\*\*  $p < 0.001$ .

### 3.3.8 Probiotic CM can attenuate proliferation of key cell types involved in atherogenesis

The effect of probiotic CM on cellular proliferation was assessed in a number of cell types involved in atherosclerosis, including monocytes, macrophages and VSMCs using representative THP-1 monocytes, THP-1 macrophages and HASMCs respectively. Several methods were used as detailed in Section 2.4.2 and illustrated in Figure 3.4.

#### 3.3.8.1 THP-1 monocytes

THP-1 monocytes treated with either vehicle or probiotic CM were counted daily for 7 days and proliferation determined as the percentage change in cell number. Linear regression was performed, and the gradient of the slopes compared by One-way ANOVA using GraphPad Prism software (Figure 3.19). Results show a significant reduction in

monocyte proliferation over the 7-day period when treated with Lab4 CM ( $p < 0.05$ ), Lab4b CM ( $p < 0.05$ ) or CUL66 CM ( $p < 0.001$ ) compared to the vehicle control. In addition, the change in cell number was assessed on individual days 2, 5 and 7 and proliferation determined as percentage change in cell number relative to the vehicle control. On day 2, treatment with either Lab4, Lab4b or CUL66 CM had resulted in non-significant reductions of 33%, 36% and 24% respectively (Figure 3.20A). By day 5, treatment with Lab4, Lab4b or CUL66 CM resulted in significant reductions of 63% ( $p < 0.001$ ), 49% ( $p = 0.001$ ) and 59% ( $p < 0.001$ ) respectively (Figure 3.20B). By day 7, treatment with Lab4 or Lab4b showed non-significant reductions of 63% and 49% respectively, while CUL66 CM showed a significant reduction of 59% ( $p = 0.023$ ) (Figure 3.20C).

### 3.3.8.2 THP-1 macrophages

THP-1 macrophages were treated with either vehicle or probiotic CM for 48 hours and cellular proliferation assessed by crystal violet staining as described in Section 2.4.2. To control for any changes in cell viability, the LDH assay was performed simultaneously as described in Section 2.4.1. Proliferation was determined as the change in cell number from day 0, where the cell number was proportional to the level of crystal violet staining. Treatment with Lab4, Lab4b or CUL66 CM significantly attenuated proliferation of THP-1 macrophages by 49% ( $p < 0.001$ ), 35% ( $p < 0.001$ ) and 28% ( $p < 0.001$ ) respectively (Figure 3.21A). No detrimental effect on cell viability was observed following 48-hour treatment with probiotic CM (Figure 3.21B). Subsequently, the BrdU Labeling and Detection Kit was used to assess the rate of proliferation after 48-hour treatment with probiotic CM. Lab4 CM significantly reduced the rate of proliferation by 33% ( $p = 0.002$ ), whereas Lab4b treatment resulted in a trend of reduction of 14% ( $p = 0.053$ ) and CUL66 had no effect (Figure 3.22).

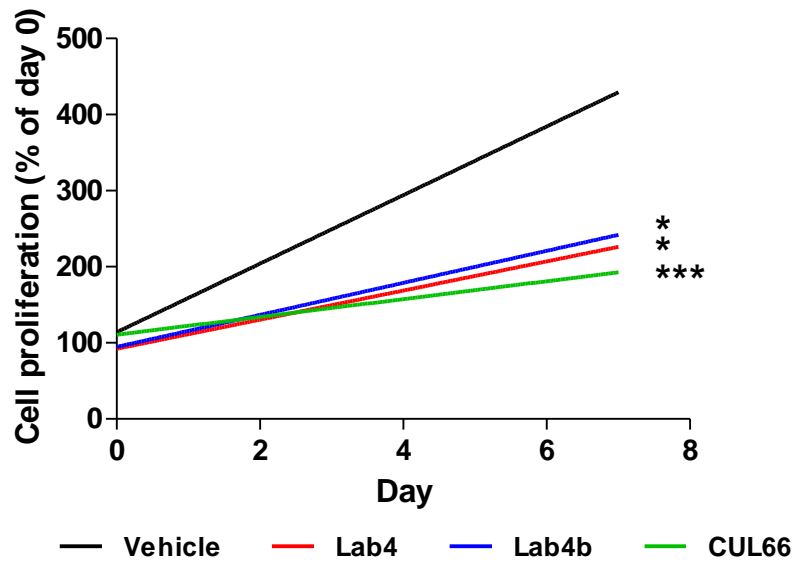


**Figure 3.19 - Probiotic CM reduces the proliferation of THP-1 monocytes over a 7-day period.** THP-1 monocytes treated with either vehicle control or probiotic CM were counted daily over a 7-day period. Data are presented as linear regression of percentage change in cell number from three independent experiments. Linear regression was performed using GraphPad Prism followed by a One-way ANOVA with Dunnett (2-sided) post-hoc test where \*  $p < 0.05$  and \*\*\*  $p < 0.001$ .

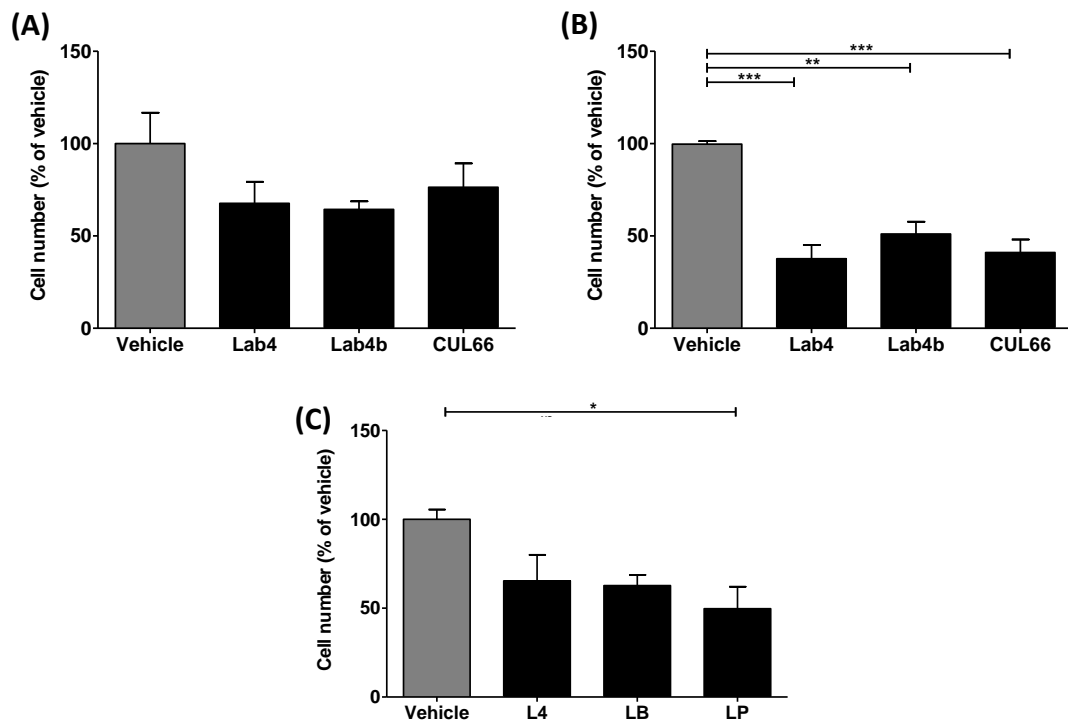


**Figure 3.20 - Probiotic CM reduces the proliferation of THP-1 monocytes over a 7-day period.** THP-1 monocytes were treated with either vehicle control or Lab4 (8  $\mu\text{g}/\text{mL}$ ), Lab4b (1.5  $\mu\text{g}/\text{mL}$ ) or CUL66 (5  $\mu\text{g}/\text{mL}$ ) CM and the cell number counted daily for 7 days. Cell numbers are displayed as a percentage relative to the Vehicle control at (A) day 2, (B) day 5 and (C) day 7, where Vehicle control was set to 100%. Data are presented as mean  $\pm$  SEM from three independent experiments. Statistical analysis was performed using a One-way ANOVA and Dunnett (2-sided) post-hoc test where \*  $p < 0.05$ , \*\*  $p < 0.01$  and \*\*\*  $p < 0.001$ .

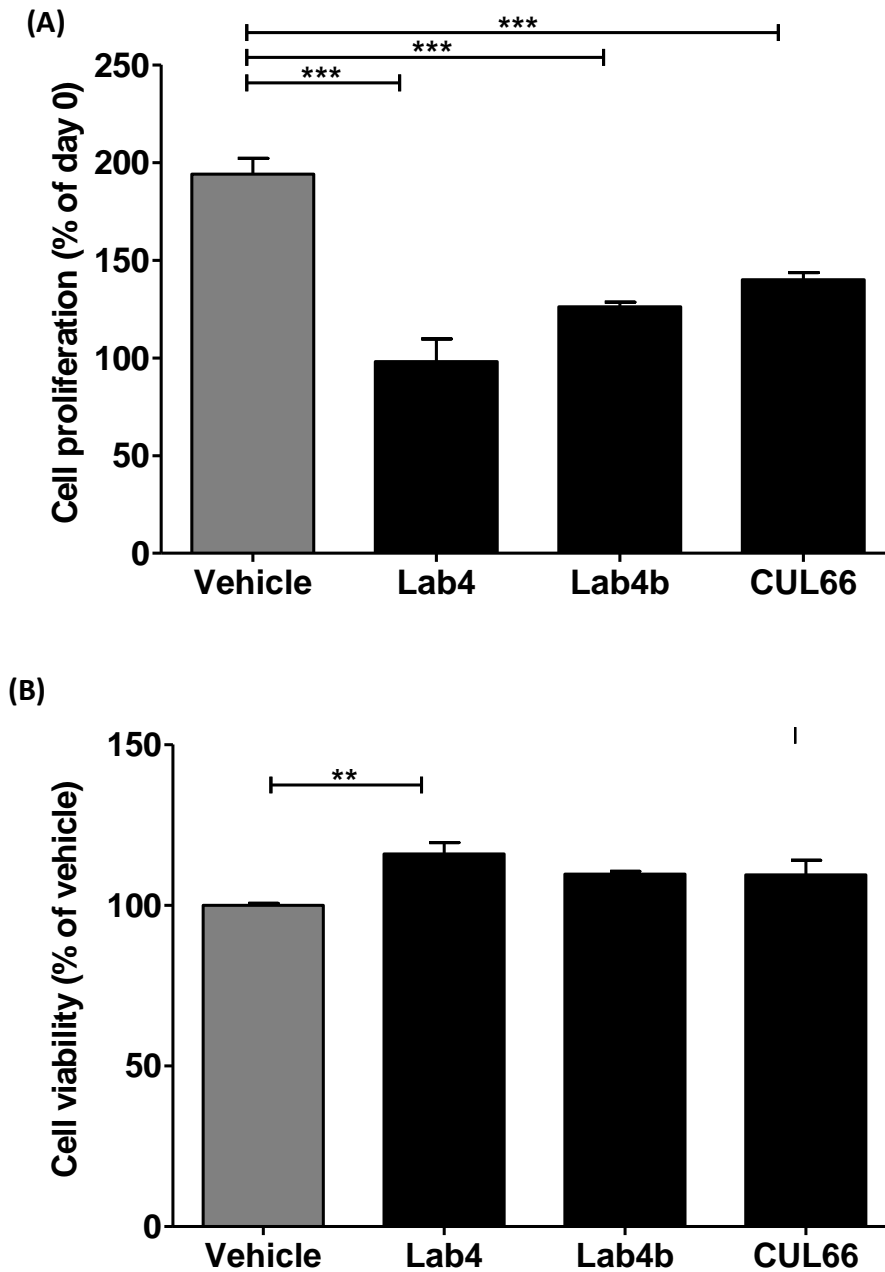


**Figure 3.21 - Proliferation of macrophages was reduced in the presence of probiotic CM.** THP-1 macrophages were treated for 48 hours with either the vehicle control or Lab4 (8 µg/mL), Lab4b (1.5 µg/mL) or CUL66 (5 µg/mL) CM. (A) Change in proliferation from day 0 was determined as a percentage relative to the vehicle control which was set to 100%. (B) Cell viability at end-point was assessed using the LDH Assay Kit, determined as a percentage relative to the vehicle control which was set to 100%. Data are presented as mean ± SEM from three independent experiments. Statistical analysis was performed using a One-way ANOVA and Dunnett T3 post-hoc test where \*\*  $p < 0.01$  and \*\*\*  $p < 0.001$ .

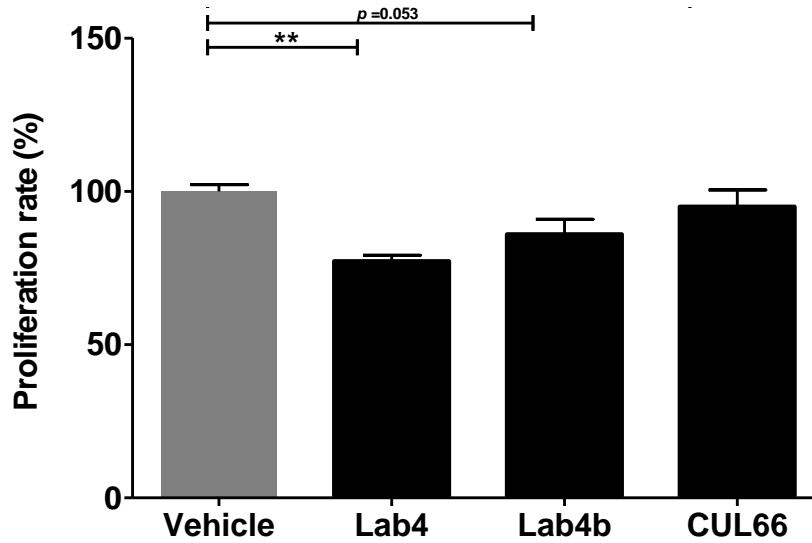


**Figure 3.22 - Probiotic CM has a strain-specific effect on the proliferation rate of THP-1 macrophages.** The proliferation rate of THP-1 macrophages was determined using the BrdU Labeling and Detection Kit following 48 hours treatment with either the vehicle control or Lab4 (8  $\mu\text{g}/\text{mL}$ ), Lab4b (1.5  $\mu\text{g}/\text{mL}$ ) or CUL66 (5  $\mu\text{g}/\text{mL}$ ) CM. Proliferation rate was determined as a percentage of the vehicle control which was set to 100%. Data are presented as mean  $\pm$  SEM from three independent experiments. Statistical analysis was performed using a One-way ANOVA and Dunnett (2-sided) post-hoc test where \*\*  $p < 0.01$ .

### 3.3.8.3 HASMCs

HASMCs were treated with either vehicle or probiotic CM and cellular proliferation assessed by crystal violet staining over a 7-day period. To ensure that the results were not affected by changes in cell viability, the LDH assay was performed on days 2, 5 and 7. Linear regression was performed followed by One-way ANOVA to compare percentage change in cell number for each probiotic CM or the vehicle control over the 7-day period (Figure 3.23). Results show a non-significant reduction in proliferation with Lab4 and Lab4b, whereas CUL66 treatment resulted in a trend of reduction ( $p = 0.08$ ). Figure 3.23 also shows the percentage change in cell numbers at day 7, where treatment with Lab4, Lab4b or CUL66 CM resulted in a 15% ( $p < 0.001$ ), 7% ( $p = 0.003$ ) and 16% ( $p < 0.001$ ) reduction in cell proliferation respectively (Figure 3.23B). Although CUL66 treatment showed a significant reduction in cell viability ( $p < 0.001$ ), this reduction was small and overall there was no detrimental effect on cell viability with either probiotic CM (Figure 3.23C). Subsequently, the BrdU Labeling and Detection Kit was used to assess the rate of proliferation after 2, 5 and 7 days treatment with probiotic CM. After 2 days treatment with Lab4b CM, the proliferation rate was reduced significantly by 59% ( $p < 0.001$ ) (Figure 3.24). No change was seen following treatment with Lab4 or CUL66 CM.

After 5 days, no significant change was seen with any CM treatment. By 7 days, Lab4 and Lab4b treatment resulted in no change, whereas CUL66 treatment resulted in a 28% ( $p = 0.010$ ) increase in proliferation rate.

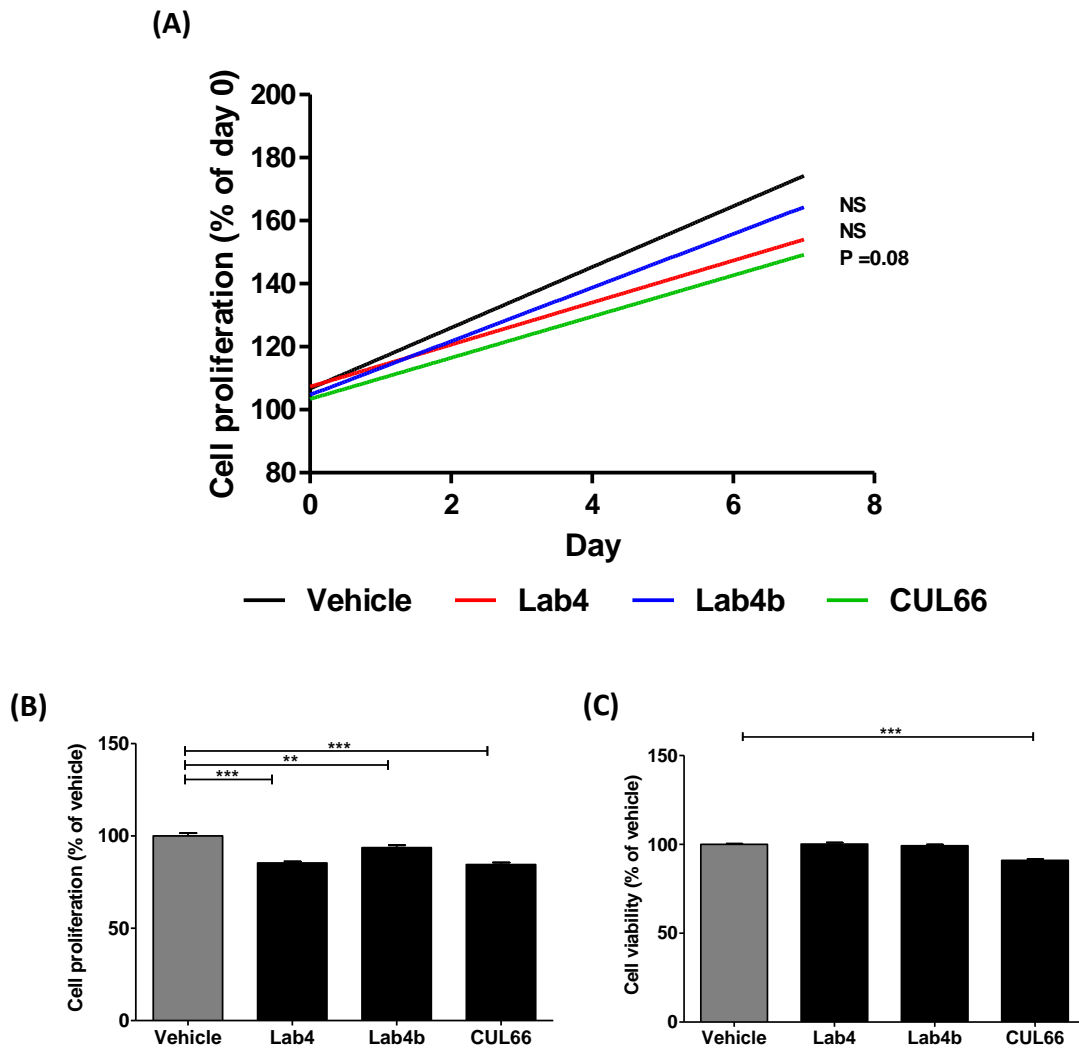


**Figure 3.23 - Probiotic CM reduces the proliferation of HASMCs over a 7-day period.** HASMCs were treated with either vehicle or Lab4 (8  $\mu\text{g}/\text{mL}$ ), Lab4b (1.5  $\mu\text{g}/\text{mL}$ ) or CUL66 (5  $\mu\text{g}/\text{mL}$ ) CM and cellular proliferation assessed by crystal violet staining over a 7-day period. (A) Linear regression of percentage change in cell numbers from day 0. (B) Cell proliferation at day 7 determined by crystal violet staining method and displayed as a percentage relative to the vehicle control which was set to 100%. (C) Cell viability at day 7 determined using the LDH Assay Kit, determined as a percentage relative to the vehicle control which was set to 100%. Data are presented as mean  $\pm$  SEM from three independent experiments. Statistical analysis was performed using a One-way ANOVA with Dunnett (2-sided) post-hoc test where \*\*  $p < 0.01$ ; \*\*\*  $p < 0.001$ .



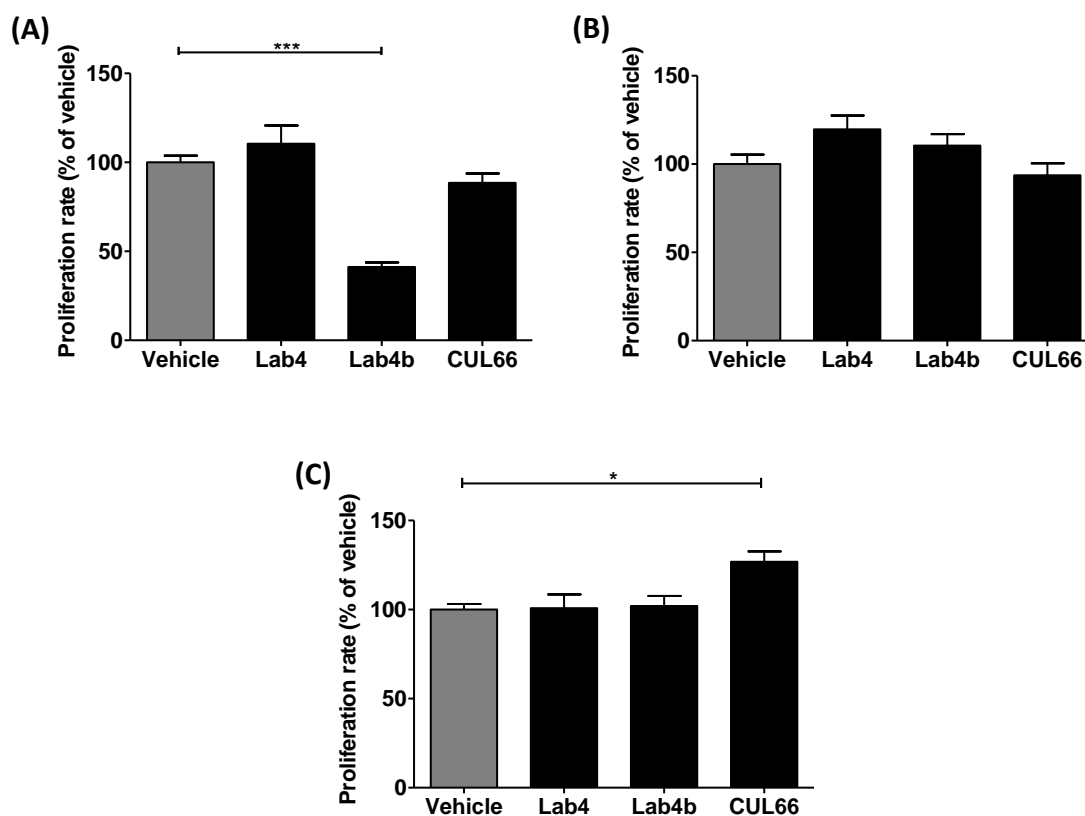


**Figure 3.24 - Probiotic CM has a strain-specific effect on the proliferation rate of HASMCs.** HASMCs were treated for (A) 2, (B) 5 or (C) 7 days with either vehicle control or Lab4 (8  $\mu\text{g}/\text{mL}$ ), Lab4b (1.5  $\mu\text{g}/\text{mL}$ ) or CUL66 (5  $\mu\text{g}/\text{mL}$ ) CM. The proliferation rate was then measured using the BrdU Labeling and Detection Kit, where data are presented as a percentage relative to the vehicle control which was set to 100%. Data are presented as mean  $\pm$  SEM from three independent experiments. Statistical analysis was performed using a One-way ANOVA and Dunnett T3 (A) or Dunnett (2-sided) (B) and (C) post-hoc tests where \*  $p < 0.05$  and \*\*\*  $p < 0.001$ .

### 3.3.9 Probiotic CM displays a strain-specific effect on the invasion of HASMCs

The effect of probiotic CM on smooth muscle cell invasion was assessed in HASMCs using a modified Boyden chamber method as described in Section 2.4.5. Briefly, HASMCs were treated with either vehicle control or probiotic CM and allowed to migrate in response to PDGF-BB. Cells treated with vehicle control in the absence of PDGF-BB were included for comparative purposes (No PDGF control). The number of migrated cells were counted and averaged from five high power fields (HPF), and expressed as fold-change to the vehicle control (Figure 3.25). HASMC invasion was significantly attenuated with Lab4 and Lab4b CM treatment by 0.48-fold ( $p < 0.001$ ) and 0.5-fold ( $p < 0.001$ ) respectively, whereas treatment with CUL66 CM had no significant effect on SMC invasion (Figure 3.25).

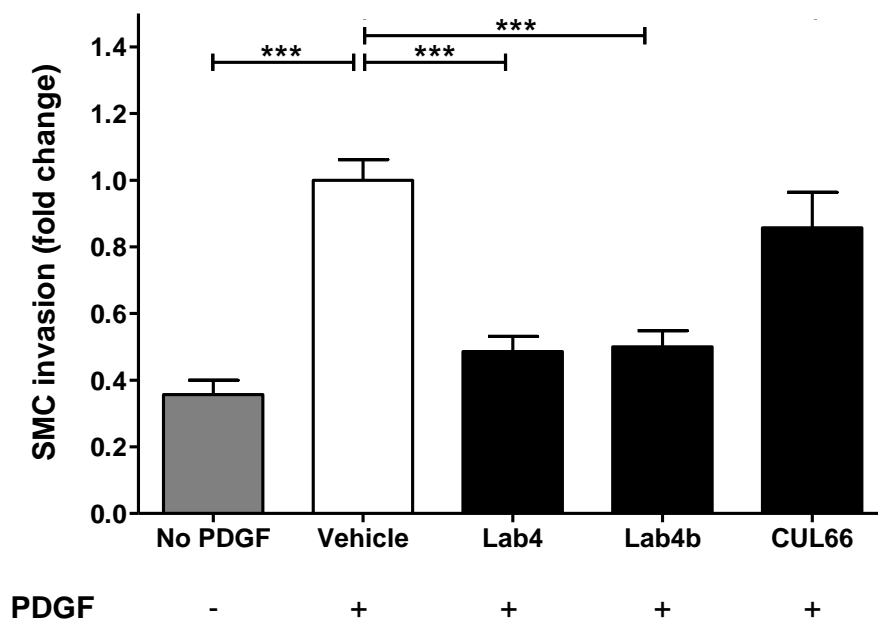


**Figure 3.25 - Invasion of HASMCs was attenuated in the presence of probiotic CM in a strain-specific manner.** The effect of probiotic CM on the invasion of VSMCs was assessed using HASMCs incubated with PDGF-BB and either vehicle control (Vehicle) or Lab4 (8  $\mu\text{g}/\text{mL}$ ), Lab4b (1.5  $\mu\text{g}/\text{mL}$ ) or CUL66 (5  $\mu\text{g}/\text{mL}$ ) CM. Cells incubated with the vehicle in the absence of PDGF-BB (No PDGF) were included for comparative purposes. The number of migrated cells were counted and averaged per five HPF, and presented as fold-change to the vehicle control which was arbitrarily set to 1.0. Data are presented as mean  $\pm$  SEM from three independent experiments. Statistical analysis was performed using a One-way ANOVA and Dunnett (2-sided) post-hot test where \*\*\*  $p < 0.001$ .

### 3.3.10 Activation of the NLRP3 inflammasome was enhanced in the presence of probiotic CM

The effect of probiotic CM on the activation of NLRP3 inflammasomes by cholesterol crystals was assessed in THP-1 macrophages using a standard ELISA protocol as outlined in Section 2.6.3. Treatment with Lab4, Lab4b or CUL66 CM resulted in a significant 47-fold ( $p < 0.001$ ), 29-fold ( $p = 0.001$ ) and 55-fold ( $p < 0.001$ ) induction of IL-1 $\beta$  production respectively (Figure 3.26).

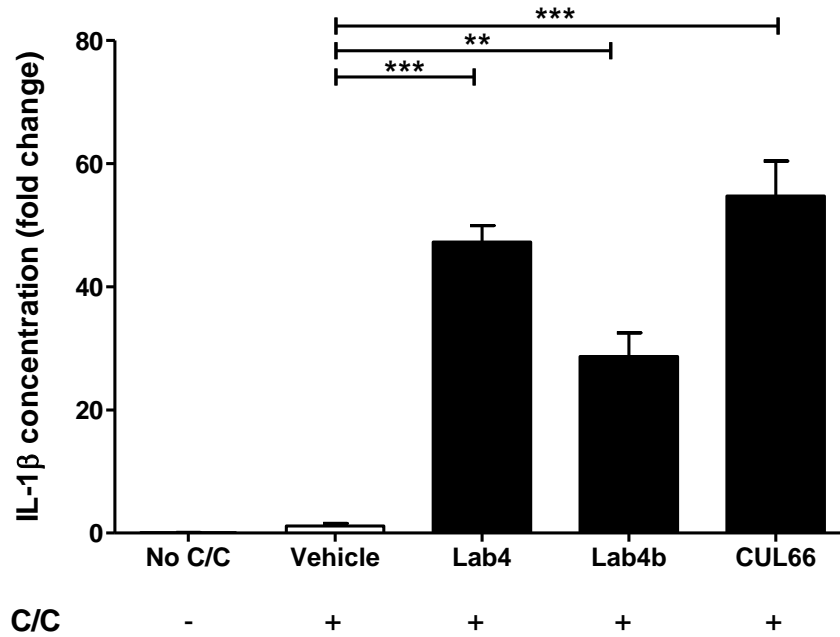


**Figure 3.26 - Inflammasome activation was significantly increased in the presence of probiotic CM.** THP-1 macrophages were stimulated with cholesterol crystals and treated with vehicle (Vehicle control) or Lab4 (8 µg/mL), Lab4b (1.5 µg/mL) or CUL66 (5 µg/mL) CM. Cells treated with vehicle control in the absence of cholesterol crystal stimulus (No C/C) were included for comparative purposes. IL-1β concentration was determined by ELISA and expressed as fold-change to the vehicle control which was arbitrarily set to 1. Data are presented as mean ± SEM from three independent experiments. Statistical analysis was performed using a One-way ANOVA with Dunnett (2-sided) post-hoc test where \*\* $p < 0.01$  and \*\*\* $p < 0.001$ . C/C, cholesterol crystals.

### 3.3.11 Probiotic CM displays a number of strain-specific effects on inflammatory gene expression in cytokine stimulated macrophages

The effect of probiotic CM on inflammatory gene expression was assessed in THP-1 macrophages stimulated with either IFN-γ (250 U/mL), IL-1β (1000 U/mL) or TNF-α (100 ng/mL) in the presence of vehicle control or probiotic CM. RNA was then extracted, reverse transcribed to cDNA and the expression levels of both MCP-1 and ICAM1 measured by qPCR as described in Section 2.5.

Macrophages showed a significant increase in the expression of both MCP-1 (86-fold;  $p < 0.001$ ) and ICAM1 (4.6-fold;  $p < 0.001$ ) with IFN-γ stimulus compared to vehicle alone (Figure 3.27A and B). Treatment of IFN-γ-stimulated macrophages with Lab4, Lab4b or CUL66 CM had no further effect on MCP-1 expression, whereas expression of ICAM1 was significantly increased by 2-fold (Lab4;  $p = 0.020$ ), 4.1-fold (Lab4b;  $p < 0.001$ ) and 2.4-fold (CUL66;  $p = 0.010$ ).

Following IL-1 $\beta$  stimulation, macrophages showed a significant increase in the expression of both MCP-1 (6-fold;  $p < 0.001$ ) and ICAM1 (4.5-fold;  $p < 0.001$ ) (Figure 3.27C and D). In the presence of Lab4b CM, IL-1 $\beta$ -induced expression of MCP-1 was significantly increased by 4.9-fold ( $p < 0.001$ ), whereas no significant change was observed in the presence of Lab4 or CUL66 CM. IL-1 $\beta$ -induced expression of ICAM1 showed no significant change with any probiotic CM treatments.

In vehicle treated macrophages, TNF- $\alpha$  stimulus had no effect on MCP-1 expression but resulted in a 1.9-fold increase in ICAM1 expression ( $p = 0.001$ ) (Figure 3.27E and F). The TNF- $\alpha$ -induced expression of MCP-1 was significantly increased by 3.2-fold with Lab4b treatment ( $p < 0.001$ ), whereas no significant changes were observed in the presence of Lab4 or CUL66 CM. The TNF- $\alpha$ -induced expression of ICAM1 was significantly reduced with Lab4 and CUL66 CM by 1.9-fold ( $p = 0.001$ ) and 2.3-fold ( $p < 0.001$ ) respectively, and non-significantly reduced by 1.5-fold ( $p = 0.075$ ) in the presence of Lab4b.

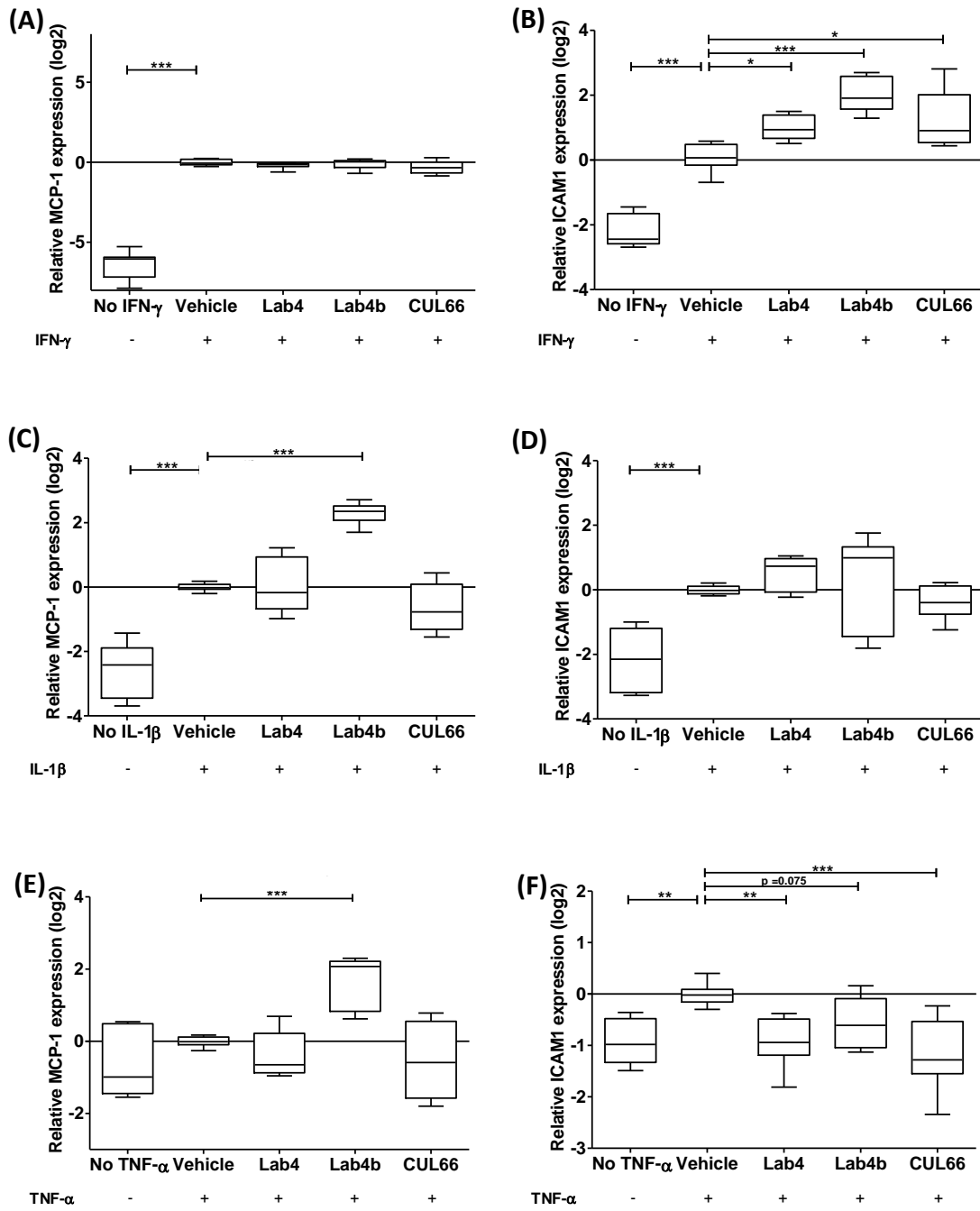


**Figure 3.27 - Probiotic CM has strain specific effects on inflammatory gene expression in cytokine stimulated macrophages.** IFN- $\gamma$  (A and B), IL-1 $\beta$  (C and D) or TNF- $\alpha$  (E and F) stimulated THP-1 macrophages were treated with either vehicle control (Vehicle) or Lab4 (8  $\mu$ g/mL), Lab4b (1.5  $\mu$ g/mL) or CUL66 (5  $\mu$ g/mL) CM. Unstimulated cells treated with the vehicle control were included for comparative purposes (No cytokine). The expression of MCP-1 and ICAM1 was determined by qPCR using the  $\Delta\Delta C_T$  method. Data are presented as box and whisker plots of log<sub>2</sub> fold-change in expression relative to the vehicle control, where whiskers represent min to max fold-change from three independent experiments. Statistical analysis was performed using a One-way ANOVA and Dunnett T3 post-hoc test where \* $p$  < 0.05, \*\* $p$  < 0.01 and \*\*\* $p$  < 0.001.

### 3.4 Discussion

Prior to the start of *in vitro* investigations, it was decided to limit batch effects by normalising CM to the same protein concentration throughout all experiments. The maximum protein concentration at which cells remain viable was determined as 8 µg/mL for Lab4, 1.5 µg/mL for Lab4b and 5 µg/mL for CUL66. Although Lab4b and CUL66 showed no detrimental effect on cell viability, higher concentrations of Lab4 CM clearly had a detrimental effect on cell survival (Figure 3.6), highlighting the importance of assessing cell viability prior to beginning *in vitro* investigations, and maintaining confidence in the data obtained. Furthermore, the total protein concentration was noted to vary between batches of CM, despite the same mass of starting probiotics, highlighting the importance of controlling for batch effects and normalising treatment throughout all experiments. Initial investigations were performed in a dose-dependent manner to determine an optimal concentration for each probiotic CM to continue for the remaining *in vitro* studies.

#### 3.4.1 Probiotic CM attenuates MCP-1-stimulated migration of monocytes

Results show that the migration of monocytes was significantly reduced at all tested concentrations of each probiotic CM (Figure 3.8). In the comparison of probiotic activity, each probiotic CM significantly attenuated MCP-1-stimulated monocyte migration (Figure 3.9). These findings suggest a role for probiotic treatment in the inhibition of monocyte migration, an important process in the initiation of atherosclerosis. Given that previous studies have shown the ability of probiotic bacteria to downregulate MCP-1 expression (Chen *et al.*, 2017), future work may involve more detailed investigation of the effects of probiotic CM on pathways involved in the induced expression of MCP-1 and its actions.

#### 3.4.2 Measurement of ROS as an indicator of antioxidant capacity

Treatment with either Lab4, Lab4b or CUL66 CM had no significant effect on TBHP-induced cellular ROS production in THP-1 monocytes (Figures 3.10 and 3.12). In contrast, in THP-1 macrophages ROS production was significantly increased with all

concentrations of each probiotic CM (Figures 3.11 and 3.13). Overall, results suggest that in the current setup, probiotic CM has no beneficial effect on TBHP-induced ROS production. However, while the reduction of ROS by antioxidant agents has previously been considered beneficial in atherosclerosis, more elaborate current therapeutic strategies target not only excess ROS but a large variety of modulators of oxidative stress (Kattoor *et al.*, 2017; Saso *et al.*, 2017) such as mitochondrial ROS (Mercer *et al.*, 2012), endothelial nitric oxide synthase (eNOS) (Antonopoulos *et al.*, 2012) or the major ROS producing enzymes NADPH oxidases (NOX) (Kattoor *et al.*, 2017; Li *et al.*, 2012). Owing to the strong link between ROS and oxidative modification of LDL, it may be more relevant in future studies to investigate more directly the ability of probiotics to mitigate LDL oxidation using a method described by Amarowicz and Pegg (2017). LDL is isolated from human plasma and oxidation induced by  $\text{Cu}^{2+}$  ions or 2,2'-azobis(2-methylpropionamide) dihydrochloride (AAPH), in the presence or absence of probiotic treatment.

### 3.4.3 Uptake of modified LDL in macrophages via macropinocytosis

Following on from monocyte migration and ROS production, the effect of probiotic CM on macropinocytosis in macrophages was initially assessed using a range of concentrations. Results show significant attenuation of LY uptake with all concentrations of Lab4, Lab4b and CUL66 CM (Figure 3.14). Notably, while effects achieved at all concentrations maintain statistical significance, a dose-dependent response is notable for each probiotic CM treatment, where attenuation of LY uptake becomes less effective at lower concentrations (Figure 3.14). These data suggest that the highest tested concentration of 8  $\mu\text{g}/\text{mL}$  for Lab4, 1.5  $\mu\text{g}/\text{mL}$  for Lab4b and 5  $\mu\text{g}/\text{mL}$  for CUL66 were the most effective and were therefore selected for continued use in *in vitro* investigations.

In the comparison of probiotic activity, each probiotic CM was able to attenuate macropinocytosis by a similar degree (Figure 3.15), suggesting that all of Lab4, Lab4b and CUL66 effectively attenuate macropinocytosis in macrophages. The excessive uptake of modified LDL is a key event in the formation of foam cells and in atherosclerosis progression. Uptake via macropinocytosis occurs independently of

receptor-mediated uptake and constitutes a substantial contribution of total lipid uptake by macrophage foam cells (Michael *et al.*, 2013). While the effect of probiotic treatment on macropinocytosis has not previously been studied, these results represent a possible mechanism leading to an attenuation of foam cell formation during atherosclerosis development.

#### 3.4.4 The effect of probiotic CM on mitochondrial function

Basal respiration was significantly increased with Lab4 or CUL66 treatment compared to the vehicle control (Figure 3.17A). This result correlates well with the significant increase in ROS production demonstrated in Section 3.3.4. Increased basal respiration has been shown to correlate with increased proton leakage and reduced mitochondrial health (Koczor *et al.*, 2013). Both Lab4 and CUL66 treatment resulted in a significant increase in maximal respiration (Figure 3.17C) and subsequently an increase in spare respiratory capacity (Figure 3.17E), suggesting that although basal respiration is increased, cells have an increased capacity to deal with the energy demand. Lab4b showed a non-significant increase in basal respiration, maximal respiration and spare respiratory capacity suggesting a similar trend with all CM treatments. In terms of mitochondrial function, results from this series of investigations suggest that while Lab4b has no effect, Lab4 shows no overall positive or negative effect and CUL66 has an overall positive effect. Studies in LDLr<sup>-/-</sup> mice have demonstrated a correlation between increased mitochondrial stress and atherosclerosis progression (Dorighello *et al.*, 2018; Wang *et al.*, 2017d), with one study showing accelerated lesion development with excessive macrophage mitochondrial stress (Wang *et al.*, 2014). Further research is required to gain a more in depth understanding of the effect of these probiotics on mitochondrial function; however, these preliminary results indicate that CUL66 in particular may exert positive effects on the mitochondrial bioenergetic profile in human macrophages.

#### 3.4.5 Phagocytic activity of macrophages was enhanced in the presence of probiotic CM

Phagocytic activity of human macrophages was assessed in THP-1 macrophages treated with either the vehicle control or probiotic CM, using the Vybrant Phagocytosis Assay



Kit. Phagocytic activity was significantly increased in the presence of all of Lab4, Lab4b and CUL66 CM (Figure 3.18). Few studies have investigated the effect of probiotic bacteria on macrophage phagocytic activity. A recent study has demonstrated increased macrophage phagocytic activity *in vitro* in response to a specific *Lactobacillus* strain (Jaffar *et al.*, 2018). This follows a previous study that demonstrated increased BMDM phagocytic activity in response to a novel strain of *Bacteroides* (Deng *et al.*, 2016). However, these previous studies were not conducted in the context of atherosclerosis. In the context of atherosclerosis, this is generally a positive result as increased phagocytosis has been associated with reduced oxLDL uptake and reduced atherosclerotic plaque formation in ApoE<sup>-/-</sup> mice (Laguna-Fernandez *et al.*, 2018). While phagocytic activity of macrophages is necessary for the removal of apoptotic cells and debris from plaques, it could potentially exert pro-atherogenic properties upon phagocytosis of lipoproteins, erythrocytes and platelets (Schrijvers *et al.*, 2007). Further research is required to investigate the effects of enhanced phagocytosis; for example, by assessing the impact of increased phagocytosis on the uptake of oxLDL.

#### 3.4.6 Differential effects of probiotic CM on the proliferation of cell types involved in atherosclerosis

In order to determine the effect of probiotic treatment on the proliferation of key cell types in atherosclerosis, THP-1 monocytes, macrophages and HASMCs were treated with either the vehicle control or probiotic CM, and proliferation measured as illustrated in Figure 3.4. For each cell type, total proliferation showed a general trend of reduction with each probiotic CM, while the rate of proliferation displayed a more strain-specific effect. For all assays, no significant reduction in cell viability occurred, suggesting that the observed reduction in cell proliferation was not due to any increase in cell death.

Treatment with probiotic CM resulted in a large attenuation of monocyte proliferation of up to 50% by day 7 (Figures 3.19 and 3.20). Although macrophage proliferation is considered to be a stronger factor in advanced lesion development, monocytes maintain an essential role particularly in early disease. This result correlates with a previous study which investigated the effect of specific probiotic strains on the proliferation of peripheral blood mononuclear cells (PBMCs) *in vitro*, demonstrating a significant

reduction in a protein concentration-dependent manner on par with that of known anti-proliferative agent dexamethasone (Kankaanpää *et al.*, 2003). HASMC proliferation also showed a trend of reduction following probiotic treatment however results were less pronounced, possibly owing to the much slower growth rate typical of this cell type compared to the THP-1 cell line. By day 7, all probiotic treatments showed a significant reduction in proliferation of HASMCs (Figure 3.23). Proliferation of VSMCs is known to be a factor involved in atherogenesis (Wang *et al.*, 2007) and while normal controlled proliferation can be beneficial, dysregulated VSMC proliferation contributes to plaque formation (Li *et al.*, 2018). This result suggests that probiotic treatment may also have a beneficial effect on dysregulated VSMC proliferation. In this series of experiments, macrophage proliferation was significantly reduced following 48 hours treatment compared to day 0 (Figure 3.21). Additionally, the rate of proliferation after 48 hours was significantly reduced with Lab4 treatment, whereas Lab4b treatment resulted in a trend of reduction and CUL66 showed no significant effect (Figure 3.22). Studies have demonstrated an association between reduced proliferation of macrophages and suppression of early atherosclerosis in LDLr<sup>-/-</sup> mice (Babaev *et al.*, 2018), as well as accelerated atherosclerosis development with increased proliferation of monocytes and macrophages in ApoE<sup>-/-</sup> mice (Kuo *et al.*, 2011). Attenuation of macrophage proliferation therefore represents a further possible mechanism by which probiotics may exert anti-atherogenic effects.

### 3.4.7 Invasion of SMCs

The effect of probiotic CM on the invasion of HASMCs was investigated using a modified Boyden chamber method. In the presence of PDGF-BB stimulus, cells treated with Lab4 or Lab4b CM showed a large reduction in invasion of approximately 50% compared to the vehicle control, whereas CUL66 had no significant effect (Figure 3.25). These results suggest that probiotic treatment may attenuate the invasion of VSMCs in a strain-specific manner. Previous studies have shown that PDGF-BB as well as the PDGF receptor beta (PDGFR $\beta$ ) are expressed in VSMCs within atherosclerotic plaques, and that their inhibition reduces migration and proliferation of SMCs and subsequently atherosclerotic lesion size (He *et al.*, 2015; Ricci and Ferri, 2015; Sano *et al.*, 2001; Wang *et al.*, 2017c). The tyrosine kinase inhibitor Imatinib blocks the activity of the PDGFR.

Diabetic ApoE<sup>-/-</sup> mice treated with Imatinib showed reduced total plaque area that correlated with a reduction in PDGF-B expression and reduced phosphorylation of PDGFR $\beta$  (Lassila *et al.*, 2004; Ricci and Ferri, 2015). Given the results of this study, it can be suggested that Lab4 and Lab4b may attenuate the pathological PDGF-induced invasion of VSMCs, possibly due to an attenuation of PDGFR expression or activity, representing an additional mechanism by which these probiotics exert beneficial effects in atherosclerosis.

### 3.4.8 The effects of probiotic CM on common inflammatory markers

This study aimed to investigate the potential anti-inflammatory effects of probiotic treatment by assessing both the activation of the NLRP3 inflammasome and cytokine-induced expression of inflammatory markers, MCP-1 and ICAM1. From Figure 3.26, it can be seen that treatment with probiotic CM resulted in a large increase in IL-1 $\beta$  production by up to 55-fold, suggesting a strong induction of the NLRP3 inflammasome in response to probiotic CM. As part of the innate immune system, the NLRP3 inflammasome is activated in response to pathogen associated molecular patterns (PAMPs). It is therefore not surprising that media conditioned by probiotic bacteria would lead to significant activation and the production of IL-1 $\beta$ . Earlier in this chapter, it was shown that treatment of THP-1 macrophages with probiotic CM leads to an increased production of TBHP-induced ROS production. It is therefore also worth considering that an increase in ROS production has previously been shown to cause activation of the NLRP3 inflammasome (Zhou *et al.*, 2010), and that these results may be linked by common mechanism(s).

As discussed previously, the anti-inflammatory effects of probiotic bacteria are highly strain-specific even within a single species. In the current study, treatment of cytokine-stimulated macrophages with probiotic CM generated strain-specific effects, particularly with regards to TNF- $\alpha$ - and IL-1 $\beta$ -induced expression of MCP-1, which was increased in response to Lab4b but not Lab4 or CUL66 CM (Figure 3.27C and E). As can be seen from Figure 3.27A-D, results suggest that none of the probiotic CM treatments exert beneficial effects in either IFN- $\gamma$  or IL-1 $\beta$  pathways. However, the TNF- $\alpha$ -induced expression of ICAM1 was significantly attenuated by both Lab4 and CUL66 treatment,

while Lab4b also demonstrated a trend of reduced expression (Figure 3.27E and F), representing one possible mechanism by which each probiotics may exert anti-inflammatory effects. This result is in agreement with a previous study which demonstrated the ability of certain *Lactobacillus* strains to effectively downregulate the production of TNF- $\alpha$  under inflammatory conditions (Aparna Sudhakaran *et al.*, 2013). While probiotic CM had no beneficial effect on the IFN- $\gamma$  and IL-1 $\beta$ -induced expression of MCP-1 and ICAM1, it should be noted that there are many pro-inflammatory cytokines and inflammatory markers that should be investigated before drawing any firm conclusions.

### 3.4.9 Future directions

The aim of this chapter was to gain a broad insight into the effects of probiotic treatment on key processes in atherosclerosis. Overall, the results indicate anti-atherosclerotic actions of probiotic treatment, demonstrating attenuated monocyte migration, macrophage macropinocytosis, VSMC invasion and proliferation of key cell types as well as increased macrophage phagocytic activity. Results for ROS production, mitochondrial function and cytokine-induced inflammatory responses suggest that these specific probiotics are less effective as an anti-oxidant or anti-inflammatory agent, at least under *in vitro* conditions. However, probiotic treatment appears to exert a number of beneficial effects on macrophage function. Macrophages are a key cell type involved in atherosclerosis with macrophage foam cell formation regarded as a critical process in atherosclerosis development. Despite the huge availability of literature pertaining to the effects of probiotics on lipid function, there is little research into probiotics and macrophage foam cell formation. Furthermore, the effects of Lab4, Lab4b or CUL66 on aspects of foam cell formation have not yet been studied. Therefore, in the following chapter, the effect of probiotic CM on macrophage foam cell formation was investigated in greater detail.

# CHAPTER 4

*The effects of probiotic CM on  
foam cell formation*

---

## 4.1 Introduction

Under normal physiological conditions, macrophage cholesterol metabolism is subject to tight homeostatic control with mechanisms regulating the uptake, intracellular metabolism and efflux of cholesterol (McLaren *et al.*, 2011a). In atherosclerosis, disruption of these mechanisms leads to the intracellular accumulation of lipids and the formation of macrophage foam cells, the hallmark of atherosclerosis. A simplified schematic representation of such mechanisms is shown in Figure 4.1. As discussed in Chapter 1, foam cells are integral to every stage in atherosclerosis progression. In early disease, foam cells accumulate and manifest as fatty streaks within the intima of medium and large arteries, providing the foundation for progression to more advanced disease. In advanced atherosclerotic plaques, apoptotic and necrotic foam cells accumulate, contributing to secondary necrosis and the formation of a necrotic core (Moore and Tabas, 2011).

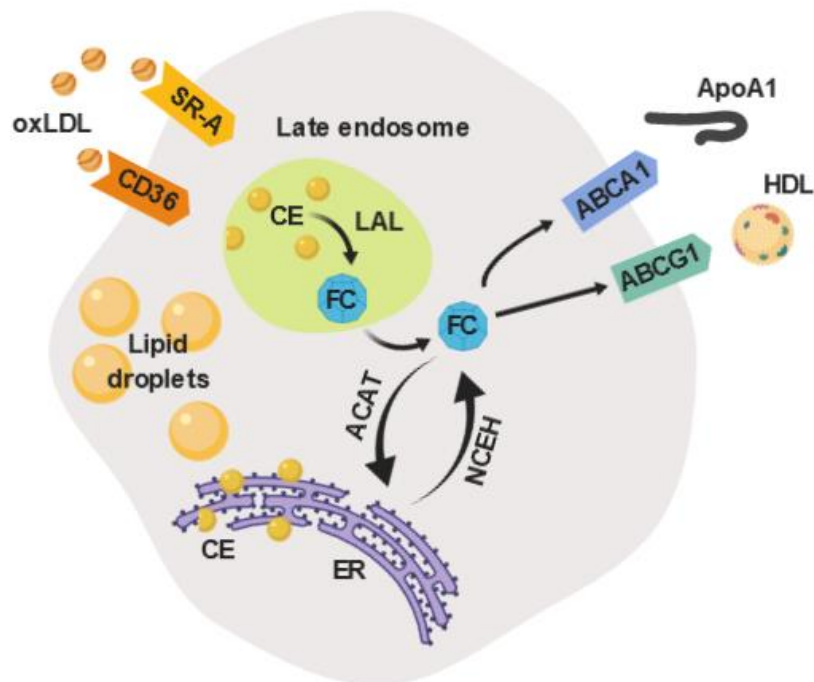


**Figure 4.1 - Schematic representation of processes involved in macrophage foam cell formation.** OxLDL is internalised and trafficked to the endosome where the CE portion is metabolised to FC via LAL. FC is then either transported out of the cell via ABC transporters to apoA1 or HDL, or trafficked to the ER and re-esterified via ACAT enzymes. Re-esterified cholesterol is then either stored within the cytoplasm as lipid droplets, or hydrolysed to FC by NCEH enzymes and transported from the cell. Image created using BioRender. Abbreviations: OxLDL, oxidised LDL; SR-A, scavenger receptor-A; CE, cholesterol esters; FC, free cholesterol; ER, endoplasmic reticulum; ACAT, acyl-CoA cholesterol acyltransferase; NCEH, neutral cholesterol ester hydrolase; ABCA1, ATP-binding cassette transporter A1; ABCG1, ATP-binding cassette transporter G1.

### 4.1.1 Uptake of modified LDL

Native (unmodified) LDL is internalised via macrophage LDL receptors, and is negatively regulated via feedback inhibition according to the level of intracellular cholesterol stores. However, modified LDL cannot use this pathway (Kzhyshkowska *et al.*, 2012) and is instead internalised in an unregulated manner, primarily via scavenger receptors. Therefore, it is not surprising that modified LDL is the primary contributor to intracellular cholesterol accumulation and foam cell formation (Bobryshev *et al.*, 2016). Modified forms of LDL isolated from atherosclerosis patients have been shown to induce the intracellular accumulation of cholesterol esters in cultured macrophages, while native LDL from healthy patients does not (Chistiakov *et al.*, 2017). In Chapter 3, it was demonstrated that the uptake of modified LDL via macropinocytosis was attenuated in THP-1 macrophages in the presence of probiotic CM. While macropinocytosis is a well-defined mechanism of modified LDL uptake, a significant amount is internalised via receptor-mediated pathways involving SR-A, CD36, and lectin-like oxLDL receptor-1 (LOX-1). As described in Chapter 1, certain scavenger receptors have high affinity for modified forms of LDL, particularly oxLDL and acLDL, which are rapidly internalised in an unregulated manner.

SR-A is a class A scavenger receptor capable of binding many ligands relevant to atherosclerosis including acLDL, oxLDL, apoE, certain types of modified collagen and ECM components. SR-A has a high affinity for acLDL in particular, and does not bind native forms of LDL or HDL (Kzhyshkowska *et al.*, 2012). CD36 is a class B scavenger receptor that also binds certain forms of modified LDL, particularly oxLDL, and its expression is upregulated with atherosclerosis progression via peroxisome proliferator-activated receptor (PPAR)- $\gamma$ -dependent pathways (Nakagawa-Toyama *et al.*, 2001). Both SR-A and CD36 are heavily implicated in the unregulated and excessive internalisation of modified LDL contributing to the formation of foam cells, and inhibition of these receptors has been shown to be beneficial in reducing atherosclerosis progression. Indeed, the uptake of oxLDL has been shown to be reduced in HMDMs derived from CD36-deficient patients (Nozaki *et al.*, 1995), while in ApoE<sup>-/-</sup> mice lacking SR-A and CD36 it was demonstrated that these receptors are responsible for the majority of modified LDL uptake and degradation (Kunjathoor *et al.*, 2002). In the same study,

cholesterol esters failed to accumulate in SR-A- and CD36-deficient macrophages, thereby suggesting that other scavenger receptors fail to compensate for the absence of SR-A and CD36 (Kunjathoor *et al.*, 2002). A more recent study demonstrated a significant reduction in aortic lesion area in ApoE<sup>-/-</sup> mice deficient in either CD36 (61-74% reduction) or SR-A (32% reduction), however no further reduction was seen upon combined absence of CD36 and SR-A (Kuchibhotla *et al.*, 2008).

To assess the effects of probiotic CM on receptor-mediated lipid uptake of oxLDL, either THP-1 macrophages or HMDMs were treated with Dil-oxLDL in the presence of vehicle control or probiotic CM, then the uptake of Dil-oxLDL was assessed by flow cytometry as described in Section 2.7.1. Additionally, the effect of probiotic CM on the expression of key genes involved in modified lipoprotein uptake (SR-A, CD36, LPL) was determined in THP-1 macrophages treated for 24 hours with either vehicle control or probiotic CM. RNA was extracted, reverse transcribed to cDNA and gene expression determined by qPCR as described in Section 2.5.

#### 4.1.2 Cholesterol efflux

In addition to increased internalisation of modified lipoproteins, reduced efflux of cholesterol from the cell is also a well-studied mechanism involved in the formation of macrophage foam cells. As discussed in Chapter 1, under normal conditions, RCT and HDL-mediated passive diffusion work to transport excess intracellular cholesterol back to the liver for degradation and excretion (Figure 1.4). In atherosclerosis these mechanisms are impaired and efflux of cholesterol is reduced, thereby promoting intracellular accumulation of modified LDL-derived cholesterol esters and subsequently foam cell formation (Favari *et al.*, 2015).

As illustrated in Figure 4.1, free cholesterol is transported out of the cell to lipid acceptors HDL and apoA1 via membrane transporters which include ATP-binding cassette transporters, namely ABCG1 and ABCA1 respectively (Tall *et al.*, 2008). Several pathways for cholesterol efflux have been described including active efflux via ABC transporters, passive diffusion, or scavenger receptor-B1 (SR-B1)-mediated efflux; however, it is cholesterol transporters ABCA1 and ABCG1 that are responsible for the



majority of cholesterol efflux from macrophages (Sekiya *et al.*, 2011). ABCA1 and ABCG1 translocate from the ER, late endosomes and other intracellular compartments to the plasma membrane, promoting the flow of intracellular cholesterol. Under normal physiological conditions, the majority of cholesterol in cells is located at the plasma membrane with only a minimal amount present in intracellular locations (Favari *et al.*, 2015). In atherosclerosis however, the expression of ABCG1 and ABCA1 is downregulated leading to reduced efflux of cholesterol and therefore accumulation of intracellular cholesterol esters (Chistiakov *et al.*, 2017). A large number of studies have demonstrated that an increase in ABCA1/G1 expression results in increased cholesterol efflux and subsequently decreased foam cell formation both *in vitro* (Adorni *et al.*, 2017; Fu *et al.*, 2014; Sun *et al.*, 2015) and *in vivo* (Huang *et al.*, 2015; Jiang *et al.*, 2017; Zou *et al.*, 2017). A number of mechanisms are known to lead to this ABCA1/G1-dependent increase in cholesterol efflux, including PPAR/LXR activation pathways in which gene expression of ABCA1 is stimulated via LXRs, which are themselves stimulated by intracellular cholesterol accumulation (Jiang *et al.*, 2017; Larrede *et al.*, 2009). ApoE is an anti-atherogenic lipoprotein synthesised largely by the liver, or locally by macrophages in atherosclerotic plaques (Valanti *et al.*, 2018) in response to differentiation, cytokine stimulation or lipid accumulation. ApoE contributes to the formation of HDL particles (Langmann *et al.*, 2003) and when synthesised in response to lipid enrichment, activates the LXR pathway and subsequently leads to the increased expression of ABCA1 and ABCG1 (Favari *et al.*, 2015).

The effect of probiotic CM on cholesterol efflux was assessed using a traditional [<sup>14</sup>C]cholesterol method, in which the efflux of [<sup>14</sup>C]cholesterol from foam cells in response to apoA1 was measured by liquid scintillation counting as described in Section 2.7.3. As the lipoprotein component of HDL, apoA1 is a highly effective cholesterol acceptor utilised in a number of previous cholesterol efflux studies (McLaren *et al.*, 2010; Michael *et al.*, 2016; Moss *et al.*, 2016). Additionally, the effect of probiotic CM on the expression of key genes involved in cholesterol efflux (ABCA1, ABCG1, LXR $\alpha$ , LXR $\beta$ , APOE) was investigated in macrophage foam cells treated for 24 hours with vehicle control or probiotic CM. RNA was extracted, reverse transcribed to cDNA and gene expression determined by qPCR as described in Section 2.5.

### 4.1.3 Intracellular cholesterol metabolism

Foam cell formation is largely driven by an imbalance between the rate of internalisation and efflux of cholesterol. However, the intracellular metabolism, storage and esterification of cholesterol also plays an important role. The intracellular metabolism of cholesterol is illustrated in Figure 4.1. Once internalised, the cholesterol ester contained within the LDL particle is unesterified to free cholesterol and fatty acids in late endosomes/lysosomes via the LAL enzyme (Chistiakov *et al.*, 2016). Free cholesterol is trafficked to the ER where it is re-esterified via ACAT enzymes, namely ACAT1 (McLaren *et al.*, 2011a). This esterified cholesterol is then either stored within the cytoplasm as lipid droplets, or hydrolysed to free cholesterol by neutral cholesterol ester hydrolase (NCEH) enzymes and transported out of the macrophage (Chistiakov *et al.*, 2016). ACAT and NCEH enzymes create a cycle of cholesterol esterification and hydrolysis which is integral to macrophage cholesterol trafficking (Sekiya *et al.*, 2011). In atherosclerosis, increased production and decreased hydrolysis of CE causes this cycle to become imbalanced, leading to an excess of CE which is stored in cytoplasmic lipid droplets. Many studies have demonstrated an athero-protective effect of ACAT1 inhibition and/or increased NCEH1 expression. In THP-1 macrophages, overexpression of NCEH1 inhibits the accumulation of CE (Okazaki *et al.*, 2008), while pharmacological or genetic inhibition of NCEH1 significantly increases the accumulation of CE in acLDL-treated macrophages (Sekiya *et al.*, 2009; Yamazaki *et al.*, 2018). Furthermore, a recent study in LDLr<sup>-/-</sup> mice demonstrated that NCEH1-deficiency results in increased lesion area, while conversely the loss of both ACAT1 and NCEH1 results in a significant reduction in lesion size (Yamazaki *et al.*, 2018). Several studies demonstrate that inhibition of ACAT1 is beneficial in reducing atherosclerosis (Huang *et al.*, 2016; Wang *et al.*, 2017a). However, additional studies have found that ACAT1 inhibition enhances lesion size in LDLr<sup>-/-</sup> mice (Fazio *et al.*, 2001), with reports of deleterious effects associated with excessive accumulation of free cholesterol, including severe skin lesions and reduced life-span in ACAT1-deficient mice (Wakabayashi *et al.*, 2018). This research suggests that while modulation of ACAT1 and NCEH1 expression can be beneficial in reducing foam cell formation and plaque area, a balance must be maintained to avoid the excessive build-up of either cholesterol esters or free cholesterol.

The formation of cholesterol esters and other major lipid classes in macrophage foam cells was assessed by measuring the incorporation of [<sup>14</sup>C]acetate into major lipid classes, a technique that has been utilised in studies of lipid metabolism for decades (Shireman *et al.*, 1988; Yamasaki *et al.*, 2018). Acetate is metabolised within the macrophage and incorporated into lipid classes which are then extracted and separated by TLC, and the radioactivity contained within each fraction measured by scintillation counting as described in Section 2.7.3. Additionally, the effect of probiotic CM on the expression of key genes involved in intracellular cholesterol metabolism (ACAT1, NCEH1) was investigated in macrophage foam cells treated for 24 hours with vehicle control or probiotic CM. RNA was extracted, reverse transcribed to cDNA and gene expression determined by qPCR as described in Section 2.5.

## 4.2 Experimental aims

This chapter aimed to investigate the effect of Lab4, Lab4b and CUL66 CM on receptor-mediated uptake of modified LDL, cholesterol efflux and intracellular cholesterol metabolism in human macrophages for the first time at the cellular level, and to investigate possible mechanisms of action at the molecular level. As in Chapter 3, Lab4, Lab4b and CUL66 CM was used at a concentration of 8, 1.5 and 5 µg/mL respectively for all experiments. Experimental strategies for each assay are illustrated in Figures 4.2-4.5 below. Specific methods are detailed in Chapter 2.

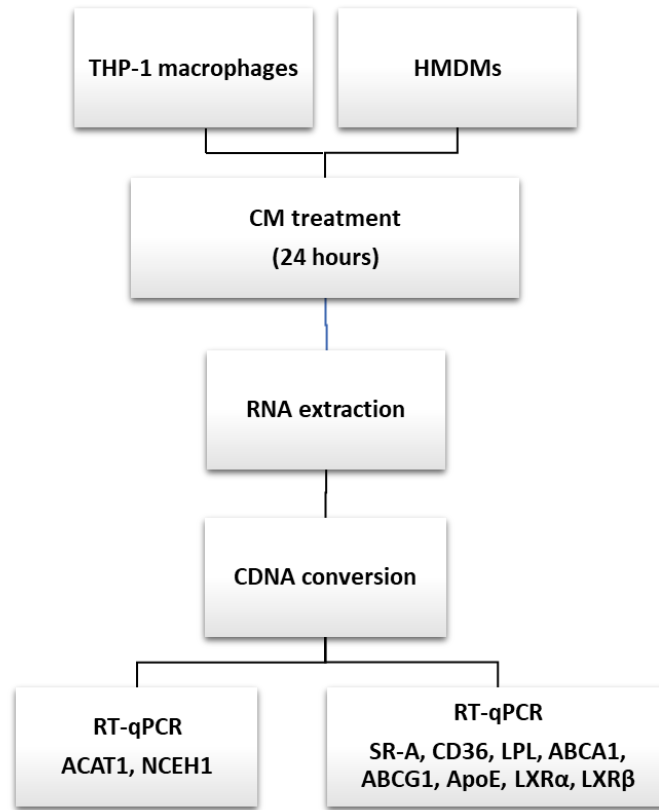


Figure 4.2 - Experimental strategy for the investigation of the effect of probiotic CM on the expression of key genes in foam cell formation.

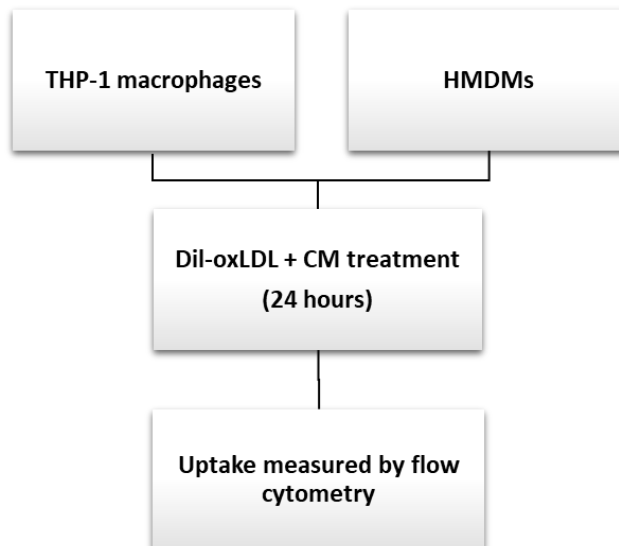


Figure 4.3 – Experimental strategy for the investigation of the effect of probiotic CM on the uptake of oxLDL.

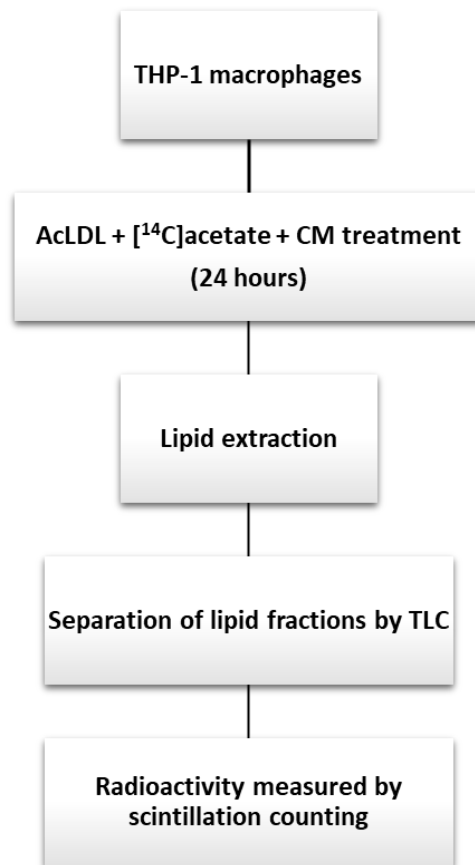


Figure 4.4 – Experimental strategy for the investigation of the effect of probiotic CM on cholesterol efflux from macrophage foam cells.

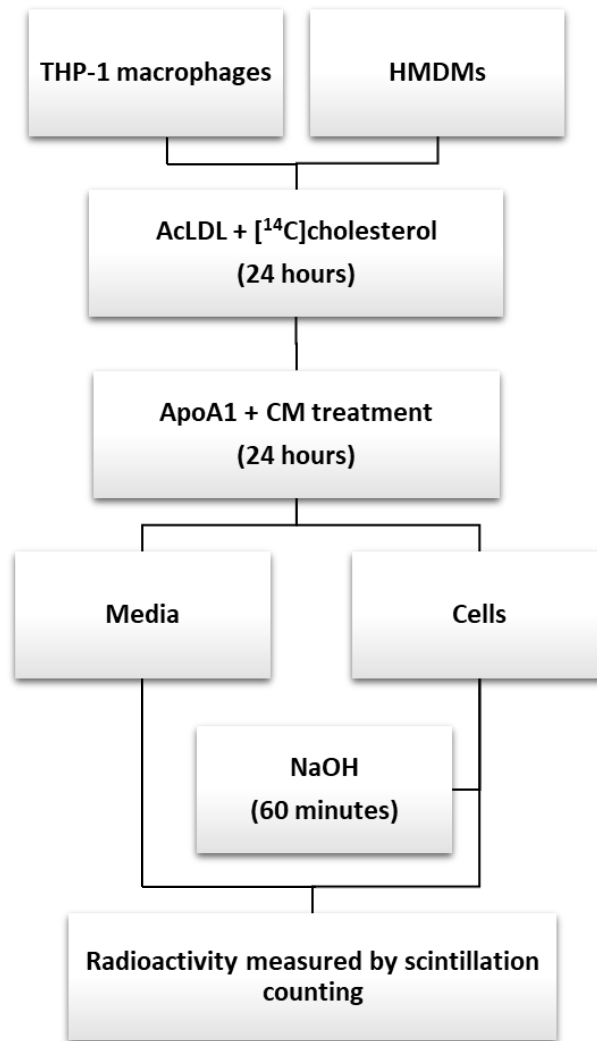
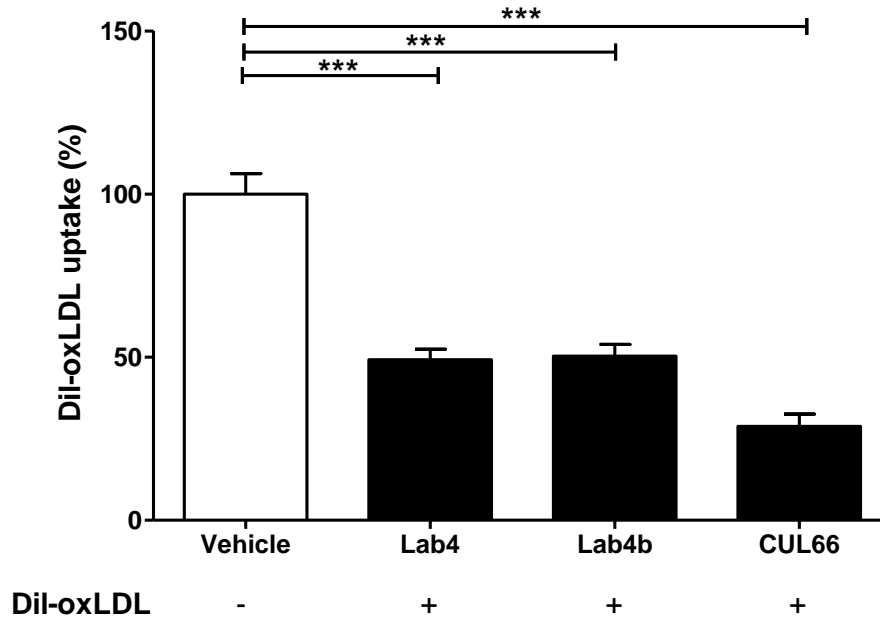


Figure 4.5 – Experimental strategy for the investigation of the effect of probiotic CM on macrophage intracellular cholesterol metabolism.

## 4.3 Results

### 4.3.1 Probiotic CM attenuates receptor-mediated uptake of modified LDL in human macrophages

To investigate the effect of probiotic CM on receptor-mediated uptake of modified LDL, THP-1 macrophages were treated with either vehicle control or probiotic CM in the presence of Dil-oxLDL as described in Section 2.7.1. Cells that had taken up Dil-oxLDL were sorted by flow cytometry and the uptake calculated as a percentage relative to the vehicle control which was set to 100% after background subtraction. In the presence of Lab4, Lab4b or CUL66 CM, the uptake of Dil-oxLDL was significantly attenuated by 51.7% ( $p < 0.001$ ), 49.7% ( $p < 0.001$ ) and 72.2% ( $p < 0.001$ ) respectively (Figure 4.6). The experiment was then repeated in primary human macrophages isolated from buffy coats using the protocol described in Section 2.3.1.4. HMDMs seeded in 12-well plates at a concentration of  $3 \times 10^6$  per mL were treated for 24 hours with vehicle control or probiotic CM plus Dil-oxLDL, following the same protocol as for THP-1 macrophages detailed above. In the presence of Lab4, Lab4b or CUL66 CM, the uptake of Dil-oxLDL by primary human macrophages was significantly attenuated by 45.1% ( $p = 0.001$ ), 54.4% ( $p = 0.002$ ) and 70.2% ( $p < 0.001$ ) respectively (Figure 4.7).



**Figure 4.6 - Receptor-mediated uptake of modified lipoproteins was attenuated in the presence of probiotic CM.** The effect of probiotic CM on receptor-mediated uptake of modified LDL was determined following 24 hours treatment with either vehicle control plus Dil-oxLDL, or Lab4 (8  $\mu\text{g}/\text{mL}$ ), Lab4b (1.5  $\mu\text{g}/\text{mL}$ ) or CUL66 (5  $\mu\text{g}/\text{mL}$ ) CM plus Dil-oxLDL. Dil-oxLDL uptake was determined as a percentage relative to the vehicle control which was arbitrarily set to 100% following background subtraction. Data are presented as mean  $\pm$  SEM from three independent experiments. Statistical analysis was performed using a One-way ANOVA with Dunnett (2-sided) post-hoc test where \*\*\*  $p < 0.001$ .

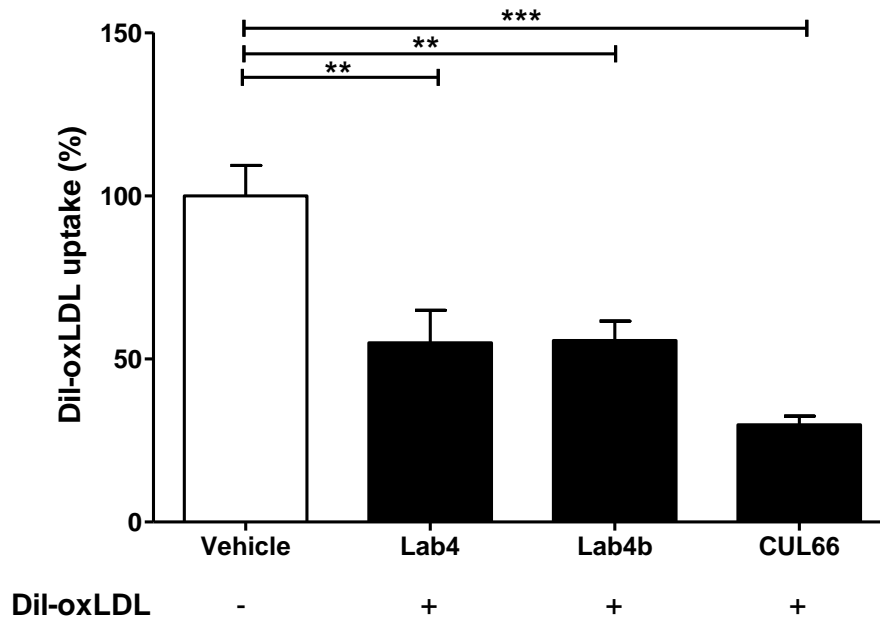


**Figure 4.7 - Probiotic CM inhibits the uptake of modified lipoproteins in primary human macrophages.** The effect of probiotic CM on receptor-mediated uptake of oxLDL was determined following treatment with either vehicle control plus Dil-oxLDL, or Lab4 (8  $\mu\text{g}/\text{mL}$ ), Lab4b (1.5  $\mu\text{g}/\text{mL}$ ) or CUL66 (5  $\mu\text{g}/\text{mL}$ ) CM plus Dil-oxLDL. Dil-oxLDL uptake was determined as a percentage relative to the vehicle control, which was arbitrarily set to 100% following background subtraction. Data are presented as mean  $\pm$  SEM from three independent experiments. Statistical analysis was performed using a One-way ANOVA with Dunnett (2-sided) post-hoc test where \*\*  $p < 0.01$ , \*\*\*  $p < 0.001$ .



### 4.3.2 Expression of macrophage scavenger receptors was attenuated following treatment with probiotic CM

To investigate the effect of probiotic CM on key genes involved in modified LDL uptake, THP-1 macrophages were treated with either vehicle control or probiotic CM for 24 hours. RNA was extracted, reverse transcribed to cDNA and gene expression determined by real-time qPCR as described in Section 2.5. As shown in Figure 4.8A, gene expression of SR-A was significantly reduced in the presence of Lab4, Lab4b or CUL66 CM by 2.5-fold ( $p < 0.001$ ), 7-fold ( $p < 0.001$ ) and 2.5-fold ( $p < 0.001$ ) respectively. Gene expression of CD36 was also significantly reduced in the presence of Lab4, Lab4b or CUL66 CM to 4.2-fold ( $p < 0.001$ ), 13.1-fold ( $p < 0.001$ ) and 2.8-fold ( $p < 0.001$ ) respectively (Figure 4.8B). Expression of LPL showed no significant change with Lab4 or CUL66 treatment, but was significantly reduced in the presence of Lab4b by 2.5-fold ( $p < 0.001$ ) (Figure 4.8C).

Changes in gene expression of macrophage scavenger receptors SR-A and CD36 were also investigated in primary human macrophages as described in Section 2.3.1.4, in order to rule out cell-line specific effects. As shown in Figure 4.9A, gene expression of SR-A was significantly reduced by 3.6-fold ( $p = 0.03$ ) following treatment with Lab4 CM, whereas no significant change in expression was seen with Lab4b or CUL66 CM. Expression of CD36 was significantly attenuated with Lab4, Lab4b and CUL66 CM by 12.2-fold ( $p < 0.001$ ), 41.1-fold ( $p < 0.001$ ) and 11.8-fold ( $p < 0.001$ ) respectively (Figure 4.9B).

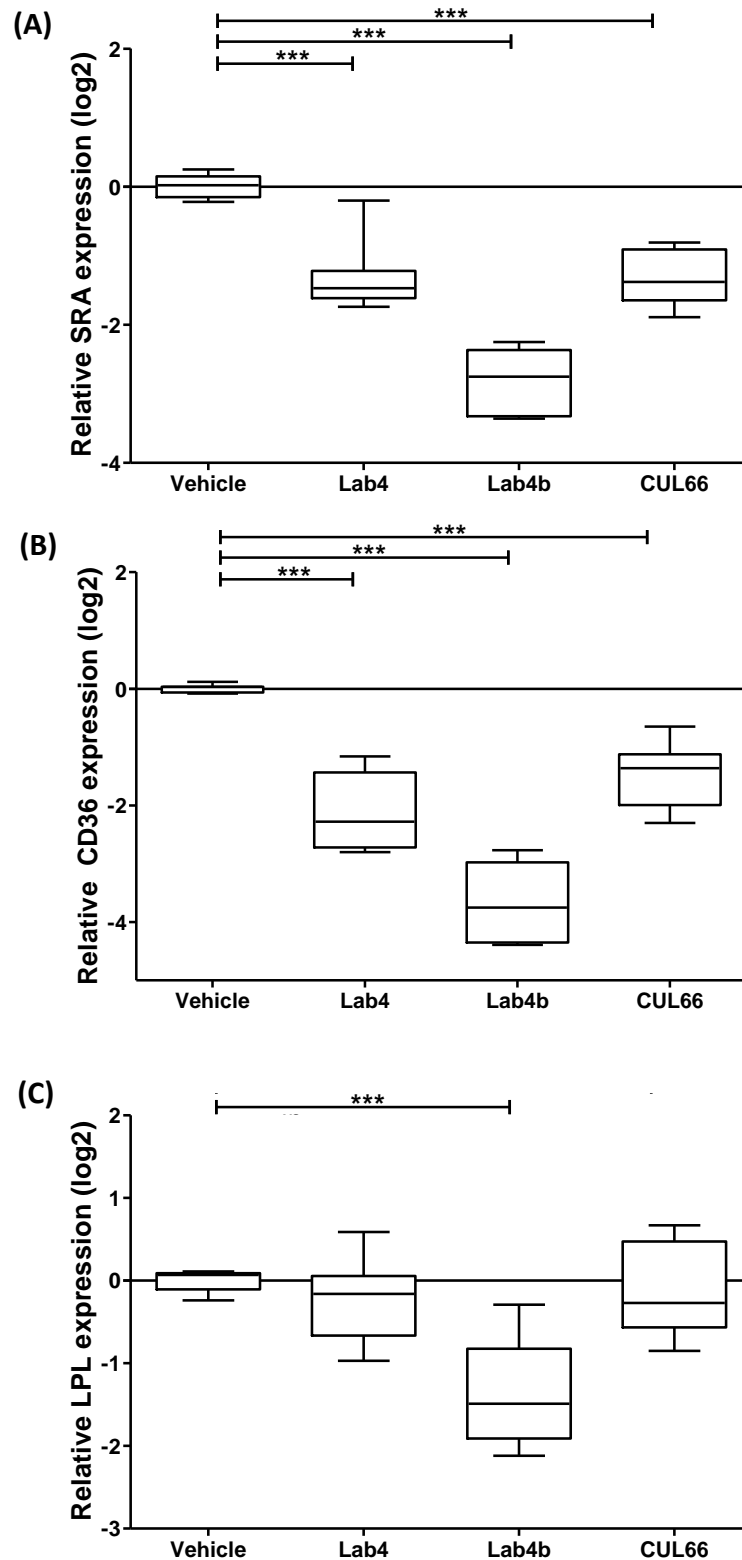


**Figure 4.8 – Gene expression of macrophage scavenger receptors was inhibited by probiotic CM treatment.** The effect of probiotic CM on the expression of scavenger receptors (A) SRA and (B) CD36 together with (C) LPL was investigated in THP-1 macrophages treated for 24 hours with either vehicle control or Lab4 (8  $\mu\text{g}/\text{mL}$ ), Lab4b (1.5  $\mu\text{g}/\text{mL}$ ) or CUL66 (5  $\mu\text{g}/\text{mL}$ ) CM. Gene expression was determined by qPCR using the  $\Delta\Delta\text{C}_T$  method. Data are presented as box and whisker plots of log<sub>2</sub> fold-change in gene expression relative to the vehicle control, where whiskers represent min to max fold-change from three independent experiments. Statistical analysis was performed using a One-way ANOVA with Dunnett (2-sided) (A and B) or Dunnett T3 (C) post-hoc test where \*\*\*  $p < 0.001$ . SRA, scavenger receptor class A; LPL, lipoprotein lipase.

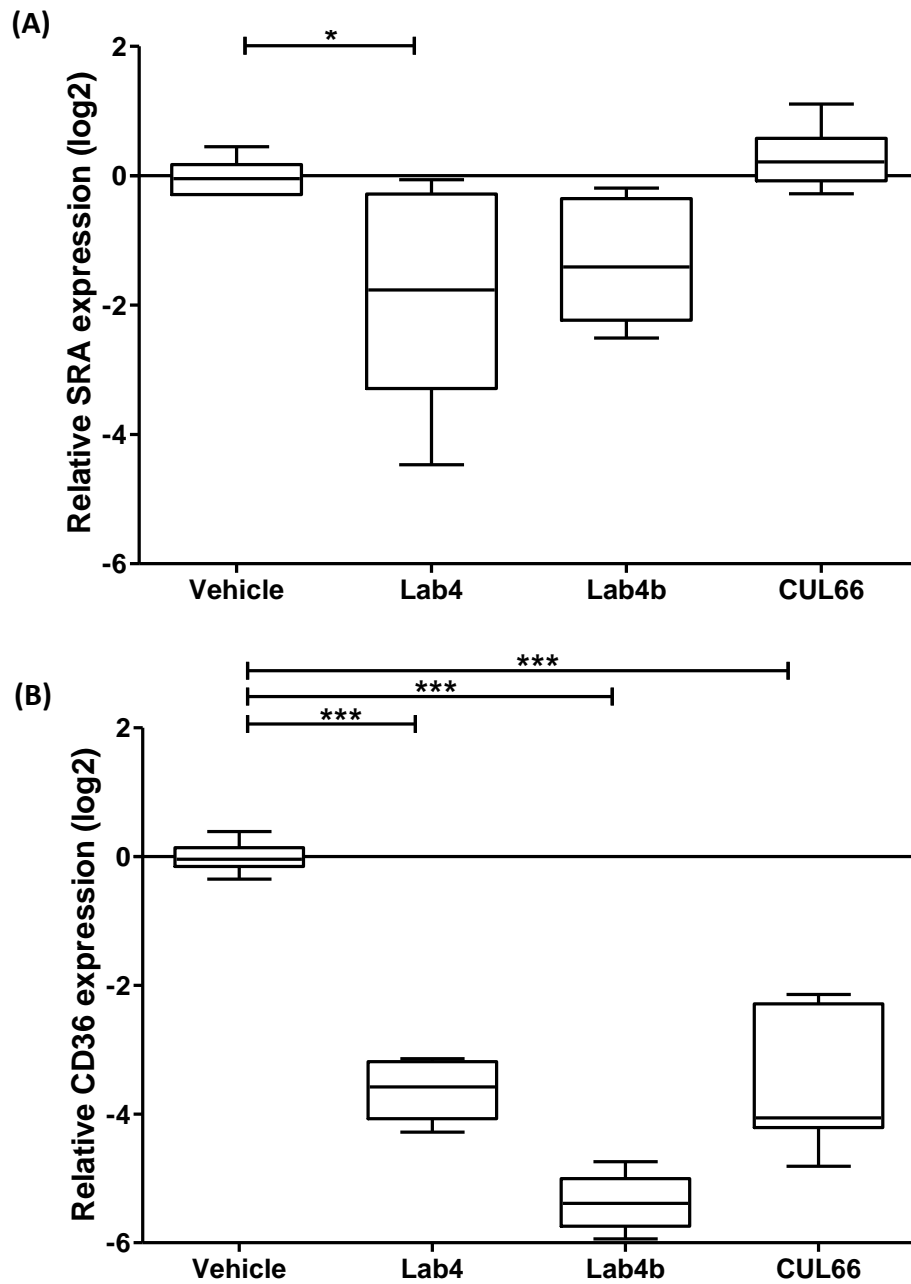


**Figure 4.9 - Probiotic CM attenuates the expression of scavenger receptor genes in primary human macrophages.** The effect of probiotic CM on the expression of scavenger receptors (A) SRA and (B) CD36 was investigated in primary human macrophages treated for 24 hours with either vehicle control or Lab4 (8  $\mu\text{g}/\text{mL}$ ), Lab4b (1.5  $\mu\text{g}/\text{mL}$ ) or CUL66 (5  $\mu\text{g}/\text{mL}$ ) CM. Gene expression was determined by qPCR using the  $\Delta\Delta\text{C}_T$  method. Data are presented as box and whisker plots of log<sub>2</sub> fold-change in gene expression relative to the vehicle control, where whiskers represent min to max fold-change from three independent experiments. Statistical analysis was performed using a One-way ANOVA with Dunnett (2-sided) post-hoc test where \* $p < 0.05$ , \*\*\*  $p < 0.001$ .

### 4.3.3 Probiotic CM enhances the efflux of cholesterol from human macrophage foam cells

The effect of probiotic CM on cholesterol efflux was assessed in THP-1 macrophages as described in Section 2.7.3. Briefly, THP-1 macrophages were converted to foam cells by incubation with acLDL (25 µg/mL), in addition to [4-<sup>14</sup>C] cholesterol (0.5 µCi/mL) for 24 hours to allow the uptake and cellular metabolism. Cells were then treated for a further 24 hours with apoA1 (10 µg/mL) and either vehicle control or probiotic CM. Cells treated with the vehicle in the absence of apoA1 were included for comparative purposes. The radioactivity in both supernatant and cellular fractions was then measured using a liquid scintillation counter, and cholesterol efflux was determined as the percentage of radioactivity present in the supernatant versus total radioactivity (supernatant plus cellular fractions). As shown in Figure 4.10, cells treated with vehicle plus apoA1 showed a significant increase in cholesterol efflux compared to vehicle alone ( $p = 0.029$ ). Treatment with Lab4, Lab4b or CUL66 CM further increased cholesterol efflux significantly by 39% ( $p = 0.03$ ), 48% ( $p < 0.001$ ) and 53% ( $p < 0.001$ ) respectively. The experiment was then repeated in primary human macrophages isolated from buffy coats using the protocol described in Section 2.3.1.4. As shown in Figure 4.11, no significant change in efflux was observed between the vehicle alone or vehicle plus apoA1. Nevertheless, treatment with Lab4 CM resulted in a significant 59% increase in efflux ( $p = 0.006$ ), while Lab4b and CUL66 resulted in non-significant increases of 19% ( $p = 0.697$ ) and 31% ( $p = 0.309$ ) respectively (Figure 4.11).

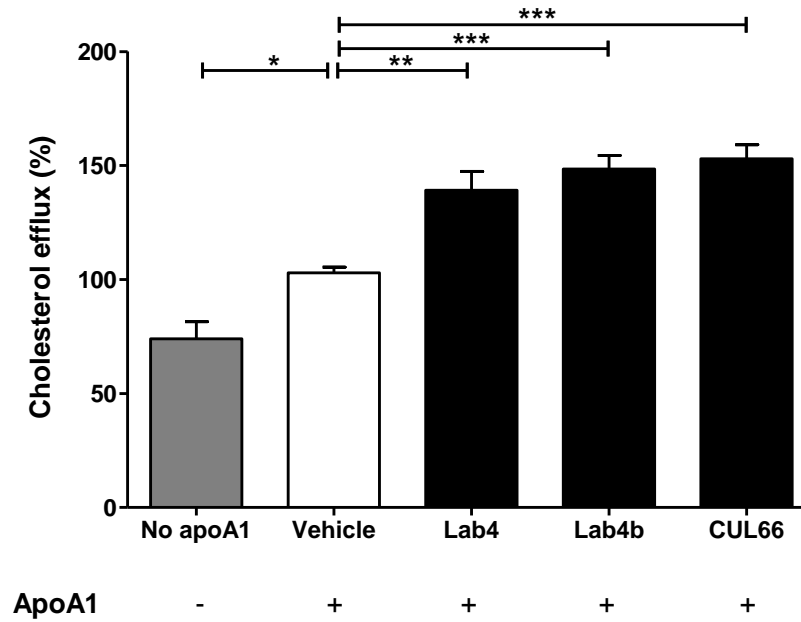


**Figure 4.10 - Treatment with probiotic CM enhances efflux of cholesterol from THP-1 macrophages.** THP-1 macrophages were treated with acLDL in addition to [4-<sup>14</sup>C] cholesterol for 24 hours followed by a further 24 hours with apoA1 and either vehicle control (Vehicle) or Lab4 (8 µg/mL), Lab4b (1.5 µg/mL) or CUL66 (5 µg/mL) CM. Cells treated with vehicle control in the absence of apoA1 were included for comparative purposes (No apoA1). Cholesterol efflux was calculated as a percentage relative to the vehicle control which was arbitrarily set to 100%. Data are presented as mean ± SEM from three independent experiments. Statistical analysis was performed using a One-way ANOVA and Dunnett (2-sided) post-hoc test where \**p* < 0.05, \*\**p* < 0.01 and \*\*\**p* < 0.001.

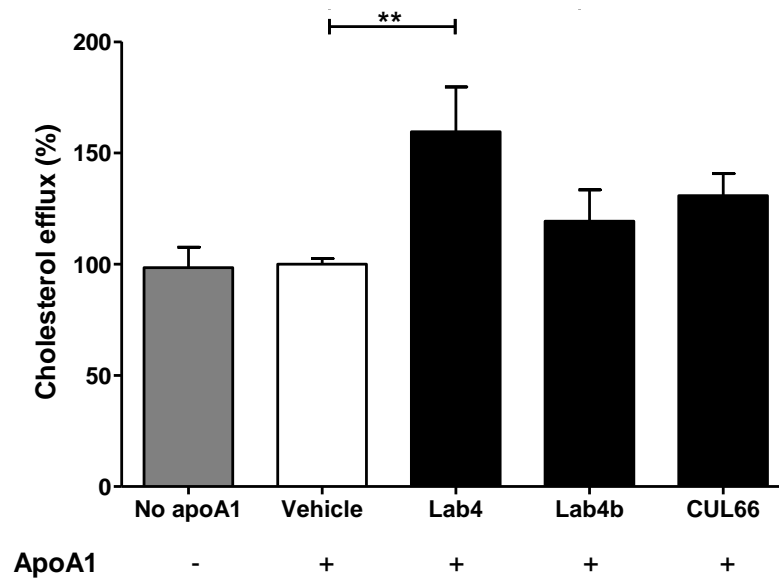


**Figure 4.11 - Probiotic CM enhances cholesterol efflux from primary human macrophages.** Primary human macrophages were treated with acLDL in addition to [4-<sup>14</sup>C] cholesterol for 24 hours followed by a further 24 hours with apoA1 and either vehicle control (Vehicle) or Lab4 (8 µg/mL), Lab4b (1.5 µg/mL) or CUL66 (5 µg/mL) CM. Cells treated with vehicle control in the absence of apoA1 were included for comparative purposes (No apoA1). Cholesterol efflux was determined as a percentage relative to the vehicle control which was arbitrarily set to 100%. Data are presented as mean ± SEM from four independent experiments. Statistical analysis was performed using a One-way ANOVA and Dunnett (2-sided) post-hoc test where \*\**p* < 0.01.

#### 4.3.4 Probiotic CM has strain-specific effects on the expression of key genes involved in cholesterol efflux

To investigate the effect of probiotic CM on key genes involved in cholesterol efflux, THP-1 macrophages were treated with acLDL for 24 hours to convert them into foam cells, followed by either vehicle control or probiotic CM for a further 24 hours. RNA was extracted, reverse transcribed to cDNA and the expression of ABCA1, ABCG1, APOE, LXR- $\alpha$  and LXR- $\beta$  determined by qPCR as described in Section 2.5. For ABCA1, treatment with Lab4 or Lab4b CM resulted in an increase in expression of 1.7-fold ( $p < 0.001$ ) and 2-fold ( $p < 0.001$ ) respectively, whereas CUL66 CM showed no significant change (Figure 4.12A). Expression of ABCG1 was significantly increased in the presence of Lab4 and Lab4b CM by 2-fold ( $p < 0.001$ ) and 3.5-fold ( $p < 0.001$ ) respectively, whereas CUL66 produced no significant changes (Figure 4.12B). LXR- $\alpha$  expression was increased by 1.6-fold ( $p = 0.013$ ) and 1.9-fold ( $p = 0.001$ ) in the presence of Lab4 or Lab4b CM respectively, with no significant change in expression following CUL66 treatment (Figure 4.12C). LXR- $\beta$  expression was significantly increased in the presence of Lab4 and Lab4b CM by 1.5-fold ( $p = 0.007$ ) and 2.5-fold ( $p < 0.001$ ) respectively, while CUL66 CM produced a significant 1.5-fold ( $p = 0.12$ ) decrease in expression (Figure 4.12D). For APOE expression, no significant changes were seen with Lab4 or Lab4b CM, while CUL66 treatment produced a 1.4-fold ( $p = 0.011$ ) reduction (Figure 4.12E). Changes in the expression of ABCA1 and ABCG1 were also analysed in primary human macrophages. Results from one independent experiment showed an increase in the expression of ABCA1 and ABCG1 following acLDL treatment, with a further increase following treatment with probiotic CM (Figure 4.13).

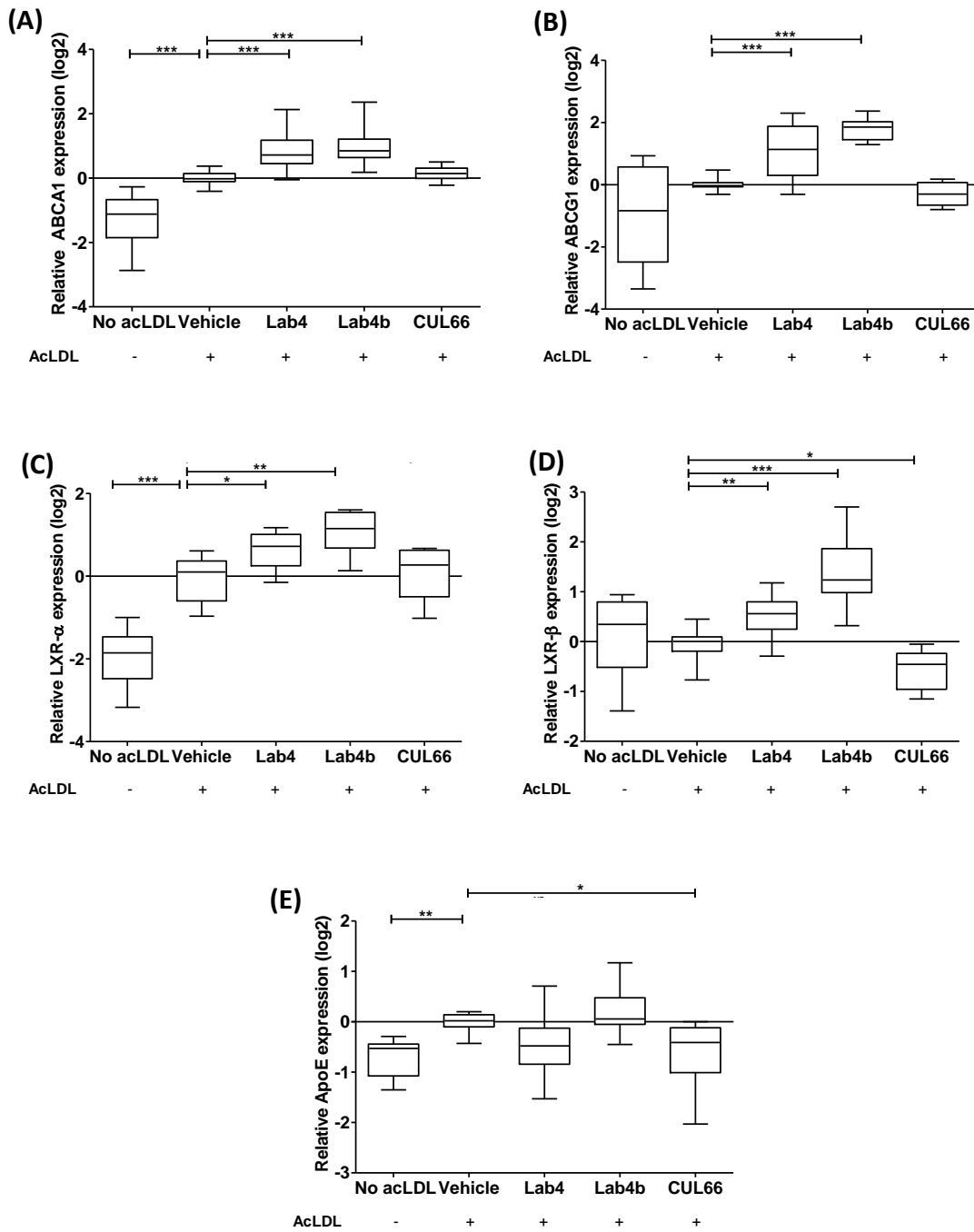


**Figure 4.12 - Probiotic CM has strain-specific effects on the expression of key genes involved in cholesterol efflux.** The effect of probiotic CM on the expression of (A) ABCA1, (B) ABCG1, (C) LXR-α, (D) LXR-β and (E) APOE was investigated in THP-1 macrophage foam cells treated for 24 hours with either vehicle control or Lab4 (8 µg/mL), Lab4b (1.5 µg/mL) or CUL66 (5 µg/mL) CM. Gene expression was determined by qPCR using the  $\Delta\Delta C_T$  method. Data are presented as box and whisker plots of log<sub>2</sub> fold-change in gene expression relative to the vehicle control, where whiskers represent min to max fold-change from three independent experiments. Statistical analysis was performed using a One-way ANOVA with Dunnett T3 (A, B or E), Dunnett (2-sided) (C and D) post-hoc tests where \**p* < 0.05, \*\**p* < 0.01 and \*\*\* *p* < 0.001.

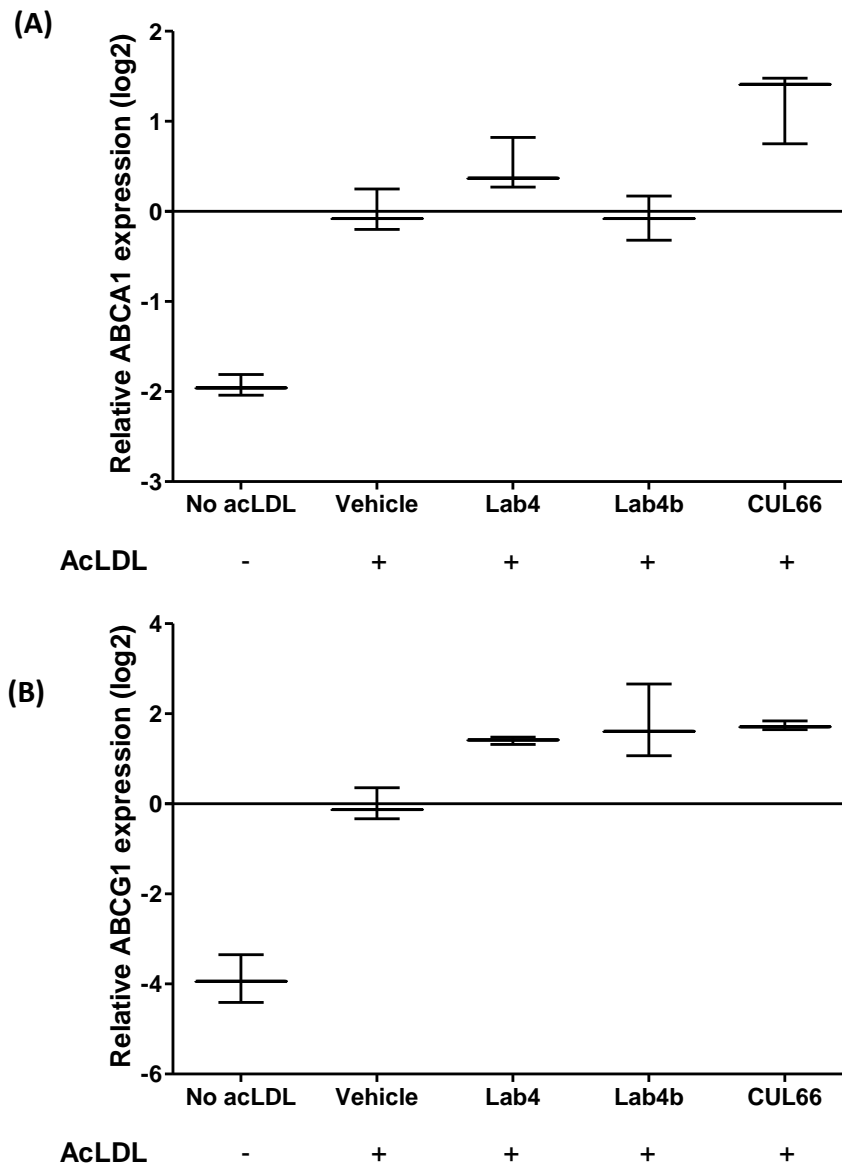


**Figure 4.13 - Probiotic CM increases the expression of key genes involved in cholesterol efflux in primary human macrophage foam cells.** The effect of probiotic CM on the expression of (A) ABCA1 and (B) ABCG1 was investigated in primary human macrophage foam cells treated for 24 hours with either vehicle control or Lab4 (8 µg/mL), Lab4b (1.5 µg/mL) or CUL66 (5 µg/mL) CM. Gene expression was determined by qPCR using the  $\Delta\Delta C_T$  method. Data are presented as box and whisker plots of log<sub>2</sub> fold-change in gene expression relative to the vehicle control, where whiskers represent min to max fold-change from one independent experiment.

#### 4.3.5 Cholesterol metabolism

The effect of probiotic CM on cholesterol metabolism was assessed in THP-1 macrophages according to a method adapted from previous studies in the laboratory (Gallagher, 2016; Moss, 2018). Briefly, THP-1 macrophages were seeded in 6-well plates



at a concentration of  $2 \times 10^6$  cells per mL, and incubated for 24 hours with either vehicle plus [ $^{14}\text{C}$ ] acetate (1  $\mu\text{Ci}/\text{mL}$ ) (negative control), vehicle plus [ $^{14}\text{C}$ ] acetate (1  $\mu\text{Ci}/\text{mL}$ ) and 25  $\mu\text{g}/\text{mL}$  acLDL (vehicle control), or probiotic CM plus [ $^{14}\text{C}$ ] acetate (1  $\mu\text{Ci}/\text{mL}$ ) and 25  $\mu\text{g}/\text{mL}$  acLDL. Lipids were then extracted using Folch's method as described in Section 2.7.4.1, and separated into major lipid classes by TLC (Section 2.7.4.2). The lipids on TLC plates were scraped and the incorporation of [ $^{14}\text{C}$ ] acetate into individual fractions was measured by liquid scintillation counting as described in Section 2.7.3. Total polar lipids (PL), triglycerides (TG), free fatty acids (FFA) cholesterol esters (CE) and free cholesterol (FC) were calculated as a percentage of total lipids. Results from one experiment are shown in Figure 4.14. The total cellular content of PL and FC was reduced with probiotic treatment, FFA were increased, with little change in TG components. Importantly, treatment with CUL66 resulted in a large decrease in CE, while Lab4 and Lab4b produced a smaller decrease in CE. However, these results are from one experiment, and additional repeats are required before any firm conclusions can be made.

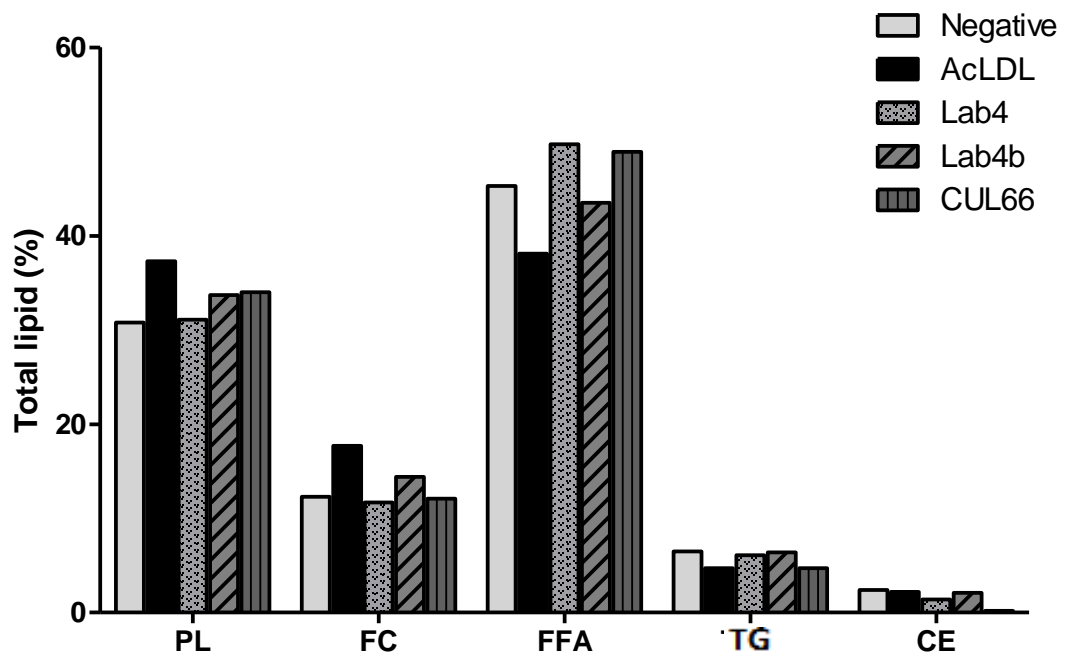


**Figure 4.14 - The effect of probiotic CM on the incorporation of [ $^{14}\text{C}$ ] acetate into major lipid classes.** THP-1 macrophages were treated with either vehicle plus [ $^{14}\text{C}$ ] acetate (Negative), vehicle plus [ $^{14}\text{C}$ ] acetate and acLDL (vehicle control; AcLDL) or Lab4 (8  $\mu\text{g}/\text{mL}$ ), Lab4b (1.5  $\mu\text{g}/\text{mL}$ ) or CUL66 (5  $\mu\text{g}/\text{mL}$ ) CM plus [ $^{14}\text{C}$ ] acetate and acLDL. Lipid classes were separated by TLC and the incorporation of [ $^{14}\text{C}$ ] acetate measured by scintillation counting. Data are presented as a percentage of the total lipids from one experiment. PL, polar lipids; FC, free cholesterol; FFA, free fatty acids; TG, triglycerides; CE, cholesterol esters.

#### 4.3.6 Probiotic CM has strain-specific effects on the expression of genes involved in intracellular cholesterol metabolism

To investigate the effect of probiotic CM on the expression of key genes involved in cholesterol metabolism, THP-1 macrophages were treated with acLDL for 24 hours followed by either vehicle control or probiotic CM for a further 24 hours. RNA was extracted, reverse transcribed to cDNA and the expression of NCEH1 and ACAT1 determined by qPCR as described in Section 2.5. As shown in Figure 4.15, the expression of NCEH1 was differentially regulated by probiotic CM with a significant 1.9-fold ( $p = 0.05$ ) increase with Lab4, no significant change with Lab4b, and a significant 3.6-fold ( $p < 0.001$ ) decrease with CUL66 CM. ACAT1 expression was significantly increased with Lab4b CM by 1.7-fold ( $p < 0.001$ ), while treatment with Lab4 or CUL66 CM showed no significant change in expression (Figure 4.15).

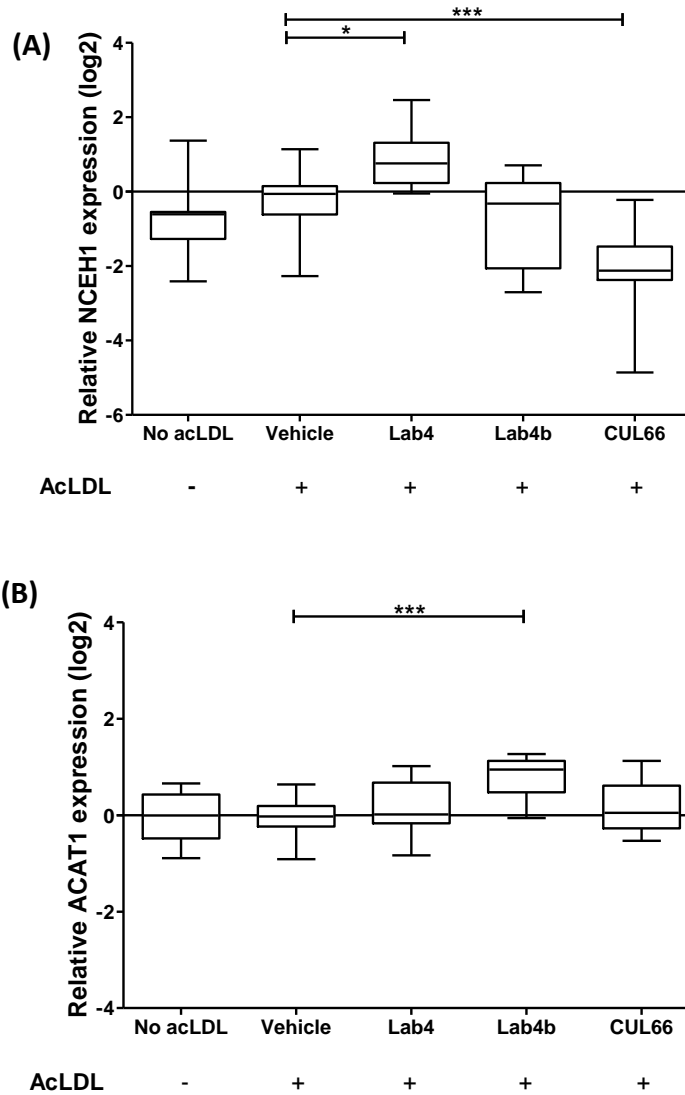


**Figure 4.15 – Probiotic CM has strain-specific effects on the expression of key genes involved in cholesterol metabolism.** The effect of probiotic CM on the expression of key genes involved in cholesterol metabolism was investigated in THP-1 macrophage foam cells treated for 24 hours with either vehicle control or Lab4 (8 µg/mL), Lab4b (1.5 µg/mL) or CUL66 (5 µg/mL) CM. Gene expression was measured by qPCR and relative expression of (A) NCEH1 and (B) ACAT1 determined using the  $\Delta\Delta C_T$  method. Data are presented as box and whisker plots of log<sub>2</sub> fold-change in gene expression relative to the vehicle control, where whiskers represent min to max fold-change from three independent experiments. Statistical analysis was performed using a One-way ANOVA with Dunnett (2-sided) post-hoc test where \* $p < 0.05$  and \*\*\*  $p < 0.001$ .

## 4.4 Discussion

Studies in the current chapter aimed to investigate the effect of probiotics on macrophage foam cell formation, and subsequently elucidate possible mechanisms underlying these effects. Initially, the effect of each probiotic CM on modified LDL uptake, cholesterol efflux and intracellular cholesterol metabolism was investigated at the cellular level. Studies then progressed to attempt to elucidate possible mechanisms underlying these effects at the molecular level by analysis of any changes in the expression of key genes involved in foam cell formation.

### 4.4.1 Modified LDL uptake

Firstly, the effect of probiotics on the uptake of modified LDL was investigated in THP-1 macrophages and HMDMs treated with Dil-oxLDL, and the uptake measured by flow cytometry. Uptake of Dil-oxLDL was significantly attenuated by 50% or more in both THP-1 macrophages (Figure 4.6) and HMDMs (Figure 4.7) treated with Lab4 or Lab4b CM, while CUL66 CM treatment resulted in greater attenuation of more than 70% in both cell model systems. Gene expression analysis in THP-1 macrophages showed that the expression of scavenger receptors SR-A and CD36 was significantly attenuated by each probiotic treatment, with Lab4b treatment resulting in notably greater attenuation of SR-A and CD36 expression in addition to a significant reduction in LPL expression (Figure 4.8). In the same series of experiments, Lab4 and CUL66 had no effect on the expression of LPL, indicating possible strain-specific mechanisms underlying the observed reduction in oxLDL uptake at the cellular level. In HMDMs, CD36 expression was significantly attenuated by each probiotic CM, consistent with findings in THP-1 macrophages (Figure 4.9). However, the expression of SR-A was attenuated with Lab4 treatment only, again indicating strain-specific effects of the probiotic bacteria.

It was previously shown that each probiotic CM significantly attenuates macropinocytosis in human macrophages (Figure 3.13). Studies presented in this chapter demonstrated that each probiotic CM also attenuates receptor-mediated uptake of oxLDL by macrophages, and that this effect is achieved at least in part by attenuation of macrophage scavenger receptors at the gene expression level.

Additionally, Lab4b specifically demonstrates an ability to attenuate the gene expression of LPL in THP-1 macrophages (Figure 4.8). LPL can associate with lipoproteins, thereby increasing the efficiency of their uptake (Serri *et al.*, 2004). It also increases the production of the proinflammatory cytokine TNF- $\alpha$ , increases monocyte adhesion to endothelial cells and increases the proliferation of VSMCs (Serri *et al.*, 2004). These findings reinforce potential further beneficial effects of Lab4b treatment via attenuation of LPL expression. Indeed, studies presented in Chapter 3 demonstrated that Lab4b treatment attenuated both monocyte migration (Figure 3.7) and VSMC proliferation (Figure 3.22). Additionally, it is notable that significant attenuation of CD36 expression was consistently achieved in both THP-1 macrophages and HMDMs with all probiotic CM treatments. This study is the first to investigate the effect of probiotic treatment on oxLDL uptake in macrophages with no similar studies appearing in the literature to date. However, a recent study investigating the effects of a specific strain of *L. plantarum* on diet-induced obesity and insulin resistance demonstrated a reduction in hepatic expression of CD36 in mice fed a high fat diet (Lee *et al.*, 2018).

#### 4.4.2 Cholesterol efflux

Overall, investigations of probiotic CM treatment on the uptake of oxLDL produced interesting results and demonstrated beneficial effects on this key aspect of macrophage foam cell formation. Next, the effect of probiotic treatment on the efflux of cholesterol was investigated in THP-1 macrophages and HMDMs. In THP-1 macrophages, treatment with apoA1 resulted in a significant increase in cholesterol efflux compared to no-apoA1 control, and treatment with all probiotic CM lead to a further significant increase in efflux of approximately 50% (Figure 4.10). In HMDMs, treatment with apoA1 alone did not produce a change in efflux of cholesterol; however, Lab4 treatment resulted in a significant increase while Lab4b and CUL66 treatment displayed a trend of increase in cholesterol efflux (Figure 4.11), which would likely reach significance upon further experimental repeats. Further studies investigated the possible mechanisms underlying this effect by analysis of ABCA1, ABCG1, APOE, LXR $\alpha$  and LXR $\beta$  expression in THP-1 macrophage foam cells. Following treatment with Lab4 or Lab4b CM, gene expression of ABCA1, ABCG1, LXR $\alpha$  and LXR $\beta$  were all significantly increased (Figure 4.12), suggesting that the observed increase in cholesterol efflux at

the cellular level may in part be due to upregulated LXR/ABC transporter pathways. Lab4 and Lab4b treatment had no effect on the expression of APOE (Figure 4.12). In contrast, treatment with CUL66 had no effect on the expression of ABCA1, ABCG1 or LXR $\alpha$ , with a decrease in the expression of LXR $\beta$  and APOE (Figure 4.12), highlighting strain-specific mechanisms of action underlying the observed increase in cholesterol efflux at the cellular level. The expression of ABCA1 and ABCG1 was also assessed in HMDMs, where treatment with each CM appears to result in increased expression (Figure 4.13). However, due to time constraints, results represent a single experimental repeat and further experiments will be required before firm conclusions can be drawn.

Treatment with Lab4 and Lab4b CM resulted in a significant increase in cholesterol efflux from both THP-1 macrophages and HMDMs (Figures 4.10 and 4.11), with a corresponding increase in the expression of ABCA1, ABCG1, LXR $\alpha$  and LXR $\beta$  (Figure 4.12). These results suggest that probiotic CM increases cholesterol efflux at least in part via LXR and ABC transporter pathways. A recent study demonstrated inhibition of LXR $\alpha$ -mediated ABCA1/ABCG1-dependent cholesterol efflux from THP-1 macrophages, resulting in an increase in lesion area and plaque lipid accumulation in ApoE $^{-/-}$  mice (Jin *et al.*, 2018). In the same study, treatment with LXR activator T0901317 increased ABCA1/ABCG1 expression both *in vitro* and *in vivo*, thereby reducing foam cell formation and atherosclerotic lesion area in THP-1 macrophages and ApoE $^{-/-}$  mice respectively (Jin *et al.*, 2018). An earlier study showed that in cholesterol-loaded THP-1 macrophages, ABCA1 was responsible for the efflux of cholesterol upon LXR activation, while silencing of ABCG1 indicated that ABCG1 expression was not necessary to achieve this effect (Larrede *et al.*, 2009).

Therapeutic strategies aimed to stimulate RCT have targeted LXR owing to subsequent effects in promoting cholesterol efflux from macrophages and HDL biosynthesis (Favari *et al.*, 2015). However, lipogenic toxicity associated with the systemic LXR agonists T0901317 and GW3965 (Favari *et al.*, 2015) is a major limitation of targeting LXRs. Despite this, the intestine-specific LXR activator GW6340 has been shown to enhance macrophage RCT while avoiding lipogenic toxicity (Yasuda *et al.*, 2010). Increased expression of ABC transporters A1/G1 as a result of LXR stimulation therefore represents a possible mechanism by which probiotic treatment enhances cholesterol efflux from

macrophages. Further research may aim to confirm these findings in a similar manner to previous studies in which PPAR $\gamma$  activity was inhibited by siRNA knockdown, abolishing the ABCA1 induced effect on cholesterol efflux (Sun *et al.*, 2015). In addition to the PPAR/LXR pathway, ABCA1 expression is known to be induced via the activation of the Janus kinase 2 (JAK2)/signal transducer and activator of transcription 3 (STAT3) pathway, in which activation of STAT3 increases ABCA1 expression and inhibition of JAK2 suppresses this effect (Fu *et al.*, 2014). With a number of possible mechanisms resulting in increased expression of ABC transporters, further investigation at the molecular and cellular level is required to elucidate the exact pathways underlying this observed effect.

#### 4.4.3 Intracellular cholesterol metabolism

The effect of probiotic CM on macrophage intracellular cholesterol metabolism was investigated for the first time in human macrophages at the cellular and gene expression levels. Formation of cholesterol esters and other major lipid classes in macrophage foam cells was assessed by following the incorporation of [ $^{14}\text{C}$ ]acetate into major lipid classes; a technique that has been utilised in studies of lipid metabolism for decades (Shireman *et al.*, 1988; Yamasaki *et al.*, 2018). Acetate is metabolised within the macrophage and incorporated into lipid classes, which can be separated by TLC and the radioactivity contained within each fraction measured by scintillation counting. As in previous studies, acLDL was used to induce foam cell formation and cholesterol ester accumulation in THP-1 macrophages (Gallagher, 2016; Lada *et al.*, 2003). Due to time constraints, only one experimental repeat was carried out and additional repeats will be required before firm conclusions can be made. Figure 4.14 shows that PL and FC fractions were reduced with probiotic CM treatment whereas FFA content was increased, with little change in TAG level. Notably, treatment with CUL66 resulted in a large decrease in CE formation, while Lab4 and Lab4b produced a smaller decrease in CE. In particular, the observed reduction in FC and CE fractions with probiotic CM treatment is of interest, suggesting an overall reduction in the amount of cholesterol stored within the cell. It should also be noted that the radioactivity contained within the media was also measured from samples collected prior to processing of cells for lipid extraction. It was noted that a higher level of [ $^{14}\text{C}$ ]acetate remained in the media when the cells were treated with probiotic CM compared to those treated with vehicle alone

(data not shown). This indicates that probiotic CM treated cells may have taken up less acetate, coinciding with the ability of probiotic CM to attenuate lipid uptake in macrophages. Additionally, in order to promote foam cell formation, the cells were treated with acLDL at a concentration of 25 µg/mL which was selected based on previous studies in the laboratory (Gallagher, 2016; Moss, 2018). One of these studies found that treatment of THP-1 macrophages with the same concentration of acLDL failed to achieve an accumulation of cholesterol esters, and so an alternative macrophage source was used (murine RAW264.7; Gallagher 2016). In the literature however, THP-1 macrophages have been successfully utilised in similar studies upon treatment with acLDL, with one study using a higher concentration of 100 µg/mL (Lada *et al.*, 2003). While THP-1 macrophages did accumulate cholesterol esters in this study, the level of accumulation was low. It could therefore be suggested that this experiment may be improved, either by using a higher concentration of acLDL or by utilising an alternative macrophage source.

The effect of probiotic CM treatment on the expression of ACAT1 and NCEH1 was also investigated in THP-1 macrophage foam cells and showed strain-specific results (Figure 4.15). Lab4 treatment resulted in a significant increase in the expression of NCEH1, but had no effect on ACAT1 expression. In this case, an increase in the presence of free cholesterol would be expected at the cellular level; however, in the current study a decrease was observed (Figure 4.15) suggesting involvement of additional mechanisms. Treatment with Lab4b resulted in no change in NCEH1 expression, but a significant increase in the expression of ACAT1 (Figure 4.15). In this case an increase in the accumulation of cholesterol esters might also be expected, contrary to the effect observed at the cellular level (Figure 4.14), again suggesting the involvement of additional mechanisms. With CUL66 treatment, the expression of NCEH1 was significantly decreased with no change in ACAT1 expression (Figure 4.15), supporting an increase in cholesterol accumulation which is again contradictory to the results obtained at the cellular level, where CUL66 treatment resulted in a large decrease in the CE fraction (Figure 4.14). Together, these results suggest that while the formation of intracellular cholesterol esters may be reduced with probiotic treatment, it is unlikely that this effect is achieved via modulation of ACAT1 and NCEH1 expression. However,



the expression of ACAT1 and NCEH1 should be investigated at the protein level, possibly by using standard Western blotting methods, before firm conclusions can be made.

#### 4.4.4 Summary and future work

In the previous chapter it was demonstrated that treatment with probiotic CM attenuated macropinocytosis in human macrophages. Studies presented in the current chapter showed that treatment of human macrophages with probiotic CM demonstrated an attenuation of receptor-mediated uptake of modified LDL, with a corresponding attenuation of scavenger receptors SR-A and CD36 at the gene expression level. Furthermore, probiotic CM treatment resulted in a significant increase in the efflux of cholesterol from the cell. However, a strain-specific mechanism was observed at the gene expression level with Lab4 and Lab4b stimulating an increase in the expression of ABCA1/G1 as well as LXR $\alpha$  and LXR $\beta$ , while CUL66 treatment resulted in an increase in the expression of APOE. Although the investigation of intracellular cholesterol metabolism was inconclusive, it's likely that the observed attenuation of modified LDL uptake together with increased efflux of cholesterol represents the primary mechanism by which probiotic CM reduces macrophage foam cell formation. Until recent years, monocyte-derived macrophages were thought to be the major contributor to foam cell accumulation in the plaque. However, it has been demonstrated that other cell types including endothelial cells and VSMCs are also able to form foam cells and can contribute substantially to foam cell accumulation (Chistiakov *et al.*, 2017). In fact, it has recently been shown that VSMCs can constitute up to 50% or more of total foam cell population in human coronary artery plaque (Dubland and Francis, 2016). Further work may therefore investigate the effect of probiotics on foam cell formation in additional cell types.

This is the first study to investigate the effect of Lab4, Lab4b and CUL66 on foam cell formation in human macrophages. Given the marked implication of foam cell accumulation in atherosclerosis, the ability of probiotics to reduce the formation of foam cells is a highly desirable effect of an anti-atherosclerotic therapy. When considered in conjunction with the beneficial effects observed in Chapter 3, it was concluded that these probiotics represent a promising candidate for anti-atherosclerotic

therapy. Research therefore progressed to *in vivo* investigation using atherosclerosis mouse models, which are presented in the next chapter.

## CHAPTER 5

*The effects of Lab4 and  
CUL66 combination on  
atherosclerosis development  
in vivo*

---

## 5.1 Introduction

In the studies presented in the previous chapters it was demonstrated that probiotic CM treatment exerted a number of beneficial effects *in vitro*, including the attenuation of monocyte migration, inhibition of macrophage foam cell formation and reduced proliferation of key cell types in atherosclerosis; highlighting their potential as an anti-atherogenic agent. While *in vitro* study is very informative, it is also limited and validation through *in vivo* study is essential for confirmation of findings in a more relevant model system. In this chapter, the effect of probiotic dietary supplementation on atherosclerotic plaque development, plaque composition and plasma lipids was investigated *in vivo* using a widely employed atherosclerosis mouse model. The LDLr<sup>-/-</sup> mutation induces hypercholesterolaemia and a plasma lipid profile resembling that of dyslipidaemic humans (Getz and Reardon, 2016), making it a particularly suited model for the study of effects on plasma lipids. While spontaneous plaque formation may be observed in other atherosclerosis mouse models such as the ApoE<sup>-/-</sup> mouse, this is not a characteristic of the LDLr<sup>-/-</sup> model where plaque and lesion development is diet induced (Getz and Reardon, 2016). The LDLr<sup>-/-</sup> mouse was therefore selected as one of the most extensively utilised atherosclerosis mouse models, and the most suitable model for use in this study.

### 5.1.1 Study design

LDLr<sup>-/-</sup> mice (8-week old; male) were randomly assigned into two groups of 15 and allocated to either HFD (control group) or HFD supplemented with probiotic (probiotic group). A novel probiotic combination of Lab4 and CUL66 was used for the study as decided by Cultech Ltd in line with company goals. Table 5.1 shows the bacteria strains included in the Lab4/CUL66 supplement. The mice were fed HFD supplemented with probiotic at a concentration of  $1 \times 10^8$  CFU/g, or 100 billion CFU/day equivalent human dose, for a period of 12 weeks. Further details on animals and feeding are described in Section 2.8.1. At study end point, mice were euthanised by increasing the levels of CO<sub>2</sub> and death confirmed by absence of a pulse. Whole blood, subcutaneous and gonadal fat, organs (heart, liver, spleen and thymus), descending aorta and rear legs were collected and stored as described in Section 2.8.2. Fat and organ weights were recorded.

Although not immediately required, many of these tissues were collected and stored for future experiments in order to minimise waste and satisfy the 3R's of animal research ethics.

Mouse body weights were analysed for any difference in final body weight or total weight gained throughout the study. Organ weights were also analysed. To assess the effect of probiotic on plaque size and lipid content, the aortic sinus was sectioned at 10 nm intervals. Sections were stained with H&E or Oil red O and the plaque area and lipid content determined respectively. Further sections of the arterial sinus were used in the immunohistochemical analysis of macrophage, T cell and SMC content using cell surface marker antibodies. Blood samples were analysed and plasma cholesterol and TG content quantified.

**Table 5.1 - Bacteria species included in the Lab4/CUL66 probiotic supplement**

Bacteria species
<i>Lactobacillus acidophilus</i> CUL21 (NCIMB 30156)
<i>Lactobacillus acidophilus</i> CUL60 (NCIMB 30157)
<i>Bifidobacterium bifidum</i> CUL20 (NCIMB 30153)
<i>Bifidobacterium animalis subsp. lactis</i> CUL34 (NCIMB 30172)
<i>Lactobacillus plantarum</i> CUL66

## 5.2 Experimental aim

The studies presented in this chapter aimed to assess the effect of probiotic supplementation on atherosclerotic plaque development, plaque composition and plasma lipid profile in LDLR<sup>-/-</sup> mice following 12 weeks feeding of HFD or HFD supplemented with Lab4/CUL66. Detailed methods for this chapter are described in Section 2.8, and an overview of the experimental strategy is presented in Figure 5.1.

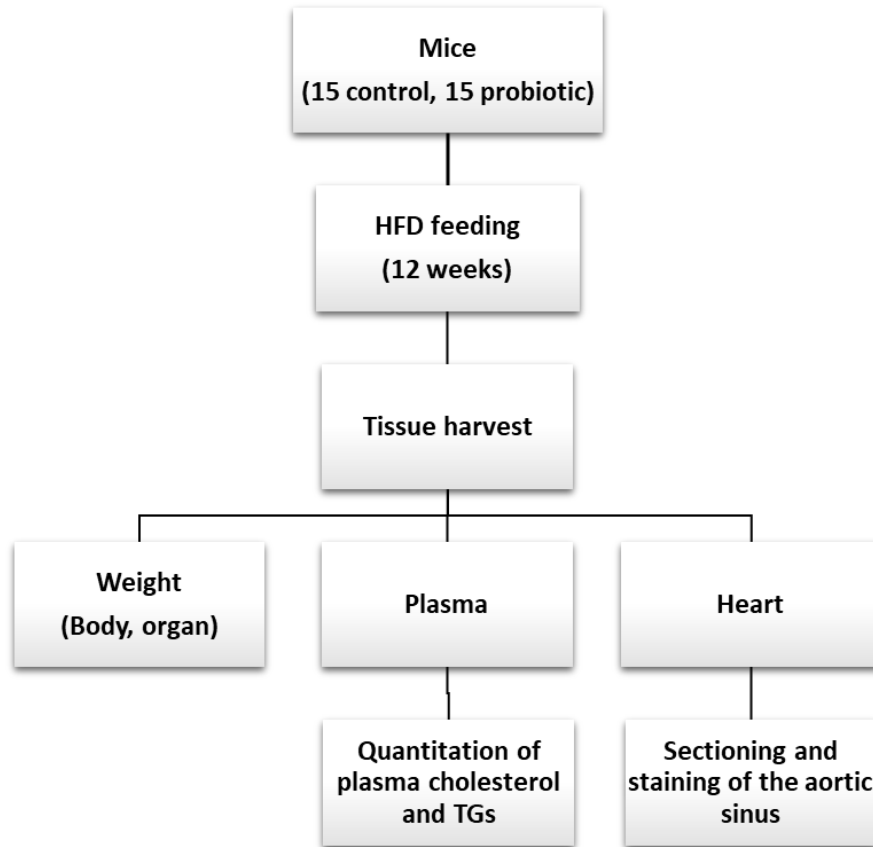


**Figure 5.1 - Experimental strategy used to assess the effect of probiotic treatment on plaque formation and lipid profile *in vivo*.** HFD, high fat diet; TGs, triglycerides.

### 5.3 Results

#### 5.3.1 Lab4/CUL66 supplementation had no effect on the body weight of LDLr<sup>-/-</sup> mice fed a high fat diet

Mouse weights were recorded at study start, then every 2-3 days for 12 weeks with a final measurement taken at study end point. Weights recorded at study start and end were used to calculate total weight gained by each mouse throughout the study. No difference in either final weight or total weight gain was observed between the control and the probiotic groups (Figure 5.2).

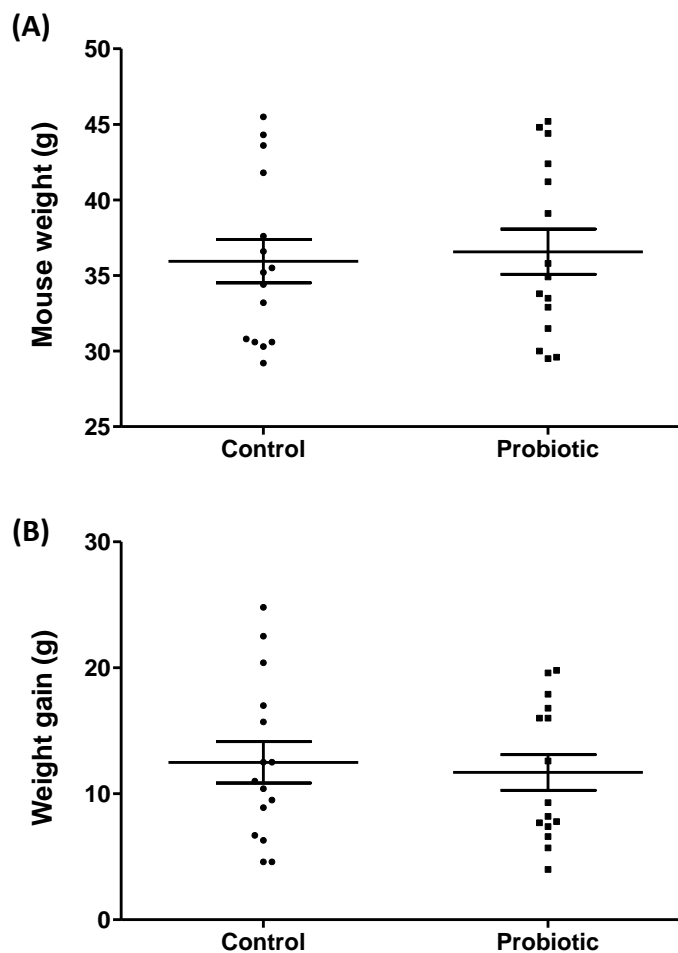


**Figure 5.2 - Probiotics have no effect on mouse body weights compared to the control group.** Mice were fed either HFD or HFD supplemented with probiotic for 12 weeks and mouse weights recorded every 2-3 days. (A) Mouse weight measured at study end; (B) Mouse weight gain from study start to end point. Data are presented as mean  $\pm$  SEM from 15 control and 15 probiotic mice. Statistical analysis was performed using a Student's t-test.

### 5.3.2 The effect of Lab4/CUL66 supplementation on mouse body fat and organ weight

Subcutaneous and gonadal fat together with liver, spleen, heart and thymus were removed and weighed at study end. Fat and organ weights are shown in Figure 5.3. No significant difference between subcutaneous fat, gonadal fat, liver, heart or thymus weight was observed between the control and the probiotic groups. However, spleen weight was significantly increased in the probiotic group compared to the control ( $p = 0.034$ ).

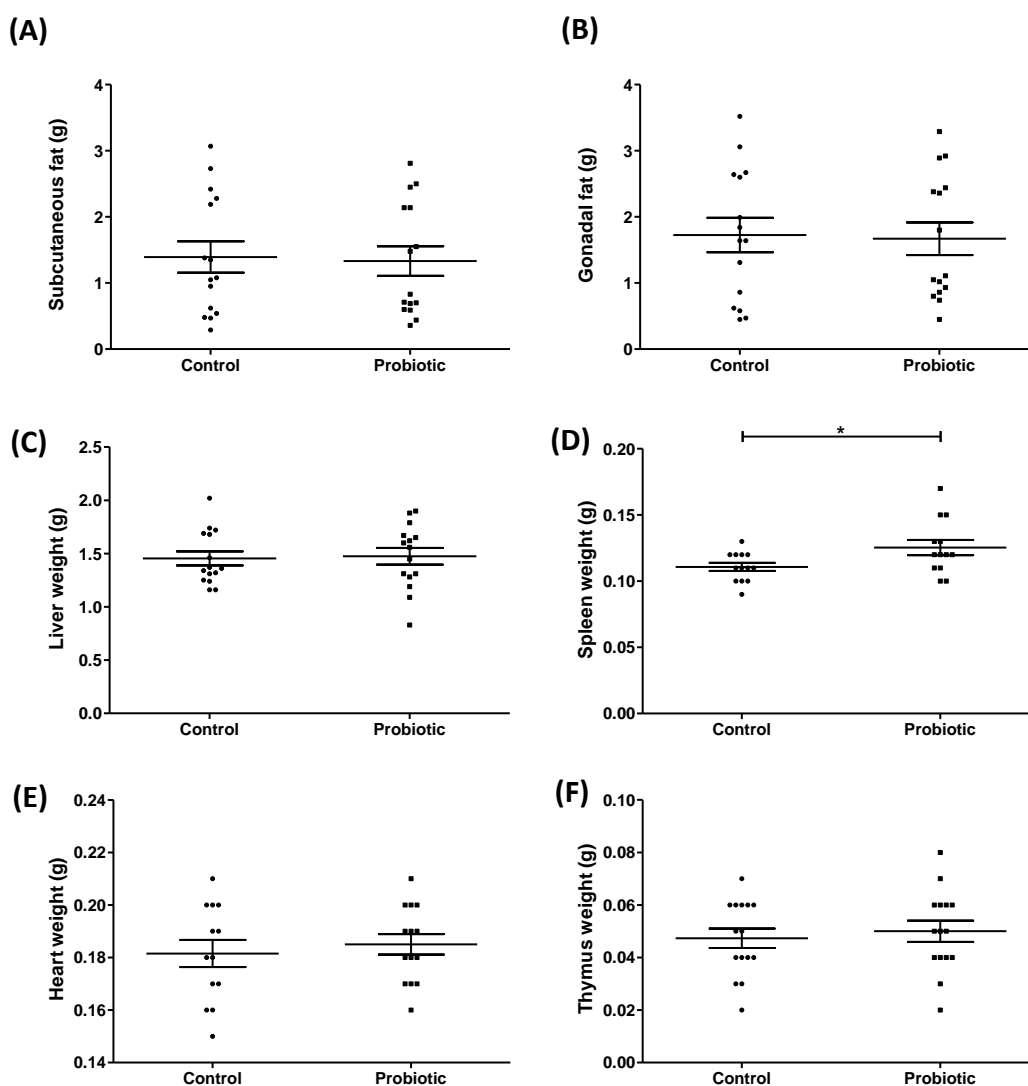


**Figure 5.3 – Mouse fat and organ weight recorded at study end.** Mice were fed either HFD (Control group) or HFD supplemented with probiotics (Probiotic group) for 12 weeks and fat and organ weights recorded at study end point. (A) Subcutaneous fat; (B) Gonadal fat; (C) Liver; (D) Spleen; (E) Heart; and (F) Thymus. Data are presented as mean  $\pm$  SEM from 15 control and 15 probiotic mice. Statistical analysis was performed using a Student's t-test where  $*p < 0.05$ .



### 5.3.3 The effect of Lab4/CUL66 supplementation on plasma cholesterol levels in mice fed a high fat diet

Total cholesterol, HDL, LDL and free cholesterol content of plasma was measured from 15 control and 15 probiotic mice as described in Section 2.8.3.1. Cholesterol ester level was determined as the difference between total and free cholesterol fractions, and ratios of LDL/HDL, TC/HDL and TC/LDL calculated. Results demonstrate a significant 32% increase in plasma HDL cholesterol ( $p = 0.041$ ), in addition to a significant 19% ( $p = 0.048$ ) decrease in LDL cholesterol in the probiotic group compared to the control. Furthermore, calculation of the LDL/HDL ratio showed a significant 39% decrease ( $p = 0.002$ ) in the probiotic group compared to the control (Figure 5.4). Probiotic treatment had no significant effect on total cholesterol, free cholesterol or cholesterol esters compared to the control. TC/HDL ratio was significantly decreased by 27% ( $p = 0.031$ ), and TC/LDL ratio increased by 45% ( $p = 0.044$ ) in the probiotic group compared to the control (Figure 5.5).

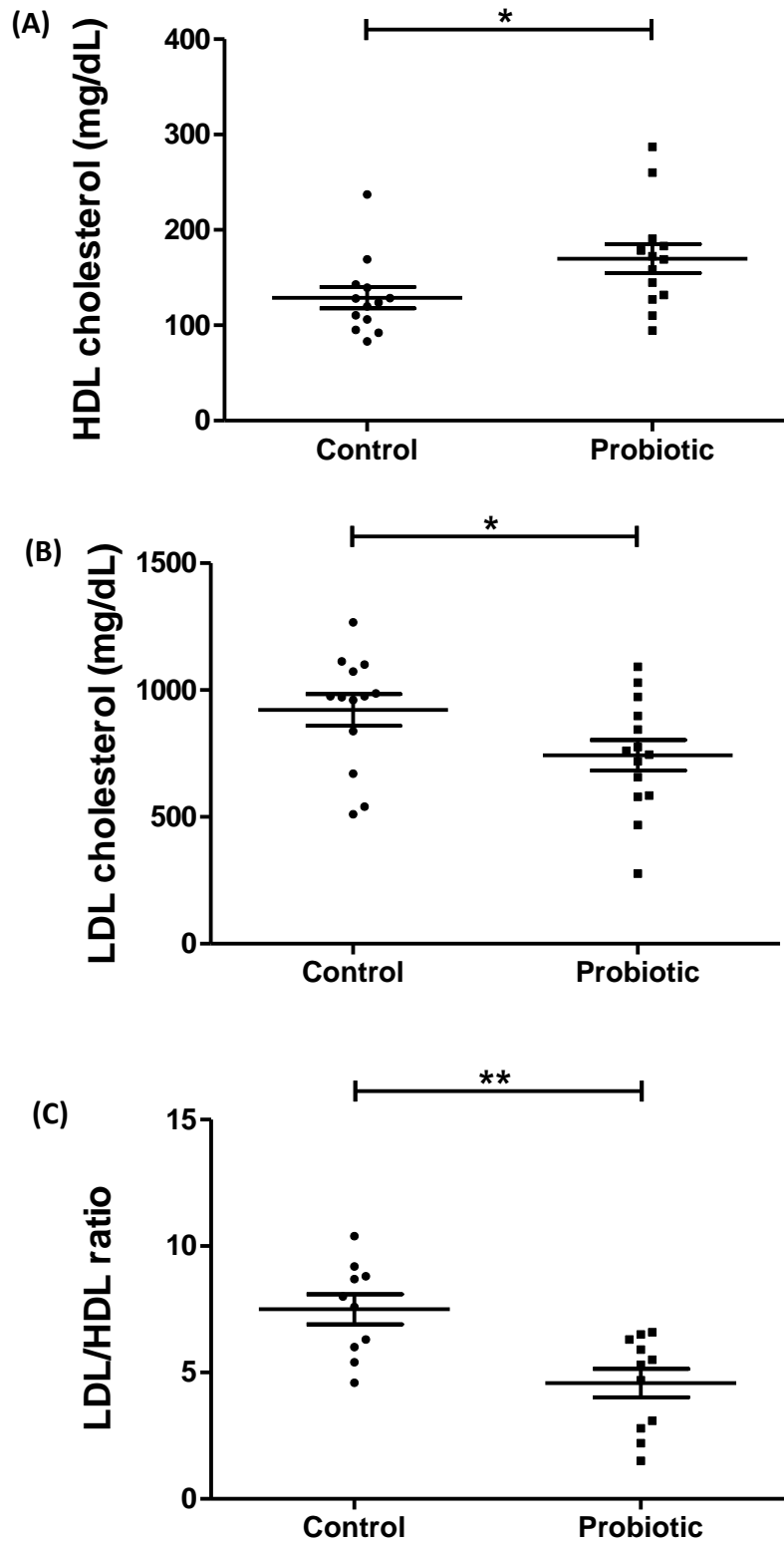


**Figure 5.4 - Increased HDL and decreased LDL cholesterol levels in probiotic mice compared to the control.** Plasma cholesterol levels were measured following 12 weeks feeding with either HFD (Control) or HFD supplemented with probiotic (Probiotic). (A) HDL cholesterol; (B) LDL cholesterol; and (C) LDL/HDL ratio. Data are presented as mean  $\pm$  SEM from 15 control and 15 probiotic mice. Statistical analysis was performed using a Student's t-test where \* $p$  < 0.05 and \*\* $p$  < 0.01.

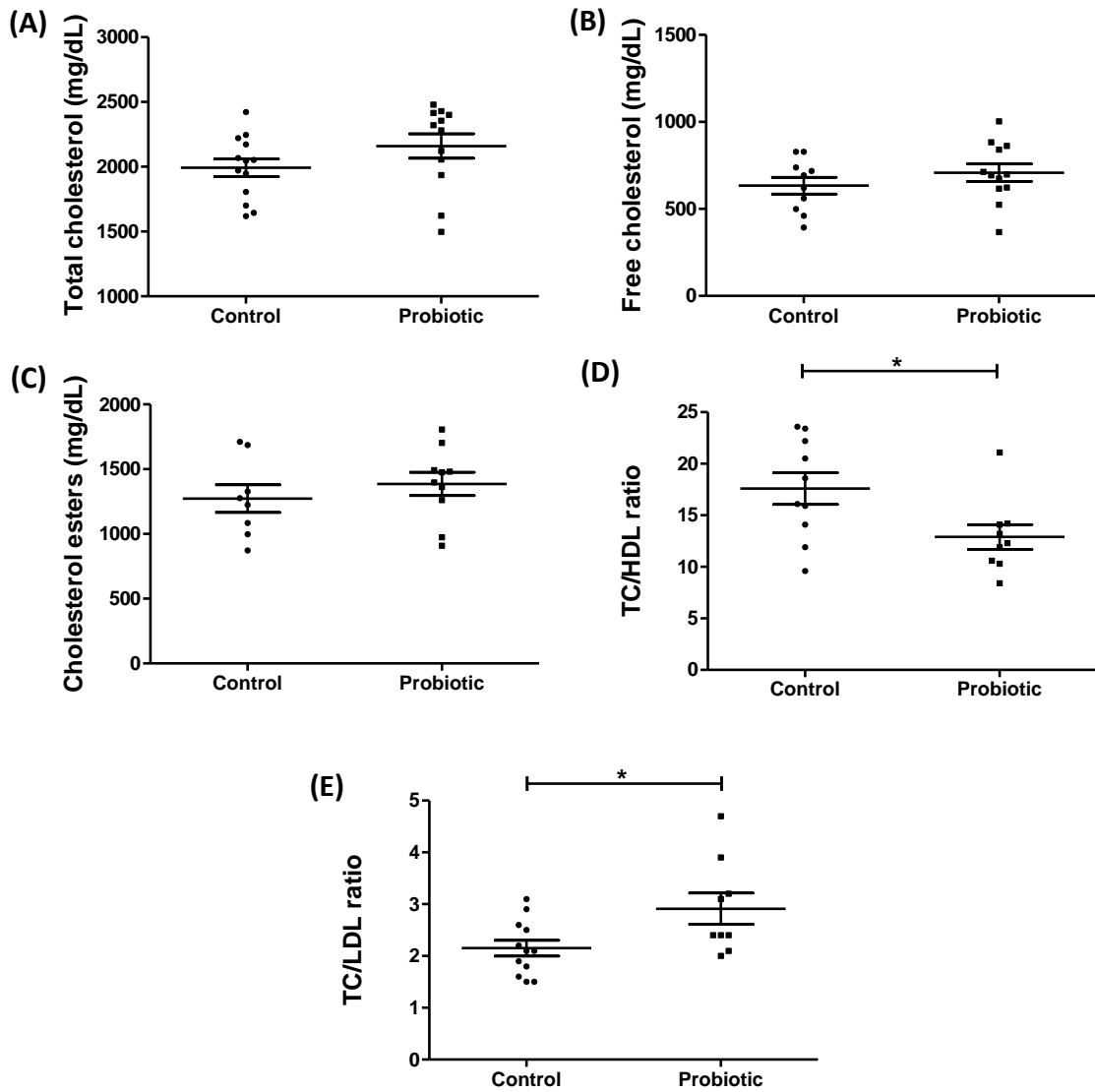


**Figure 5.5 – Probiotic treatment has beneficial effects on cholesterol ratios compared to the control.** Plasma cholesterol levels were measured following 12 weeks feeding with either HFD (Control) or HFD supplemented with probiotic (Probiotic). (A) Total cholesterol; (B) free cholesterol; and (C) cholesterol esters were measured and used in the calculation of (D) TC/HDL ratio and (E) TC/LDL ratio. Data are presented as mean  $\pm$  SEM from 15 control and 15 probiotic mice. Statistical analysis was performed using a Student's t-test where  $*p < 0.05$ .

### 5.3.4 Triglycerides were increased in the plasma of probiotic mice compared to the control

Plasma TG levels were measured from 15 control and 15 probiotic treated mice as described in section 2.8.3.2. TG levels were significantly increased in the plasma of the probiotic group compared to the control ( $p = 0.019$ ) (Figure 5.6).

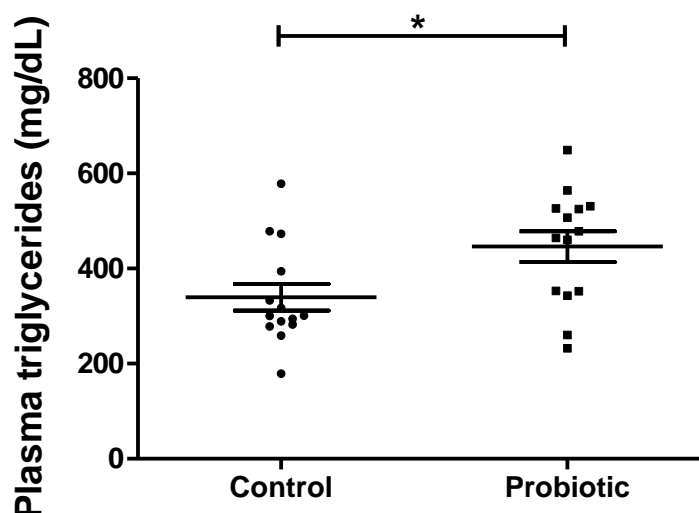


**Figure 5.6 - Plasma triglyceride levels were increased in the probiotic compared to the control group.** Plasma triglyceride levels were measured following 12 weeks feeding with either HFD (Control) or HFD supplemented with probiotic (Probiotic). Data are presented as mean  $\pm$  SEM from 15 control and 15 probiotic mice. Statistical analysis was performed using a Student's t-test where \* $p < 0.05$ .

### 5.3.5 Plaque area and lipid content was reduced with Lab4/CUL66 supplementation

Sections of the aortic sinus were stained with H&E and Oil Red O as described in Sections 2.8.5.2 and 2.8.5.3 respectively. Figure 5.7 shows representative H&E and Oil red O stained sections from control and probiotic groups. H&E and Oil red O stained sections from 12 control and 11 probiotic mice were used in the measurement of plaque area and lipid content respectively, using Image J software. Plaque area was significantly reduced by 39% in the probiotic mice compared to the control ( $p = 0.021$ ) (Figure 5.8). Lipid content determined as percentage staining of the plaque was significantly reduced by 35% ( $p < 0.001$ ) compared to the control (Figure 5.9).

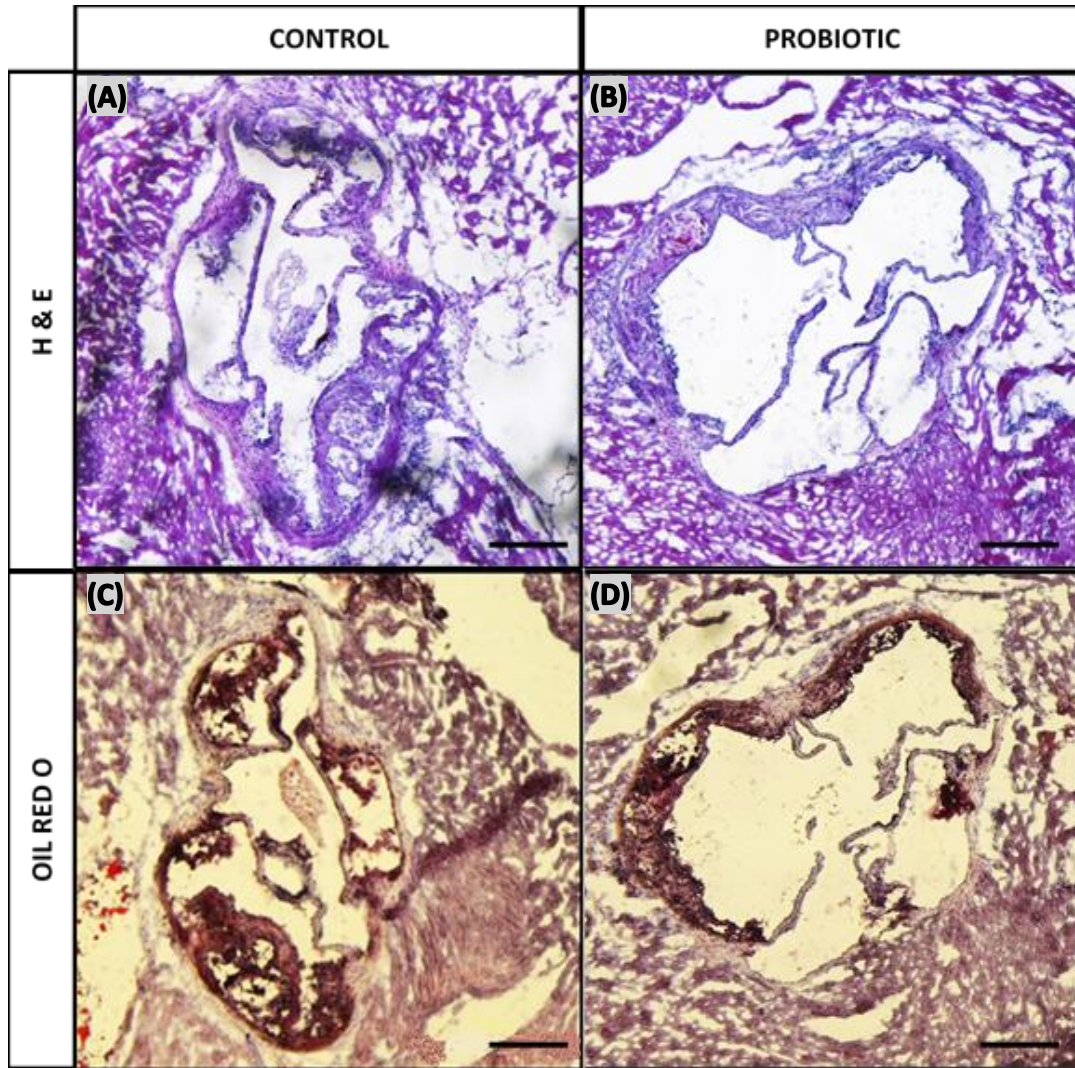


**Figure 5.7 - H&E and Oil Red O staining of the aortic sinus in the control and probiotic groups.** Sections of the aortic sinus following 12 weeks feeding with HFD (Control; n=12) or HFD supplemented with probiotic (Probiotic; n=11). Images show H&E stained sections from (A) control and (B) probiotic mice and Oil red O stained sections from (C) control and (D) probiotic mice. Images taken at X40 magnification. Scale bar represents 50  $\mu$ M.

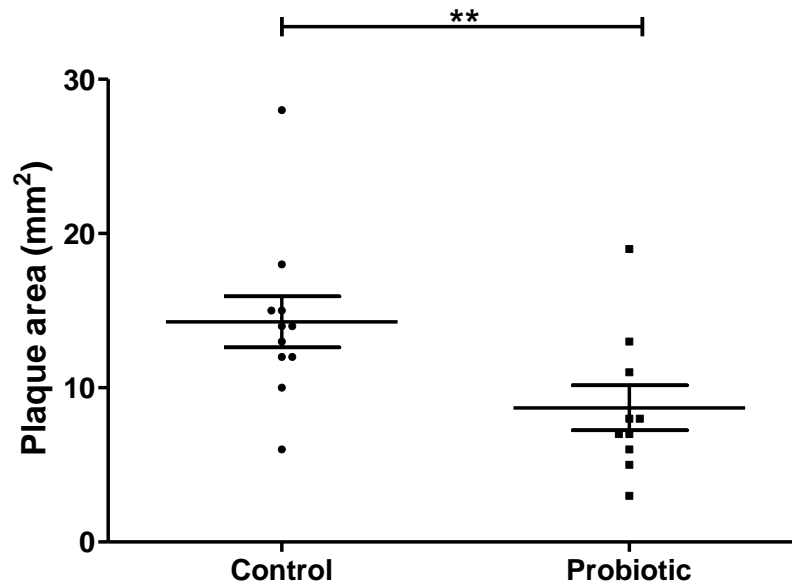


**Figure 5.8 - Plaque area was significantly reduced in probiotic mice compared to the control.** Plaque area was measured in sections of the aortic sinus following 12 weeks feeding with either HFD (Control) or HFD supplemented with probiotic (Probiotic). Sections were stained with H&E and plaque area quantified using Image J software. Data are presented as mean  $\pm$  SEM from 12 control and 11 probiotic mice. Statistical analysis was performed using a Student's t-test where  $**p < 0.01$ .

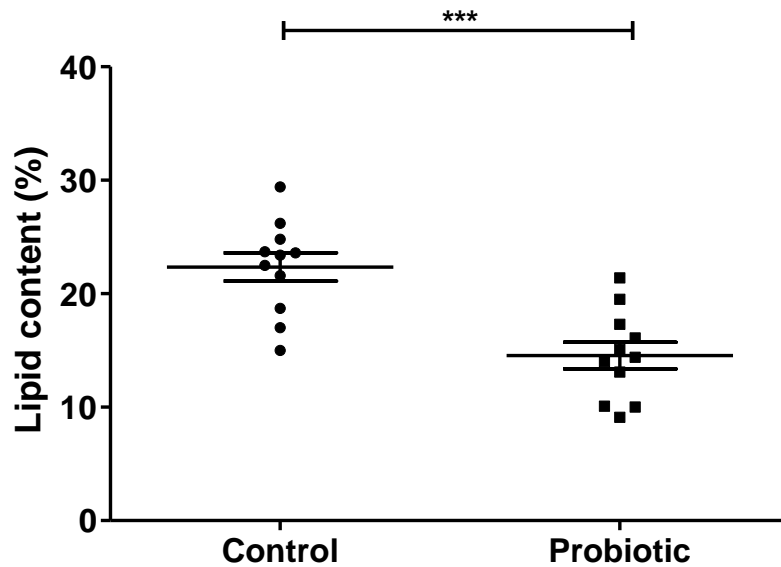


**Figure 5.9 – Lipid content was significantly reduced in the aortic sinus of probiotic mice compared to the control.** Following 12 weeks feeding with either HFD (Control) or HFD supplemented with probiotic (Probiotic), the aortic sinus were sectioned and lipid content assessed. Sections were stained with Oil red O and lipid content determined as percentage staining of the plaque using Image J software. Data are presented as mean  $\pm$  SEM from 12 control and 11 probiotic mice. Statistical analysis was performed using a Student's t-test where  $***p < 0.001$ .

### 5.3.6 The effects of Lab4/CUL66 supplementation on macrophage, SMC and T cell content of plaques

Immunofluorescent staining was carried out using sections of the aortic sinus as described in Section 2.8.5.4. Briefly, cell surface marker antibodies were used to detect macrophages (anti-mouse MOMA-2), SMCs (anti-mouse  $\alpha$ SMA) and T cells (anti-mouse CD3). Images were captured at X40 magnification (X4/0.13 objective). DAPI, FITC and AF-488 filters were applied for imaging of DAPI, AF-594 and AF-488 fluorophores respectively. All images were captured using consistent exposure, intensity and contrast settings for comparable downstream analyses. Intensity of staining within the plaque was quantified using ImageJ software where raw intensity values were determined in relation to maximum intensity values of segmented images. Representative images obtained for control and probiotic groups are presented in Figures 5.10 – 5.12. Macrophage, SMC and T cell content of sections obtained from control and probiotic groups are presented as a percentage staining of plaque in Figure 5.13. Macrophage content was significantly reduced by 39% in the probiotic group compared to the control ( $p = 0.024$ ). T cell content was also reduced by 34% showing a non-significant trend of decrease ( $p = 0.096$ ) in the probiotic group. Additionally, a significant 40% reduction ( $p = 0.024$ ) in smooth muscle cell content was observed in the probiotic group. For each section, the corresponding ISO control contained little to no staining (Figures 5.10 – 12), showing that the staining was specific for the target site and not due to non-specific background binding.

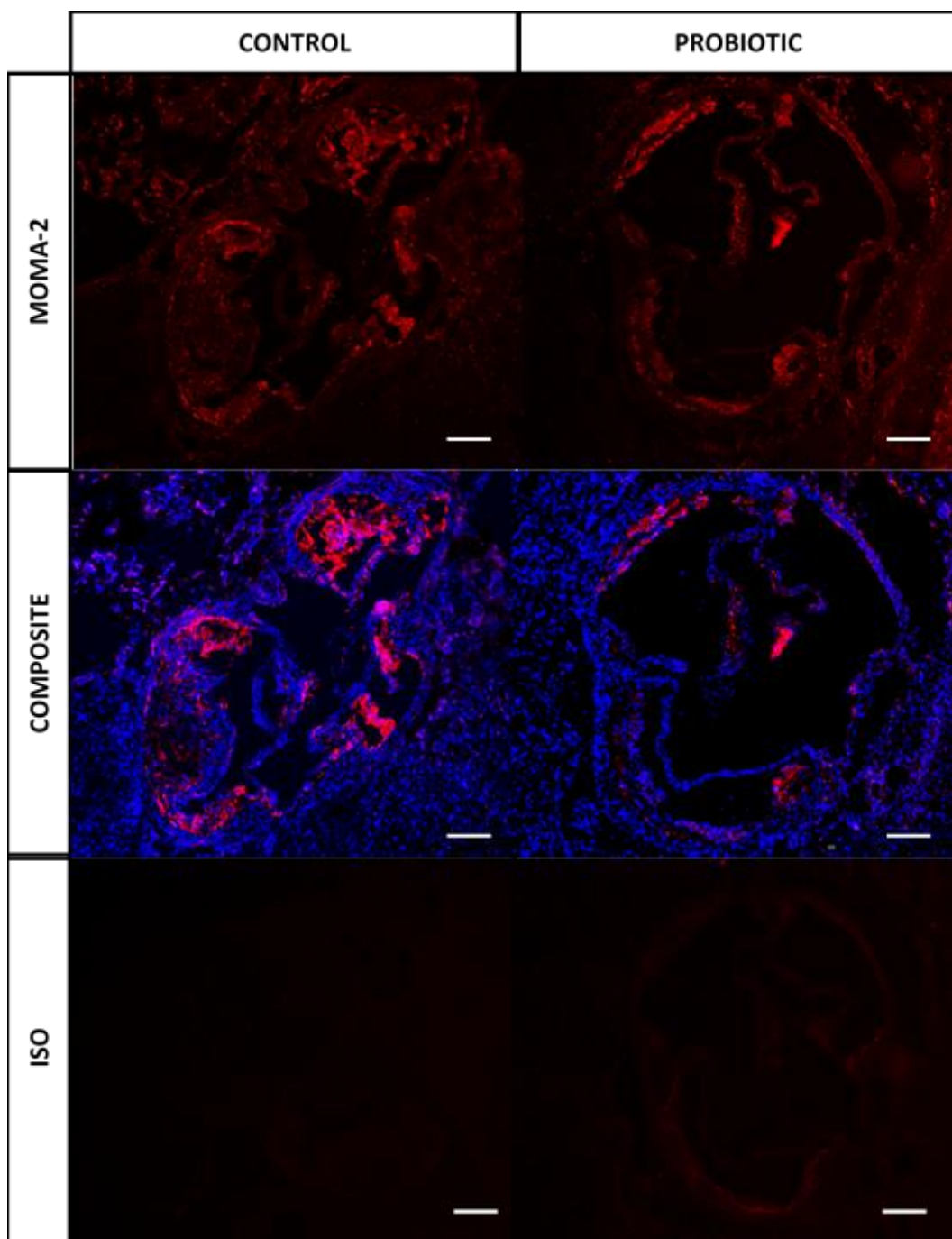


**Figure 5.10 - Immunofluorescent staining of macrophages present in sections of the aortic sinus.** Following 12 weeks feeding with either HFD (Control) or HFD supplemented with probiotic (Probiotic), the aortic sinus was sectioned and the macrophage content analysed by immunohistochemistry using cell surface marker antibodies. Sections were stained using the MOMA-2 cell surface antibody, mounted with DAPI and images captured by fluorescent microscopy. Representative images are presented for control and probiotic groups showing MOMA-2 staining (MOMA-2), MOMA-2 and DAPI staining (Composite) and IgG isotype control (ISO). Scale bars represent 50  $\mu$ M. Red, MOMA-2 AF-488; Blue, DAPI.



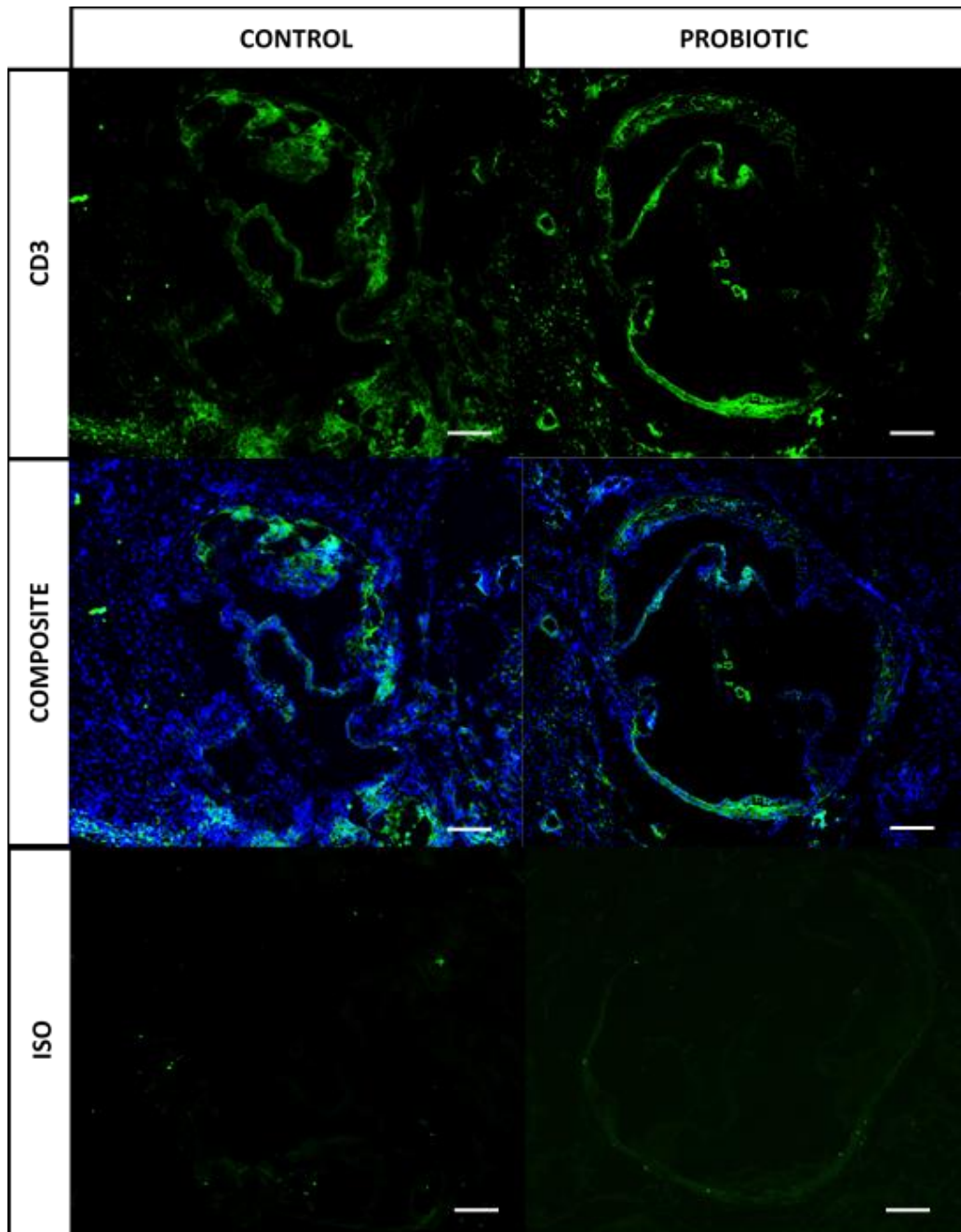


**Figure 5.11 - Immunofluorescent staining of T cells present in sections of the aortic sinus.** Following 12 weeks feeding with either HFD (Control) or HFD supplemented with probiotic (Probiotic), the aortic sinus was sectioned and the T cell content analysed by immunohistochemistry using cell surface marker antibodies. Sections were stained using the CD3 cell surface antibody, mounted with DAPI, and the images visualised and captured by fluorescent microscopy. Representative images are presented for control and probiotic groups showing CD3 staining (CD3), CD3 and DAPI staining (Composite) and IgG isotype control (ISO). Scale bars represent 50  $\mu$ M. Green, CD3 AF-594; Blue, DAPI.

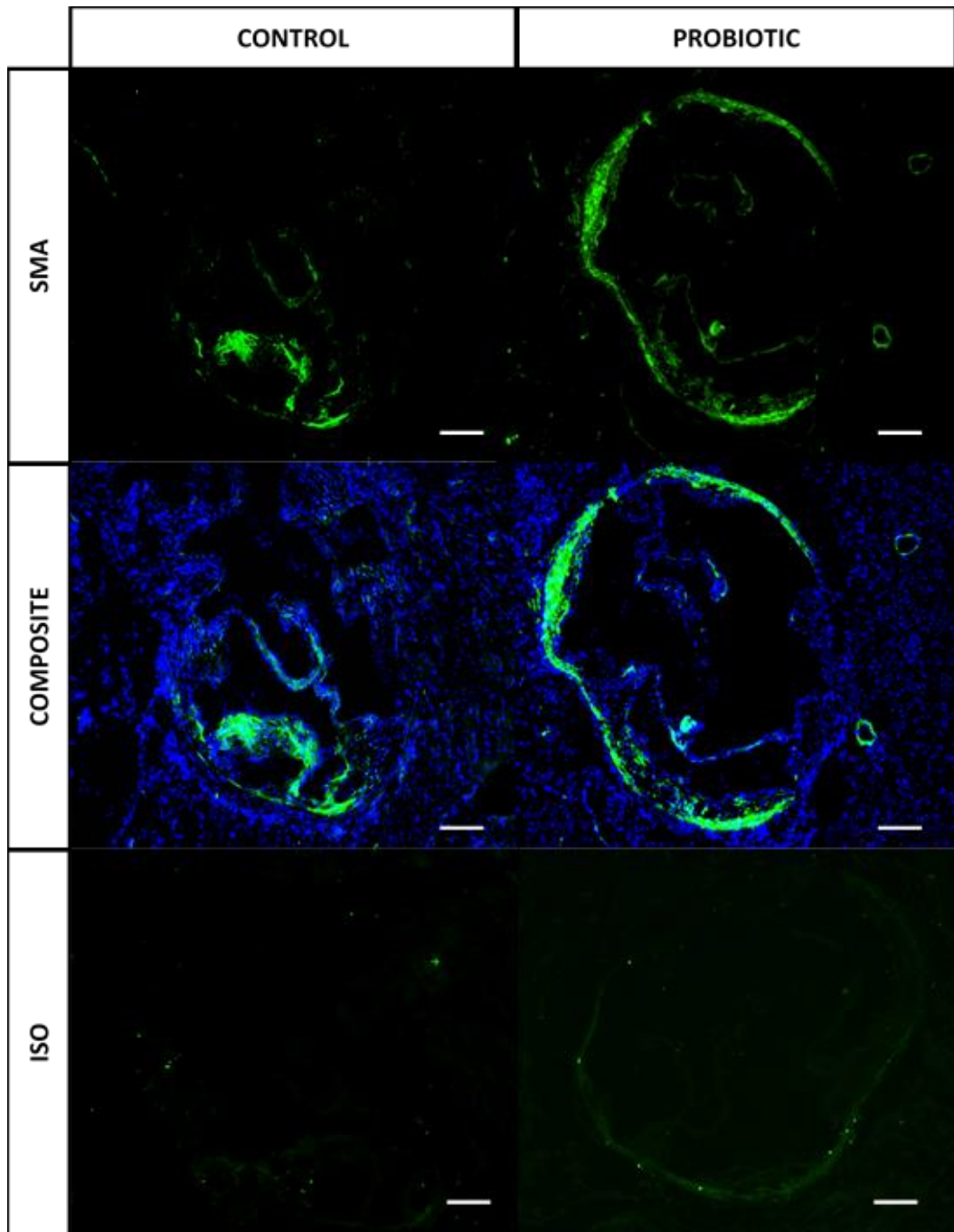


**Figure 5.12 - Immunofluorescent staining of SMCs present in sections of the aortic sinus.** Following 12 weeks feeding with either HFD (Control) or HFD supplemented with probiotic (Probiotic), the aortic sinus was sectioned and the SMC content analysed by immunohistochemistry using cell surface marker antibodies. Sections were stained using the  $\alpha$ SMA cell surface antibody, mounted with DAPI and images visualised and captured by fluorescent microscopy. Representative images are presented for control and probiotic groups showing  $\alpha$ SMA staining (SMA),  $\alpha$ SMA and DAPI staining (Composite) and IgG isotype control (ISO). Scale bars represent 50  $\mu$ M. Green,  $\alpha$ SMA AF-594; Blue, DAPI.

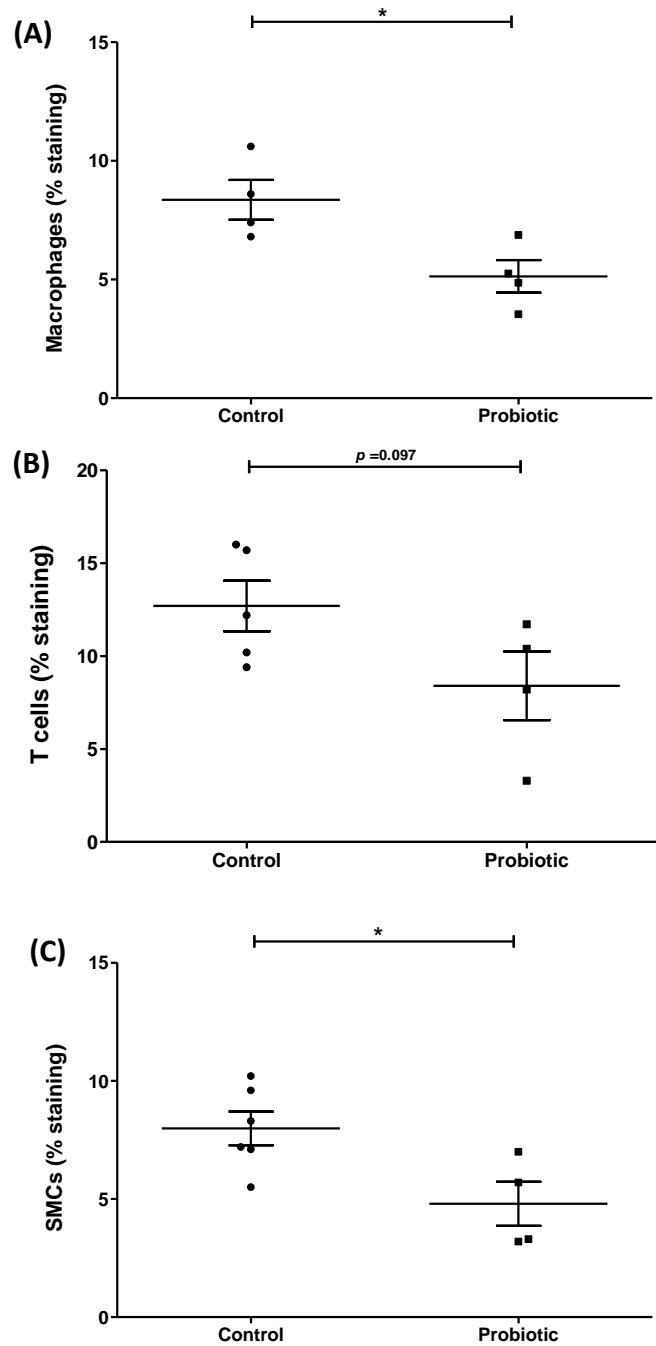


**Figure 5.13 – Macrophage, SMC and T cell content was significantly reduced in the aortic sinus of probiotic mice compared to the control.** Following 12 weeks feeding with either HFD (Control) or HFD supplemented with probiotic (Probiotic), the aortic sinus was sectioned and (A) macrophage, (B) T cell and (C) SMC content analysed by immunohistochemistry using cell surface marker antibodies. Images were captured using fluorescence microscopy. Regions of staining were quantified using ImageJ software and presented as percentage staining of plaque. Data are presented as mean  $\pm$  SEM from either 4 (A), 5 (B) or 6 (C) control and 4 probiotic mice. Statistical analysis was performed using a Student's t-test where  $*p < 0.05$ .

## 5.4 Discussion

Following on from the promising results obtained from *in vitro* studies, the investigation of the effect of probiotics on atherosclerosis was continued *in vivo* using atherosclerosis mouse models. In this chapter, the effect of Lab4/CUL66 supplementation on plaque development, plaque composition and plasma lipid profile was assessed in LDLr<sup>-/-</sup> mice following 12 weeks feeding with either HFD or HFD supplemented with Lab4/CUL66 in combination.

### 5.4.1 The effect of Lab4/CUL66 supplementation on mouse body and organ weights

At study end, there was no significant difference in body weights in control versus probiotic groups (Figure 5.2A). Mouse body weight at the study start was subtracted from the weight at study end to determine total weight gain for individual mice over the period of the study. Probiotic supplementation had no effect on the total weight gained throughout the study (Figure 5.2B). Previous studies investigating the effects of probiotic supplementation in a range of mouse models have shown strain-specific effects with regards to weight gain. A previous study using ApoE<sup>-/-</sup> mice demonstrated highly strain-specific effects on weight gain upon administration of different strains of *L. reuteri*. A significant reduction in weight gain was observed with *L. reuteri* ATCC treatment while conversely, treatment with *L. reuteri* L6798 resulted in a significant increase in weight gain (Fåk and Bäckhed, 2012). Another recent study demonstrated that treatment with different probiotic compositions resulted in strain-specific variation, with *L. casei* IMV B-7280 (separately) and a composition of *B. animalis* VKL/*B. animalis* VKB/*L. casei* IMV B-7280 having greater effect in decreasing body weight in high-calorie-induced obesity (Bubnov *et al.*, 2017). Recently, an acute study of Lab4/CUL66 supplementation in C57BL/6J mice reported suppression of diet-induced weight gain after a period of 2-weeks (Michael *et al.*, 2017). Further studies in C57BL/6 mice have reported suppression of HFD-induced weight gain with *L. acidophilus* strain NS1 (Song *et al.*, 2015) or *L. acidophilus* AD031 (Li *et al.*, 2016) supplementation. However, a comparative meta-analysis of the effect of *Lactobacillus* species on weight gain reported

an overall significant weight gain in both humans and animal models administered *L. acidophilus* in a large number of studies (Million *et al.*, 2012). The same meta-analysis reported inconsistent findings of both weight loss and gain with *L. plantarum* (Million *et al.*, 2012), supporting the notion that the effect of probiotic consumption on body weight is not only species-specific but highly strain-specific.

In addition to body weight, organ weight was also recorded and analysed at study end. No difference was observed in heart, liver or thymus weights; however, spleen weight was significantly increased in the probiotic group compared to the control (Figure 5.3). Increased spleen size has been associated with reduced atherosclerosis and plaque development in LDLr<sup>-/-</sup> mice (Whitman *et al.*, 2002). However, the mechanism of this association is unclear. In ApoE<sup>-/-</sup> mice fed an atherogenic diet, splenectomy has been shown to greatly accelerate atherosclerosis compared to a control group subjected to sham operation (Caligiuri *et al.*, 2002), implying an atheroprotective effect of the spleen (Witztum, 2002). More recently, Grasset *et al.* (2015) investigated an athero-protective role of the spleen via induction of a protective B cell response, highlighting the importance of the spleen in atherosclerosis-associated immunity. The B cell response involves the induction of atheroprotective antibodies against modified lipoproteins including oxLDL by antigens presenting oxidation-specific epitopes, such as phosphorylcholine (PC), leading to plaque reduction (Grasset *et al.*, 2015). This mechanism in which oxidation-specific epitopes give rise to an anti-PC response and reduction of atherosclerosis has been demonstrated in a number of studies (Binder *et al.*, 2003; Ketelhuth and Hansson, 2016; Kimura *et al.*, 2015). Together, these results suggest that the observed increase in spleen weight in the probiotic group may be associated with an anti-atherosclerotic response and may be a result of an enhanced B-cell response and induced production of atheroprotective anti-PC antibodies.

#### 5.4.2 Lab4/CUL66 supplementation has beneficial effects on plasma lipid profile

Elevated blood cholesterol is an important atherosclerosis risk factor and plasma lipids are routinely used as risk markers of atherosclerosis disease progression (Huang *et al.*, 2013). As discussed previously, among the beneficial effects attributed to probiotic

supplementation, their reported ability to lower plasma cholesterol levels is of particular interest in the prevention and management of CVD. In order to assess the effect of probiotic supplementation on plasma lipid profile, total cholesterol, HDL, LDL, free cholesterol and triglyceride content of plasma was measured from 15 control and 15 probiotic mice following 12 weeks feeding with HFD or HFD supplemented with Lab4/CUL66. Cholesterol ester level was determined as the difference between total and free cholesterol fractions, and ratios of LDL/HDL, TC/HDL and TC/LDL calculated.

In this study, total cholesterol was largely increased across both groups, an effect commonly associated with the LDLr<sup>-/-</sup> mouse model (Getz and Reardon, 2016). Probiotic supplementation had no significant effect on total cholesterol levels compared to the control (Figure 5.5A). Few similar studies have investigated the effect of probiotic supplementation on plasma lipid profiles of LDLr<sup>-/-</sup> mice. However, there are studies reporting varying effects in alternative animal models. Almost a decade ago it was demonstrated that probiotic supplementation had the potential to positively affect plasma lipid profiles in hypercholesterolemic rabbits, although no change in total cholesterol was observed (Cavallini *et al.*, 2009). A later study investigating the effect of a number of *Lactobacillus* and *Bifidobacterium* strains in obese mice reported that *L. casei* IMV B-7280 was particularly effective at lowering total plasma cholesterol, in comparison to *B. animalis* VKB/*B. animalis* VKL treatment which showed no effect (Bubnov *et al.*, 2017). Moreover, a meta-analysis of randomised clinical trials investigating the effect of probiotics on blood lipid concentrations revealed a highly strain-specific effect on total cholesterol, with strains of *L. acidophilus* and *E. faecium* showing a net reduction in total cholesterol levels while *L. plantarum* and *L. helveticus* showed no significant net change (Cho and Kim, 2015). It is therefore not surprising that the effects of probiotics on plasma lipids and total cholesterol level also displays strain-specific variation. In the current study, probiotic supplementation had no effect on total cholesterol; however, it is more relevant to consider HDL and LDL fractions individually and in relation to each other as an HDL/LDL ratio.

Circulating levels of HDL cholesterol are inversely associated with atherosclerosis disease risk and is classified as a negative risk factor for CVD (Bandeali and Farmer, 2012). In this study, supplementation with Lab4/CUL66 resulted in a significant 32%

increase in plasma HDL levels compared to the control (Figure 5.4A). Furthermore, the ratio of total cholesterol to HDL cholesterol (TC/HDL) was significantly decreased in the probiotic group compared to the control (Figure 5.5D) demonstrating that HDL levels were increased in relation to the total cholesterol level. In a meta-analysis of randomised controlled trials investigating the effect of probiotics on blood lipid concentrations, Cho and Kim (2015) reported a significant net increase in HDL cholesterol in studies utilising strains of *L. acidophilus* or a combination of *L. acidophilus/B. lactis*. In contrast, they also reported a significant net decrease with *L. plantarum* and *L. helveticus*, in addition to no net change in HDL levels with *E. faecium* (Cho and Kim, 2015). Interestingly, Lab4 contains two different species of *L. acidophilus*, suggesting that these bacteria may be responsible for the increase in HDL cholesterol observed in this study. Although multifactorial, the anti-atherogenic association with increased HDL levels is considered to be primarily due to its role in RCT where it is the major cholesterol carrier (Bandeali and Farmer, 2012). As discussed previously in Chapters 1 and 3, cholesterol is passed from lipid laden foam cells to HDL via a number of mechanisms but is largely achieved via interaction with the membrane transporter ABCA1. As demonstrated in Chapter 4, efflux of cholesterol from macrophage foam cells is enhanced in the presence of Lab4 and CUL66 (Figure 4.10), which is accompanied by an increase in the expression of ABCA1 at the mRNA level (Figure 4.12A). Together, these results suggest that Lab4/CUL66 may exert anti-atherosclerotic effects by enhancing ABCA1-associated efflux of cholesterol from lipid laden foam cells to increased levels of circulating HDL cholesterol, thereby permitting enhanced transport of cholesterol to the hepatic biliary excretion system.

Mutations in the LDLr gene disrupt the receptor-mediated clearance of LDL and is the most common cause of the autosomal dominant disorder, FH (Linton *et al.*, 2000). FH is associated with highly elevated levels of LDL cholesterol and consequently premature atherosclerotic disease. A recent consensus statement from the European Atherosclerosis Society Consensus Panel reviewed evidence from epidemiological, genetic and clinical studies, concluding that LDL burden is a central determining factor in the initiation and progression of atherosclerosis (FERENCE *et al.*, 2017). It was also concluded that the lower the level of LDL cholesterol that could be achieved by an agent, the greater the clinical benefit (FERENCE *et al.*, 2017). Indeed, the association between

LDL cholesterol lowering and reduced atherosclerosis disease risk has long been established with human studies showing significant attenuation of plaque progression with lipid-lowering treatment (Pinkosky *et al.*, 2016; Shimada and Cannon, 2015; Shin *et al.*, 2017). LDLr<sup>-/-</sup> mice used in this study naturally develop high levels of LDL cholesterol; however, supplementation with Lab4/CUL66 resulted in a significant 19% reduction LDL cholesterol levels (Figure 5.4B). Furthermore, the ratio of total cholesterol to LDL cholesterol (TC/LDL) was significantly increased in the probiotic group compared to the control (Figure 5.5D) demonstrating that LDL levels were increased in relation to the total cholesterol levels. In a meta-analysis of the effect of probiotics on plasma lipids, Cho and Kim (2015) reported a significant decrease in LDL cholesterol as demonstrated in a total of 20 out of 23 randomised controlled trials (Cho and Kim, 2015), suggesting that while strain-specific variation exists, the ability to lower LDL cholesterol is a common feature across probiotic strains. Furthermore, many human studies have demonstrated a reduction in LDL levels and generally improved lipid profile with probiotic supplementation as outlined in a recent literature review (Sharma *et al.*, 2018).

So far in this chapter, it has been shown that supplementation with Lab4/CUL66 can positively modulate plasma lipids, by increasing levels of HDL and decreasing levels of LDL cholesterol, both independently and in relation to total cholesterol levels. Although this information is very useful when assessing cardiovascular and atherosclerosis disease risk, even more relevant is the ratio of LDL to HDL cholesterol. In this study, the LDL/HDL cholesterol ratio was calculated and found to be significantly reduced by 27% in the probiotic group compared to the control (Figure 5.4C). This is a highly encouraging result suggesting that Lab4/CUL66 supplementation may exert athero-protective effects via the modulation of plasma lipid profile.

In addition to cholesterol levels, plasma TG was also analysed as a further important indicator of atherosclerosis risk. Raised levels of circulating TG is a marker for several atherogenic lipoproteins, including TG-rich lipoproteins, VLDL remnants and chylomicron remnants, all of which are capable of enhancing atherosclerosis (Moss, 2018; Talayero and Sacks, 2011). In fact, while elevated LDL cholesterol is considered a major risk factor for cardiovascular and atherosclerosis disease, hypertriglyceridemia has been considered as an independent risk factor (Sarwar *et al.*, 2007) so much that



when LDL cholesterol is maintained at goal levels, patients with hypertriglyceridemia have been reported to remain at significant risk (Talayero and Sacks, 2011). In this study, Lab4/CUL66 supplementation was unable to lower plasma TG, in fact TG levels were significantly increased in the probiotic group compared to the control (Figure 5.6). Upon review of the numerous animal and human studies carried out, it is clear that the effect of probiotic supplementation on plasma TG level is also subject to species-specific variations. While a number of *in vivo* studies have shown a significant decrease in TG levels following probiotic supplementation (Fhoula *et al.*, 2018; Huang *et al.*, 2013; Kumar *et al.*, 2011; Wang *et al.*, 2012), others have shown no effect (Greany *et al.*, 2008; Razmpoosh *et al.*, 2019; Sharma *et al.*, 2018). In a randomised double-blind controlled study, patients with hypertriglyceridemia showed a significant reduction in TG following 12 weeks supplementation with *L. curvatus* HY7601 and *L. plantarum* KY1032 (Ahn *et al.*, 2015). Moreover, the effect was more pronounced in patients with higher fasting TG at study start. These findings suggests the possibility that results are dependent not only on the strain and the dose of the probiotic administered but also on the existing level of hypertriglyceridemia in the subject.

#### 5.4.3 Lab4/CUL66 supplementation reduces plaque size and lipid content in LDLr<sup>-/-</sup> mice

This study aimed to elucidate the effect of Lab4/CUL66 supplementation on atherosclerotic plaque formation. Sections of the aortic sinus were stained with H&E in order to quantify plaque size and observe morphology, while staining with Oil red O was carried out to determine plaque lipid content. Both plaque area and lipid content was found to be significantly reduced by 39% and 35% respectively in the probiotic group compared to the control (Figures 5.8 and 5.9). As can be seen in the representative images shown in Figure 5.7, mice in the control group presented with large plaques and distortion of the aorta. Although this specific probiotic mix has not previously been investigated in LDLr<sup>-/-</sup> mice, these results do correlate with previous studies investigating the effect of various probiotics on atherosclerotic plaque formation (Chan *et al.*, 2016b). As discussed previously, the VSL#3 probiotic consortium has been investigated for its effects on plaque formation in ApoE<sup>-/-</sup> mice, demonstrating significant reduction in

atherosclerotic lesion development (Chan, 2012; Chan *et al.*, 2016b). Similar to Lab4/CUL66 combination, VSL#3 contains a mix of different *Lactobacillus* and *Bifidobacterium* strains (Kühbacher *et al.*, 2006) with both consortiums containing *L. plantarum* and *L. acidophilus*. In contrast, supplementation with *L. reuteri* strains ATCC 4659, DSM or L6798 was unsuccessful in reducing lesion development in a similar model using ApoE<sup>-/-</sup> mice. Although the number of studies investigating atherosclerotic plaque development with probiotic supplementation are relatively few, it is not surprising that again the effects of probiotic supplementation have been shown to be strain-specific.

#### 5.4.4 The effect of Lab4/CUL66 supplementation on plaque composition

The presence of immune cells, particularly macrophages and T cells within plaques is associated with plaque destabilisation and rupture (Shaikh *et al.*, 2012). The vulnerable plaque is characterised by a thin fibrous cap, along with large accumulation of T cells and macrophages in relation to reduced numbers of SMCs, and a large collagen-poor, lipid-rich necrotic core (Newby *et al.*, 2009). In the current study, the effect of Lab4/CUL66 supplementation on macrophage, T cell and SMC composition of plaque lesions was assessed by immunohistochemistry. Sections of the aortic sinus were stained with anti-mouse cell surface marker primary antibodies, followed by fluorophore-conjugated secondary antibodies. Antibodies raised against MOMA-2,  $\alpha$ SMA and CD3 have been used previously to successfully target macrophages, SMCs and T cells in the plaque respectively (Dong *et al.*, 2016; Gajda *et al.*, 2008; Xiong *et al.*, 2017). Details of antibodies used are given in Section 2.8.5. To control for non-specific staining, an isotype control was included for each section. The isotype is serum IgG correlating to the species in which the primary antibodies were raised; any secondary antibody binding is therefore non-specific. Figures 5.10 – 5.12 include representative ISO images which were used during analysis to deduct any background staining for individual sections. Images were captured by fluorescence microscopy using consistent exposure, intensity and contrast settings for comparable downstream analyses. DAPI, FITC and AF-488 filters were applied for detection of DAPI (blue), AF-594 (green) and AF-488 (red) fluorescence respectively. Macrophage, SMC and T cell content was quantified using ImageJ software where images were first segmented, then percentage staining of plaque was determined by raw intensity values in relation to maximum intensity values.

Intensity analysis was chosen in preference to simple pixel quantification as a more accurate method of quantifying cellular presence in immunofluorescent images. Results show that macrophage and SMC content of plaques was significantly reduced in the probiotic group compared to the control, while T cell content also displays a trend of reduction (Figure 5.10 – 5.12). For each section, the corresponding ISO control contained little to no staining, showing that staining is specific for the target site and not due to non-specific background binding.

MOMA-2 staining showed a large accumulation of macrophages in sections from the control group, particularly within the area of plaque where staining is more intense (Figure 5.10). Interestingly in Figure 5.10, the image representing the control group is showing an absence of intense staining within one of the plaque lesions, suggesting that a necrotic core may be present here. This result correlates with previous chapters in which it was shown that probiotic CM attenuates monocyte recruitment (Figure 3.9) and monocyte (Figure 3.20) and macrophage (Figure 3.21) proliferation *in vitro*. Macrophage foam cells are the predominant source of extracellular proteases, particularly MMPs, which directly degrade ECM components leading to plaque destabilisation (Newby *et al.*, 2009). Additionally, regions of dense accumulation of macrophages as seen in the control group are prone to more frequent apoptosis and formation of a necrotic core (De Meyer *et al.*, 2012), further contributing to plaque vulnerability and rupture. Prevention or depletion of plaque macrophage accumulation is considered athero-protective; therefore, these results suggest that Lab4/CUL66 supplementation leads to the attenuation of macrophage accumulation and consequently possible reduction of plaque destabilisation.

After macrophages, T cells represent the second largest population of immune cells in the atherosclerotic plaque (Shaikh *et al.*, 2012). Although different classes of T cells can exert different effects within an atherosclerotic lesion, in general T cells are considered to exacerbate atherosclerosis, particularly in advanced lesions where T cells and B cells are largely responsible for driving inflammation and plaque progression (Tse *et al.*, 2013). CD3, previously known as T3, is ubiquitously presented by all T cell classes. In this study, staining of CD3 shows accumulation of T cells within the area of the plaque, particularly visible in the control group compared to probiotic group where plaque area

is relatively small (Figure 5.11). Overall, reduced staining was observed in the probiotic group (Figure 5.13B) and although this result did not reach significance, it did show a trend of reduction with a p-value of 0.097. As mentioned previously, the CD3 protein is presented by all T cells, therefore this result gives a general assessment of T cell content. As the most abundant T cell subset present in the atherosclerotic plaque, it is likely that the pro-inflammatory helper Th1 lymphocyte (Shaikh *et al.*, 2012) represents the majority of CD3 staining observed in this study. Future work may aim to elucidate the exact contribution of individual T cell subtypes beginning with T helper (CD4+) and T cytotoxic (CD8+) cells, thereby providing additional detail for more informed conclusions.

VSMC proliferation and infiltration into an atherosclerotic lesion can be either pro- or anti-atherogenic depending on the stage of disease progression. It is generally accepted that VSMC accumulation confers stability to advanced atherosclerotic plaques via formation of a protective fibrous cap (Zernecke, 2017), which consists primarily of VSMC-derived collagen, elastin, proteoglycans and ECM. Apoptosis and senescence of VSMCs results in loss of collagen and ECM proteins, promoting atherosclerosis progression with degradation of the fibrous cap and subsequent plaque vulnerability and rupture (Fernández-Hernando *et al.*, 2009; Wang *et al.*, 2015a). In the current study, VSMC presence in sections of the aortic sinus was quantified by immunohistochemistry using antibodies targeting the SMC protein  $\alpha$ SMA. Results show a significant 40% reduction in VSMC in the probiotic group compared to the control (Figure 5.13C). In Figure 5.12, differential accumulation of VSMCs can be seen; in the probiotic group, a small amount of staining is visible within the plaque while more intense staining is visible within the vessel wall; however, in the control group intense staining can be seen particularly around the outside of the plaque. This pattern of staining suggests that VSMCs may have formed a thick protective cap over the plaque, representative of a more advanced but stable lesion. The amount of staining present in the probiotic group was significantly reduced compared to the control group (Figure 5.13C). However, this may simply be due to the presence of less advanced plaque in sections from the probiotic group. For more conclusive results a larger sample size would be required.

### 5.4.5 Summary and future work

Results in this chapter have laid a strong foundation in the investigation of the effect of Lab4/CUL66 supplementation in atherosclerosis development *in vivo*. Firstly, it was shown that probiotic supplementation had no effect on mouse body or organ weight, with the exception of spleen weight which was significantly increased in the probiotic group compared to the control, possibly via an enhanced athero-protective B cell response. Next, it was shown that Lab4/CUL66 supplementation had the ability to beneficially modulate plasma lipid profile with mice in the probiotic group demonstrating increased HDL levels, decreased LDL levels and beneficially altered TC/HDL, TC/LDL and HDL/LDL cholesterol ratios. Drawing on results from previous chapters, it is possible that Lab4/CUL66 may exert anti-atherosclerotic effects by enhancing ABCA1-associated efflux of cholesterol from lipid laden foam cells to increased levels of circulating HDL cholesterol, thereby permitting enhanced transport of cholesterol to the hepatic biliary excretion system. This beneficial effect of Lab4/CUL66 on plasma lipid profile is a highly encouraging result given the clinical importance of plasma lipids in atherosclerosis risk assessment and disease monitoring. Furthermore, it was demonstrated that Lab4/CUL66 supplementation led to a large reduction in plaque area in the probiotic group compared to the control; in fact, sections from the control group featured large plaques with extensive lipid accumulation and distortion of the aorta. Distortion of the aorta was not observed in any of the sections obtained from the probiotic group. Finally, investigation of plaque composition revealed a significant reduction in macrophage accumulation, another exciting finding correlating with reduced atherosclerosis disease progression in the probiotic group. In addition to macrophages, accumulation of T cells also displayed a trend of reduction in the probiotic group. Since the most likely abundance of T cells is the pro-inflammatory helper Th1 cells (Ilhan and Kalkanli, 2015), it can be suggested that this result shows anti-atherogenic potential; however, more specific investigation of the contribution of individual T cell subsets is required. While VSMC staining is reduced in the probiotic group, the distribution of the staining is particularly notable, with the position of staining in the control group being suggestive of the formation of a protective VSMC-dense fibrous cap. While these results are encouraging, the availability of suitable sections for

immunohistochemical analysis of plaque composition was limited. For more conclusive interpretation of the results obtained by immunofluorescent staining, a larger sample size would be required.

Following on from the results presented in this chapter, investigation continued to attempt to elucidate the mechanisms underlying these observed anti-atherosclerotic effects. In the studies presented in the next chapter, stored tissues were utilised to explore bone marrow stem cell populations and expression of atherosclerosis-associated genes using qPCR microarrays.

## CHAPTER 6

*Mechanisms underlying the  
athero-protective effects of  
Lab4/CUL66 supplementation  
in atherosclerosis*

---

## 6.1 Introduction

The effect of probiotics on atherosclerosis was investigated in LDLr<sup>-/-</sup> mice fed for 12 weeks with HFD or HFD supplemented with Lab4/CUL66 probiotic combination. Data presented in Chapter 5 showed that Lab4/CUL66 supplementation attenuated atherosclerotic plaque formation by 39% compared to the control, and beneficially modulated plasma lipid profiles resulting in increased HDL with decreased LDL cholesterol levels. Additionally, plaque composition was shown to be altered, notably showing a reduction in plaque macrophage content as well reduced SMC and T cell content. In light of these important results, the aims of the studies presented in this chapter was to further investigate the effects of Lab4/CUL66 supplementation and to elucidate the mechanisms underlying the results presented in the previous chapter.

In the studies presented in Chapter 3, the CM from either Lab4 or CUL66 was shown to significantly affect gene expression, in particular genes involved in foam cell formation. It's possible that the reduced plaque formation observed *in vivo* is in part due to similar alterations in gene expression. However, given the full range of the effects observed, it is likely that there are multiple contributory mechanisms. Due to the high number of genes involved in atherosclerosis, it was decided to screen a large number of genes simultaneously using a qPCR microarray method. The liver plays a central role in metabolism and the production of plasma proteins, all of which contribute to atherogenesis, and is a common source of mRNA in the study of atherosclerosis gene expression (Pan *et al.*, 2018; Recinos *et al.*, 2004; States *et al.*, 2012). Liver gene expression was therefore analysed following 12 weeks feeding with HFD (control group) or HFD supplemented with Lab4/CUL66 (probiotic group), using Qiagen Atherosclerosis RT<sup>2</sup> Profiler PCR Array plates. The PCR microarray plates contained a large panel of 84 atherosclerosis-associated genes implicated in the control of inflammation, cell adhesion, lipid metabolism, apoptosis and more. A table of the 84 genes included in the qPCR microarray plate is shown in Appendix 1.

Alteration in bone marrow cell populations has been reported to play an important role in hypercholesterolemia and atherosclerosis disease progression (Lang and Cimato, 2014; Ma and Feng, 2016). Therefore, in addition to the analysis of gene expression, the



effect of Lab4/CUL66 supplementation on key bone marrow cell populations was investigated in *LDLr<sup>-/-</sup>* mice following 12 weeks feeding with HFD (control) or HFD supplemented with Lab4/CUL66 probiotic combination. Bone marrow populations of stem cells, progenitor cells and lineage differentiated cells were analysed using a method modified from one previously used in the laboratory (Moss, 2018). A simplified representation of bone marrow cell population lineage is shown in Figure 6.1. Haematopoietic stem/progenitor cells (HSPCs) are responsible for the generation of all blood cells. Within the HSPC population, haematopoietic stem cells (HSCs) generate multipotent progenitors (MPPs) which subsequently generate progenitor cells, lineage-specific precursors and finally fully differentiated blood cells (Gao *et al.*, 2014).

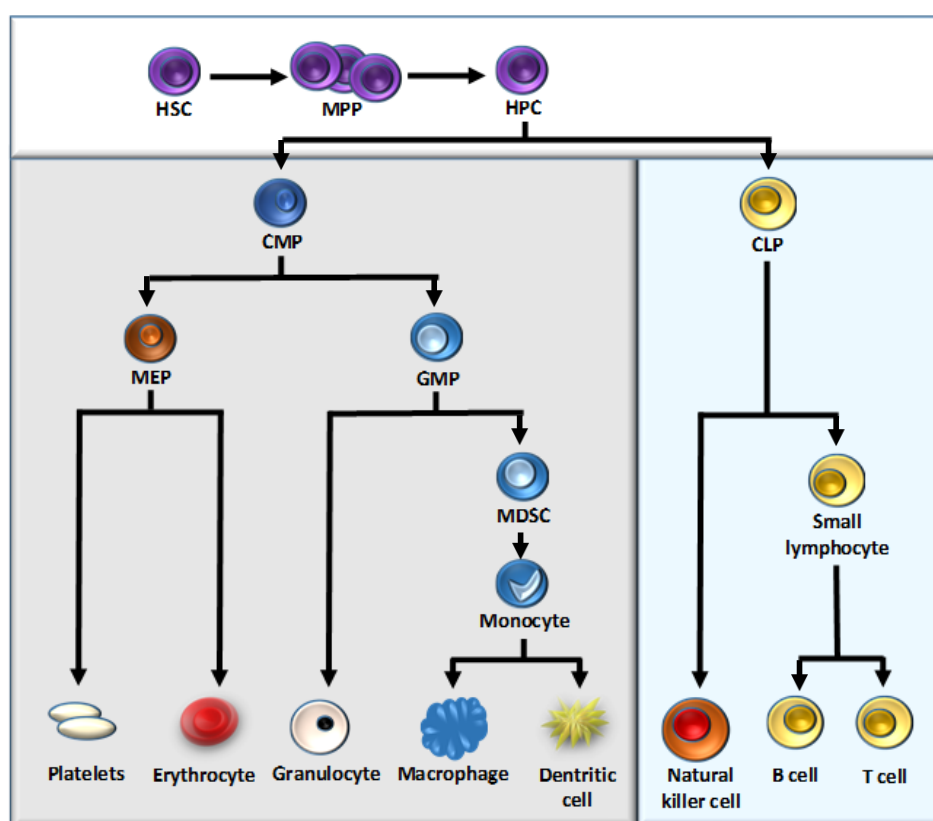


**Figure 6.1 - Simplified representation of bone marrow cell populations.** Abbreviations: HSC, haematopoietic stem cell; MPP, multipotent progenitor; HPC, haematopoietic progenitor cell; CMP, common myeloid progenitor; CLP, common lymphoid progenitor; MEP, megakaryocyte-erythroid progenitor; GMP, granulocyte-macrophage progenitor; MDSC, myeloid-derived suppressor cell.

Bone marrow contains heterogeneous populations of cells and so analysis of populations of interest requires a method of discerning one cell type from another. In the current study, this was achieved using a technique known as immunophenotyping in which heterogeneous cell populations are stained with antibodies targeting cell-

specific surface antigens. Antibodies are typically conjugated to fluorophores and are detected using flow cytometric analysis, allowing the identification of the presence and proportion of cell populations of interest. (Sykora and Reschke, 2019) Staining of a mixture of cell types with a cocktail of antibodies targeting one or more cell surface antigens, known as markers or identifiers, can therefore be used to discern one cell type from another. In this study fluorochrome-conjugated antibodies targeting cell specific surface markers were used to analyse key cell populations in the bone marrow using flow cytometry. A list of all cell types with their corresponding identifier is given in Table 2.8.

## 6.2 Experimental aim

The studies presented in this chapter aimed to assess the effect of Lab4/CUL66 supplementation on atherosclerosis-associated gene expression and bone marrow cell populations in LDLr<sup>-/-</sup> mice following 12 weeks feeding of HFD or HFD supplemented with Lab4/CUL66. Detailed methods for this chapter are described in Section 2.8.6 and 2.8.4 respectively. An overview of the experimental strategy is presented in Figure 6.2. Gating strategy applied in the analysis of bone marrow cell populations is outlined in Figure 6.3.

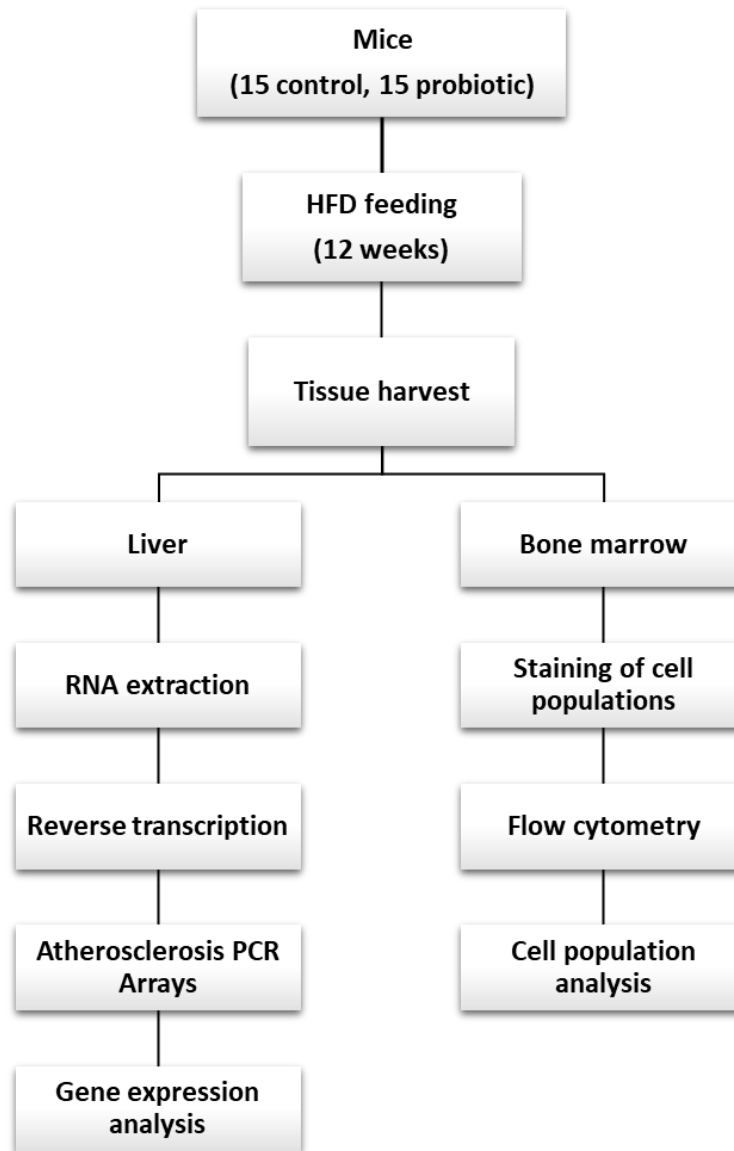
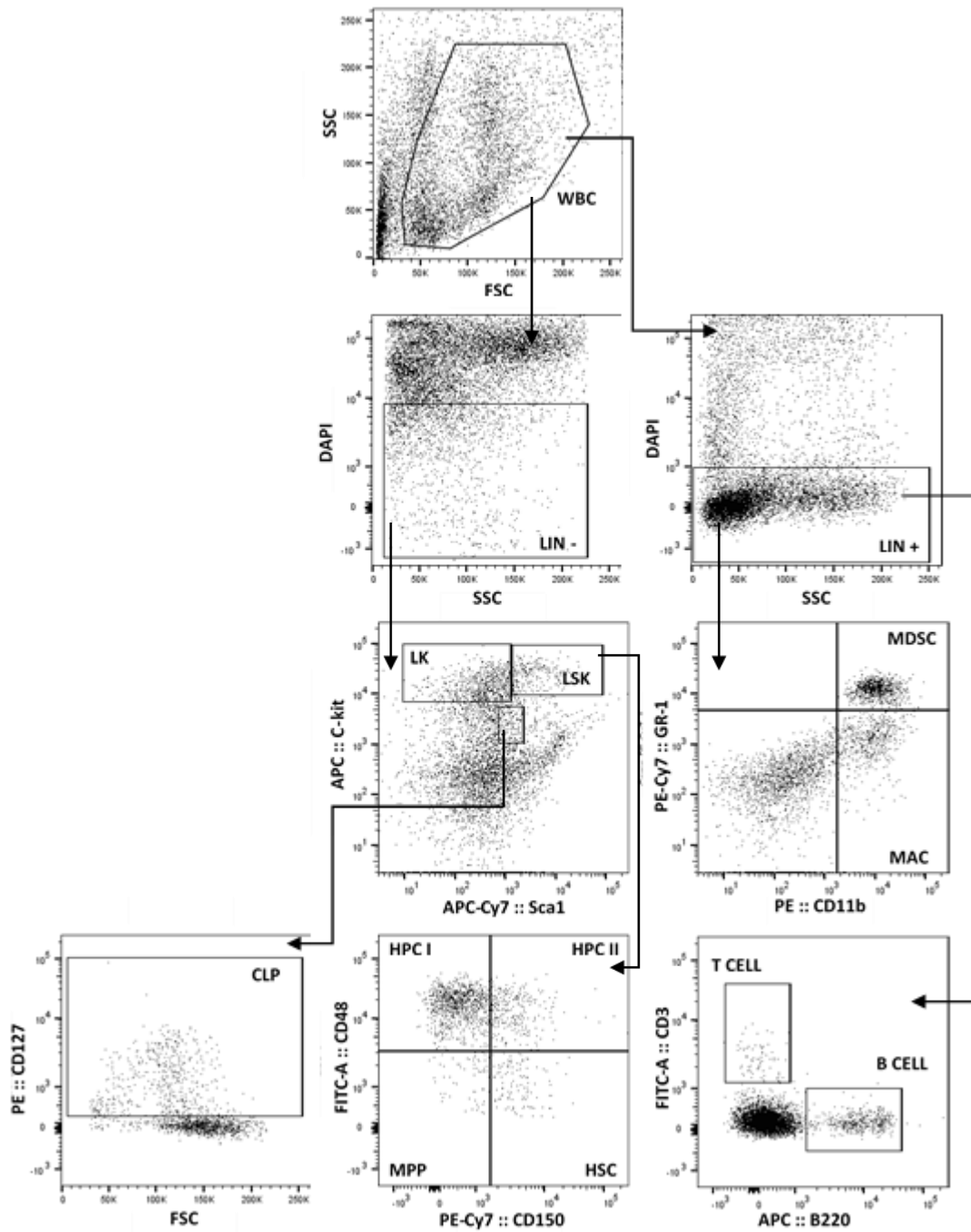


Figure 6.2 - Experimental strategy for the analysis of liver gene expression and bone marrow cell populations.



**Figure 6.3 – Representative flow plots outlining the gating strategy utilised in the analysis of haematopoietic cell populations by flow cytometry.** In flow cytometry, forward scatter (FSC) provides a measurement of cell size by determining the amount of light which passes around it. Side scatter (SSC-A) provides a measurement of granularity by determining the amount of light which is reflected by particles within the cells. Application of filters and gating is used to isolate cell populations of interest. WBC, white blood cells; LIN, lineage; CLP, common lymphoid progenitor; HPC, haematopoietic progenitor cell; MPP, multipotent progenitor; HSC, haematopoietic stem cell; MDSC, myeloid-derived suppressor cells; MAC, macrophages; Sca1, stem cells antigen 1; FITC, Fluorescein isothiocyanate; PE, Phycoerythrin; APC, allophycocyanin.

## 6.3 Results

### 6.3.1 The effects of Lab4/CUL66 supplementation on the expression of key genes involved in atherosclerosis

To investigate the expression of key genes involved in atherosclerosis, samples of liver which were snap frozen at study end point were selected at random to a total of 8 each from control and probiotic groups. RNA was extracted from the liver tissue, reverse transcribed and amplified by qPCR using Atherosclerosis RT<sup>2</sup> Profiler PCR Array plates as described in Section 2.8.6. For all test wells, C<sub>T</sub> values greater than 35 were not included in downstream analysis due to the increased risk of non-specific amplification. In addition to test wells, each microarray plate included the following controls:

- Genomic DNA control (GDC): A C<sub>T</sub> value of ≤35 was indicative of the presence of genomic DNA contamination;
- Reverse transcription control (RTC): Included to assess the efficiency of the RT reaction. Average C<sub>T</sub> values of the positive PCR control (PPC; see below) were deducted from the RTC, and a value greater than 5 was indicative of impurities and reduced RT reaction efficiency;
- PPC: Included to assess the efficiency of the PCR reaction, where average C<sub>T</sub> values of approximately 20 ± 2 cycles was considered efficient. A large variation in PPC values was considered indicative of the presence of PCR amplification inhibitors, while C<sub>T</sub> values consistently greater than 22 indicated inefficient PCR reaction conditions.

In addition to GDC, RTC and PPC controls, the C<sub>T</sub> values of housekeeping genes (*Actb*, *B2m*, *Gapdh*, *Gusb*, *Hsp90ab1*) were checked for stability within 2 cycles. Melting curve analysis was carried out on individual samples where a single peak representing amplification of a single product was acceptable. Fold-change in gene expression was calculated using the  $\Delta\Delta C_T$  method. A full list of expression changes for genes included in the Atherosclerosis RT<sup>2</sup> Profiler PCR Array is shown in Table 6.1. Genes for which changes in expression reached significance are listed in Table 6.2 in addition to fold-change increase/decrease and p values. Of the 84 genes tested, 63 achieved a minimum of 10%

change in expression, while 19 achieved significant change and a further 51 showed a trend in change in expression ( $p < 0.100$ ). A volcano plot showing global changes in gene expression was produced using R software (Figure 6.4).

**Table 6.1 - Changes in the expression of each gene tested using the Atherosclerosis RT<sup>2</sup> Profiler PCR Arrays**

<b>Gene</b>	<b>GenBank ID</b>	<b>Fold-change</b>	<b>P value</b>	<b>Change</b>
<i>Abca1</i>	NM_013454	1.27	0.129	Increase
<i>Ace</i>	NM_009598	1.19	0.403	Decrease
<i>Apoa1</i>	NM_009692	1.06	0.756	Increase
<i>Apob</i>	NM_009693	1.18	0.048	Decrease
<i>Apoe</i>	NM_009696	1.05	0.372	Increase
<i>Bax</i>	NM_007527	1.41	0.073	Decrease
<i>Bcl2</i>	NM_009741	1.23	0.275	Increase
<i>Bcl2a1a</i>	NM_009742	1.19	0.704	Decrease
<i>Bcl2l1</i>	NM_009743	1.47	0.074	Decrease
<i>Bid</i>	NM_007544	1.18	0.427	Decrease
<i>Birc3</i>	NM_007464	1.03	0.572	Increase
<i>Ccl2</i>	NM_011333	2.08	0.111	Decrease
<i>Ccl5</i>	NM_013653	1.79	0.179	Decrease
<i>Ccr1</i>	NM_009912	1.70	0.003	Decrease
<i>Ccr2</i>	NM_009915	1.63	0.006	Decrease
<i>Cd44</i>	NM_009851	1.93	0.178	Decrease
<i>Cdh5</i>	NM_009868	1.08	0.980	Decrease
<i>Cflar</i>	NM_009805	1.23	0.017	Decrease
<i>Col3a1</i>	NM_009930	2.38	0.253	Decrease
<i>Csf2</i>	NM_009969	1.79	0.317	Decrease
<i>Ctgf</i>	NM_010217	1.25	0.814	Decrease
<i>Cxcl1</i>	NM_008176	3.09	0.087	Decrease
<i>Eln</i>	NM_007925	1.07	0.684	Increase
<i>Eng</i>	NM_007932	1.10	0.311	Increase
<i>Fabp3</i>	NM_010174	1.21	0.241	Increase
<i>Fas</i>	NM_007987	1.19	0.315	Decrease
<i>Fga</i>	NM_010196	1.12	0.542	Decrease
<i>Fgb</i>	NM_181849	1.30	0.211	Increase

<b>Gene</b>	<b>GenBank ID</b>	<b>Fold-change</b>	<b>P value</b>	<b>Change</b>
<i>Fgf2</i>	NM_008006	1.11	0.807	Decrease
<i>Fn1</i>	NM_010233	1.30	0.124	Increase
<i>Hbegf</i>	NM_010415	1.13	0.024	Decrease
<i>Icam1</i>	NM_010493	1.34	0.025	Decrease
<i>Ifng</i>	NM_008337	2.40	0.000	Decrease
<i>Il1a</i>	NM_010554	1.47	0.110	Decrease
<i>Il1b</i>	NM_008361	1.03	0.477	Increase
<i>Il1r1</i>	NM_008362	1.17	0.007	Decrease
<i>Il1r2</i>	NM_010555	1.30	0.815	Decrease
<i>Il2</i>	NM_008366	1.76	0.048	Decrease
<i>Il3</i>	NM_010556	1.12	0.154	Increase
<i>Il4</i>	NM_021283	1.21	0.183	Decrease
<i>Il5</i>	NM_010558	1.29	0.435	Decrease
<i>Itga2</i>	NM_008396	1.72	0.000	Decrease
<i>Itga5</i>	NM_010577	1.67	0.620	Decrease
<i>Itgax</i>	NM_021334	1.23	0.246	Decrease
<i>Itgb2</i>	NM_008404	1.32	0.001	Decrease
<i>Kdr</i>	NM_010612	1.05	0.462	Increase
<i>Klf2</i>	NM_008452	1.29	0.695	Increase
<i>Lama1</i>	NM_008480	1.28	0.171	Decrease
<i>Ldlr</i>	NM_010700	1.00	0.713	Increase
<i>Lif</i>	NM_008501	1.03	0.540	Increase
<i>Lpl</i>	NM_008509	1.21	0.161	Decrease
<i>Lypla1</i>	NM_008866	2.52	0.014	Decrease
<i>Mmp1a</i>	NM_032006	1.80	0.000	Decrease
<i>Mmp3</i>	NM_010809	1.50	0.018	Decrease
<i>Msr1</i>	NM_031195	1.40	0.351	Decrease
<i>Nfkb1</i>	NM_008689	1.09	0.310	Increase
<i>Npy</i>	NM_023456	1.86	0.282	Decrease
<i>Nr1h3</i>	NM_013839	1.05	0.395	Increase



<b>Gene</b>	<b>GenBank ID</b>	<b>Fold-change</b>	<b>P value</b>	<b>Change</b>
<i>Pdgfa</i>	NM_008808	1.31	0.019	Increase
<i>Pdgfb</i>	NM_011057	1.07	0.678	Decrease
<i>Pdgfrb</i>	NM_008809	1.06	0.900	Increase
<i>Plin2</i>	NM_007408	1.12	0.187	Decrease
<i>Ppara</i>	NM_011144	1.09	0.074	Increase
<i>Ppard</i>	NM_011145	1.12	0.153	Increase
<i>Pparg</i>	NM_011146	1.40	0.046	Decrease
<i>Ptgs1</i>	NM_008969	1.04	0.455	Increase
<i>Rxra</i>	NM_011305	1.32	0.239	Increase
<i>Sele</i>	NM_011345	1.56	0.005	Decrease
<i>Sell</i>	NM_011346	1.42	0.414	Decrease
<i>Selp</i>	NM_011347	1.17	0.171	Decrease
<i>Selplg</i>	NM_009151	1.12	0.554	Decrease
<i>Serpinb2</i>	NM_011111	1.12	0.553	Decrease
<i>Serpine1</i>	NM_008871	2.27	0.001	Decrease
<i>Sod1</i>	NM_011434	1.02	0.639	Increase
<i>Spp1</i>	NM_009263	1.00	0.515	Increase
<i>Tgfb1</i>	NM_011577	1.09	0.266	Increase
<i>Tgfb2</i>	NM_009367	1.17	0.818	Decrease
<i>Thbs4</i>	NM_011582	1.09	0.385	Increase
<i>Tnc</i>	NM_011607	1.16	0.349	Decrease
<i>Tnf</i>	NM_013693	1.28	0.035	Decrease
<i>Tnfaip3</i>	NM_009397	2.26	0.098	Decrease
<i>Vcam1</i>	NM_011693	1.37	0.082	Decrease
<i>Vegfa</i>	NM_009505	1.51	0.126	Decrease
<i>Vwf</i>	NM_011708	1.13	0.336	Increase

Gene expression was assessed in the livers of mice following 12 weeks feeding with HFD or HFD supplemented with Lab4/CUL66. Table shows gene, GenBank reference, fold-change in expression, *p* value and increase/decrease in gene expression. A list of full gene names is included in Appendix 1. Statistical analysis was performed using an unpaired Student's t-test.

**Table 6.2 – Atherosclerosis-associated genes showing significant change, or trend of change in expression.**

<b>Gene</b>	<b>GenBank ID</b>	<b>Fold-change</b>	<b>P value</b>	<b>Change</b>
<i>Apob</i>	NM_009693	1.18	0.048	Decrease
<i>Bax</i>	NM_007527	1.41	0.073*	Decrease
<i>Bcl2l1</i>	NM_009743	1.47	0.074*	Decrease
<i>Ccr1</i>	NM_009912	1.70	0.003	Decrease
<i>Ccr2</i>	NM_009915	1.63	0.006	Decrease
<i>Cflar</i>	NM_009805	1.23	0.017	Decrease
<i>Cxcl1</i>	NM_008176	3.09	0.087*	Decrease
<i>Hbegf</i>	NM_010415	1.13	0.024	Decrease
<i>Icam1</i>	NM_010493	1.34	0.025	Decrease
<i>Ifng</i>	NM_008337	2.40	0.000	Decrease
<i>Il1r1</i>	NM_008362	1.17	0.007	Decrease
<i>Il2</i>	NM_008366	1.76	0.048	Decrease
<i>Itga2</i>	NM_008396	1.72	0.000	Decrease
<i>Itgb2</i>	NM_008404	1.32	0.001	Decrease
<i>Lypla1</i>	NM_008866	2.52	0.014	Decrease
<i>Mmp1a</i>	NM_032006	1.80	0.000	Decrease
<i>Mmp3</i>	NM_010809	1.50	0.018	Decrease
<i>Pdgfa</i>	NM_008808	1.31	0.019	Increase
<i>Ppara</i>	NM_011144	1.09	0.074*	Increase
<i>Pparg</i>	NM_011146	1.40	0.046	Decrease
<i>Sele</i>	NM_011345	1.56	0.005	Decrease
<i>Serpine1</i>	NM_008871	2.27	0.001	Decrease
<i>Tnf</i>	NM_013693	1.28	0.035	Decrease
<i>Tnfaip3</i>	NM_009397	2.26	0.098*	Decrease
<i>Vcam1</i>	NM_011693	1.37	0.082*	Decrease

Table shows gene, GenBank reference, fold-change in expression, *p* value and increase/decrease in gene expression. Statistical analysis was performed using an unpaired Student's t-test. \* Trend towards significance where *p* < 0.100.

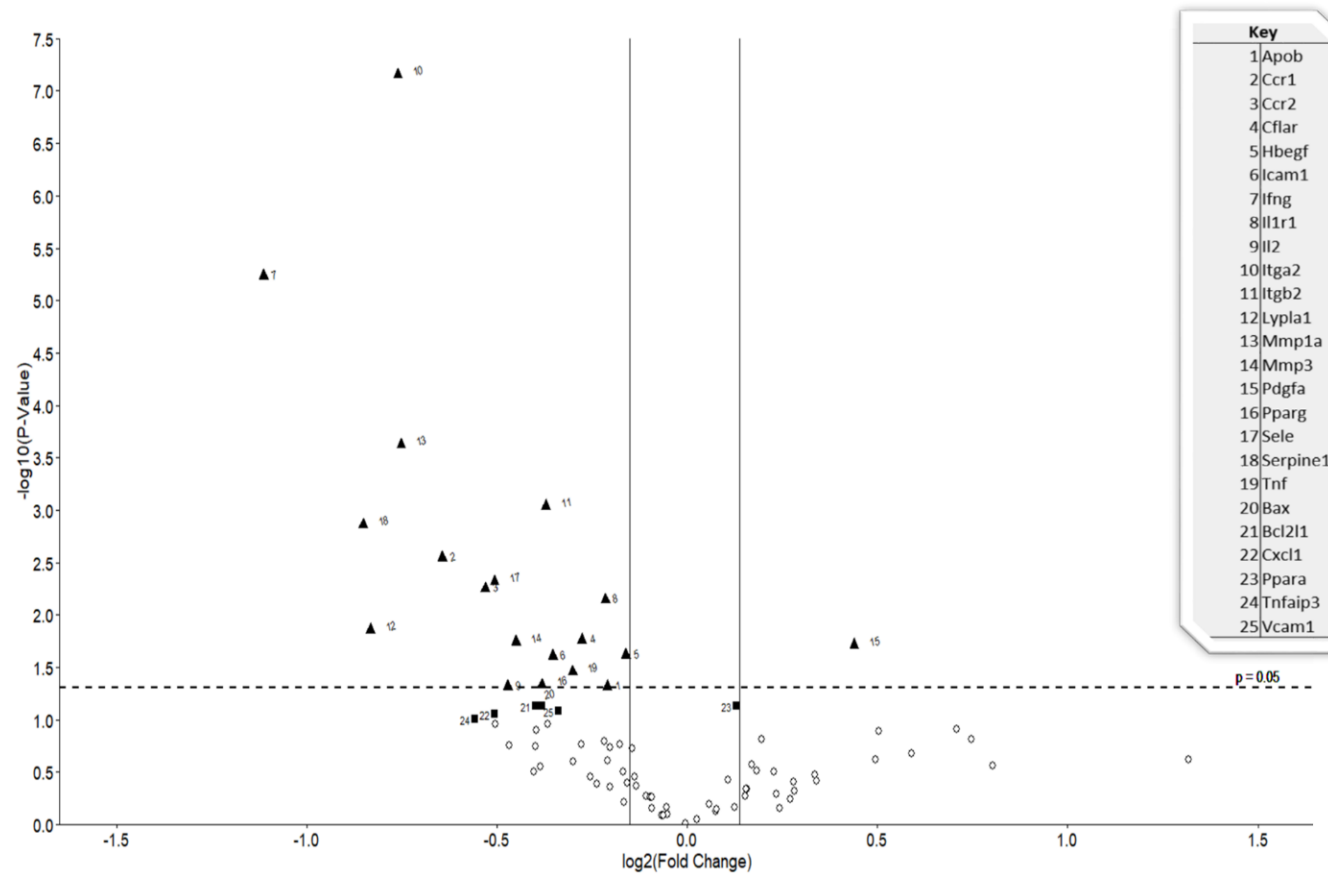


**Figure 6.4 - Volcano plot showing changes in gene expression with Lab4/CUL66 supplementation compared to the control.** The effect of Lab4/CUL66 on atherosclerosis-associated gene expression was assessed in liver samples from 8 control and 8 probiotic mice following 12 weeks feeding with either HFD (control group) or HFD supplemented with Lab4/CUL66. Data are presented as mean fold-change in gene expression in the probiotic group compared to the control. The  $\log_2$  fold-change in gene expression is represented on the x-axis. The y-axis shows the  $-\log_{10}$  of the p value. A p value of 0.05 (dashed line) and fold change of  $\pm 10\%$  (solid lines) are indicated. A black triangle indicates genes showing significant changes in expression, and a black square indicates genes showing a trend towards significance ( $p < 0.100$ )

The 84 atherosclerosis-associated genes included in the Atherosclerosis RT<sup>2</sup> Profiler PCR Array were arranged into groups of related genes based on their function. Cluster analysis was performed and a heatmap produced for each group of related genes using the online tool Morpheus, where colour and intensity gives visual representation of the changes in gene expression for all genes (Figure 6.5).

Groups of related genes that show significant changes in expression are presented graphically in Figure 6.6. Some genes are pleiotropic and are therefore included in more than one related group. Fold-change increase/decrease together with the p-value for each gene is given in Table 6.2. Of the genes involved in the inflammatory response (Figure 6.6A) the expression of all of *Ccr1*, *Ccr2*, *Infg*, *Il2*, *Itgb2*, *Pparg* and *Tnf* was significantly reduced in the probiotic group compared to the control. Similarly, the expression of genes involved in lipid transport and metabolism (*Abob*, *Lypla1* and *Pparg*) was decreased (Figure 6.6B). Expression of a number of genes involved in cell adhesion were also significantly reduced (*Icam*, *Itga1*, *Itgb2*, *Sele*) (Figure 6.6C). For genes involved in cell growth and proliferation, the expression of *Hbegf*, *Il2* and *Ifng* was significantly decreased while that for *Pdgfa* was increased (Figure 6.6D). Expression of genes involved in transcription regulation (*Pparg*, *Ifng*) and apoptosis (*Cflar*, *Ifng*) were also significantly decreased (Figures 6.6E and 6.6F). Finally, the largest group of genes that showed significant change in expression code for extracellular matrix molecules (Figure 6.6G), where the expression of *Serpine1*, *Mmp1a*, *Mmp3*, *Hbegf*, *Infg*, *Il1r1*, *Il2*, *Itga2*, *Itgb2* and *Sele* decreased and that for *Pdgfa* increased.

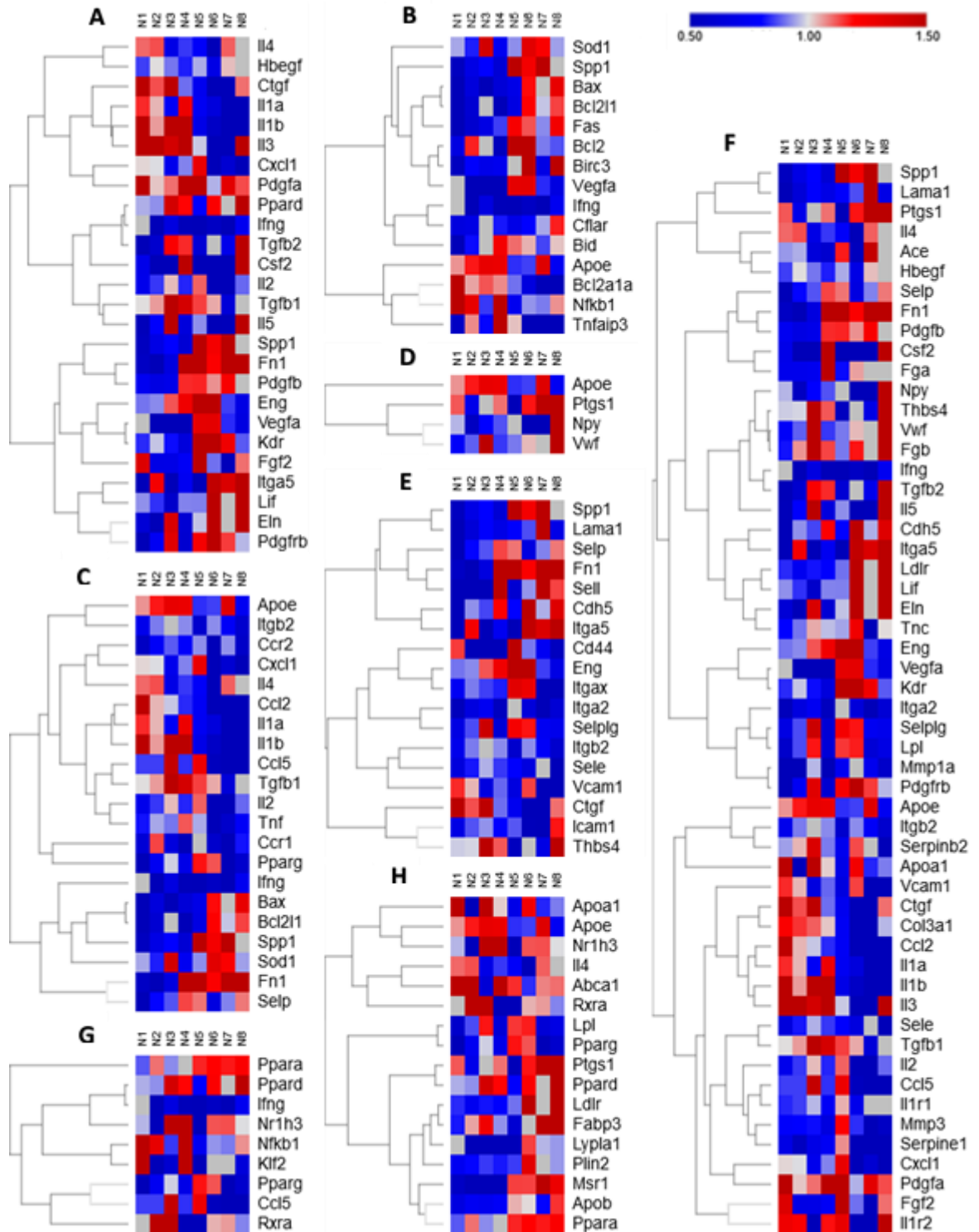


**Figure 6.5 – Heatmaps showing a visual representation of fold-change in gene expression with Lab4/CUL66 supplementation.** The effect of Lab4/CUL66 on atherosclerosis-associated gene expression was assessed in liver samples from 8 control and 8 probiotic treated mice following 12 weeks feeding with either HFD (control group) or HFD supplemented with Lab4/CUL66. Each heatmap consists of a family of related genes where (A) Cell growth and proliferation; (B) Apoptosis; (C) Stress responses; (D) Blood coagulation and circulation; (E) Cell adhesion molecules; (F) Extracellular matrix molecules; (G) Transcriptional regulation; and (H) Lipid transport and metabolism. Box colour and intensity represents fold-change in gene expression as depicted by the scale. Clustering displayed on the left of each heatmap is according to similarity of expression pattern between genes in each related group. Fold-change in gene expression was determined using the  $\Delta\Delta C_T$  method. Cluster analysis was performed and heatmaps produced using Morpheus software. A list of full gene names is included in Appendix 1.

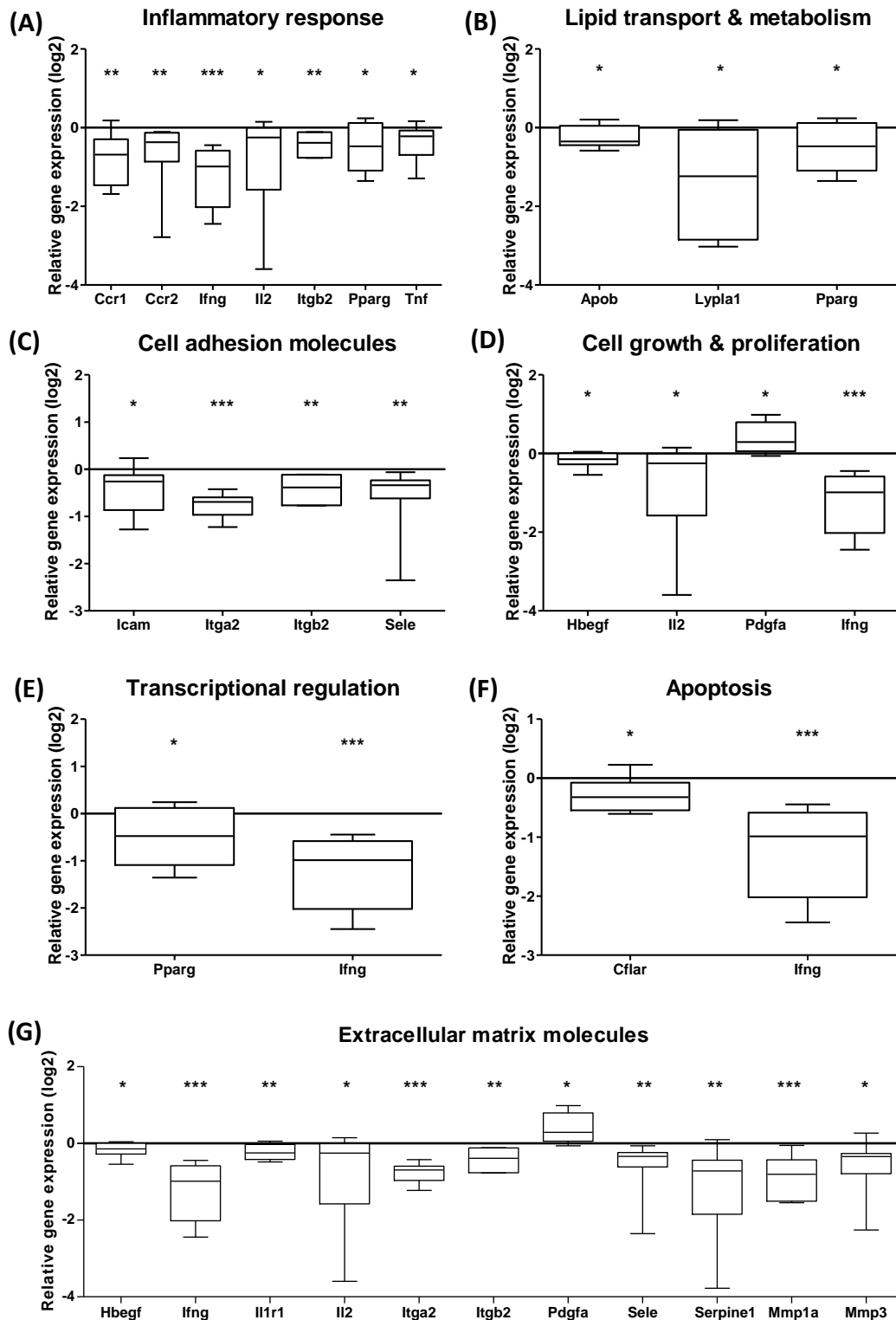


**Figure 6.6 – Related genes show significant change in expression with Lab4/CUL66 supplementation compared to the control.** The effect of Lab4/CUL66 on atherosclerosis-associated gene expression was assessed in liver samples from 8 control and 8 probiotic mice following 12 weeks feeding with either HFD (control group) or HFD supplemented with Lab4/CUL66 (probiotic group). Genes showing significant change in expression were sorted into related groups involved in (A) inflammatory responses, (B) lipid transport and metabolism, (C) cell adhesion, (D) cell growth and proliferation, (E) transcriptional regulation, (F) apoptosis and (G) extracellular matrix molecules. Data are presented as box and whisker plots of log<sub>2</sub> fold-change in gene expression in the probiotic group relative to the control, where whiskers represent min to max fold-change. Statistical analysis was performed using an unpaired Student's t-test where \**p* < 0.05, \*\**p* < 0.01, \*\*\**p* < 0.001.

### 6.3.2 The effect of Lab4/CUL66 supplementation on key bone marrow cell populations

Following 12 weeks feeding with HFD (control) or HFD supplemented with Lab4/CUL66, the bone marrow was extracted and cell populations analysed by immunophenotyping as described in Section 2.8.4. Stem cell populations including HSCs, MPPs and HPC I and II, were identified using antibodies targeting cell surface glycoproteins CD150 and CD48. CD150 is also known as signalling lymphocyte activation molecule (SLAM) and hence these populations are referred to as SLAM. For CLP, CD127 was used as an identifier. For lineage positive differentiated cells, B cells were identified via the B220 marker, T cells via the CD3 marker and macrophages, granulocytes and MDSCs via GR1 and Mac1 markers. The composition of antibody cocktails used in the preparation of SLAM, progenitor and lineage positive cell populations is detailed in Table 2.7. Cell populations of interest were identified using the gating strategy shown in Figure 6.3, and analysed using FlowJo software. Total WBC counts were first analysed, and no significant change in WBC count between the control and the probiotic groups was confirmed (Figure 6.7). The proportion of each cell population was then determined as a frequency of the WBC count for each individual sample.

Results for stem cell populations are shown in Figure 6.8. No significant change was seen in the proportion of MPP or HPC I cell populations between the control and the probiotic groups. In contrast, the proportions of HPC II ( $p < 0.048$ ) and HSC ( $p < 0.034$ ) populations were significantly increased in the probiotic group compared to control. For progenitor CLP, populations showed no significant change between the control and probiotic groups (Figure 6.9). In the category of lineage positive differentiated cells, B cells showed no significant change between control and probiotic groups (Figure 6.10). However, the proportion of T cells was significantly reduced ( $p < 0.005$ ), and both MDSC ( $p < 0.041$ ) and macrophage ( $p < 0.046$ ) populations were significantly reduced in the probiotic group compared to control.

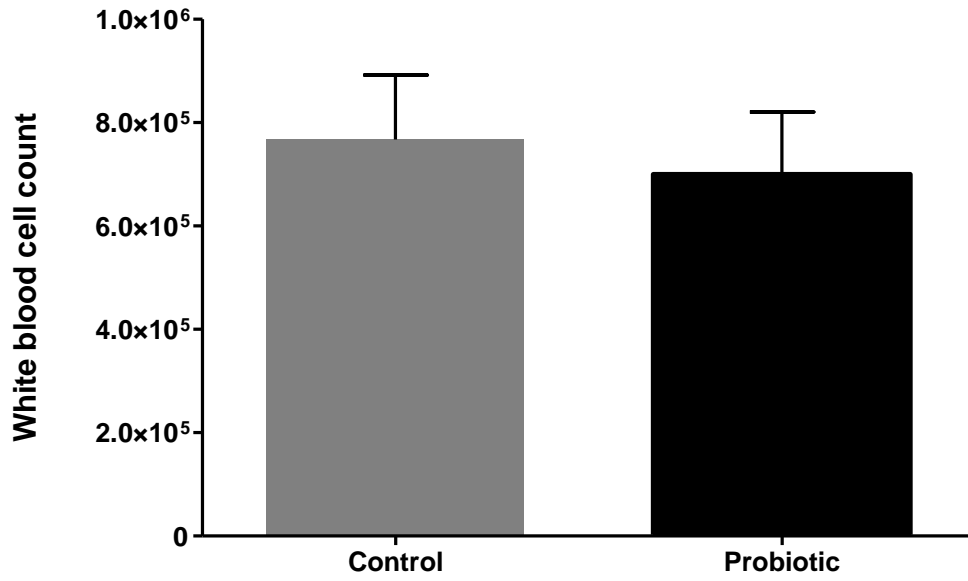


**Figure 6.7 – Treatment with Lab4/CUL66 had no significant effect on white blood cell counts in the bone marrow.** Immunophenotyping of bone marrow stem cell populations from LDLr<sup>-/-</sup> mice was performed following 12 weeks feeding with either HFD (Control) or HFD supplemented with Lab4/CUL66 (Probiotic). Graph represents the total white blood cell counts from the Control and Probiotic groups. Data are presented as mean  $\pm$  SEM from 15 control and 15 probiotic mice. Statistical analysis was performed using an unpaired Student's t-test.



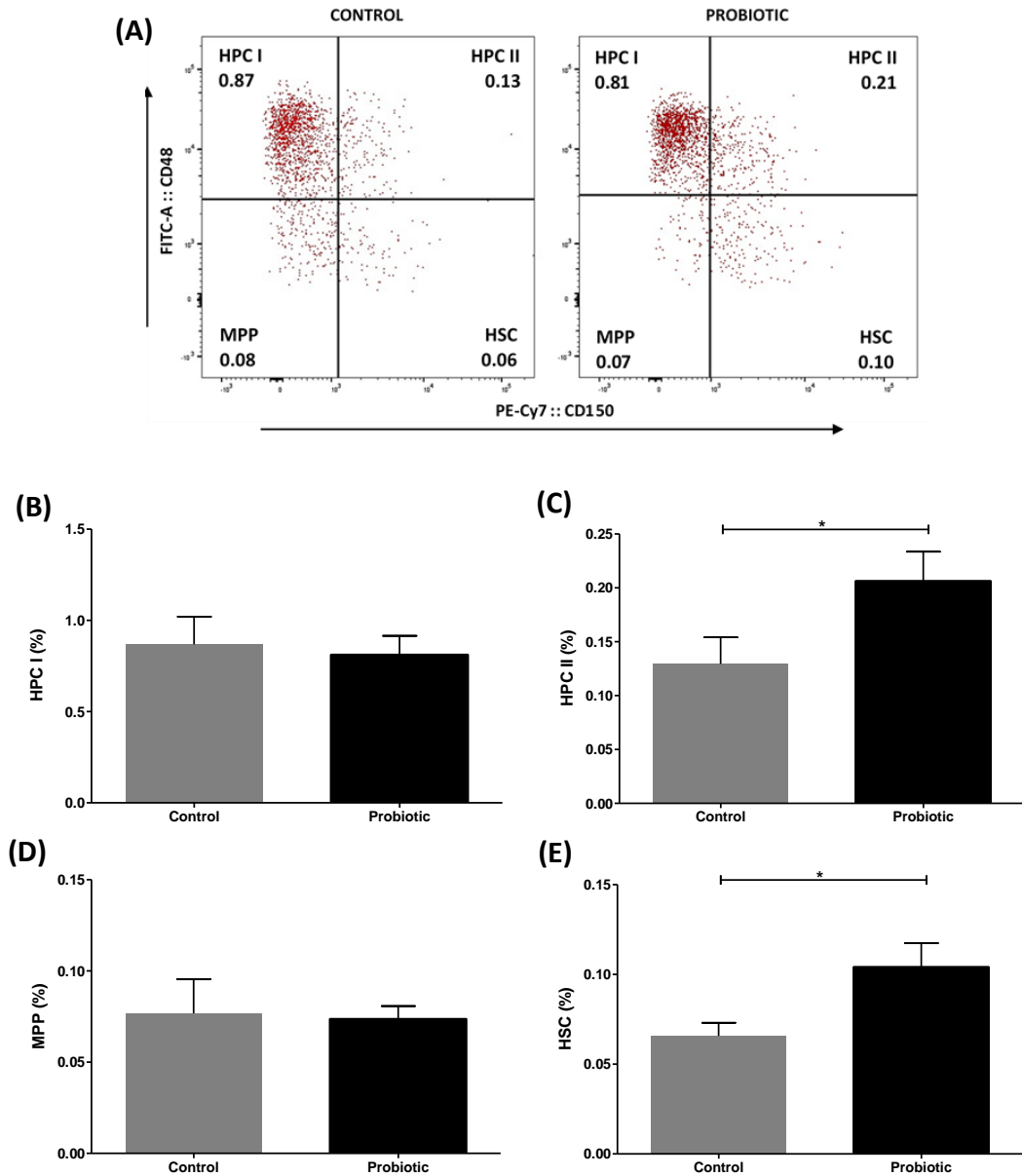


**Figure 6.8 – The effect of Lab4/CUL66 supplementation on bone marrow stem cell populations.** Immunophenotyping of bone marrow stem cell populations from *LDLr<sup>-/-</sup>* mice was performed following 12 weeks feeding with either HFD (Control) or HFD supplemented with Lab4/CUL66 (Probiotic). (A) Representative flow plots showing stem cell populations in control and probiotic groups. Gating shows position of populations representing HPC I (CD48<sup>+</sup>CD150<sup>-</sup>), HPC II (CD48<sup>+</sup>CD150<sup>+</sup>), MPP (CD48<sup>-</sup>CD150<sup>-</sup>) and HSC (CD48<sup>-</sup>CD150<sup>+</sup>) cells. Graphs represent total (B) HPC I; (C) HPC II; (D) MPP; and (E) HSC populations as a frequency of total white blood cells. Data are presented as mean  $\pm$  SEM from 15 control and 15 probiotic mice. Statistical analysis was performed using an unpaired Student's t-test where \* $p < 0.05$ .

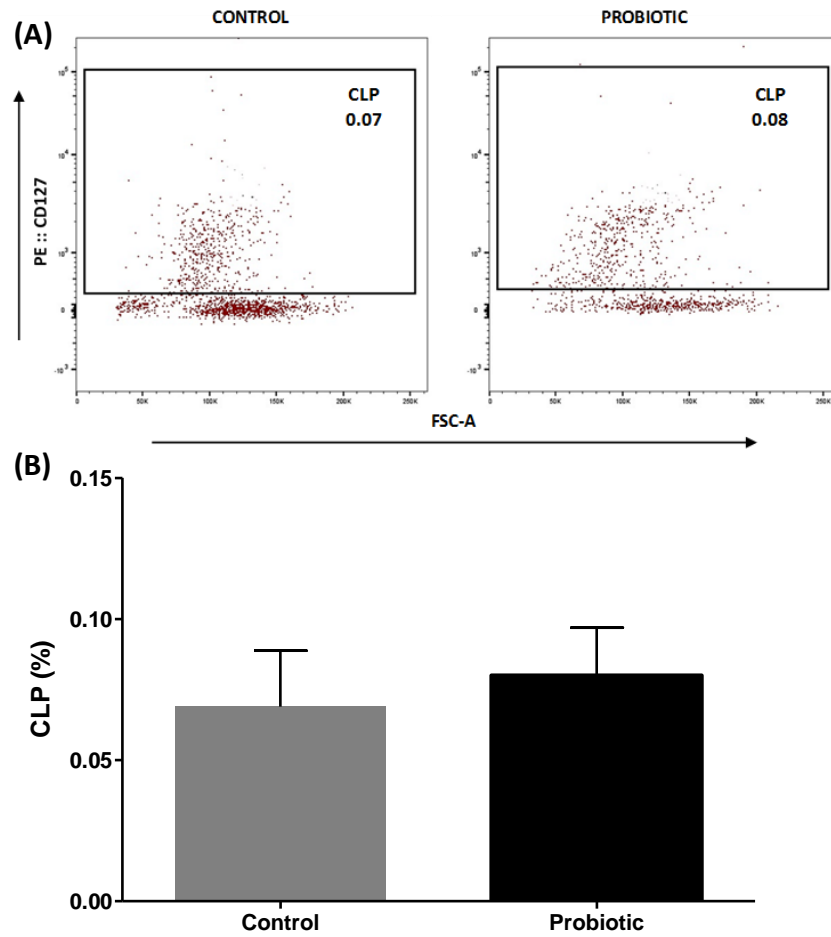


**Figure 6.9 - The effect of Lab4/CUL66 supplementation on bone marrow CLP progenitor cell populations.** Immunophenotyping of bone marrow stem cell populations from LDLr<sup>-/-</sup> mice was performed following 12 weeks feeding with either HFD (Control) or HFD supplemented with Lab4/CUL66 (Probiotic). (A) Representative flow plots showing CLP progenitor cell populations in control and probiotic groups. (B) Graph represents total CLP populations as a frequency of total white blood cells. Data are presented as mean  $\pm$  SEM from 15 control and 15 probiotic mice. Statistical analysis was performed using an unpaired Student's t-test where \* $p$  < 0.05, \*\* $p$  < 0.01.

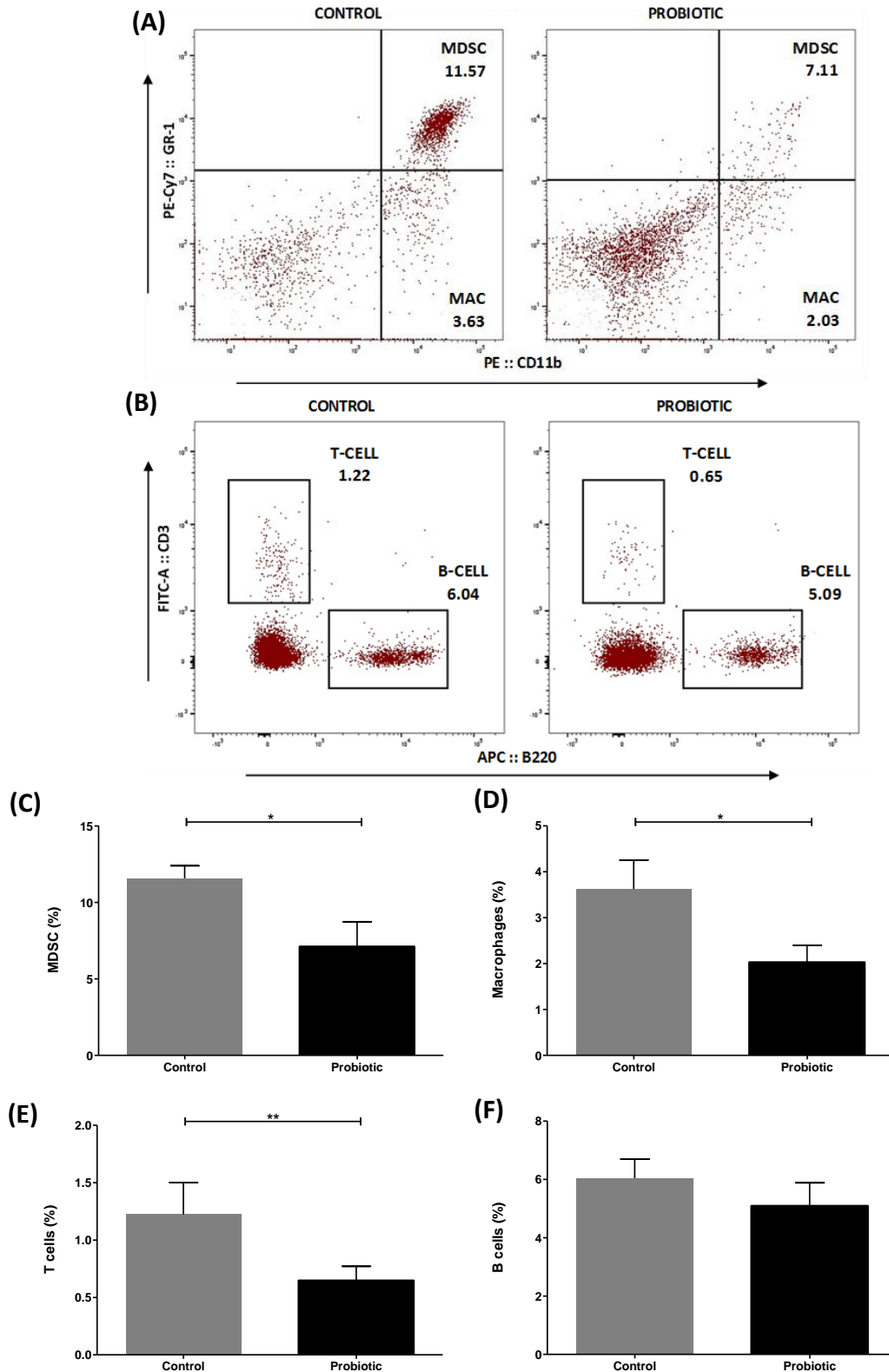


**Figure 6.10 - The effect of Lab4/CUL66 supplementation on bone marrow lineage differentiated cell populations.** Immunophenotyping of bone marrow stem cell populations from *LDLr<sup>-/-</sup>* mice was performed following 12 weeks feeding with either HFD (control) or HFD supplemented with Lab4/CUL66 (probiotic). (A) Representative flow plots showing lineage positive cell populations in control and probiotic groups. Gating shows position of populations representing MDSC (GR-1<sup>+</sup>CD11b<sup>+</sup>), monocytes/macrophages (MAC; GR-1<sup>+</sup>CD11b<sup>+</sup>), (B) T Cells (CD3<sup>+</sup>B220<sup>-</sup>) and B Cells (CD3<sup>-</sup>B220<sup>+</sup>) cells. Graphs represent total (C) MDSC; (D) Monocyte/macrophage; (E) T cell; and (F) B cell populations as a frequency of total white blood cells. Data are presented as mean ± SEM from 15 control and 15 probiotic mice. Statistical analysis was performed using an unpaired Student's t-test where \**p* < 0.05, \*\**p* < 0.01.

## 6.4 Discussion

The current study aimed to investigate the mechanisms underlying the findings from initial *in vivo* investigations which were presented in Chapter 5. The hepatic gene expression of 84 key genes involved in atherosclerosis was investigated following 12 weeks feeding with HFD (control) or HFD supplemented with Lab4/CUL66. Gene expression was determined by qPCR using the Atherosclerosis RT<sup>2</sup> Profiler PCR Array, and fold-change in gene expression was calculated using the  $\Delta\Delta C_T$  method. Of the 84 genes tested, a total of 63 achieved a minimum of 10% change in expression, with 19 of these genes achieving significance and a further 6 displaying a trend towards significance. Genes showing a significant change in expression were further analysed and grouped into related sets as shown in Figure 6.6.

### 6.4.1 Lab4/CUL66 supplementation significantly attenuated the expression of key genes involved in cell adhesion

The expression of a number of genes involved in cell adhesion was significantly decreased in the probiotic group compared to the control (Figure 6.6C). *Icam* and *Sele* encode cell adhesion molecules ICAM1 and E-selectin respectively, both expressed at high levels on the surface of activated endothelial cells in response to pro-inflammatory cytokines, including TNF- $\alpha$ , and are involved in the induction of monocyte recruitment and migration (Hoffman *et al.*, 2018). Mice deficient in cell adhesion molecules have been shown to display reduced atherosclerotic lesion size (Collins *et al.*, 2000; Galkina and Ley, 2007). Moreover, in LDLr<sup>-/-</sup> mice, the inhibition of the expression of cytokines and adhesion molecules including ICAM1, has been shown to attenuate atherosclerosis progression independent of changes in lipid profile (Srivastava *et al.*, 2015). In the studies presented in Chapter 3, it was shown that probiotic CM attenuated monocyte migration *in vitro* (Figure 3.9). It could therefore be suggested that Lab4/CUL66 supplementation attenuates monocyte recruitment *in vivo*. Interestingly, in the current study the expression of IFN- $\gamma$  and TNF- $\alpha$  was also significantly decreased in the probiotic group compared to the control (Figure 6.6A). IFN- $\gamma$  potentiates the expression of adhesion molecules induced by proinflammatory cytokines including TNF- $\alpha$ , thereby

promoting monocyte recruitment (Voloshyna *et al.*, 2014). It could therefore be suggested that attenuation of the expression of pro-atherogenic cytokines including IFN- $\gamma$  and TNF- $\alpha$ , and subsequently adhesion molecules such as ICAM-1, represents one possible mechanism underlying the probiotic-mediated attenuation of monocyte recruitment and migration. As the TNF- $\alpha$ -induced expression of adhesion molecules ICAM-1 and E-selectin requires the transcription factor NF- $\kappa$ B (Baker *et al.*, 2011), it would be useful to investigate the possible involvement of this pathway in future work.

*Itga2* and *Itgb2* encode integrin subunits  $\alpha$ 2 and  $\beta$ 2 respectively. Integrins are heterodimer transmembrane proteins consisting of two subunits, alpha and beta, each of which binds to ECM molecules (Adorno-Cruz and Liu, 2019). Integrin subunit  $\alpha$ 2 forms a heterodimer with the  $\beta$ 1 subunit to form a collagen-binding integrin (Table 6.2), while subunit  $\beta$ 2 is part of the leukocyte-specific  $\beta$ 2 integrin involved in the recognition of cell adhesion molecules on the activated endothelium (Adorno-Cruz and Liu, 2019).  $\beta$ 2 integrins recognise adhesion molecules ICAM1 and E-selectin, and following activation by CC chemokine ligand (CCL) 2 binding, mediate firm adhesion of monocytes to the endothelial layer (Liu *et al.*, 2008). Previous studies have demonstrated the ability of  $\beta$ 2 integrins to modulate the initiation and progression of atherosclerosis in LDLr<sup>-/-</sup> mice (Merched *et al.*, 2010).

*Ccr1* and *Ccr2* encode CC chemokine receptors 1 (CCR1) and 2 (CCR2). CCR1 and CCR2 are chemokine receptors for CCL1/CCL5 and CCL2 (MCP-1) respectively, and are involved in the recruitment of leukocytes across the arterial wall (Boring *et al.*, 1998). Studies investigating the effect of CCR1 on atherosclerosis progression have shown conflicting results though many concur that the receptor is athero-protective (Boring *et al.*, 1998; Braunersreuther *et al.*, 2007; Wan and Murphy, 2013). However, this has not been the case for CCR2 which is known to be pro-atherogenic and pro-inflammatory in nature (Wan and Murphy, 2013). A number of studies in both ApoE<sup>-/-</sup> and LDLr<sup>-/-</sup> mice have demonstrated that CCR2 deficiency leads to attenuation of atherosclerosis (Dawson *et al.*, 1999; Gu *et al.*, 1998; Guo *et al.*, 2003). In the current study, the expression of genes encoding chemokine receptors CCR1 and CCR2 in addition to integrin subunits was significantly decreased, along with genes encoding cell adhesion molecules ICAM1 and

E-selectin. These findings further support the role of probiotic supplementation in the attenuation of monocyte recruitment and migration.

#### 6.4.2 The effect of Lab4/CUL66 supplementation on the expression of genes involved in the regulation of the extracellular matrix

ECM is the major constituent of vascular walls. Genes associated with ECM molecules represent the largest group of associated genes showing significant changes in expression (Figure 6.6G). As discussed previously, the ECM is essential for plaque stability and the formation of a fibrous cap; when components of the ECM are compromised, destabilisation of the fibrous cap leads to plaque rupture and subsequent clinical complications. Of the genes presented in Figure 6.6G, *Serpine1*, *Mmp1a* and *Mmp3* are discussed here in addition to the association of *Ifng* and *Il2* with ECM molecules. *Itga2*, *Itgb2* and *Sele* encode cell adhesion molecules and have been discussed previously in Section 6.4.1, while *Hbegf*, *Il1r1* and *Pdgfa* are included in Table 6.3.

*Serpine1* encodes plasminogen activator inhibitor 1 (PAI-1), a glycoprotein from the serpin family and the primary inhibitor of plasminogen activators in vascular fibrinolysis (Rouch *et al.*, 2015). PAI-1 is known to be involved in the pathogenesis of many conditions, including vascular thrombosis and atherosclerosis (Rouch *et al.*, 2015); in fact, and increased level of PAI-1 in the blood has been highlighted as an independent risk factor for atherosclerosis progression and plaque rupture (Lijnen, 2005; Milenkovic *et al.*, 2017). Upregulation of PAI-1 expression has been demonstrated in human atherosclerotic lesions (Milenkovic *et al.*, 2017; Schneiderman *et al.*, 1992), while studies in ApoE<sup>-/-</sup> mice have reported an athero-protective effect of PAI-1 inhibition or deficiency (Eitzman *et al.*, 2000). Additionally, PAI-1 expression is induced by a range of cytokines including TNF- $\alpha$ .

*Mmp1a* and *Mmp3* encode matrix metalloprotease (MMP)-1a and MMP-3 respectively. Metalloproteinases are a family of enzymes responsible for the degradation of ECM components and are classified into several groups, including collagenases (MMP-1, -8, and -13), gelatinases (MMP-2 and -9), and stromelysins (MMP-3, -10, and -11) (Ye,

2015). Degradative action of MMP enzymes on ECM components breaks down the fibrous cap leading to plaque instability and rupture. Macrophage-derived foam cells accumulated within atherosclerotic lesions have been identified as a major source of MMPs including MMP-3 (Magdalena *et al.*, 2006). The correlation between MMP activity and atherosclerosis is widely known; increased expression of MMPs is associated with enhanced development of atherosclerotic lesions and increased SMC migration (Magdalena *et al.*, 2006; Prescott *et al.*, 1999) and many studies have demonstrated attenuation of plaque progression with deficiency of various MMPs, including MMP-10 (Purroy *et al.*, 2018), MMP-9 (Jin *et al.*, 2015) and MMP-3 (Beaudeau *et al.*, 2003). In the current study, the expression of MMP-1 and MMP-3 was downregulated in the livers of probiotic supplemented mice compared to the control. These results are encouraging and suggest that Lab4/CUL66 supplementation exerts positive effects via potential downregulation of the expression of MMP enzymes. However, studies investigating the effects of MMP -1 and -3 is limited while alternative MMPs dominate the literature. For future studies, investigation of the expression of a wider range of MMPs at the gene and protein level may be carried out at alternative sites including the aorta, providing a more comprehensive view of the effect of probiotic supplementation on MMP activity. Furthermore, the activity of MMP enzymes is counterbalanced by the presence of tissue inhibitors of MMPs (TIMPs), which are also expressed in atherosclerotic lesions (Heeneman *et al.*, 2003). A better indication of potential levels of ECM degradation would be provided if further studies aimed to assess the expression of TIMPs in addition to MMPs.

*Ifng* and *Il2* encode pro-inflammatory cytokines IFN- $\gamma$  and IL-2 respectively and have been discussed previously in relation to the atherosclerotic inflammatory response in Section 6.4.1. They are considered here in relation to the ECM. Both IFN- $\gamma$  and IL-2 induce the release of MMPs, thereby promoting the degradation of the ECM (Wang *et al.*, 2015b) resulting in reduced plaque stability with eventual destabilisation and rupture (Voloshyna *et al.*, 2014; Weng *et al.*, 2014). In the current study, the expression of IFN- $\gamma$  and IL-2, in addition to MMP-1 and -3, was significantly reduced with Lab4/CUL66 supplementation compared to the control, suggesting a potential athero-protective role of Lab4/CUL66 in maintaining plaque stability.

### 6.4.3 Lipid transport and metabolism

*ApoB* encodes the protein apoB, a key component of atherogenic lipoproteins as discussed in Chapter 1. ApoB is an important predictor of atherosclerosis and a known positive correlation exists between apoB levels and atherosclerotic conditions, with decreased apoB expression reported to have a protective effect against hypercholesterolemia (Dhingra and Bansal, 2005). In fact, it has been proposed that apoB is a superior indicator of atherosclerosis risk (Harper and Jacobson, 2010), as reported in a number of human trials where apoB was shown to be a more accurate predictor of disease risk than the traditionally used LDL or non-HDL cholesterol levels (Holme *et al.*, 2008; McQueen *et al.*, 2008; Walldius *et al.*, 2001). This is particularly the case for a subgroup of at-risk patients who exhibit low or normal levels of LDL cholesterol despite high numbers of lipoprotein particles (Harper and Jacobson, 2010). In the current study, the expression of *ApoB* was attenuated by probiotic supplementation at the gene expression level (Figure 6.6), correlating with results in Chapter 5 where probiotic supplementation was shown to significantly reduce plasma levels of LDL cholesterol (Figure 5.4). However, decreased expression of apoB at the mRNA level cannot be directly associated with decreased levels of plasma LDL cholesterol, and plasma apoB protein levels would need to be measured before firm conclusions can be drawn. In future work it would be useful to analyse plasma levels of apoB in the probiotic group compared to the control, and to consider this in relation to the levels of non-HDL cholesterol.

In addition to *ApoB*, expression of *Lypla1* and *Pparg* was also significantly decreased in the probiotic group compared to control. Lysophospholipase A1 (LYPLA1) is a cytosolic serine hydrolase and is partially responsible for the metabolism of lysophospholipids (Wepy *et al.*, 2019). Under conditions of oxidative stress, up to half of the phosphatidylcholine held within an LDL particle is converted to lysophosphatidylcholine (LPC) (Wepy *et al.*, 2019). LPC is a major bioactive phospholipid component of oxLDL which is hydrolysed by lysophospholipases to form lysophosphatidic acid (LPA) (Bao *et al.*, 2018). LPC levels in the circulation are associated with the development of atherosclerotic plaques and endothelial cell dysfunction, and the LPC content of circulating modified LDL has been shown to be increased in atherosclerosis patients (Bao



*et al.*, 2018; Zakiev *et al.*, 2016). LPA is also pro-atherogenic and is abundant in the necrotic core of atherosclerotic plaques. In the current study, *Lypla1* expression was significantly decreased in the probiotic group compared to control. This result indicates the possibility of a corresponding reduction in the levels of LPC and LPA; however, further investigations would be required to investigate this proposition.

*Pparg*, encoding PPAR- $\gamma$ , has been discussed in Section 6.4.1 with regards to its role in inflammatory responses. PPAR- $\gamma$  is highly expressed in macrophage foam cells within atherosclerotic lesions (Li *et al.*, 2000) where activation has been reported to promote monocyte/macrophage differentiation and induce the expression of CD36 (Tontonoz *et al.*, 1998). Endogenous PPAR- $\gamma$  ligands have been identified within serum oxLDL, and it has been suggested that atherogenic lipoproteins including oxLDL may induce their own uptake via PPAR- $\gamma$ -induced upregulation of CD36, thereby promoting foam cell formation (Rosen and Spiegelman, 2000). Despite these findings, PPAR- $\gamma$  agonists have been shown to inhibit atherosclerosis development in animal (Li *et al.*, 2000) and human studies (Ivanova *et al.*, 2017; Skochko and Kaidashev, 2017). PPAR- $\gamma$  agonists are used as therapeutic agents in a number of conditions associated with cardiovascular risk including diabetes mellitus and hypertension (Ivanova *et al.*, 2015, 2017); however, it is possible that some of the anti-atherogenic effect of these agents are achieved via non-PPAR- $\gamma$ -related mechanisms (i.e. non-genomic effects). In the current study, gene expression of PPAR- $\gamma$  was significantly decreased in the probiotic group compared to control. However, the effects of PPAR- $\gamma$  are complex and further investigation is required to ascertain the effect of attenuated PPAR- $\gamma$  expression in atherogenesis.

#### 6.4.4 Lab4/CUL66 supplementation attenuates gene expression of key pro-inflammatory cytokines

Investigation of inflammatory gene expression *in vitro* displayed few notable effects in THP-1 macrophages treated with probiotic CM compared to control (Figure 3.27). In contrast, the expression of genes involved in the inflammatory response *in vivo* suggests a beneficial effect of Lab4/CUL66 supplementation, with genes encoding key pro-inflammatory molecules displaying decreased expression. *Ifng*, *Tnf* and *Il2* encode key pro-inflammatory and pro-atherogenic cytokines IFN- $\gamma$ , TNF- $\alpha$  and IL-2 respectively,

each of which is integral to atherosclerosis development and the expression of all was significantly reduced with probiotic supplementation (Figure 6.6A).

As discussed in Chapter 1, IFN- $\gamma$  is a T cell and macrophage-derived proinflammatory cytokine known to be highly expressed in atherosclerotic lesions and deficiency of this cytokine has been shown to attenuate atherosclerosis in both ApoE<sup>-/-</sup> and LDLr<sup>-/-</sup> mouse models (Koga *et al.*, 2007; Niwa *et al.*, 2004). IFN- $\gamma$  is a master regulator involved in all stages of atherosclerosis initiation, development and progression, including monocyte recruitment, foam cell formation, plaque formation and rupture, as well as the Th1-associated immune responses (Voloshyna *et al.*, 2014). Additionally, IFN- $\gamma$  promotes apoptotic cell death in human macrophages (Inagaki *et al.*, 2002) and VSMCs (Geng *et al.*, 1996), thereby contributing to the formation of a necrotic core and decreased plaque stability. An increase in IFN- $\gamma$  has also been shown to significantly increase the T cell content of atherosclerotic lesions (Voloshyna *et al.*, 2014; Whitman *et al.*, 2000). With respect to the effect of IFN- $\gamma$  on the T cell content of the plaque, this observed decrease in *Ifng* expression correlates with results in Chapter 5 where it was shown that Lab4/CUL66 supplementation led to a reduction in the T cell content of plaque in the probiotic group compared to the control (Figure 5.13). The Janus kinase (JAK)-Signal Transducers and Activators of Transcription (STAT) pathway represents the primary IFN- $\gamma$  signalling pathway (Moss and Ramji, 2015). As IFN- $\gamma$  represents such a promising target for anti-atherosclerotic therapeutics, future work should involve more in-depth investigation of Lab4/CUL66 supplementation on IFN- $\gamma$ -associated responses.

Activation of macrophages by IFN- $\gamma$  leads to the production of further proinflammatory cytokines, including TNF- $\alpha$  (Voloshyna *et al.*, 2014), the gene expression of which was also shown to be decreased with Lab4/CUL66 supplementation. Like IFN- $\gamma$ , TNF- $\alpha$  is a key cytokine implicated in many stages of atherosclerosis exhibiting strong pro-atherogenic effects, and attenuation of TNF- $\alpha$  action has been shown to diminish atherosclerosis development (Br n n *et al.*, 2004; Ohta *et al.*, 2005). Additionally, *Il2* encodes IL-2, a pro-atherogenic cytokine involved in cell-mediated immune responses and is primarily produced by activated T cells. Suppression of IL-2 action has demonstrated anti-atherogenic outcomes, with one study reporting enhanced atherosclerosis with IL-2 injection in addition to a reduction in atherosclerosis following

injection with anti-IL-2 antibodies (Ramji and Davies, 2015; Upadhy *et al.*, 2004). In the current study, IL-2 mRNA expression was significantly decreased, presenting a further anti-atherogenic effect of Lab4/CUL66 supplementation.

**Table 6.3 - Further genes showing significant changes in expression and their role in atherosclerosis**

Gene	Pathway	Role in atherosclerosis
<i>Cflar</i>	Apoptosis	CASP8 and FADD-like apoptosis regulator CFLAR. Overexpression attenuates metabolic disorders associated with cardiovascular risk (Wang <i>et al.</i> , 2017b)
<i>Hbegf</i>	Cell growth & proliferation	Heparin-binding EGF-like growth factor (HBEGF), a potent mitogen and chemoattractant for VSMCs (Nakata <i>et al.</i> 1996). HBEGF expression positively correlates with cardiovascular risk (Kim <i>et al.</i> , 2017)
<i>Il1r1</i>	Extracellular matrix molecules	IL-1 receptor 1 (IL-1R1), involved in vascular remodelling. IL-1R1 deficiency reduces atherosclerosis in <i>Il1r1<sup>-/-</sup>/ApoE<sup>-/-</sup></i> mice (Alexander <i>et al.</i> , 2012)
<i>Itga2</i>	Cell adhesion molecules	Integrin subunit $\alpha 2$ forms collagen-binding integrin, involved in monocyte attachment to collagen IV (Wang <i>et al.</i> , 2010)
<i>Pdgfa</i>	Cell growth & proliferation	PDGF alpha, stimulates migration and proliferation of VSMCs. Promotes vascular disease and atherosclerosis progression (Brown <i>et al.</i> , 2010)

#### 6.4.5 The effect of Lab4/CUL66 supplementation on key cell populations in the bone marrow of *LDLr<sup>-/-</sup>* mice

In addition to the analysis of gene expression, the effect of Lab4/CUL66 supplementation on key bone marrow cell populations was investigated using a method of immunophenotyping. To identify cell populations of interest, bone marrow extract was incubated with antibodies targeting specific cell surface markers and flow cytometry was carried out. Cell populations were identified and the proportion of each cell type was determined as a frequency of total white blood cells from absolute cell

numbers. Results are presented in Figures 6.8 - 6.10. Bone marrow cell populations that demonstrated significant changes are highlighted in Figure 6.11.

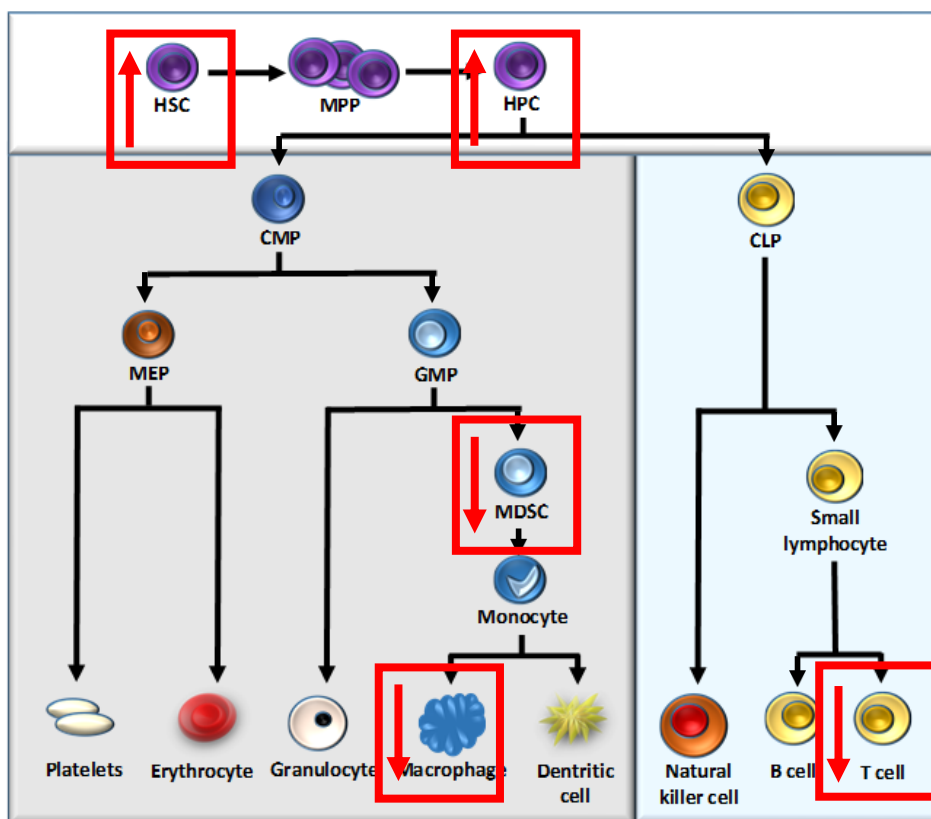


**Figure 6.11 - Bone marrow cell populations showing significant changes with probiotic supplementation.** Simplified representation of bone marrow cell populations. Red squares highlight cell populations which were significantly increased (upwards arrow) or decreased (downwards arrow) in the bone marrow of probiotic supplemented mice compared to the control. HSC, haematopoietic stem cell; MPP, multipotent progenitor; HPC, haematopoietic progenitor cell; CMP, common myeloid progenitor; CLP, common lymphoid progenitor; MEP, megakaryocyte-erythroid progenitor; GMP, granulocyte-macrophage progenitor; MDSC, myeloid-derived suppressor cell.

As discussed previously, LSK (Lin<sup>-</sup> Sca-1<sup>+</sup> c-Kit<sup>+</sup>) populations give rise to HSC, MPP and subsequently HPC populations. In the current study, bone marrow populations of HSCs and HPCs were significantly increased following probiotic supplementation (Figure 6.8). An increase in HSPCs is known to correlate with hypercholesterolaemia (Feng *et al.*, 2012; Lang and Cimato, 2014), where a reduction in cholesterol level has been shown to attenuate hypercholesterolaemia-induced HSPC expansion (Ma and Feng, 2016). To the contrary in the current study, probiotic supplementation resulted in an increase in HSPCs (HSC and HPC), independent of a significant decrease in LDL cholesterol as demonstrated in Chapter 5 (Figure 5.4). It is therefore likely that the observed increase in bone marrow HSPC population is unrelated to plasma cholesterol levels. Additionally, increased bone marrow HSC proliferation is associated with increased leukocyte

production (Hanna and Hedrick, 2014). However, in the current study probiotic supplementation had no effect on the CLP cell population, and resulted in a significant decrease in the CD3+ T cell population (Figure 6.10). The production and maturation of T cells is complex and their role in atherosclerosis is dependent upon many factors, including the specific phenotypic subset. The CD3 marker is a defining feature of T cells and is particularly useful in the identification of bone marrow T cells, where the CD3+CD4-CD8- phenotype represents over a third of the total population (Sykes, 1990). T cell numbers may be used as an indirect marker of inflammatory status, therefore the observed reduction in bone marrow T cells indicates a possible anti-inflammatory and anti-atherogenic effect. However the origin, composition and fate of bone marrow T cell populations is highly complex and largely unclear, and further research is required before any firm conclusions can be drawn. In addition to a reduction in bone marrow CD3+ T cells, it was shown in Chapter 5 that probiotic supplementation also resulted in a trend of reduction of T cell content in atherosclerotic plaque (Figure 5.11), suggesting that Lab4/CUL66 may exert beneficial effects via the modulation of T cells. In future studies, it would be informative to perform similar immunophenotyping of T cell populations in the plasma and/or the aorta, to gain a more in-depth understanding of the T cell-mediated effects of Lab4/CUL66. Furthermore, it would also be useful to determine the frequency of T cell subsets in these tissues, such as the pro-atherogenic Th1 cells, or athero-protective regulatory T cells (Getz and Reardon, 2018).

The LK (Lin- cKit+) cell population within the bone marrow gives rise to myeloid progenitors and subsequently all myeloid cells. CMPs are responsible for the generation of both MEPs and GMPs, where GMPs give rise to MDSCs and finally monocytes and macrophages. In the current study, both MDSCs and macrophages were significantly reduced (Figure 6.10). Few studies have investigated the role of MDSCs in atherosclerosis disease and the relationship remains unclear. One study reported that MDSCs in the bone marrow of LDLr<sup>-/-</sup> mice strongly suppress the proliferation of T-cells, particularly pro-inflammatory Th1 and Th17 cells in atherosclerotic conditions, and this effect is associated with increased monocyte MDSCs (Foks *et al.*, 2016). In the current study, probiotic supplementation led to an increase in MDSCs (Figure 6.10). However, monocyte/macrophage MDSCs in addition to the T-cell content of atherosclerotic plaques was significantly reduced. This result indicates that the observed increase in

MDSC population did not significantly contribute to atherosclerosis disease progression in the current study.

Finally, the bone marrow monocyte/macrophage population was significantly decreased in the probiotic group compared to control. As shown in Figure 6.10A, monocytes/macrophages are CD11b (MAC1)+GR1- and distinguishable from the MDSC CD11b+GR1+ population. Monocytes and macrophages are integral to atherosclerosis initiation, development and progression and a reduction in these cells could lead to decreased recruitment of monocytes, reduced foam cell formation and reduced plaque formation. Plaque macrophages are known to drive many processes in atherosclerosis disease progression; however, the role of bone marrow macrophages is unknown. It was demonstrated in Chapter 5 that the macrophage content of atherosclerotic lesions was significantly reduced in the probiotic group compared to control (Figure 5.13), indicating a reduction in infiltrating monocytes possibly due to a reduction of circulating monocytes. Macrophage populations in the bone marrow are largely erythroblastic island macrophages and HSC niche macrophages (Kaur *et al.*, 2017), therefore it could be suggested that it is the CD11b+GR1- monocyte population that has greater relevance in relation to atherosclerosis. Future work should aim to further distinguish populations identified by the CD11b+GR1- marker. It would also be useful to identify and assess the proportion of these cell populations in the plasma using a similar immunophenotyping method.

#### 6.4.6 Summary

Studies in this chapter have revealed a number of probiotic-induced changes in atherosclerosis-associated gene expression. A significant decrease in the expression of genes involved in cell adhesion was observed (Figure 6.6C), which when considered together with the reduction in monocyte migration observed during *in vitro* investigations (Figure 3.10), supports the probiotic-induced reduction in monocyte recruitment via downregulation of the expression of genes involved in cell adhesion. In addition, downregulation of genes involved in lipid transport and metabolism (Figure 6.6B) supports the reduction in plasma LDL-C and increase in HDL-C demonstrated in Chapter 5 (Figure 5.4), while the significant downregulation of genes encoding ECM

molecules (Figure 6.6G) suggests a potential role of probiotic supplementation in fibrous cap formation and the maintenance of plaque stability. Furthermore, the downregulation of genes encoding key pro-inflammatory cytokines, including IFN- $\gamma$  and TNF- $\alpha$ , represents a possible anti-inflammatory effect of Lab4/CUL66 supplementation. Since IFN- $\gamma$  and TNF- $\alpha$  are implicated in every stage of atherosclerosis initiation and progression, downregulation of expression of these cytokines at the molecular level may also be a contributing factor in the probiotic-induced reduction of monocyte recruitment, foam cell formation, plaque formation, and T cell content of plaque as observed in the current study.

In addition to gene expression changes, bone marrow populations of MDSCs, monocytes/macrophages and T cells were significantly decreased in the probiotic group compared to control. These changes are potentially anti-atherogenic in nature and may correlate with the observed reduction in plaque macrophage and T cell content. While this initial assessment of cell populations is useful, further research is required to assess the proportion of more specific subsets of cell populations both in the plaque and in the bone marrow; particularly T cell subsets which are numerous and variable in their effects in atherosclerosis.

# CHAPTER 7

*General Discussion*

---



## 7.1 Introduction

Despite advances in therapeutic strategies, CVD remains the leading cause of death worldwide with an estimated one in three deaths attributed to the disease. Furthermore, the prevalence of CVD presents a tremendous financial burden, costing the UK economy an estimated 19 billion annually. Atherosclerosis is a chronic inflammatory disorder of the medium and large arteries and is the primary cause of CVD-related morbidity and mortality. Atherosclerosis develops over a life-time with a number of risk factors known to accelerate disease progression, including cigarette smoking, hypertension, hyperglycaemia, dyslipidaemia and a genetic predisposition to the disease.

The most commonly prescribed first-line pharmaceutical agents are statins, a class of lipid-lowering agents known for their ability to inhibit the HMG CoA reductase enzyme. Statins have shown some success as lipid-lowering agents; however, statin therapy even in combination with life-style changes achieves relatively limited success and considerable cardiovascular risk remains (Cannon *et al.*, 2015). Furthermore, subsets of patients suffer intolerable statin-related side effects, are non-compliant, or fail to achieve target LDL-C levels even at the highest dose (Stroes *et al.*, 2015; Whayne, 2013). Due to the limitations of statin therapy, the search continues for more alternative or additional agents including co-therapy with non-statin agents, PCSK9 inhibitors, monoclonal antibodies or nutraceuticals.

Probiotics have shown great potential as anti-atherogenic agents with studies demonstrating beneficial effects of probiotic treatment on atherosclerotic lesion formation, as well as a number of cardiovascular risk factors including dyslipidaemia, hypertension, hypercholesterolaemia and chronic inflammation. The Lab4 and Lab4b probiotic consortia developed by Cultech Ltd are composed of distinct populations of *Lactobacillus* spp. and *Bifidobacterium* spp. Over the previous 15 years, clinical studies have shown the benefit of both Lab4 and Lab4b in a variety of functions including digestive health, immune health, mood and cognition in adults, children and babies (Allen *et al.*, 2014; Hepburn *et al.*, 2013; Owen *et al.*, 2014; Williams *et al.*, 2009). In addition, the probiotic *L. plantarum* CUL66 has demonstrated cholesterol-lowering

ability, and in a preliminary short-term feeding study Lab4/CUL66 supplementation was shown to attenuate hypercholesterolaemia in C57BL/6J mice fed a HFD (Michael *et al.*, 2016, 2017). Results from these preliminary studies are promising, and when considered in conjunction with previously demonstrated immunomodulatory effects, highlight the potential benefits of Lab4, Lab4b or CUL66 supplementation as potential athero-protective agents. While several clinical studies have demonstrated the beneficial effects of Lab4 and Lab4b consortia in a variety of conditions, their role in atherosclerosis has not previously been investigated.

The overall aim of this project was therefore to assess the anti-atherogenic effects of Lab4, Lab4b and CUL66 on key processes in atherosclerosis development. Initial investigations were performed *in vitro* using human monocytes, macrophages and VSMCs, and key findings confirmed in primary human macrophages. The project then progressed to determine anti-atherogenic effects of supplementation with Lab4 combined with CUL66 *in vivo* using an atherosclerosis mouse model.

## 7.2 Summary of key findings

Overall results from this project have highlighted Lab4, Lab4b, CUL66, and the Lab4/CUL66 combination as potential anti-atherosclerotic agents capable of exerting beneficial effects in a variety of atherogenic processes both *in vitro* and *in vivo*. The key anti-atherosclerotic effects of these probiotic consortia, as identified from results presented in this study, are illustrated in Figure 7.1. In this section, results from each experimental chapter are summarised, and key findings from *in vitro* and *in vivo* studies are presented in Tables 7.1 and 7.2 respectively.

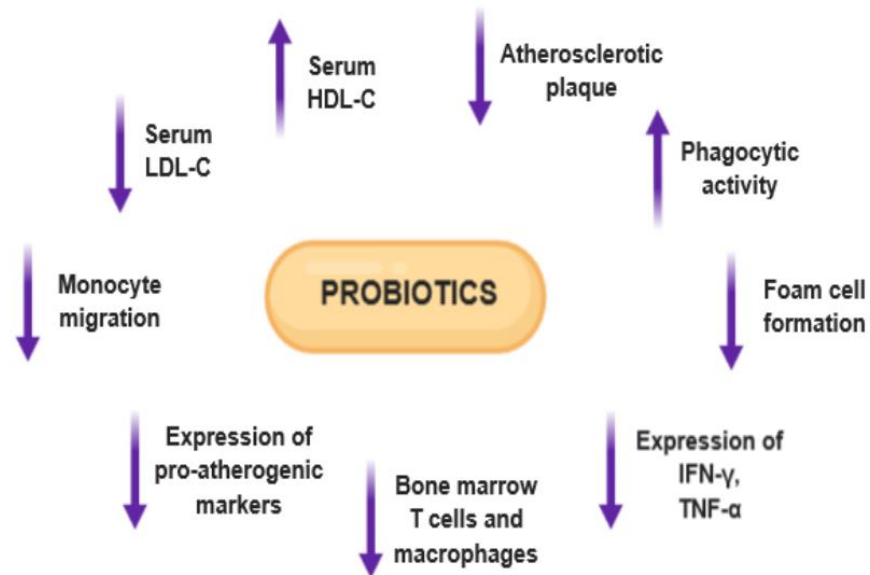


Figure 7.1 - Key anti-atherosclerotic effects of Lab4, Lab4b, CUL66 and Lab4/CUL66.

**Chapter 3.** Prior to the start of experiments on atherosclerosis-associated parameters, probiotic CM concentration was optimised to the maximum protein concentration at which cells maintain viability. Initial investigations were then carried out *in vitro* using THP-1 monocytes and PMA-differentiated THP-1 macrophages to determine the effect of Lab4, Lab4b and CUL66 on a number of key processes in atherosclerosis development. Key results from these initial investigations suggested that all of Lab4/Lab4b/CUL66 can attenuate MCP-1-induced monocyte migration (Figure 3.9), dramatically attenuate macropinocytosis by macrophages (Figure 3.15), increase macrophage phagocytic activity (Figure 3.18), and reduce proliferation of monocytes, macrophages and VSMCs (Figures 3.20-24). Upon investigation of the effect of probiotics on inflammatory gene expression, it was found that each of Lab4/Lab4b/CUL66 was able to attenuate TNF- $\alpha$ -induced expression of ICAM1 but not MCP-1 (Figure 3.27). Additionally, CUL66 demonstrated the ability to increase mitochondrial respiratory capacity in macrophages while Lab4 and Lab4b had no effect (Figure 3.17). In addition, Lab4 and Lab4b attenuated VSMC invasion while CUL66 had no effect (Figure 3.25). Overall, results from this chapter demonstrated the anti-atherosclerotic potential of each probiotic across key processes in atherosclerosis development.

**Chapter 4.** In the previous chapter, it was found that probiotic treatment had a profound effect on macropinocytosis in macrophages, suggesting a possible role for probiotics in the prevention of lipoprotein uptake. Given the strong association between probiotics and lipid modulation, investigations continued *in vitro* with a more specific focus on the uptake, metabolism and efflux of cholesterol and macrophage foam cell formation. All of Lab4/Lab4b/CUL66 inhibited macrophage uptake of oxLDL by a minimum of 50% (Figure 4.6), with a corresponding decrease in gene expression of SR-A, CD36 and LPL (Figure 4.8). Furthermore, all of Lab4/Lab4b/CUL66 increased efflux of cholesterol from macrophage foam cells (Figure 4.10) where Lab4 and Lab4b resulted in a corresponding increase in ABCA1, ABCG1 and LXRs at the gene expression level (Figure 4.12). Intracellular cholesterol metabolism was also investigated and initial results suggest that probiotic treatment can reduce the accumulation of cholesterol esters (Figure 4.14); however, further repeats are required before any firm conclusions can be drawn. Together, results from this chapter strongly suggest that these probiotics can reduce or even prevent the formation of macrophage foam cells, a critical process in atherosclerosis development.

**Chapter 5.** Following on from the promising results demonstrated in *in vitro* investigations, studies continued to assess the anti-atherosclerotic effects of Lab4/CUL66 supplementation *in vivo* using an atherosclerosis mouse model. LDLr<sup>-/-</sup> mice were fed HFD (control) or HFD supplemented with Lab4/CUL66 (probiotic) for a period of 12 weeks. Mice were then sacrificed and tissues collected. Plaque area was significantly reduced by 39% in the probiotic group compared to control, in addition to a 35% reduction in lipid content (Figures 5.8-9). The composition of plaque was also altered where the probiotic group had a reduced level of macrophages, SMCs and a trend of reduction in the T cell content compared to the control group (Figure 5.13). Analysis of plasma lipids revealed a remarkable reduction in LDL-C with increased HDL-C despite no change in TC levels. Furthermore, the ratios of LDL/HDL, TC/HDL and TC/LDL were all beneficially altered (Figures 5.4-6). Together, these results show that Lab4/CUL66 supplementation has beneficial anti-atherosclerotic effects *in vivo*, including a significant improvement of plasma lipid profile and a remarkable reduction in atherosclerotic plaque formation. In studies presented in Chapter 6, further tissues

were analysed in an attempt to delineate the possible mechanisms underlying these observed anti-atherosclerotic effects.

**Chapter 6.** To investigate the mechanisms underlying the anti-atherosclerotic effects demonstrated in Chapter 5, hepatic gene expression and bone marrow cell populations were analysed. Immunophenotyping of bone marrow cell populations was carried out by flow cytometry and key cell types identified. Stem cell populations were found to be overall increased in the probiotic group compared to control (Figure 6.8). In the lymphocytic cell lineage, T-cell populations were significantly reduced (Figure 6.10). In the myeloid lineage, populations of monocytes/macrophages were also significantly reduced in the probiotic group compared to control (Figure 6.10). Gene expression was determined by qPCR using the Atherosclerosis RT<sup>2</sup> Profiler PCR Array, and the fold-change in gene expression calculated using the  $\Delta\Delta C_T$  method. Of the 84 genes tested, a total of 63 achieved a minimum of 10% change in expression, while 19 of these genes achieved significance and a further 6 displayed a trend of significance (Table 6.2). Of the genes showing significant changes in expression, many were found to encode a number of key molecules involved in atherosclerotic processes, including inflammatory responses (IFN- $\gamma$ , TNF- $\alpha$ , IL-2), cell adhesion (ICAM1, CCR2, E-selectin, integrins), lipid transport (apoB), and ECM molecules (MMPs, IL-1R1, PAI-1). Overall, results from this chapter correlate with anti-atherogenic effects observed in previous chapters and provides insight into the mechanisms by which Lab4/CUL66 supplementation may exert these effects.

**Table 7.1 - Summary of key findings from *in vitro* investigations of the effects of Lab4, Lab4b and CUL66 on key processes in atherosclerosis.**

Investigation	Lab4	Lab4b	CUL66
Monocyte migration	↓	↓	↓
Macropinocytosis	↓	↓	↓
Receptor-mediated uptake of oxLDL	↓	↓	↓
Cholesterol efflux	↑	↑	↑
VSMC invasion	↓	↓	–
Phagocytosis	↑	↑	↑
Gene expression changes	SR-A	↓	↓
	CD36	↓	↓
	LPL	–	↓
	ABCA1	↑	↑
	ABCG1	↑	↑
	LXR $\alpha$	↑	↑
	LXR $\beta$	↑	↑

**Table 7.2 - Summary of key findings from *in vivo* investigation of the effect of Lab4/CUL66 supplementation in LDLr<sup>-/-</sup> mice.**

Parameter	Effect of Lab4/CUL66 supplementation
Plaque formation	Reduced plaque area
Plaque composition	Reduced plaque lipid content; reduced plaque macrophage, T cell and SMC content
Fat and organ weights	Increased spleen weight
Plasma lipids	Increased HDL-C; reduced LDL-C and HDL/LDL ratio; no change in TC; reduced TC/HDL and increased TC/LDL ratios
Gene expression	Significant changes in expression of 19 atherosclerosis-associated genes
Bone marrow cell populations	Increased stem cell and progenitor populations; reduced T cells and monocytes/macrophages

### 7.3 Mechanisms of action

It is clear from *in vivo* studies that Lab4/CUL66 supplementation can reduce the formation of atherosclerotic lesions in the aortic sinus of LDLr<sup>-/-</sup> mice fed a HFD. Furthermore, Lab4/CUL66 supplementation demonstrated plasma LDL-C lowering capability as well as the ability to increase HDL-C, suggesting that this probiotic combination may be an effective lipid-modulating agent for patients with high LDL-C and/or low HDL-C levels. Dyslipidaemia is a major risk factor for atherosclerosis development and it is likely that these lipid-modulating effects of probiotic treatment is in part responsible for the observed reduction in plaque formation. However, while lipid-lowering agents are known to reduce cardiovascular risk, the beneficial effects of the Lab4 consortia in combination with CUL66 extends beyond lipid-modulation to a number of atherogenic processes. Figure 7.2 shows an overview of atherosclerosis progression highlighting key processes in which Lab4, Lab4b, CUL66 or Lab4/CUL66 combination have demonstrated beneficial anti-atherosclerotic effects. The possible mechanisms underlying these effects are discussed in the next section.

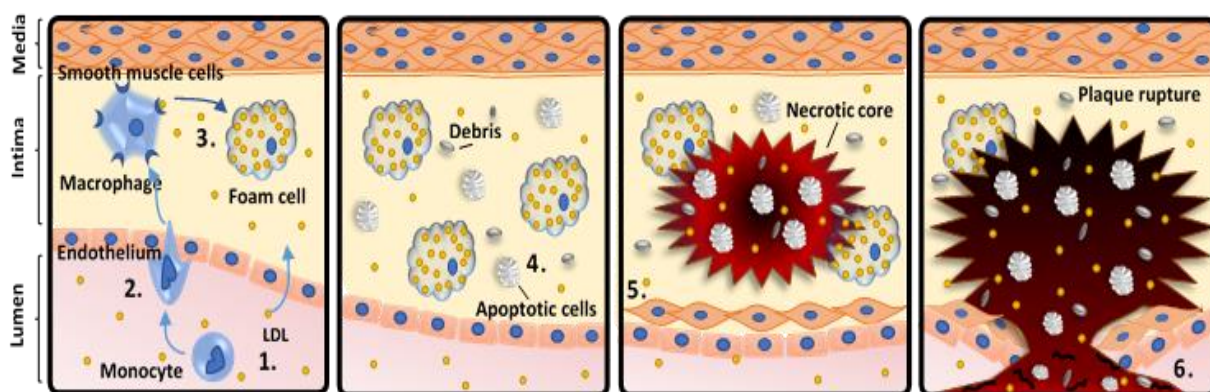


**Figure 7.2 - Probiotics exert effects in a number of key stages in atherosclerosis development.** 1. Plasma lipids. Lab4/CUL66 supplementation lowers LDL-C and increases HDL-C *in vivo*. 2. Monocyte migration was attenuated *in vitro*. *In vivo* expression of genes encoding ICAM1, selectins and integrins involved in monocyte recruitment, adhesion and transendothelial migration was also attenuated by Lab4/CUL66 supplementation. 3. Foam cell formation was attenuated by probiotic treatment *in vitro* with attenuated uptake and increased efflux of cholesterol and corresponding changes in expression of related genes. *In vivo* Lab4/CUL66 supplementation led to reduced plaque formation and reduced plaque lipid content. 4. Macrophage phagocytic activity was increased *in vitro*. 5. SMC accumulation in the plaque was reduced *in vivo*. 6. Lab4/CUL66 supplementation attenuated *In vivo* expression of genes encoding proteins involved in the degradation of the protective fibrotic cap.

### 7.3.1 Plasma lipid modulation

The ability of probiotics to modulate plasma lipids is well documented in the literature with a high number of studies reporting significant beneficial lipid-modulating effects (Fortes *et al.*, 2018; Guo *et al.*, 2011; Han *et al.*, 2019; Mahboobi *et al.*, 2018; Sharma *et al.*, 2018). In a preliminary short-term feeding study carried out by Cultech Ltd, Lab4/CUL66 supplementation was shown to attenuate hypercholesterolaemia in C57BL/6J mice fed a HFD (Michael *et al.*, 2017). This study reported no change in plasma TC, LDL-C, HDL-C or triglycerides which is contrary to the findings of this project, likely due to differences in models used (C57BL/6J v/s LDLR<sup>-/-</sup>) and duration of HFD feeding (2 weeks v/s 12 weeks). However, it is notable that an increase in total and unconjugated bile acids was reported in the faeces of probiotic-fed mice, implicating BSH activity as a possible mechanism of cholesterol-lowering activity. Deconjugation of bile salts by probiotic BSH activity, together with the ability of probiotics to bind and to assimilate cholesterol in the intestine (Pereira and Gibson, 2002) are thought to largely contribute to their cholesterol-lowering capability (Kumar *et al.*, 2012). In the same study by Michael *et al.* (2017), the ability of Lab4 to hydrolyse bile salts, assimilate cholesterol and regulate cholesterol transport by polarised Caco-2 enterocytes was also demonstrated. It can therefore be suggested that supplementation with a combination of Lab4/CUL66 has the ability to lower plasma cholesterol levels and that this is achieved at least in part via assimilation of cholesterol in the intestine, and by deconjugation of bile acids due to probiotic BSH activity. The enterohepatic circulation (EHC) describes the movement of bile acid molecules from the liver to the intestine and back to the liver. The EHC functions to maintain a large pool of bile acids and under normal conditions, approximately 95% of bile acids are reabsorbed from the intestine and transported back to the liver, with only a small volume lost in the faeces (Cai and Chen, 2014). *De novo* synthesis of bile acids from cholesterol molecules compensates for this faecal loss. The BSH enzyme produced by many probiotic bacteria in the gut catalyses the deconjugation of bile acids, increasing the volume lost in faeces and therefore increasing *de novo* synthesis of bile acids from hepatic cholesterol in order to compensate (Tsai *et al.*, 2014). By this mechanism, probiotic BSH activity is thought to contribute to the cholesterol-lowering capability of probiotics including Lab4/CUL66 combination.



In addition to cholesterol assimilation and BSH activity of Lab4/CUL66 demonstrated previously, in the current study gene expression of apoB was significantly reduced in mice supplemented with Lab4/CUL66 compared to control (Table 6.2). As discussed in Chapter 1, apoB is an essential component of atherogenic cholesterol-rich lipoproteins which are considered a key causal agent in atherosclerosis disease (Shapiro and Fazio, 2017). ApoB-containing lipoproteins represent the primary source of cholesterol in atherosclerosis, particularly LDL, which is implicated as a key driver of the initiation and progression of atherosclerotic plaques (Tabas *et al.*, 2007). Since all atherogenic particles (VLDL, IDL, LDL) contain one apoB molecule, the level of apoB is a useful indicator of the number of atherogenic particles (Kumar *et al.*, 2012). In fact the direct link between plasma cholesterol, apoB-containing lipoproteins and atherosclerosis led to the discovery and development of statins (Shapiro and Fazio, 2017). Few studies have investigated the effect of probiotics on apoB levels; however, in one study BSH-active *L. reuteri* effectively lowered plasma apoB-100 in addition to LDL-C and TC in hypercholesterolaemic patients (Jones *et al.*, 2012). A recent study similarly reported a reduction in apoB, TC and LDL-C in low cardiovascular risk patients following 12 weeks supplementation with *B. longum* and red yeast rice extract (Ruscica *et al.*, 2019). In the current study, Lab4/CUL66 supplementation led to a reduction in apoB at the gene expression level. This result is indicative of an additional mechanism by which Lab4/CUL66 modulates plasma lipid levels and correlates with the observed decrease in apoB-containing lipoproteins in the plasma. However, for a firmer conclusion future work may include measurement of serum apoB where a reduction at the protein level would further support the cholesterol-lowering capability of this probiotic combination.

### 7.3.2 Foam cell formation

As discussed previously, disruption of normal homeostatic mechanisms governing macrophage cholesterol metabolism can result in the excessive uptake of modified lipoproteins, particularly oxLDL via macrophage scavenger receptors, together with decreased efflux of cholesterol and accumulation of intracellular cholesterol esters (Chistiakov *et al.*, 2017). Cholesterol esters are stored within cytoplasmic lipid droplets, which accumulate forming lipid-laden foam cells. Macrophage foam cells exhibit altered physiology, including reduced mobility and phagocytic activity in addition to increased

apoptotic cell death. The formation, accumulation and apoptosis of foam cells is a key driver of atherosclerosis progression and the discovery of novel agents capable of interrupting this process may be highly beneficial in atherosclerosis prevention or even regression. Despite the plethora of evidence supporting the lipid-modulating effect of probiotics, no previous studies were found that investigated the effect of probiotic supplementation on macrophage foam cell formation in atherosclerosis. Few studies have however reported probiotic-induced decrease in the expression of CD36 (Lee *et al.*, 2018) and ABCA1/ABCG1 (Wang *et al.*, 2010).

In the current study, *in vitro* investigations revealed that all of Lab4, Lab4b and CUL66 were capable of dramatically attenuating receptor-mediated uptake of oxLDL at the cellular level by a minimum of 50%, with a corresponding decrease in scavenger receptors SR-A and CD36 at the gene expression level (Figure 4.6-8). The correlation between SR-A/CD36 expression and the uptake of oxLDL is well established (Cruet *et al.*, 2013; Sun *et al.*, 2007), and the ability of Lab4/Lab4b/CUL66 to attenuate oxLDL uptake via attenuation of scavenger receptor expression represents a further likely anti-atherogenic mechanism. Lab4b also significantly reduced gene expression of LPL while Lab4 and CUL66 had no effect (Figure 4.8C), suggesting the presence of an additional strain specific mechanism related to the different *Lactobacillus* species present in the Lab4b consortium compared to Lab4. Furthermore, *in vitro* investigations also revealed a significant increase in cholesterol efflux from macrophage foam cells with Lab4, Lab4b or CUL66 treatment (Figure 4.10). Again for Lab4 and Lab4b this result at the cellular level was confounded by a correlating increase in the expression of efflux machinery, ABCA1 and ABCG1, in addition to increased expression of LXRs at the gene expression level (Figure 4.12). Interestingly, gene expression of these key molecules involved in cholesterol efflux was unchanged or even reduced with CUL66 treatment (Figure 4.12), suggesting that an alternative mechanism underlies the observed CUL66-induced increase in cholesterol efflux at the cellular level. For Lab4 and Lab4b consortia, these results suggest that their ability to increase the efflux of cholesterol from macrophage foam cells may be at least in part due to an increase in ABCA1 and ABCG1 expression, induced via the upregulation LXR- $\alpha$  and LXR- $\beta$  in response to intracellular cholesterol accumulation (Bobryshev *et al.*, 2016). In addition to cholesterol efflux, preliminary investigation of intracellular cholesterol metabolism suggested that all of Lab4, Lab4b

and particularly CUL66 had the ability to reduce cholesterol ester accumulation. However due to time constraints, this result is from a single experiment and further repeats are required before any firm conclusions can be made.

Although many studies were carried out *in vitro*, *in vivo* results were also supportive of a decrease in foam cell accumulation. Lab4/CUL66 supplementation resulted in a significantly lower plaque lipid content compared to control, as well as significantly reduced macrophage content and corresponding reduction in monocyte/macrophage populations within the bone marrow. Furthermore, analysis of gene expression showed a non-significant increase in ABCA1 expression (Table 6.1). Other key genes involved in the uptake, intracellular metabolism and efflux of cholesterol were not present in the Atherosclerosis RT<sup>2</sup> Profiler Arrays, therefore future work could include the investigation of, CD36, ABCG1 and LXR expression not only in the liver but also in samples of aorta obtained from *in vivo* studies.

Together, results from the current study highlight Lab4/Lab4b/CUL66 as potential foam cell-targeting agents capable of reducing or preventing their formation. Investigation of the underlying mechanisms have revealed probiotic-induced reduction of oxLDL uptake via a decrease in the expression of SR-A and CD36 scavenger receptors, as well as increased cholesterol efflux via LXR activation and subsequent increase in ABCA1/ABCG1 expression.

### 7.3.3 Monocyte recruitment

As previously discussed, monocyte recruitment in response to endothelial cell activation represents one of the earliest events in atherogenesis. A number of cytokines and cell adhesion molecules are involved in monocyte recruitment (MCP-1, TNF- $\alpha$ , M-CSF), adhesion to endothelial cells (E- and P-selectins, integrins, VCAM1 and ICAM1) and finally transmigration into the arterial intima (Gerhardt and Ley, 2015). Overall, results of the current study strongly indicate a role of probiotic supplementation in the attenuation of monocyte recruitment and adherence. At the cellular level, *In vitro* investigations demonstrated significant attenuation of MCP-1-induced monocyte migration in the presence of Lab4, Lab4b or CUL66, while gene expression of the MCP-1

receptor CCR2 was shown to be significantly decreased *in vivo* (Table 6.2). MCP-1 is a key chemoattractant involved in monocyte migration and studies in atherosclerosis mouse models deficient in MCP-1 or its receptor have demonstrated decreased subendothelial monocyte accumulation and protection against lesion development (Combadière *et al.*, 2008; Mestas and Ley, 2008; Raghu *et al.*, 2017). The ability of Lab4/Lab4b/CUL66 to attenuate MCP-1-induced monocyte migration via downregulation of CCR2 expression therefore indicates a further potential anti-atherosclerotic mechanism of probiotic treatment.

Analysis of gene expression in LDLr<sup>-/-</sup> mice supplemented with Lab4/CUL66 revealed significant changes in the expression of a number of genes encoding key proteins involved in monocyte recruitment and adhesion (Figure 6.6C). Lab4/CUL66 supplementation led to a significant reduction in the expression of cell adhesion molecules ICAM1 and E-selectin in addition to integrin subunit  $\beta$ 2, and a non-significant reduction in expression of VCAM1. All of ICAM1, VCAM1, selectins and integrins are expressed on the surface of activated endothelial cells in response to pro-inflammatory cytokines including TNF- $\alpha$  and IFN- $\gamma$  (Gerhardt and Ley, 2015), expression of which was also significantly reduced with Lab4/CUL66 supplementation. Given the positive correlation between reduced expression of cell adhesion molecules and attenuation of atherosclerosis (Collins *et al.*, 2000; Galkina and Ley, 2007), these results further support the role of Lab4/Lab4b/CUL66 in the reduction of monocyte recruitment and present a possible mechanism by which this effect is achieved.

#### 7.3.4 Additional mechanisms of action

Atherosclerosis is a chronic inflammatory disorder and as such inflammatory pathways are involved at every stage of atherosclerosis initiation and progression. Inflammation is therefore a popular target for atherosclerosis intervention and research into suitable anti-inflammatory agents has increased in recent decades (Fava and Montagnana, 2018). Probiotics have previously been identified as having immunomodulatory effects on inflammatory cytokine production (Djaldetti and Bessler, 2017), increased production of anti-atherogenic regulatory T cells (Karimi *et al.*, 2009) and suppression of pro-atherogenic T helper cells (Ding *et al.*, 2017). However, these effects are highly

strain-specific and some strains have been reported to promote the production of T helper cells and pro-inflammatory cytokines and/or suppress the production of anti-inflammatory cytokines (Ding *et al.*, 2017). Initial investigation of the anti-inflammatory potential of Lab4, Lab4b and CUL66 was carried out *in vitro* where probiotic treatment either had no effect on, or resulted in an increase in IFN- $\gamma$  or IL-1 $\beta$ -induced expression of MCP-1 and ICAM1 (Figure 3.27). TNF- $\alpha$ -induced expression of ICAM1, however, was reduced with all of Lab4, Lab4b and CUL66 treatment (Figure 3.27). Investigation of the effects of Lab4/CUL66 *in vivo* presented a more promising outcome with regards to anti-inflammatory actions. Gene expression analysis revealed a significant reduction in the expression of pro-inflammatory and pro-atherogenic cytokines IFN- $\gamma$ , TNF- $\alpha$  and IL-2 in the probiotic group compared to control (Figure 6.6A). Additionally, Lab4/CUL66 supplementation led to a significant reduction in T cell and macrophage populations in the bone marrow, as well as a significant decrease in macrophage content and a trend of reduction of T cell content of aortic plaques (Figure 5.13). Together, these results suggest that Lab4/Lab4b/CUL66 and combinations thereof possess immunomodulatory effects; however, inflammatory processes in atherosclerosis are highly complex and further research is required to determine more specific interactions.

A further mechanism by which probiotics may exert anti-atherogenic effects is by enhancing macrophage phagocytic activity. In atherosclerosis, phagocytosis becomes ineffective with an increasing burden of apoptotic cells and debris leading to the formation of a lipid-rich necrotic core characteristic of progressive atherosclerotic lesions (Tabas, 2009). Although previous studies have demonstrated an athero-protective effect of increased phagocytic activity (Laguna-Fernandez *et al.*, 2018), the effect of probiotics on macrophage phagocytic activity in the context of atherosclerosis has not been studied. In the current study, treatment with Lab4, Lab4b or CUL66 was shown to significantly enhance phagocytic activity of macrophages *in vitro* (Figure 3.18), presenting a possible mechanism by which Lab4/Lab4b/CUL66 treatment may enhance the clearance of apoptotic cells and debris and thereby reduce or delay necrotic core formation.

In advanced atherosclerosis, the balance between the generation and degradation of ECM molecules maintains the presence of a thick fibrous protective cap. When

degradation exceeds the generation of ECM proteins, the fibrous cap is compromised and the plaque becomes unstable and vulnerable to rupture, thrombus formation and subsequent clinical complications. ECM-degrading proteins, namely MMPs and serine proteases, are secreted primarily by macrophage foam cells and are strongly implicated in fibrous cap thinning (Magdalena *et al.*, 2006). In the current study, *in vivo* gene expression analysis revealed a significant reduction of MMP-1a and MMP-3 expression in the probiotic group compared to the control (Table 6.2). Previous studies have demonstrated that MMP deficiency, including that of MMP-3, is associated with increased plaque stability and attenuation of plaque progression (Beaudeau *et al.*, 2003; Brown *et al.*, 2017). It is therefore possible that Lab4/CUL66 supplementation exerts further anti-atherogenic effects via the modulation of the expression of ECM-degrading proteins and hence contributes to the maintenance of plaque stabilisation and improved prognosis.

#### 7.4 Further work and future perspectives

There are a number of further experiments that may provide data to compliment results from the current study, particularly with regards to additional analysis of stored tissues and faeces obtained from the *in vivo* investigation of Lab4/CUL66 supplementation in LDLr<sup>-/-</sup> mice. As Lab4 and CUL66 are known to exhibit BSH activity, it would be useful to assess the level of deconjugated bile acids in the faeces collected at study end. An increase in the presence of bile acids would be indicative of increased BSH activity, and further support the hypothesis that the observed cholesterol-reducing capability of Lab4/CUL66 is at least in part due to probiotic-induced *de novo* synthesis of bile acids from cholesterol. Furthermore, it would be very informative to obtain a measure of the levels of specific cytokines and proteins present in mouse plasma collected at study end. For example, measurement of plasma apoB levels may compliment the observed reduction in gene expression of *ApoB*, while plasma levels of pro-inflammatory cytokines such as IFN- $\gamma$ , TNF- $\alpha$  and IL-2, and anti-inflammatory cytokines such as IL-10 and TGF- $\beta$  will aid in further understanding of probiotic immunomodulatory effects. Additionally, immunophenotyping of bone marrow cell populations as carried out in the current study may be applied to plasma cell populations, providing further information on the effect of Lab4/CUL66 on circulating populations such as specific T cell and monocyte subtypes.

Future work could therefore include appropriate collection and processing of plasma at study end for the purpose immunophenotyping using flow cytometry.

A further protein of interest for future research is the transmembrane protein NPC1L1, expressed on enterocytes. NPC1L1 is an essential requirement for intestinal cholesterol absorption (Altmann *et al.*, 2004) and is the molecular target of cholesterol-lowering agent ezetimibe (Betters and Yu, 2010). It has been suggested that inhibition of both intestinal and hepatic NPC1L1 expression can promote excretion of biliary cholesterol, the final step in the RCT pathway (Betters and Yu, 2010). Furthermore, few studies have reported the ability of probiotics to inhibit cholesterol absorption via downregulation of NPC1L1 expression (Huang *et al.*, 2010, 2014). Deficiency of NPC1L1 has been shown to significantly reduce the absorption of cholesterol, promote resistance to diet-induced hypercholesterolaemia, and prevent atherosclerotic aortic lesion formation in apoE<sup>-/-</sup> mice (Davis *et al.*, 2007). Therefore, for the purpose of delineating mechanisms underlying the cholesterol-lowering effects of Lab4/CUL66, assessment of any changes in the expression of NPC1L1 both at the gene expression and protein levels may provide valuable insight.

The question of active components present in probiotic CM is an important one and although it is beyond the scope of this study, isolation of these active components could prove invaluable in future research and in disease intervention. During the production of probiotic CM, bacteria are pelleted and removed, and the resulting CM is treated with pen/strep and filter sterilised as described in Section 2.2. This limits possible components remaining in the media; however, bacterial metabolites such as short chain fatty acids (SCFAs), long chain fatty acids (LCFAs), biogenic amines, serpins and bacterial DNA all represent potential candidates. A number of studies have considered bacterial metabolites as active components (Engevik and Versalovic, 2017). For example, histamine produced by *L. reuteri* has been shown to inhibit TNF- $\alpha$  expression via modulation of the PKA/ERK pathway (Thomas *et al.*, 2012). Additionally,  $\gamma$ -aminobutyric acid (GABA) produced by certain probiotic bacteria, largely *Lactobacillus* strains, functions as an inhibitory neurotransmitter and mediates a range of effects on the host (Engevik and Versalovic, 2017). Many beneficial effects of GABA are related to the gut-brain axis where GABA has been shown to exert neuroprotective effects (Cho *et al.*,

2007); however, GABA has also been reported to reduce blood pressure in both animal and human studies (Engevik and Versalovic, 2017; Hayakawa *et al.*, 2004) indicating a possible cardio-protective role for this probiotic metabolite. Furthermore, cell-free bacterial DNA is known to exert immunomodulatory effects on the host, likely owing to the presence of 20-fold greater frequency of unmethylated CpG dinucleotides in microbial DNA (Krieg, 2002). It has been shown that DNA from probiotic bacteria can exert beneficial effects on the host where VSL#3 DNA has been shown to attenuate systemic release of TNF- $\alpha$  in mice in response to *Escherichia coli* DNA injection (Jijon *et al.*, 2004). A further study also showed VSL#3 DNA-induced anti-inflammatory effects in wild type mice and in addition demonstrated absence of such effects with DNase-treated probiotics (Rachmilewitz *et al.*, 2004). A more recent study investigated the effect of *L. plantarum* genomic DNA on LPS-induced inflammatory markers *in vitro*, demonstrating inhibition of LPS-induced TNF- $\alpha$  production accompanied by suppression of TLR2, TLR4 and TLR9 expression (Hee Kim *et al.*, 2012). The reported anti-inflammatory potential of probiotic DNA is encouraging; however, further research is required to gain understanding of these effects and strain-specific mechanisms of action.

In the current study, results obtained from *in vivo* investigation of Lab4/CUL66 supplementation in LDLR<sup>-/-</sup> mice highlighted this probiotic combination as a promising candidate for atherosclerosis intervention. Since Lab4, Lab4b and CUL66 are already included in current probiotic products available on the market, a logical next step is progression to clinical trials in the context of Lab4/CUL66 as an anti-atherosclerotic agent. It would be useful in the clinical setting to assess the effect of Lab4/CUL66 combination on TC, LDL-C, HDL-C, triglycerides, in addition to other major cardiovascular risk factors such as chronic inflammation and hypertension. Extended clinical studies would also provide insight into the effects of Lab4/CUL66 supplementation on atherosclerosis risk over a longer period where incidence of clinical outcomes can be monitored and reported. Furthermore, given the multifactorial nature of atherosclerosis aetiology and pathology, it can also be considered that probiotics may be administered in combination with additional nutraceuticals that exert anti-atherosclerotic effects via alternative mechanisms, such as antioxidant activity. As discussed in Chapter 1, hydroxytyrosol is associated with reduced cardiovascular risk owing in part due to its



high antioxidant capacity and subsequent ability to reduce oxidative stress (Colica *et al.*, 2017). This antioxidant activity in combination with the lipid and immunomodulatory effects of Lab4/CUL66 represents an even stronger candidate for atherosclerosis intervention. Furthermore, Lab4/CUL66 may be considered in combination with statin therapy. Lab4/CUL66 has demonstrated the ability to reduce cholesterol levels through decreased intestinal absorption, and by depletion of cholesterol stores as a result of increased synthesis of bile acids due to BSH activity. Lab4/CUL66 supplementation has also shown the ability to reduce apoB at the gene expression level (Figure 6.6). This ability of Lab4/CUL66 to reduce cholesterol levels by alternative mechanisms may be of particular benefit for the subset of high risk patients that are unable to achieve target cholesterol levels with HMG CoA inhibitors alone; where the cholesterol-reducing ability of Lab4/CUL66 in combination with inhibition of *de novo* cholesterol synthesis could provide an exceptionally high level of cholesterol reduction, finally achieving target levels in these patients. The effects of probiotic versus statin treatment have been compared (Cavallini *et al.*, 2009), but have not previously been investigated as a novel combination for the management of cardiovascular risk.

## 7.5 Conclusions

The current study aimed to investigate the anti-atherosclerotic effects of Lab4, Lab4b and CUL66, and to delineate possible mechanisms underlying these effects. *In vivo* investigation of a Lab4/CUL66 combination demonstrated a significant 39% reduction in plaque formation in the probiotic group compared to control. Analysis of plasma lipids revealed a reduction in LDL-C with a corresponding increase in HDL-C compared to control, demonstrating probiotic lipid-modulating capability. Results from previous *in vivo* and *in vitro* investigations suggest that the observed cholesterol-lowering effects of Lab4 and CUL66 may be attributed to probiotic BSH activity and reduced intestinal absorption of cholesterol. Further to lipid-modulating capability, the current study demonstrated the ability of Lab4, Lab4b, CUL66 and a Lab4/CUL66 combination to exert beneficial effects on a number of key processes in atherosclerosis development including inflammatory responses, monocyte migration and macrophage foam cell formation, which was further supported by results from investigation of the underlying mechanisms.

Together, results from the current study highlight Lab4, Lab4b, CUL66 or combinations of these consortia as promising candidates for atherosclerosis intervention. Furthermore, these probiotic consortia may also be considered in combination with additional nutraceuticals or even statins for more effective atherosclerosis intervention in a wider patient group. Additional clinical trials of Lab4/CUL66 are required in the context of atherosclerosis; however, due to the lack of adverse side effects, in addition to the relatively low cost compared to traditional pharmaceutical agents, this work supports the potential for world-wide application of probiotics as part of ongoing atherosclerotic CVD prevention and management strategies.

**Appendix 1 - Full list of genes included in the RT<sup>2</sup> Atherosclerosis Array**

<b>Symbol</b>	<b>GenBank ID</b>	<b>Description</b>
<i>Abca1</i>	NM_013454	ATP-binding cassette, sub-family A (ABC1), member 1
<i>Ace</i>	NM_009598	Angiotensin I converting enzyme (peptidyl-dipeptidase A) 1
<i>Apoa1</i>	NM_009692	Apolipoprotein A-I
<i>Apob</i>	NM_009693	Apolipoprotein B
<i>Apoe</i>	NM_009696	Apolipoprotein E
<i>Bax</i>	NM_007527	Bcl2-associated X protein
<i>Bcl2</i>	NM_009741	B-cell leukemia/lymphoma 2
<i>Bcl2a1a</i>	NM_009742	B-cell leukemia/lymphoma 2 related protein A1a
<i>Bcl2l1</i>	NM_009743	Bcl2-like 1
<i>Bid</i>	NM_007544	BH3 interacting domain death agonist
<i>Birc3</i>	NM_007464	Baculoviral IAP repeat-containing 3
<i>Ccl2</i>	NM_011333	Chemokine (C-C motif) ligand 2
<i>Ccl5</i>	NM_013653	Chemokine (C-C motif) ligand 5
<i>Ccr1</i>	NM_009912	Chemokine (C-C motif) receptor 1
<i>Ccr2</i>	NM_009915	Chemokine (C-C motif) receptor 2
<i>Cd44</i>	NM_009851	CD44 antigen
<i>Cdh5</i>	NM_009868	Cadherin 5
<i>Cflar</i>	NM_009805	CASP8 and FADD-like apoptosis regulator
<i>Col3a1</i>	NM_009930	Collagen, type III, alpha 1
<i>Csf2</i>	NM_009969	Colony stimulating factor 2 (granulocyte-macrophage)
<i>Ctgf</i>	NM_010217	Connective tissue growth factor
<i>Cxcl1</i>	NM_008176	Chemokine (C-X-C motif) ligand 1
<i>Eln</i>	NM_007925	Elastin
<i>Eng</i>	NM_007932	Endoglin
<i>Fabp3</i>	NM_010174	Fatty acid binding protein 3, muscle and heart
<i>Fas</i>	NM_007987	Fas (TNF receptor superfamily member 6)
<i>Fga</i>	NM_010196	Fibrinogen alpha chain
<i>Fgb</i>	NM_181849	Fibrinogen beta chain
<i>Fgf2</i>	NM_008006	Fibroblast growth factor 2
<i>Fn1</i>	NM_010233	Fibronectin 1
<i>Hbegf</i>	NM_010415	Heparin-binding EGF-like growth factor
<i>Icam1</i>	NM_010493	Intercellular adhesion molecule 1
<i>Ifng</i>	NM_008337	Interferon gamma
<i>Il1a</i>	NM_010554	Interleukin 1 alpha
<i>Il1b</i>	NM_008361	Interleukin 1 beta
<i>Il1r1</i>	NM_008362	Interleukin 1 receptor, type I
<i>Il1r2</i>	NM_010555	Interleukin 1 receptor, type II

## APPENDIX

<b>Symbol</b>	<b>GenBank ID</b>	<b>Description</b>
<i>Il2</i>	NM_008366	Interleukin 2
<i>Il3</i>	NM_010556	Interleukin 3
<i>Il4</i>	NM_021283	Interleukin 4
<i>Il5</i>	NM_010558	Interleukin 5
<i>Itga2</i>	NM_008396	Integrin alpha 2
<i>Itga5</i>	NM_010577	Integrin alpha 5 (fibronectin receptor alpha)
<i>Itgax</i>	NM_021334	Integrin alpha X
<i>Itgb2</i>	NM_008404	Integrin beta 2
<i>Kdr</i>	NM_010612	Kinase insert domain protein receptor
<i>Klf2</i>	NM_008452	Kruppel-like factor 2 (lung)
<i>Lama1</i>	NM_008480	Laminin, alpha 1
<i>Ldlr</i>	NM_010700	Low density lipoprotein receptor
<i>Lif</i>	NM_008501	Leukemia inhibitory factor
<i>Lpl</i>	NM_008509	Lipoprotein lipase
<i>Lypla1</i>	NM_008866	Lysophospholipase 1
<i>Mmp1a</i>	NM_032006	Matrix metalloproteinase 1a (interstitial collagenase)
<i>Mmp3</i>	NM_010809	Matrix metalloproteinase 3
<i>Msr1</i>	NM_031195	Macrophage scavenger receptor 1
<i>Nfkb1</i>	NM_008689	Nuclear factor of kappa light polypeptide gene enhancer in B-cells 1, p105
<i>Npy</i>	NM_023456	Neuropeptide Y
<i>Nr1h3</i>	NM_013839	Nuclear receptor subfamily 1, group H, member 3
<i>Pdgfa</i>	NM_008808	Platelet derived growth factor, alpha
<i>Pdgfb</i>	NM_011057	Platelet derived growth factor, B polypeptide
<i>Pdgfrb</i>	NM_008809	Platelet derived growth factor receptor, beta polypeptide
<i>Plin2</i>	NM_007408	Perilipin 2
<i>Ppara</i>	NM_011144	Peroxisome proliferator activated receptor alpha
<i>Ppard</i>	NM_011145	Peroxisome proliferator activator receptor delta
<i>Pparg</i>	NM_011146	Peroxisome proliferator activated receptor gamma
<i>Ptgs1</i>	NM_008969	Prostaglandin-endoperoxide synthase 1
<i>Rxra</i>	NM_011305	Retinoid X receptor alpha
<i>Sele</i>	NM_011345	Selectin, endothelial cell
<i>Sell</i>	NM_011346	Selectin, lymphocyte
<i>Selp</i>	NM_011347	Selectin, platelet
<i>Selplg</i>	NM_009151	Selectin, platelet (p-selectin) ligand
<i>Serpib2</i>	NM_011111	Serine (or cysteine) peptidase inhibitor, clade B, member 2
<i>Serpine1</i>	NM_008871	Serine (or cysteine) peptidase inhibitor, clade E, member 1
<i>Sod1</i>	NM_011434	Superoxide dismutase 1, soluble
<i>Spp1</i>	NM_009263	Secreted phosphoprotein 1
<i>Tgfb1</i>	NM_011577	Transforming growth factor, beta 1
<i>Tgfb2</i>	NM_009367	Transforming growth factor, beta 2

## APPENDIX

<b>Symbol</b>	<b>GenBank ID</b>	<b>Description</b>
<i>Thbs4</i>	NM_011582	Thrombospondin 4
<i>Tnc</i>	NM_011607	Tenascin C
<i>Tnf</i>	NM_013693	Tumor necrosis factor
<i>Tnfaip3</i>	NM_009397	Tumor necrosis factor, alpha-induced protein 3
<i>Vcam1</i>	NM_011693	Vascular cell adhesion molecule 1
<i>Vegfa</i>	NM_009505	Vascular endothelial growth factor A
<i>Vwf</i>	NM_011708	Von Willebrand factor homolog

## REFERENCES

- Adorni, M. P., Cipollari, E., Favari, E., Zanotti, I., Zimetti, F., Corsini, A., Ricci, C., Bernini, F. and Ferri, N. (2017) Inhibitory effect of PCSK9 on Abca1 protein expression and cholesterol efflux in macrophages. *Atherosclerosis*. 256, pp. 1–6.
- Adorno-Cruz, V. and Liu, H. (2019) Regulation and functions of integrin  $\alpha 2$  in cell adhesion and disease. *Genes and Diseases*. 6 (1), pp. 16–24.
- Agilent Technologies (2019) Seahorse XF Cell Mito Stress Test Kit User Guide. Available from: [https://www.agilent.com/cs/library/usermanuals/public/XF\\_Cell\\_Mito\\_Stress\\_Test\\_Kit\\_User\\_Guide.pdf](https://www.agilent.com/cs/library/usermanuals/public/XF_Cell_Mito_Stress_Test_Kit_User_Guide.pdf) [Accessed 2 June 2019].
- Ahn, H. Y., Kim, M., Chae, J. S., Ahn, Y.-T., Sim, J.-H., Choi, I.-D., Lee, S.-H. and Lee, J. H. (2015) Supplementation with two probiotic strains, *Lactobacillus curvatus* HY7601 and *Lactobacillus plantarum* KY1032, reduces fasting triglycerides and enhances apolipoprotein A-V levels in non-diabetic subjects with hypertriglyceridemia. *Atherosclerosis*. 241 (2), pp. 649–56.
- Aiello, R. J., Bourassa, P.-A. K., Lindsey, S., Weng, W., Natoli, E., Rollins, B. J. and Milos, P. M. (1999) Monocyte chemoattractant protein-1 accelerates atherosclerosis in apolipoprotein e-deficient mice. *Arteriosclerosis, Thrombosis, and Vascular Biology*. 19 (6), pp. 1518–1525.
- Alexander, M. R., Moehle, C. W., Johnson, J. L., Yang, Z., Lee, J. K., Jackson, C. L. and Owens, G. K. (2012) Genetic inactivation of IL-1 signaling enhances atherosclerotic plaque instability and reduces outward vessel remodeling in advanced atherosclerosis in mice. *Journal of Clinical Investigation*. 122 (1), pp. 70–79.
- Allen, S. J., Jordan, S., Storey, M., Thornton, C. A., Gravenor, M. B., Garaiova, I., Plummer, S. F., Wang, D. and Morgan, G. (2014) Probiotics in the prevention of eczema: a randomised controlled trial. *Archives of Disease in Childhood*. 99 (11), pp. 1014–1019.
- Allen, S. J., Jordan, S., Storey, M., Thornton, C. A., Gravenor, M., Garaiova, I., Plummer, S. F., Wang, D. and Morgan, G. (2010) Dietary supplementation with *Lactobacilli* and *Bifidobacteria* is well tolerated and not associated with adverse events during late pregnancy and early infancy. *The Journal of Nutrition*. 140 (3), pp. 483–488.
- Altmann, S. W., Davis, H. R., Zhu, L.-J., Yao, X., Hoos, L. M., Tetzloff, G., *et al.* (2004) Niemann-pick C1 like 1 protein is critical for intestinal cholesterol absorption. *Science*. 303 (5661), pp.

## REFERENCES

1201–1204.

Amarowicz, R. and Pegg, R. B. (2017) The potential protective effects of phenolic compounds against low-density lipoprotein oxidation. *Current Pharmaceutical Design*. 23 (19), pp. 2754–2766.

Antonopoulos, A. S., Margaritis, M., Lee, R., Channon, K. and Antoniades, C. (2012) Statins as anti-inflammatory agents in atherogenesis: molecular mechanisms and lessons from the recent clinical trials. *Current Pharmaceutical Design*. 18 (11), pp. 1519–30.

Aparna Sudhakaran, V., Panwar, H., Chauhan, R., Duary, R. K., Rathore, R. K., Batish, V. K. and Grover, S. (2013) Modulation of anti-inflammatory response in lipopolysaccharide stimulated human THP-1 cell line and mouse model at gene expression level with indigenous putative probiotic lactobacilli. *Genes and Nutrition*. 8 (6), pp. 637–648.

Araya, M., Morelli, L., Reid, G., Sanders, M.E., Stanton, C., Pineiro, M. and Ben Embarek, P. (2002). Guidelines for the evaluation of probiotics in food. *Report of a Joint FAO/WHO working group on drafting guidelines for the evaluation of probiotics in food, London, Ontario, Canada*.

Averna, M., Cefalù, A. B., Casula, M., Noto, D., Arca, M., Bertolini, S., *et al.* (2017) Familial hypercholesterolemia: The Italian Atherosclerosis Society Network (LIPIGEN). *Atherosclerosis Supplements*. 29, pp. 11–16.

Babaev, V. R., Huang, J., Ding, L., Zhang, Y., May, J. M. and Linton, M. F. (2018) Loss of rictor in monocyte/macrophages suppresses their proliferation and viability reducing atherosclerosis in LDLR null mice. *Frontiers in Immunology*. 9, pp. 215.

Bai, L., Li, Z., Li, Q., Guan, H., Zhao, S., Liu, R., *et al.* (2017) Mediator 1 is atherosclerosis protective by regulating macrophage polarization. *Arteriosclerosis, Thrombosis, and Vascular Biology*. 37 (8), pp. 1470–1481.

Bajaj, J. S. and Hays, R. A. (2019) Manipulation of the gut-liver axis using microbiome restoration therapy in primary sclerosing cholangitis. *The American Journal of Gastroenterology*. (1).

Baker, R. G., Hayden, M. S. and Ghosh, S. (2011) NF- $\kappa$ B, inflammation, and metabolic disease.

## REFERENCES

*Cell Metabolism*. 13 (1), pp. 11–22.

Bandeali, S. and Farmer, J. (2012) High-density lipoprotein and atherosclerosis: the role of antioxidant activity. *Current Atherosclerosis Reports*. 14 (2), pp. 101–107.

Bao, L., Qi, J., Wang, Y., Xi, Q., Tserennadmid, T., Zhao, P., Qi, J. and Damirin, A. (2018) The atherogenic actions of LPC on vascular smooth muscle cells and its LPA receptor mediated mechanism. *Biochemical and Biophysical Research Communications*. 503 (3), pp. 1911–1918.

Bayat, A., Azizi-Soleiman, F., Heidari-Beni, M., Feizi, A., Iraj, B., Ghiasvand, R. and Askari, G. (2016) Effect of cucurbita ficifolia and probiotic yogurt consumption on blood glucose, lipid profile, and inflammatory marker in type 2 diabetes. *International Journal of Preventive Medicine*. 7, pp. 30.

Beaudeau, J.-L., Giral, P., Bruckert, E., Bernard, M., Foglietti, M.-J. and Chapman, M. J. (2003) Serum matrix metalloproteinase-3 and tissue inhibitor of metalloproteinases-1 as potential markers of carotid atherosclerosis in infraclinical hyperlipidemia. *Atherosclerosis*. 169 (1), pp. 139–46.

Bennett, B. J., Vallim, T. Q. de A., Wang, Z., Shih, D. M., Meng, Y., Gregory, J., *et al.* (2013) Trimethylamine-N-Oxide, a metabolite associated with atherosclerosis, exhibits complex genetic and dietary regulation. *Cell Metabolism*. 17 (1), pp. 49–60.

Bernini, L. J., Simão, A. N. C., Alfieri, D. F., Lozovoy, M. A. B., Mari, N. L., de Souza, C. H. B., Dichi, I. and Costa, G. N. (2016) Beneficial effects of *Bifidobacterium lactis* on lipid profile and cytokines in patients with metabolic syndrome: A randomized trial. Effects of probiotics on metabolic syndrome. *Nutrition*. 32 (6), pp. 716–719.

Bertrand, M.-J. and Tardif, J.-C. (2017) Inflammation and beyond: new directions and emerging drugs for treating atherosclerosis. *Expert Opinion on Emerging Drugs*. 22 (1), pp. 1–26.

Bettters, J. L. and Yu, L. (2010) NPC1L1 and Cholesterol Transport. *FEBS Letters*. 584 (13), pp. 2740.

Bhaskar, V., Yin, J., Mirza, A. M., Phan, D., Vanegas, S., Issafras, H., Michelson, K., Hunter, J. J. and Kantak, S. S. (2011) Monoclonal antibodies targeting IL-1 beta reduce biomarkers of



## REFERENCES

atherosclerosis in vitro and inhibit atherosclerotic plaque formation in Apolipoprotein E-deficient mice. *Atherosclerosis*. 216 (2), pp. 313–320.

Bhatt, D. L. (2019) REDUCE-IT: Residual cardiovascular risk in statin-treated patients with elevated triglycerides: Now we can REDUCE-IT. *European Heart Journal*. 40 (15), pp. 1174–1175.

BHF (2018) Heart statistics - Heart and Circulatory Diseases in the UK - BHF. Available from: <https://www.bhf.org.uk/what-we-do/our-research/heart-statistics> [Accessed 19 April 2019].

Binder, C. J., Hörkkö, S., Dewan, A., Chang, M.-K., Kieu, E. P., Goodyear, C. S., *et al.* (2003) Pneumococcal vaccination decreases atherosclerotic lesion formation: molecular mimicry between *Streptococcus pneumoniae* and oxidized LDL. *Nature Medicine*. 9 (6), pp. 736–743.

Bjerg, A. T., Sørensen, M. B., Krych, L., Hansen, L. H., Astrup, A., Kristensen, M. and Nielsen, D. S. (2015) The effect of *Lactobacillus paracasei* subsp. *paracasei* L. casei W8® on blood levels of triacylglycerol is independent of colonisation. *Beneficial Microbes*. 6 (3), pp. 263–269.

Bobryshev, Y. V, Ivanova, E. A., Chistiakov, D. A., Nikiforov, N. G. and Orekhov, A. N. (2016) Macrophages and their role in atherosclerosis: Pathophysiology and transcriptome analysis. *BioMed Research International*. 2016, pp. 9582430.

Boehme, B., Schelski, N., Makridakis, M., Henze, L., Vlahou, A., Lang, F., Pieske, B., Alesutan, I. and Voelkl, J. (2018) Role of Cytosolic Serine Hydroxymethyl Transferase 1 (SHMT1) in phosphate-induced vascular smooth muscle cell calcification. *Kidney and Blood Pressure Research*. 43 (4), pp. 1212–1221.

Bohula, E. A., Wiviott, S. D., Giugliano, R. P., Blazing, M. A., Park, J.-G., Murphy, S. A., *et al.* (2017) Prevention of stroke with the addition of ezetimibe to statin therapy in patients with acute coronary syndrome in IMPROVE-IT (Improved Reduction of Outcomes: Vytorin Efficacy International Trial). *Circulation*. 136 (25), pp. 2440–2450.

Borges, N. A., Stenvinkel, P., Bergman, P., Qureshi, A. R., Lindholm, B., Moraes, C., Stockler-Pinto, M. B. and Mafra, D. (2018) Effects of probiotic supplementation on trimethylamine-n-oxide plasma levels in hemodialysis patients: a pilot study. *Probiotics and Antimicrobial Proteins*. 11 (2), pp. 648–654.

## REFERENCES

- Boring, L., Gosling, J., Cleary, M. and Charo, I. F. (1998) Decreased lesion formation in CCR2<sup>-/-</sup> mice reveals a role for chemokines in the initiation of atherosclerosis. *Nature*. 394 (6696), pp. 894–897.
- Brånén, L., Hovgaard, L., Nitulescu, M., Bengtsson, E., Nilsson, J. and Jovinge, S. (2004) Inhibition of tumor necrosis factor- $\alpha$  reduces atherosclerosis in Apolipoprotein E knockout mice. *Arteriosclerosis, Thrombosis, and Vascular Biology*. 24 (11), pp. 2137–2142.
- Braunersreuther, V., Zerneck, A., Arnaud, C., Liehn, E. A., Steffens, S., Shagdarsuren, E., *et al.* (2007) Ccr5 but not ccr1 deficiency reduces development of diet-induced atherosclerosis in mice. *Arteriosclerosis, Thrombosis, and Vascular Biology*. 27 (2), pp. 373–379.
- Brown, B. A., Williams, H. and George, S. J. (2017) Evidence for the involvement of Matrix-Degrading Metalloproteinases (MMPs) in atherosclerosis, in: *Progress in Molecular Biology and Translational Science*. 147, pp. 197–237.
- Brown, X. Q., Bartolak-Suki, E., Williams, C., Walker, M. L., Weaver, V. M. and Wong, J. Y. (2010) Effect of substrate stiffness and PDGF on the behavior of vascular smooth muscle cells: Implications for atherosclerosis. *Journal of Cellular Physiology*. 225 (1), pp. 115–122.
- Bu, J. and Wang, Z. (2018) Cross-talk between gut microbiota and heart via the routes of metabolite and immunity. *Gastroenterology Research and Practice*. 2018, pp. 1–8.
- Bubnov, R. V., Babenko, L. P., Lazarenko, L. M., Mokrozub, V. V., Demchenko, O. A., Nechypurenko, O. V. and Spivak, M. Y. (2017) Comparative study of probiotic effects of Lactobacillus and Bifidobacteria strains on cholesterol levels, liver morphology and the gut microbiota in obese mice. *EPMA Journal*. 8 (4), pp. 357–376.
- Cai, J.-S. and Chen, J.-H. (2014) The mechanism of enterohepatic circulation in the formation of gallstone disease. *The Journal of Membrane Biology*. 247 (11), pp. 1067–82.
- Caligiuri, G., Nicoletti, A., Poirier, B. and Hansson, G. K. (2002) Protective immunity against atherosclerosis carried by B cells of hypercholesterolemic mice. *The Journal of Clinical Investigation*. 109 (6), pp. 745–53.
- Camaré, C., Pucelle, M., Nègre-Salvayre, A. and Salvayre, R. (2017) Angiogenesis in the

## REFERENCES

atherosclerotic plaque. *Redox Biology*. 12, pp. 18–34.

Cambeiro-Pérez, N., Hidalgo-Cantabrana, C., Moro-García, M. A., Alonso-Arias, R., Simal-Gándara, J., Sánchez, B. and Martínez-Carballo, E. (2018) A metabolomics approach reveals immunomodulatory effects of proteinaceous molecules derived from gut bacteria over human peripheral blood mononuclear cells. *Frontiers in Microbiology*. 9, pp. 2701.

Cannon, C. P., Blazing, M. A., Giugliano, R. P., McCagg, A., White, J. A., Theroux, P., *et al.* (2015) Ezetimibe added to statin therapy after acute coronary syndromes. *New England Journal of Medicine*. 372 (25), pp. 2387–2397.

Cavallini, D. C. U., Bedani, R., Bomdespacho, L. Q., Vendramini, R. C. and Rossi, E. a (2009) Effects of probiotic bacteria, isoflavones and simvastatin on lipid profile and atherosclerosis in cholesterol-fed rabbits: a randomized double-blind study. *Lipids in Health and Disease*. 8, pp. 1.

Chan, Y. K. (2012) *Modulation of atherosclerosis by probiotic bacteria VSL#3 and LGG in ApoE<sup>-/-</sup> mice*. University of Hong Kong.

Chan, Y. K., Brar, M. S., Kirjavainen, P. V, Chen, Y., Peng, J., Li, D., Leung, F. C.-C. and El-Nezami, H. (2016a) High fat diet induced atherosclerosis is accompanied with low colonic bacterial diversity and altered abundances that correlates with plaque size, plasma A-FABP and cholesterol: a pilot study of high fat diet and its intervention with *Lactobacillus rhamno*. *BMC Microbiology*. 16 (1), pp. 264.

Chan, Y. K., El-Nezami, H., Chen, Y., Kinnunen, K. and Kirjavainen, P. V (2016b) Probiotic mixture VSL#3 reduce high fat diet induced vascular inflammation and atherosclerosis in ApoE(-/-) mice. *AMB Express*. 6 (1), pp. 61.

Chanput, W., Mes, J. J. and Wichers, H. J. (2014) THP-1 cell line: An in vitro cell model for immune modulation approach. *International Immunopharmacology*. 23 (1), pp. 37–45.

Chen, C., Yan, Y. and Liu, X. (2018) microRNA-612 is downregulated by platelet-derived growth factor-BB treatment and has inhibitory effects on vascular smooth muscle cell proliferation and migration via directly targeting AKT2. *Experimental and Therapeutic Medicine*. 15 (1), pp. 159–165.

## REFERENCES

- Chen, L., Liu, W., Li, Y., Luo, S., Liu, Q., Zhong, Y., Jian, Z. and Bao, M. (2013) Lactobacillus acidophilus ATCC 4356 attenuates the atherosclerotic progression through modulation of oxidative stress and inflammatory process. *International Immunopharmacology*. 17 (1), pp. 108–115.
- Chen, M.-F., Weng, K.-F., Huang, S.-Y., Liu, Y.-C., Tseng, S.-N., Ojcius, D. M. and Shih, S.-R. (2017) Pretreatment with a heat-killed probiotic modulates monocyte chemoattractant protein-1 and reduces the pathogenicity of influenza and enterovirus 71 infections. *Mucosal Immunology*. 10 (1), pp. 215–227.
- Chistiakov, D. A., Bobryshev, Y. V and Orekhov, A. N. (2016) Macrophage-mediated cholesterol handling in atherosclerosis. *Journal of Cellular and Molecular Medicine*. 20 (1), pp. 17–28.
- Chistiakov, D. A., Melnichenko, A. A., Myasoedova, V. A., Grechko, A. V. and Orekhov, A. N. (2017) Mechanisms of foam cell formation in atherosclerosis. *Journal of Molecular Medicine*. 95 (11), pp. 1153–1165.
- Cho, Y. A. and Kim, J. (2015) Effect of probiotics on blood lipid concentrations: a meta-analysis of randomized controlled trials. *Medicine*. 94 (43), pp. e1714.
- Cho, Y. R., Chang, J. Y. and Chang, H. C. (2007) Production of gamma-aminobutyric acid (GABA) by Lactobacillus buchneri isolated from kimchi and its neuroprotective effect on neuronal cells. *Journal of Microbiology and Biotechnology*. 17 (1), pp. 104–9.
- Choi, S.-H., Sviridov, D. and Miller, Y. I. (2017) Oxidized cholesteryl esters and inflammation. *Biochimica et Biophysica Acta (BBA) - Molecular and Cell Biology of Lipids*. 1862 (4), pp. 393–397.
- Chou, M.-Y., Hartvigsen, K., Hansen, L. F., Fogelstrand, L., Shaw, P. X., Boullier, A., Binder, C. J. and Witztum, J. L. (2008) Oxidation-specific epitopes are important targets of innate immunity. *Journal of Internal Medicine*. 263 (5), pp. 479–88.
- Colica, C., Di Renzo, L., Trombetta, D., Smeriglio, A., Bernardini, S., Cioccoloni, G., *et al.* (2017) Antioxidant effects of a hydroxytyrosol-based pharmaceutical formulation on body composition, metabolic state, and gene expression: a randomized double-blinded, placebo-controlled crossover trial. *Oxidative Medicine and Cellular Longevity*. 2017, pp. 2473495.

## REFERENCES

- Colin, S., Chinetti-Gbaguidi, G. and Staels, B. (2014) Macrophage phenotypes in atherosclerosis. *Immunological Reviews*. 262 (1), pp. 153–166.
- Collins, R. G., Velji, R., Guevara, N. V, Hicks, M. J., Chan, L. and Beaudet, A. L. (2000) P-Selectin or intercellular adhesion molecule (ICAM)-1 deficiency substantially protects against atherosclerosis in apolipoprotein E-deficient mice. *The Journal of Experimental Medicine*. 191 (1), pp. 189–94.
- Combadière, C., Potteaux, S., Rodero, M., Simon, T., Pezard, A., Esposito, B., *et al.* (2008) Combined inhibition of CCL2, CX3CR1, and CCR5 abrogates Ly6C<sup>hi</sup> and Ly6C<sup>lo</sup> monocytosis and almost abolishes atherosclerosis in hypercholesterolemic mice. *Circulation*. 117 (13), pp. 1649–1657.
- Corthésy, B., Gaskins, H. R. and Mercenier, A. (2007) Cross-talk between probiotic bacteria and the host immune system. *The Journal of Nutrition*. 137 (3), pp. 781S–790S.
- Costabile, A., Buttarazzi, I., Kolida, S., Quercia, S., Baldini, J., Swann, J. R., Brigidi, P. and Gibson, G. R. (2017) An in vivo assessment of the cholesterol-lowering efficacy of *Lactobacillus plantarum* ECGC 13110402 in normal to mildly hypercholesterolaemic adults. *PLoS One*. 12 (12), pp. e0187964.
- Crowther, M. A. (2005) Pathogenesis of atherosclerosis. *Hematology. American Society of Hematology. Education Program*. 2005 (1), pp. 436–41.
- Crucet, M., Wüst, S. J. A., Spielmann, P., Lüscher, T. F., Wenger, R. H. and Matter, C. M. (2013) Hypoxia enhances lipid uptake in macrophages: Role of the scavenger receptors Lox1, SRA, and CD36. *Atherosclerosis*. 229 (1), pp. 110–117.
- Dang, A. T. and Marsland, B. J. (2019) Microbes, metabolites, and the gut–lung axis. *Mucosal Immunology*.
- Davies, T. S., Plummer, S. F., Jack, A. A., Allen, M. D. and Michael, D. R. (2018) *Lactobacillus* and bifidobacterium promote antibacterial and antiviral immune response in human macrophages. *Journal of Probiotics & Health*. 06 (01), pp. 1–7.
- Davis, H. R., Hoos, L. M., Tetzloff, G., Maguire, M., Zhu, L., Graziano, M. P. and Altmann, S. W.

## REFERENCES

- (2007) Deficiency of Niemann-Pick C1 Like 1 prevents atherosclerosis in ApoE<sup>-/-</sup> mice. *Arteriosclerosis, Thrombosis, and Vascular Biology*. 27 (4), pp. 841–849.
- Dawson, T. C., Kuziel, W. A., Osahar, T. A. and Maeda, N. (1999) Absence of CC chemokine receptor-2 reduces atherosclerosis in apolipoprotein E-deficient mice. *Atherosclerosis*. 143 (1), pp. 205–11.
- De Melo Pereira, G. V., de Oliveira Coelho, B., Magalhães Júnior, A. I., Thomaz-Soccol, V. and Soccol, C. R. (2018) How to select a probiotic? A review and update of methods and criteria. *Biotechnology Advances*. 36 (8), pp. 2060–2076.
- De Meyer, I., Martinet, W. and De Meyer, G. R. Y. (2012) Therapeutic strategies to deplete macrophages in atherosclerotic plaques. *British Journal of Clinical Pharmacology*. 74 (2), pp. 246–63.
- Deng, H., Li, Z., Tan, Y., Guo, Z., Liu, Y., Wang, Y., *et al.* (2016) A novel strain of *Bacteroides fragilis* enhances phagocytosis and polarises M1 macrophages. *Scientific Reports*. 6 (1), pp. 29401.
- Denny, J. E., Powers, J. B., Castro, H. F., Zhang, J., Joshi-Barve, S., Campagna, S. R. and Schmidt, N. W. (2019) Differential sensitivity to plasmodium yoelii infection in C57BL/6 mice impacts gut-liver axis homeostasis. *Scientific Reports*. 9 (1), pp. 3472.
- Deshmane, S. L., Kremlev, S., Amini, S. and Sawaya, B. E. (2009) Monocyte chemoattractant protein-1 (MCP-1): an overview. *Journal of Interferon and Cytokine Research*. 29 (6), pp. 313–26.
- Dhingra, S. and Bansal, M. P. (2005) Hypercholesterolemia and apolipoprotein B expression: Regulation by selenium status. *Lipids in Health and Disease*. 4 (1), pp. 28.
- Di Pietro, N., Formoso, G. and Pandolfi, A. (2016) Physiology and pathophysiology of oxLDL uptake by vascular wall cells in atherosclerosis. *Vascular Pharmacology*. 84, pp. 1–7.
- Diez-Juan, A., Pérez, P., Aracil, M., Sancho, D., Bernad, A., Sánchez-Madrid, F. and Andrés, V. (2004) Selective inactivation of p27Kip1 in hematopoietic progenitor cells increases neointimal macrophage proliferation and accelerates atherosclerosis. *Blood*. 103 (1), pp. 158–161.

## REFERENCES

- Dinan, T. G. and Cryan, J. F. (2017) Brain–gut–microbiota axis — mood, metabolism and behaviour. *Nature Reviews Gastroenterology & Hepatology*. 14 (2), pp. 69–70.
- Ding, Y.-H., Qian, L.-Y., Pang, J., Lin, J.-Y., Xu, Q., Wang, L.-H., Huang, D.-S. and Zou, H. (2017) The regulation of immune cells by Lactobacilli: a potential therapeutic target for anti-atherosclerosis therapy. *Oncotarget*. 8 (35), pp. 59915–59928.
- Djaldetti, M. and Bessler, H. (2017) Probiotic strains modulate cytokine production and the immune interplay between human peripheral blood mononuclear cells and colon cancer cells. *FEMS Microbiology Letters*. 364 (3), pp. fnx014.
- Dolgin, E. (2017) Anti-inflammatory drug cuts risk of heart disease — and cancer. *Nature Reviews Drug Discovery*. 16 (10), pp. 665–667.
- Dong, R., Li, F., Qin, S., Wang, Y., Si, Y., Xu, X., *et al.* (2016) Dataset on inflammatory proteins expressions and sialic acid levels in apolipoprotein E-deficient mice with administration of N-acetylneuraminic acid and/or quercetin. *Data in Brief*. 8, pp. 613–7.
- Dorighello, G. G., Paim, B. A., Leite, A. C. R., Vercesi, A. E. and Oliveira, H. C. F. (2018) Spontaneous experimental atherosclerosis in hypercholesterolemic mice advances with ageing and correlates with mitochondrial reactive oxygen species. *Experimental Gerontology*. 109, pp. 47–50.
- Dubland, J. A. and Francis, G. A. (2016) So much cholesterol. *Current Opinion in Lipidology*. 27 (2), pp. 155–161.
- Dumas, A., Bernard, L., Poquet, Y., Lugo-Villarino, G. and Neyrolles, O. (2018) The role of the lung microbiota and the gut-lung axis in respiratory infectious diseases. *Cellular Microbiology*. 20 (12), pp. e12966.
- Eitzman, D. T., Westrick, R. J., Xu, Z., Tyson, J. and Ginsburg, D. (2000) Plasminogen activator inhibitor-1 deficiency protects against atherosclerosis progression in the mouse carotid artery. *Blood*. 96 (13), pp. 4212–5.
- Ejtahed, H. S., Mohtadi-Nia, J., Homayouni-Rad, A., Niafar, M., Asghari-Jafarabadi, M., Mofid, V. and Akbarian-Moghari, A. (2011) Effect of probiotic yogurt containing Lactobacillus

## REFERENCES

- acidophilus and *Bifidobacterium lactis* on lipid profile in individuals with type 2 diabetes mellitus. *Journal of Dairy Science*. 94 (7), pp. 3288–3294.
- Engevik, M. A. and Versalovic, J. (2017) Biochemical features of beneficial microbes: foundations for therapeutic microbiology. *Microbiology Spectrum*. 5 (5).
- Enns, J. E., Yeganeh, A., Zarychanski, R., Abou-Setta, A. M., Friesen, C., Zahradka, P. and Taylor, C. G. (2014) The impact of omega-3 polyunsaturated fatty acid supplementation on the incidence of cardiovascular events and complications in peripheral arterial disease: a systematic review and meta-analysis. *BMC Cardiovascular Disorders*. 14, pp. 70.
- Fåkk, F. and Bäckhed, F. (2012) *Lactobacillus reuteri* prevents diet-induced obesity, but not atherosclerosis, in a strain dependent fashion in Apoe<sup>-/-</sup> mice. *PLoS One*. 7 (10), pp. e46837.
- Farrer, S. (2018) Beyond statins: emerging evidence for HDL-increasing therapies and diet in treating cardiovascular disease. *Advances in Preventive Medicine*. 2018, pp. 1–9.
- Fava, C. and Montagnana, M. (2018) Atherosclerosis is an inflammatory disease which lacks a common anti-inflammatory therapy: how human genetics can help to this issue. a narrative review. *Frontiers in Pharmacology*. 9, pp. 55.
- Favari, E., Chroni, A., Tietge, U. J. F., Zanotti, I., Escolà-Gil, J. C. and Bernini, F. (2015) Cholesterol efflux and reverse cholesterol transport, in: von Eckardstein, A. and Kardassis, D. (eds.) *High Density Lipoproteins. Handbook of Experimental Pharmacology*, vol 224. Springer, Cham, pp. 181–206.
- Fazio, S., Major, A. S., Swift, L. L., Gleaves, L. A., Accad, M., Linton, M. F. and Farese, R. V. (2001) Increased atherosclerosis in LDL receptor-null mice lacking ACAT1 in macrophages. *Journal of Clinical Investigation*. 107 (2), pp. 163–171.
- Febbraio, M., Guy, E. and Silverstein, R. L. (2004) Stem cell transplantation reveals that absence of macrophage CD36 is protective against atherosclerosis. *Arteriosclerosis, Thrombosis, and Vascular Biology*. 24 (12), pp. 2333–2338.
- Feng, B., Yao, P. M., Li, Y., Devlin, C. M., Zhang, D., Harding, H. P., *et al.* (2003) The endoplasmic reticulum is the site of cholesterol-induced cytotoxicity in macrophages. *Nature Cell Biology*. 5



(9), pp. 781–792.

Feng, Q., Chen, W.-D. and Wang, Y.-D. (2018) Gut microbiota: an integral moderator in health and disease. *Frontiers in Microbiology*. 9, pp. 151.

Feng, Y., Schouteden, S., Geenens, R., Van Duppen, V., Herijgers, P., Holvoet, P., Van Veldhoven, P. P. and Verfaillie, C. M. (2012) Hematopoietic stem/progenitor cell proliferation and differentiation is differentially regulated by high-density and low-density lipoproteins in mice. *PLoS One*. 7 (11), pp. e47286.

Ference, B. A., Ginsberg, H. N., Graham, I., Ray, K. K., Packard, C. J., Bruckert, E., *et al.* (2017) Low-density lipoproteins cause atherosclerotic cardiovascular disease. 1. Evidence from genetic, epidemiologic, and clinical studies. A consensus statement from the European Atherosclerosis Society Consensus Panel. *European Heart Journal*. 38 (32), pp. 2459–2472.

Fernández-Hernando, C., József, L., Jenkins, D., Di Lorenzo, A. and Sessa, W. C. (2009) Absence of akt1 reduces vascular smooth muscle cell migration and survival and induces features of plaque vulnerability and cardiac dysfunction during atherosclerosis. *Arteriosclerosis, Thrombosis, and Vascular Biology*. 29 (12), pp. 2033–2040.

Fhoula, I., Rehaïem, A., Najjari, A., Usai, D., Boudabous, A., Sechi, L. A. and Hadda-Imene, O. (2018) Functional probiotic assessment and *in vivo* cholesterol-lowering efficacy of *Weissella* sp. associated with arid lands living-hosts. *BioMed Research International*. 2018, pp. 1–11.

Firouzi, S., Majid, H. A., Ismail, A., Kamaruddin, N. A. and Barakatun-Nisak, M.-Y. (2017) Effect of multi-strain probiotics (multi-strain microbial cell preparation) on glycemic control and other diabetes-related outcomes in people with type 2 diabetes: a randomized controlled trial. *European Journal of Nutrition*. 56 (4), pp. 1535–1550.

Fitó, M., Cladellas, M., de la Torre, R., Martí, J., Alcántara, M., Pujadas-Bastardes, M., *et al.* (2005) Antioxidant effect of virgin olive oil in patients with stable coronary heart disease: a randomized, crossover, controlled, clinical trial. *Atherosclerosis*. 181 (1), pp. 149–158.

Fitó, M., Cladellas, M., de la Torre, R., Martí, J., Muñoz, D., Schröder, H., *et al.* (2008) Anti-inflammatory effect of virgin olive oil in stable coronary disease patients: a randomized, crossover, controlled trial. *European Journal of Clinical Nutrition*. 62 (4), pp. 570–574.

## REFERENCES

- Foks, A. C., Van Puijvelde, G. H. M., Wolbert, J., Kröner, M. J., Frodermann, V., Van Der Heijden, T., *et al.* (2016) CD11b<sup>+</sup> Gr-1<sup>+</sup> myeloid-derived suppressor cells reduce atherosclerotic lesion development in LDLr deficient mice. *Cardiovascular Research*. 111 (3), pp. 252–261.
- Folch, J., Lees, M. and Sloane Stanley, G. H. (1957) A simple method for the isolation and purification of total lipides from animal tissues. *The Journal of Biological Chemistry*. 226 (1), pp. 497–509.
- Fortes, P. M., Marques, S. M., Viana, K. A., Costa, L. R., Naghettini, A. V. and Costa, P. S. (2018) The use of probiotics for improving lipid profiles in dyslipidemic individuals: an overview protocol. *Systematic Reviews*. 7 (1), pp. 165.
- Fu, H., Tang, Y., Ouyang, X., Tang, S., Su, H., Li, X., *et al.* (2014) Interleukin-27 inhibits foam cell formation by promoting macrophage ABCA1 expression through JAK2/STAT3 pathway. *Biochemical and Biophysical Research Communications*. 452 (4), pp. 881–887.
- Fu, Y., Mukhamedova, N., Ip, S., D'Souza, W., Henley, K. J., DiTommaso, T., *et al.* (2013) ABCA12 regulates ABCA1-dependent cholesterol efflux from macrophages and the development of atherosclerosis. *Cell Metabolism*. 18 (2), pp. 225–238.
- Gajda, M., Jawień, J., Mateuszuk, L., Lis, G. J., Radziszewski, A., Chłopicki, S. and Litwin, J. A. (2008) Triple immunofluorescence labeling of atherosclerotic plaque components in apoE/LDLR<sup>-/-</sup> mice. *Folia Histochemica et Cytobiologica*. 46 (2), pp. 143–6.
- Galkina, E. and Ley, K. (2007) Vascular adhesion molecules in atherosclerosis. *Arteriosclerosis, Thrombosis, and Vascular Biology*. 27 (11), pp. 2292–2301.
- Gallagher, H. (2016) *Anti-atherogenic actions of dihomo-gamma-linolenic acid in macrophages*. Cardiff University.
- Gao, M., Zhao, D., Schouteden, S., Sorci-Thomas, M. G., Van Veldhoven, P. P., Eggermont, K., Liu, G., Verfaillie, C. M. and Feng, Y. (2014) Regulation of high-density lipoprotein on hematopoietic stem/progenitor cells in atherosclerosis requires scavenger receptor type BI expression. *Arteriosclerosis, Thrombosis, and Vascular Biology*. 34 (9), pp. 1900–9.
- Garaiova, I., Muchová, J., Nagyová, Z., Wang, D., Li, J. V., Országhová, Z., Michael, D. R.,

## REFERENCES

- Plummer, S. F. and Ďuračková, Z. (2015) Probiotics and vitamin C for the prevention of respiratory tract infections in children attending preschool: a randomised controlled pilot study. *European Journal of Clinical Nutrition*. 69 (3), pp. 373–9.
- Garbus, J., Deluca, H. F., Loomans, M. E. and Strong, F. M. (1963) The rapid incorporation of phosphate into mitochondrial lipids. *The Journal of Biological Chemistry*. 238, pp. 59–63.
- Garcia-Calvo, M., Lisnock, J., Bull, H. G., Hawes, B. E., Burnett, D. A., Braun, M. P., *et al.* (2005) The target of ezetimibe is Niemann-Pick C1-Like 1 (NPC1L1). *Proceedings of the National Academy of Sciences*. 102 (23), pp. 8132–8137.
- Geng, Y. J., Wu, Q., Muszynski, M., Hansson, G. K. and Libby, P. (1996) Apoptosis of vascular smooth muscle cells induced by in vitro stimulation with interferon-gamma, tumor necrosis factor-alpha, and interleukin-1 beta. *Arteriosclerosis, Thrombosis, and Vascular Biology*. 16 (1), pp. 19–27.
- Gerhardt, T. and Ley, K. (2015) Monocyte trafficking across the vessel wall. *Cardiovascular Research*. 107 (3), pp. 321–30.
- Getz, G. and Reardon, C. A. (2018) T Cells in Atherosclerosis in Ldlr<sup>-/-</sup> and Apoe<sup>-/-</sup> Mice. *Journal of Immunological Sciences*. 2 (3), pp. 69–76.
- Getz, G. S. and Reardon, C. A. (2015) Use of mouse models in atherosclerosis research, in: Andrés, V. and Dorado, B. (eds.) *Methods in Mouse Atherosclerosis. Methods in Molecular Biology, vol 1339*. Humana Press, New York, NY, pp. 1–16.
- Getz, G. S. and Reardon, C. A. (2016) Do the Apoe<sup>-/-</sup> and Ldlr<sup>-/-</sup> mice yield the same insight on atherogenesis? *Arteriosclerosis, Thrombosis, and Vascular Biology*. 36 (9), pp. 1734–41.
- Giacco, F. and Brownlee, M. (2010) Oxidative stress and diabetic complications. *Circulation Research*. 107 (9), pp. 1058–1070.
- Gijbers, L., Ding, E. L., Malik, V. S., de Goede, J., Geleijnse, J. M. and Soedamah-Muthu, S. S. (2016) Consumption of dairy foods and diabetes incidence: a dose-response meta-analysis of observational studies. *The American Journal of Clinical Nutrition*. 103 (4), pp. 1111–1124.

## REFERENCES

- Gijsberts, C. M., Seneviratna, A., de Carvalho, L. P., den Ruijter, H. M., Vidanapthirana, P., Sorokin, V., *et al.* (2015) Ethnicity modifies associations between cardiovascular risk factors and disease severity in parallel dutch and singapore coronary cohorts. *PLoS One*. 10 (7), pp. e0132278.
- Gimeno, E., de la Torre-Carbot, K., Lamuela-Raventós, R. M., Castellote, A. I., Fitó, M., de la Torre, R., Covas, M.-I. and Carmen López-Sabater, M. (2007) Changes in the phenolic content of low density lipoprotein after olive oil consumption in men. A randomized crossover controlled trial. *British Journal of Nutrition*. 98 (6), pp. 1243–1250.
- Goldstein, J. L., Ho, Y. K., Basu, S. K. and Brown, M. S. (1979) Binding site on macrophages that mediates uptake and degradation of acetylated low density lipoprotein, producing massive cholesterol deposition. *Proceedings of the National Academy of Sciences of the United States of America*. 76 (1), pp. 333–7.
- Goncharov, N. V, Avdonin, P. V, Nadeev, A. D., Zharkikh, I. L. and Jenkins, R. O. (2015) Reactive oxygen species in pathogenesis of atherosclerosis. *Current Pharmaceutical Design*. 21 (9), pp. 1134–46.
- Gosling, J., Slaymaker, S., Gu, L., Tseng, S., Zlot, C. H., Young, S. G., Rollins, B. J. and Charo, I. F. (1999) MCP-1 deficiency reduces susceptibility to atherosclerosis in mice that overexpress human apolipoprotein B. *The Journal of Clinical Investigation*. 103 (6), pp. 773–8.
- Grasset, E. K., Duhlin, A., Agardh, H. E., Ovchinnikova, O., Hägglöf, T., Forsell, M. N., *et al.* (2015) Sterile inflammation in the spleen during atherosclerosis provides oxidation-specific epitopes that induce a protective B-cell response. *Proceedings of the National Academy of Sciences of the United States of America*. 112 (16), pp. E2030-8.
- Greany, K. A., Bonorden, M. J. L., Hamilton-Reeves, J. M., McMullen, M. H., Wangen, K. E., Phipps, W. R., Feirtag, J., Thomas, W. and Kurzer, M. S. (2008) Probiotic capsules do not lower plasma lipids in young women and men. *European Journal of Clinical Nutrition*. 62 (2), pp. 232–237.
- Greenow, K., Pearce, N. J. and Ramji, D. P. (2005) The key role of apolipoprotein E in atherosclerosis. *Journal of Molecular Medicine*. 83 (5), pp. 329–342.

## REFERENCES

- Groh, L., Keating, S. T., Joosten, L. A. B., Netea, M. G. and Riksen, N. P. (2018) Monocyte and macrophage immunometabolism in atherosclerosis. *Seminars in Immunopathology*. 40 (2), pp. 203–214.
- Gu, L., Okada, Y., Clinton, S. K., Gerard, C., Sukhova, G. K., Libby, P. and Rollins, B. J. (1998) Absence of monocyte chemoattractant protein-1 reduces atherosclerosis in low density lipoprotein receptor-deficient mice. *Molecular Cell*. 2 (2), pp. 275–81.
- Guo, J., Van Eck, M., Twisk, J., Maeda, N., Benson, G. M., Groot, P. H. E. and Van Berkel, T. J. C. (2003) Transplantation of monocyte CC-chemokine receptor 2-deficient bone marrow into apoe3-leiden mice inhibits atherogenesis. *Arteriosclerosis, Thrombosis, and Vascular Biology*. 23 (3), pp. 447–453.
- Guo, Z., Liu, X. M., Zhang, Q. X., Shen, Z., Tian, F. W., Zhang, H., Sun, Z. H., Zhang, H. P. and Chen, W. (2011) Influence of consumption of probiotics on the plasma lipid profile: A meta-analysis of randomised controlled trials. *Nutrition, Metabolism and Cardiovascular Diseases*. 21 (11), pp. 844–850.
- Han, M.-M., Sun, J.-F., Su, X.-H., Peng, Y.-F., Goyal, H., Wu, C.-H., Zhu, X.-Y. and Li, L. (2019) Probiotics improve glucose and lipid metabolism in pregnant women: a meta-analysis. *Annals of Translational Medicine*. 7 (5), pp. 99–99.
- Hanna, R. N. and Hedrick, C. C. (2014) Stressing out stem cells: linking stress and hematopoiesis in cardiovascular disease. *Nature Medicine*. 20 (7), pp. 707–8.
- Harper, C. R. and Jacobson, T. A. (2010) Using apolipoprotein B to manage dyslipidemic patients: time for a change? *Mayo Clinic Proceedings*. 85 (5), pp. 440–5.
- Hayakawa, K., Kimura, M., Kasaha, K., Matsumoto, K., Sansawa, H. and Yamori, Y. (2004) Effect of a gamma-aminobutyric acid-enriched dairy product on the blood pressure of spontaneously hypertensive and normotensive Wistar-Kyoto rats. *The British Journal of Nutrition*. 92 (3), pp. 411–7.
- He, C., Medley, S. C., Hu, T., Hinsdale, M. E., Lupu, F., Virmani, R. and Olson, L. E. (2015) PDGFR $\beta$  signalling regulates local inflammation and synergizes with hypercholesterolaemia to promote atherosclerosis. *Nature Communications*. 6 (1), pp. 7770.

## REFERENCES

- He, J., Zhang, F. and Han, Y. (2017) Effect of probiotics on lipid profiles and blood pressure in patients with type 2 diabetes. *Medicine*. 96 (51), pp. e9166.
- Hee Kim, C., Geun Kim, H., Yun Kim, J., Ra Kim, N., Jun Jung, B., Hye Jeong, J. and Kyun Chung, D. (2012) Probiotic genomic DNA reduces the production of pro-inflammatory cytokine tumor necrosis factor-alpha. *FEMS Microbiology Letters*. 328 (1), pp. 13–19.
- Heeneman, S., Cleutjens, J. P., Faber, B. C., Creemers, E. E., van Suylen, R.-J., Lutgens, E., Cleutjens, K. B. and Daemen, M. J. (2003) The dynamic extracellular matrix: intervention strategies during heart failure and atherosclerosis. *The Journal of Pathology*. 200 (4), pp. 516–525.
- Hemarajata, P. and Versalovic, J. (2013) Effects of probiotics on gut microbiota: mechanisms of intestinal immunomodulation and neuromodulation. *Therapeutic Advances in Gastroenterology*. 6 (1), pp. 39–51.
- Hendijani, F. and Akbari, V. (2018) Probiotic supplementation for management of cardiovascular risk factors in adults with type II diabetes: A systematic review and meta-analysis. *Clinical Nutrition*. 37 (2), pp. 532–541.
- Heo, W., Lee, E. S., Cho, H. T., Kim, J. H., Lee, J. H., Yoon, S. M., Kwon, H. T., Yang, S. and Kim, Y.-J. (2018) *Lactobacillus plantarum* LRCC 5273 isolated from Kimchi ameliorates diet-induced hypercholesterolemia in C57BL/6 mice. *Bioscience, Biotechnology, and Biochemistry*. 82 (11), pp. 1964–1972.
- Hepburn, N. J., Garaiova, I., Williams, E. A., Michael, D. R. and Plummer, S. (2013) Probiotic supplement consumption alters cytokine production from peripheral blood mononuclear cells: a preliminary study using healthy individuals. *Beneficial Microbes*. 4 (4), pp. 313–317.
- Hinton, W., McGovern, A., Coyle, R., Han, T. S., Sharma, P., Correa, A., Ferreira, F. and Lusignan, S. de (2018) Incidence and prevalence of cardiovascular disease in English primary care: a cross-sectional and follow-up study of the Royal College of General Practitioners (RCGP) Research and Surveillance Centre (RSC). *BMJ Open*. 8 (8), pp. e020282.
- Hoffman, M., Ipp, H., Phatlhane, D. V., Erasmus, R. T. and Zemlin, A. E. (2018) E-Selectin and markers of HIV disease severity, inflammation and coagulation in HIV-infected treatment-naïve

## REFERENCES

individuals. *African Health Sciences*. 18 (4), pp. 1066–1075.

Holme, I., Cater, N. B., Faergeman, O., Kastelein, J. J. P., Olsson, A. G., Tikkanen, M. J., *et al.* (2008) Lipoprotein predictors of cardiovascular events in statin-treated patients with coronary heart disease. Insights from the Incremental Decrease In End-points Through Aggressive Lipid-lowering Trial (IDEAL). *Annals of Medicine*. 40 (6), pp. 456–64.

Hong, Y.-F., Kim, H., Kim, H. S., Park, W. J., Kim, J.-Y. and Chung, D. K. (2016) *Lactobacillus acidophilus* K301 inhibits atherogenesis via induction of 24 (s), 25-epoxycholesterol-mediated ABCA1 and ABCG1 production and cholesterol efflux in macrophages. *PLoS One*. 11 (4), pp. e0154302.

Hooper, L., Thompson, R. L., Harrison, R. A., Summerbell, C. D., Ness, A. R., Moore, H. J., *et al.* (2006) Risks and benefits of omega 3 fats for mortality, cardiovascular disease, and cancer: systematic review. *BMJ (Clinical Research Ed.)*. 332 (7544), pp. 752–60.

Hove, K. D., Brøns, C., Færch, K., Lund, S. S., Rossing, P. and Vaag, A. (2015) Effects of 12 weeks of treatment with fermented milk on blood pressure, glucose metabolism and markers of cardiovascular risk in patients with type 2 diabetes: a randomised double-blind placebo-controlled study. *European Journal of Endocrinology*. 172 (1), pp. 11–20.

Hovingh, G. K., Kuivenhoven, J. A., Bischoff, R. J., Groen, A. K., Dam, M., Tol, A., *et al.* (2004) HDL deficiency and atherosclerosis: lessons from Tangier disease. *Journal of Internal Medicine*. 255 (2), pp. 299–301.

Hsu, S.-P., Wu, M.-S., Yang, C.-C., Huang, K.-C., Liou, S.-Y., Hsu, S.-M. and Chien, C.-T. (2007) Chronic green tea extract supplementation reduces hemodialysis-enhanced production of hydrogen peroxide and hypochlorous acid, atherosclerotic factors, and proinflammatory cytokines. *The American Journal of Clinical Nutrition*. 86 (5), pp. 1539–1547.

Huang, L.-H., Melton, E. M., Li, H., Sohn, P., Rogers, M. A., Mulligan-Kehoe, M. J., *et al.* (2016) Myeloid Acyl-CoA:Cholesterol Acyltransferase 1 Deficiency reduces lesion macrophage content and suppresses atherosclerosis progression. *The Journal of Biological Chemistry*. 291 (12), pp. 6232–44.

Huang, L., Chambliss, K. L., Gao, X., Yuhanna, I. S., Behling-Kelly, E., Bergaya, S., *et al.* (2019) SR-

## REFERENCES

- B1 drives endothelial cell LDL transcytosis via DOCK4 to promote atherosclerosis. *Nature*. pp. 1.
- Huang, L., Fan, B., Ma, A., Shaul, P. W. and Zhu, H. (2015) Inhibition of ABCA1 protein degradation promotes HDL cholesterol efflux capacity and RCT and reduces atherosclerosis in mice. *Journal of Lipid Research*. 56 (5), pp. 986–997.
- Huang, Y., Wang, J., Cheng, Y. and Zheng, Y. (2010) The hypocholesterolaemic effects of *Lactobacillus acidophilus* American Type Culture Collection 4356 in rats are mediated by the down-regulation of Niemann-Pick C1-Like 1. *British Journal of Nutrition*. 104 (06), pp. 807–812.
- Huang, Y., Wang, J., Quan, G., Wang, X., Yang, L. and Zhong, L. (2014) *Lactobacillus acidophilus* ATCC 4356 prevents atherosclerosis via inhibition of intestinal cholesterol absorption in apolipoprotein E-knockout mice. *Applied and Environmental Microbiology*. 80 (24), pp. 7496–504.
- Huang, Y., Wang, X., Wang, J., Wu, F., Sui, Y., Yang, L. and Wang, Z. (2013) *Lactobacillus plantarum* strains as potential probiotic cultures with cholesterol-lowering activity. *Journal of Dairy Science*. 96 (5), pp. 2746–2753.
- Huang, Z. H., Lin, C. Y., Oram, J. F. and Mazzone, T. (2001) Sterol efflux mediated by endogenous macrophage ApoE expression is independent of ABCA1. *Arteriosclerosis, Thrombosis, and Vascular Biology*. 21 (12), pp. 2019–25.
- Hujber, Z., Horváth, G., Petővári, G., Krencz, I., Dankó, T., Mészáros, K., *et al.* (2018) GABA, glutamine, glutamate oxidation and succinic semialdehyde dehydrogenase expression in human gliomas. *Journal of Experimental and Clinical Cancer Research*. 37 (1), pp. 271.
- Hütt, P., Songisepp, E., Rätsep, M., Mahlapuu, R., Kilk, K. and Mikelsaar, M. (2015) Impact of probiotic *Lactobacillus plantarum* TENSIA in different dairy products on anthropometric and blood biochemical indices of healthy adults. *Beneficial Microbes*. 6 (3), pp. 233–243.
- Ilhan, F. and Kalkanli, S. T. (2015) Atherosclerosis and the role of immune cells. *World Journal of Clinical Cases*. 3 (4), pp. 345–52.
- Inagaki, Y., Yamagishi, S., Amano, S., Okamoto, T., Koga, K. and Makita, Z. (2002) Interferon-gamma-induced apoptosis and activation of THP-1 macrophages. *Life Sciences*. 71 (21), pp.



## REFERENCES

2499–508.

Ishimwe, N., Daliri, E. B., Lee, B. H., Fang, F. and Du, G. (2015) The perspective on cholesterol-lowering mechanisms of probiotics. *Molecular Nutrition and Food Research*. 59 (1), pp. 94–105.

Ivanova, E. A., Myasoedova, V. A., Melnichenko, A. A. and Orekhov, A. N. (2017) Peroxisome Proliferator-Activated Receptor (PPAR) gamma agonists as therapeutic agents for cardiovascular disorders: focus on atherosclerosis. *Current Pharmaceutical Design*. 23 (7), pp. 1119–1124.

Ivanova, E. A., Parolari, A., Myasoedova, V., Melnichenko, A. A., Bobryshev, Y. V. and Orekhov, A. N. (2015) Peroxisome proliferator-activated receptor (PPAR) gamma in cardiovascular disorders and cardiovascular surgery. *Journal of Cardiology*. 66 (4), pp. 271–278.

Jaffar, N., Okinaga, T., Nishihara, T. and Maeda, T. (2018) Enhanced phagocytosis of *Aggregatibacter actinomycetemcomitans* cells by macrophages activated by a probiotic *Lactobacillus* strain. *Journal of Dairy Science*. 101 (7), pp. 5789–5798.

Jaiswal, S., Natarajan, P., Silver, A. J., Gibson, C. J., Bick, A. G., Shvartz, E., *et al.* (2017) Clonal hematopoiesis and risk of atherosclerotic cardiovascular disease. *New England Journal of Medicine*. 377 (2), pp. 111–121.

Jiang, C., Zhang, H., Zhang, W., Kong, W., Zhu, Y., Zhang, H., Xu, Q., Li, Y. and Wang, X. (2009) Homocysteine promotes vascular smooth muscle cell migration by induction of the adipokine resistin. *American Journal of Physiology-Cell Physiology*. 297 (6), pp. C1466–C1476.

Jiang, T., Ren, K., Chen, Q., Li, H., Yao, R., Hu, H., Lv, Y.-C. and Zhao, G.-J. (2017) Leonurine prevents atherosclerosis via promoting the expression of ABCA1 and ABCG1 in a ppar $\gamma$ /I $\kappa$ B signaling pathway-dependent manner. *Cellular Physiology and Biochemistry*. 43 (4), pp. 1703–1717.

Jiang, Y., Jiang, L.-L. I., Maimaitirexiati, X.-M. Z. Y., Zhang, Y. and Wu, L. (2015) Irbesartan attenuates TNF- $\alpha$ -induced ICAM-1, VCAM-1, and E-selectin expression through suppression of NF- $\kappa$ B pathway in HUVECs. *European Review for Medical and Pharmacological Sciences*. 19 (17), pp. 3295–302.

## REFERENCES

- Jiang, Y., Wang, M., Huang, K., Zhang, Z., Shao, N., Zhang, Y., Wang, W. and Wang, S. (2012) Oxidized low-density lipoprotein induces secretion of interleukin-1 $\beta$  by macrophages via reactive oxygen species-dependent NLRP3 inflammasome activation. *Biochemical and Biophysical Research Communications*. 425 (2), pp. 121–126.
- Jijon, H., Backer, J., Diaz, H., Yeung, H., Thiel, D., McKaigney, C., De Simone, C. and Madsen, K. (2004) DNA from probiotic bacteria modulates murine and human epithelial and immune function. *Gastroenterology*. 126 (5), pp. 1358–73.
- Jin, P., Bian, Y., Wang, K., Cong, G., Yan, R., Sha, Y., *et al.* (2018) Homocysteine accelerates atherosclerosis via inhibiting LXR $\alpha$ -mediated ABCA1/ABCG1-dependent cholesterol efflux from macrophages. *Life Sciences*. 214, pp. 41–50.
- Jin, Z.-X., Xiong, Q., Jia, F., Sun, C.-L., Zhu, H.-T. and Ke, F.-S. (2015) Investigation of RNA interference suppression of matrix metalloproteinase-9 in mouse model of atherosclerosis. *International Journal of Clinical and Experimental Medicine*. 8 (4), pp. 5272–8.
- Jo, E.-K., Kim, J. K., Shin, D.-M. and Sasakawa, C. (2016) Molecular mechanisms regulating NLRP3 inflammasome activation. *Cellular and Molecular Immunology*. 13 (2), pp. 148–59.
- Johnson, J. L. and Newby, A. C. (2009) Macrophage heterogeneity in atherosclerotic plaques. *Current Opinion in Lipidology*. 20 (5), pp. 370–8.
- Jones, M. L., Martoni, C. J., Parent, M. and Prakash, S. (2012) Cholesterol-lowering efficacy of a microencapsulated bile salt hydrolase-active *Lactobacillus reuteri* NCIMB 30242 yoghurt formulation in hypercholesterolaemic adults. *British Journal of Nutrition*. 107 (10), pp. 1505–1513.
- Kankaanpää, P., Sütas, Y., Salminen, S. and Isolauri, E. (2003) Homogenates derived from probiotic bacteria provide down-regulatory signals for peripheral blood mononuclear cells. *Food Chemistry*. 83 (2), pp. 269–277.
- Karimi, K., Inman, M. D., Bienenstock, J. and Forsythe, P. (2009) *Lactobacillus reuteri* -induced regulatory T cells protect against an allergic airway response in mice. *American Journal of Respiratory and Critical Care Medicine*. 179 (3), pp. 186–193.

## REFERENCES

- Katsi, V., Zerdes, I., Manolakou, S., Makris, T., Nihoyannopoulos, P., Tousoulis, D. and Kallikazaros, I. (2014) Anti-VEGF anticancer drugs: Mind the hypertension. *Recent Advances in Cardiovascular Drug Discovery*. 9 (2), pp. 63–72.
- Kattoor, A. J., Pothineni, N. V. K., Palagiri, D. and Mehta, J. L. (2017) Oxidative Stress in Atherosclerosis. *Current Atherosclerosis Reports*. 19 (11), pp. 42.
- Kaur, S., Raggatt, L. J., Batoon, L., Hume, D. A., Levesque, J.-P. and Pettit, A. R. (2017) Role of bone marrow macrophages in controlling homeostasis and repair in bone and bone marrow niches. *Seminars in Cell and Developmental Biology*. 61, pp. 12–21.
- Kekkonen, R.-A., Lummela, N., Karjalainen, H., Latvala, S., Tynkkynen, S., Jarvenpaa, S., *et al.* (2008) Probiotic intervention has strain-specific anti-inflammatory effects in healthy adults. *World Journal of Gastroenterology*. 14 (13), pp. 2029–36.
- Kennedy, P. J., Cryan, J. F., Dinan, T. G. and Clarke, G. (2017) Kynurenine pathway metabolism and the microbiota-gut-brain axis. *Neuropharmacology*. 112 (Pt B), pp. 399–412.
- Ketelhuth, D. F. J. and Hansson, G. K. (2016) Adaptive response of T and B cells in atherosclerosis. *Circulation Research*. 118 (4), pp. 668–678.
- Khalesi, S., Sun, J., Buys, N. and Jayasinghe, R. (2014) Effect of probiotics on blood pressure: a systematic review and meta-analysis of randomized, controlled trials. *Hypertension*. 64 (4), pp. 897–903.
- Khunti, K., Danese, M. D., Kutikova, L., Catterick, D., Sorio-Vilela, F., Gleeson, M., Kondapally Seshasai, S. R., Brownrigg, J. and Ray, K. K. (2018) Association of a combined measure of adherence and treatment intensity with cardiovascular outcomes in patients with atherosclerosis or other cardiovascular risk factors treated with statins and/or ezetimibe. *JAMA Network Open*. 1 (8), pp. e185554.
- Kiessling, G., Schneider, J. and Jahreis, G. (2002) Long-term consumption of fermented dairy products over 6 months increases HDL cholesterol. *European Journal of Clinical Nutrition*. 56 (9), pp. 843–9.
- Kim, J., Jang, S.-W., Park, E., Oh, M., Park, S. and Ko, J. (2014) The role of heat shock protein 90

## REFERENCES

- in migration and proliferation of vascular smooth muscle cells in the development of atherosclerosis. *Journal of Molecular and Cellular Cardiology*. 72, pp. 157–67.
- Kim, S., Yang, L., Kim, S., Lee, R. G., Graham, M. J., Berliner, J. A., *et al.* (2017) Targeting hepatic heparin-binding EGF-like growth factor (HB-EGF) induces anti-hyperlipidemia leading to reduction of angiotensin II-induced aneurysm development. *PLoS One*. 12 (8), pp. e0182566.
- Kimura, T., Tse, K., Sette, A. and Ley, K. (2015) Vaccination to modulate atherosclerosis. *Autoimmunity*. 48 (3), pp. 152–160.
- Klein, A., Friedrich, U., Vogelsang, H. and Jahreis, G. (2008) *Lactobacillus acidophilus* 74-2 and *Bifidobacterium animalis* subsp *lactis* DGCC 420 modulate unspecific cellular immune response in healthy adults. *European Journal of Clinical Nutrition*. 62 (5), pp. 584–593.
- Koczor, C. A., Torres, R. A., Fields, E., Qin, Q., Park, J., Ludaway, T., Russ, R. and Lewis, W. (2013) Transgenic mouse model with deficient mitochondrial polymerase exhibits reduced state IV respiration and enhanced cardiac fibrosis. *Laboratory Investigation*. 93 (2), pp. 151–158.
- Koga, M., Kai, H., Yasukawa, H., Yamamoto, T., Kawai, Y., Kato, S., *et al.* (2007) Inhibition of progression and stabilization of plaques by postnatal interferon- $\gamma$  function blocking in apoE-knockout mice. *Circulation Research*. 101 (4), pp. 348–356.
- Kojima, Y., Volkmer, J.-P., McKenna, K., Civelek, M., Lusic, A. J., Miller, C. L., *et al.* (2016) CD47-blocking antibodies restore phagocytosis and prevent atherosclerosis. *Nature*. (7614), pp. 1–20.
- Konstantinov, S. R., Smidt, H., de Vos, W. M., Bruijns, S. C. M., Singh, S. K., Valence, F., *et al.* (2008) S layer protein A of *Lactobacillus acidophilus* NCFM regulates immature dendritic cell and T cell functions. *Proceedings of the National Academy of Sciences*. 105 (49), pp. 19474–19479.
- Kort, R., Westerik, N., Mariela Serrano, L., Douillard, F. P., Gottstein, W., Mukisa, I. M., *et al.* (2015) A novel consortium of *Lactobacillus rhamnosus* and *Streptococcus thermophilus* for increased access to functional fermented foods. *Microbial Cell Factories*. 14 (1), pp. 195.

## REFERENCES

- Kouvari, M., Panagiotakos, D. B., Chrysohoou, C., Georgousopoulou, E., Notara, V., Tousoulis, D., Pitsavos, C. and The Attica Greeks Studies Investigators (2018) Gender-specific, lifestyle-related factors and 10-year cardiovascular disease risk; the ATTICA and GREECS cohort studies. *Current Vascular Pharmacology*.
- Krieg, A. M. (2002) CpG motifs in bacterial DNA and their immune effects. *Annual Review of Immunology*. 20 (1), pp. 709–760.
- Kruth, H. S., Huang, W., Ishii, I. and Zhang, W.-Y. (2002) Macrophage foam cell formation with native low density lipoprotein. *Journal of Biological Chemistry*. 277 (37), pp. 34573–34580.
- Kuchibhotla, S., Vanegas, D., Kennedy, D. J., Guy, E., Nimako, G., Morton, R. E. and Febbraio, M. (2008) Absence of CD36 protects against atherosclerosis in ApoE knock-out mice with no additional protection provided by absence of scavenger receptor A I/II. *Cardiovascular Research*. 78 (1), pp. 185–196.
- Kühbacher, T., Ott, S. J., Helwig, U., Mimura, T., Rizzello, F., Kleessen, B., *et al.* (2006) Bacterial and fungal microbiota in relation to probiotic therapy (VSL#3) in pouchitis. *Gut*. 55 (6), pp. 833–41.
- Kumar, M., Nagpal, R., Kumar, R., Hemalatha, R., Verma, V., Kumar, A., *et al.* (2012) Cholesterol-lowering probiotics as potential biotherapeutics for metabolic diseases. *Experimental Diabetes Research*. 2012, pp. 902917.
- Kumar, R., Grover, S. and Batish, V. K. (2011) Hypocholesterolaemic effect of dietary inclusion of two putative probiotic bile salt hydrolase-producing *Lactobacillus plantarum* strains in Sprague-Dawley rats. *The British Journal of Nutrition*. 105 (4), pp. 561–73.
- Kunjathoor, V. V., Febbraio, M., Podrez, E. A., Moore, K. J., Andersson, L., Koehn, S., *et al.* (2002) Scavenger receptors class a-I/II and CD36 are the principal receptors responsible for the uptake of modified low density lipoprotein leading to lipid loading in macrophages. *Journal of Biological Chemistry*. 277 (51), pp. 49982–49988.
- Kuo, C.-L., Murphy, A. J., Sayers, S., Li, R., Yvan-Charvet, L., Davis, J. Z., *et al.* (2011) *Cdkn2a* is an atherosclerosis modifier locus that regulates monocyte/macrophage proliferation. *Arteriosclerosis, Thrombosis, and Vascular Biology*. 31 (11), pp. 2483–2492.

## REFERENCES

- Kzhyshkowska, J., Neyen, C. and Gordon, S. (2012) Role of macrophage scavenger receptors in atherosclerosis. *Immunobiology*. 217 (5), pp. 492–502.
- Lada, A. T., Rudel, L. L. and Clair, R. W. St. (2003) Effects of LDL enriched with different dietary fatty acids on cholesteryl ester accumulation and turnover in THP-1 macrophages. *Journal of Lipid Research*. 44 (4), pp. 770–779.
- Laguna-Fernandez, A., Checa, A., Carracedo, M., Artiach, G., Petri, M. H., Baumgartner, R., *et al.* (2018) ERV1/ChemR23 signaling protects against atherosclerosis by modifying oxidized low-density lipoprotein uptake and phagocytosis in macrophages. *Circulation*. 138 (16), pp. 1693–1705.
- Lang, J. K. and Cimato, T. R. (2014) Cholesterol and hematopoietic stem cells: inflammatory mediators of atherosclerosis. *STEM CELLS Translational Medicine*. 3 (5), pp. 549–552.
- Langmann, T., Schumacher, C., Morham, S. G., Honer, C., Heimerl, S., Moehle, C. and Schmitz, G. (2003) ZNF202 is inversely regulated with its target genes ABCA1 and apoE during macrophage differentiation and foam cell formation. *Journal of Lipid Research*. 44 (5), pp. 968–77.
- Lappas, M. (2017) The IL-1 $\beta$  signalling pathway and its role in regulating pro-inflammatory and pro-labour mediators in human primary myometrial cells. *Reproductive Biology*. 17 (4), pp. 333–340.
- Larrede, S., Quinn, C. M., Jessup, W., Frisdal, E., Olivier, M., Hsieh, V., *et al.* (2009) Stimulation of cholesterol efflux by LXR agonists in cholesterol-loaded human macrophages is ABCA1-dependent but ABCG1-independent. *Arteriosclerosis, Thrombosis, and Vascular Biology*. 29 (11), pp. 1930–1936.
- Lassila, M., Allen, T. J., Cao, Z., Thallas, V., Jandeleit-Dahm, K. A., Candido, R. and Cooper, M. E. (2004) Imatinib attenuates diabetes-associated atherosclerosis. *Arteriosclerosis, Thrombosis, and Vascular Biology*. 24 (5), pp. 935–942.
- Lau, K., Srivatsav, V., Rizwan, A., Nashed, A., Liu, R., Shen, R. and Akhtar, M. (2017) Bridging the gap between gut microbial dysbiosis and cardiovascular diseases. *Nutrients*. 9 (8), pp. E859.

## REFERENCES

- Lee, E., Jung, S.-R., Lee, S.-Y., Lee, N.-K., Paik, H.-D. and Lim, S.-I. (2018) Lactobacillus plantarum strain Ln4 attenuates diet-induced obesity, insulin resistance, and changes in hepatic mRNA levels associated with glucose and lipid metabolism. *Nutrients*. 10 (5), pp. E643.
- Lee, J., Son, H. and Ryu, O.-H. (2017) Management status of cardiovascular disease risk factors for dyslipidemia among Korean adults. *Yonsei Medical Journal*. 58 (2), pp. 326.
- Li, A. C., Brown, K. K., Silvestre, M. J., Willson, T. M., Palinski, W. and Glass, C. K. (2000) Peroxisome proliferator-activated receptor  $\gamma$  ligands inhibit development of atherosclerosis in LDL receptor-deficient mice. *Journal of Clinical Investigation*. 106 (4), pp. 523–531.
- Li, D. Y. and Tang, W. H. W. (2017) Gut microbiota and atherosclerosis. *Current Atherosclerosis Reports*. 19 (10), pp. 39.
- Li, H., Xia, N. and Förstermann, U. (2012) Cardiovascular effects and molecular targets of resveratrol. *Nitric Oxide*. 26 (2), pp. 102–110.
- Li, M., Qian, M., Kyler, K. and Xu, J. (2018) Endothelial-vascular smooth muscle cells interactions in atherosclerosis. *Frontiers in Cardiovascular Medicine*. 5, pp. 151.
- Li, R., Yang, J., Saffari, A., Jacobs, J., Baek, K. I., Hough, G., *et al.* (2017) Ambient ultrafine particle ingestion alters gut microbiota in association with increased atherogenic lipid metabolites. *Scientific Reports*. 7 (1), pp. 42906.
- Li, S.-C., Hsu, W.-F., Chang, J.-S. and Shih, C.-K. (2019) Combination of lactobacillus acidophilus and bifidobacterium animalis subsp. lactis shows a stronger anti-inflammatory effect than individual strains in HT-29 cells. *Nutrients*. 11 (5), pp. 969.
- Li, Z., Jin, H., Oh, S. Y. and Ji, G. E. (2016) Anti-obese effects of two Lactobacilli and two Bifidobacteria on ICR mice fed on a high fat diet. *Biochemical and Biophysical Research Communications*. 480 (2), pp. 222–227.
- Libby, P. and Ebert, B. L. (2018) CHIP (Clonal Hematopoiesis of Indeterminate Potential). *Circulation*. 138 (7), pp. 666–668.
- Lijnen, H. R. (2005) Pleiotropic functions of plasminogen activator inhibitor-1. *Journal of*

## REFERENCES

*Thrombosis and Haemostasis*. 3 (1), pp. 35–45.

Linton, M. F., Yancey, P. G., Davies, S. S., Jerome, W. G., Linton, E. F., Song, W. L., Doran, A. C. and Vickers, K. C. (2019) *The Role of Lipids and Lipoproteins in Atherosclerosis*. In: Feingold KR, Anawalt B, Boyce A, et al., editors. Endotext [Internet]. South Dartmouth (MA): MDText.com, Inc.; 2000-. Available from: <https://www.ncbi.nlm.nih.gov/books/NBK343489/>.

Litvinov, D. Y., Savushkin, E. V, Garaeva, E. A. and Dergunov, A. D. (2016) Cholesterol efflux and reverse cholesterol transport: experimental approaches. *Current Medicinal Chemistry*. 23 (34), pp. 3883–3908.

Liu, C., Yang, L., Han, Y., Ouyang, W., Yin, W. and Xu, F. (2019) Mast cells participate in regulation of lung-gut axis during *Staphylococcus aureus* pneumonia. *Cell Proliferation*. 52 (2), pp. e12565.

Liu, D.-Q., Li, L.-M., Guo, Y.-L., Bai, R., Wang, C., Bian, Z., Zhang, C.-Y. and Zen, K. (2008) Signal regulatory protein alpha negatively regulates beta2 integrin-mediated monocyte adhesion, transendothelial migration and phagocytosis. *PloS One*. 3 (9), pp. e3291.

Lloyd-Jones, D. M. (2014) Niacin and HDL cholesterol — Time to face facts. *New England Journal of Medicine*. 371 (3), pp. 271–273.

Louis, S. F. and Zahradka, P. (2010) Vascular smooth muscle cell motility: From migration to invasion. *Experimental and Clinical Cardiology*. 15 (4), pp. e75-85.

Lubin, J. H., Couper, D., Lutsey, P. L. and Yatsuya, H. (2017) Synergistic and non-synergistic associations for cigarette smoking and non-tobacco risk factors for cardiovascular disease incidence in the atherosclerosis risk in communities (ARIC) study. *Nicotine and Tobacco Research*. 19 (7), pp. 826–835.

Lubomski, M., Tan, A. H., Lim, S.-Y., Holmes, A. J., Davis, R. L. and Sue, C. M. (2019) Parkinson's disease and the gastrointestinal microbiome. *Journal of Neurology*. pp. 1–17.

Ma, X. and Feng, Y. (2016) Hypercholesterolemia tunes hematopoietic stem/progenitor cells for inflammation and atherosclerosis. *International Journal of Molecular Sciences*. 17 (7), pp. 1162.



## REFERENCES

- Madden, J. A. J., Plummer, S. F., Tang, J., Garaiova, I., Plummer, N. T., Herbison, M., *et al.* (2005) Effect of probiotics on preventing disruption of the intestinal microflora following antibiotic therapy: A double-blind, placebo-controlled pilot study. *International Immunopharmacology*. 5 (6), pp. 1091–1097.
- Madjd, A., Taylor, M. A., Mousavi, N., Delavari, A., Malekzadeh, R., Macdonald, I. A. and Farshchi, H. R. (2016) Comparison of the effect of daily consumption of probiotic compared with low-fat conventional yogurt on weight loss in healthy obese women following an energy-restricted diet: a randomized controlled trial. *The American Journal of Clinical Nutrition*. 103 (2), pp. 323–9.
- Magdalena, K., Magdalena, K. and Grazyna, S. (2006) The role of matrix metalloproteinase-3 in the development of atherosclerosis and cardiovascular events. *Electronic Journal of IFCC*. 17 (1), pp. 2–5.
- Mahboobi, S., Rahimi, F. and Jafarnejad, S. (2018) Effects of prebiotic and synbiotic supplementation on glycaemia and lipid profile in type 2 diabetes: a meta-analysis of randomized controlled trials. *Advanced Pharmaceutical Bulletin*. 8 (4), pp. 565–574.
- Mahdy Ali, K., Wonnerth, A., Huber, K. and Wojta, J. (2012) Cardiovascular disease risk reduction by raising HDL cholesterol--current therapies and future opportunities. *British Journal of Pharmacology*. 167 (6), pp. 1177–94.
- Makinen, P. I., Lappalainen, J. P., Heinonen, S. E., Leppanen, P., Lahtenvuo, M. T., Aarnio, J. V., Heikkila, J., Turunen, M. P. and Yla-Herttuala, S. (2010) Silencing of either SR-A or CD36 reduces atherosclerosis in hyperlipidaemic mice and reveals reciprocal upregulation of these receptors. *Cardiovascular Research*. 88 (3), pp. 530–538.
- Martin, F.-P. J., Wang, Y., Sprenger, N., Yap, I. K. S., Lundstedt, T., Lek, P., *et al.* (2008) Probiotic modulation of symbiotic gut microbial–host metabolic interactions in a humanized microbiome mouse model. *Molecular Systems Biology*. 4, pp. 157.
- Matsuyama, T., Tanaka, Y., Kamimaki, I., Nagao, T. and Tokimitsu, I. (2008) Catechin safely improved higher levels of fatness, blood pressure, and cholesterol in children. *Obesity*. 16 (6), pp. 1338–1348.

## REFERENCES

- McCarthy, M. (2014) Niacin fails to reduce vascular events in large randomised trial. *BMJ (Clinical Research Ed.)*. 349, pp. g4774.
- McLaren, J. E., Michael, D. R., Ashlin, T. G. and Ramji, D. P. (2011a) Cytokines, macrophage lipid metabolism and foam cells: implications for cardiovascular disease therapy. *Progress in Lipid Research*. 50 (4), pp. 331–47.
- McLaren, J. E., Michael, D. R., Guschina, I. A., Harwood, J. L. and Ramji, D. P. (2011b) Eicosapentaenoic acid and docosahexaenoic acid regulate modified LDL uptake and macropinocytosis in human macrophages. *Lipids*. 46 (11), pp. 1053–1061.
- McLaren, J. E., Michael, D. R., Salter, R. C., Ashlin, T. G., Calder, C. J., Miller, A. M., Liew, F. Y. and Ramji, D. P. (2010) IL-33 reduces macrophage foam cell formation. *Journal of Immunology*. 185 (2), pp. 1222–9.
- McLaren, J. E. and Ramji, D. P. (2009) Interferon gamma: A master regulator of atherosclerosis. *Cytokine and Growth Factor Reviews*. 20 (2), pp. 125–135.
- McQueen, M. J., Hawken, S., Wang, X., Ounpuu, S., Sniderman, A., Probstfield, J., *et al.* (2008) Lipids, lipoproteins, and apolipoproteins as risk markers of myocardial infarction in 52 countries (the INTERHEART study): a case-control study. *The Lancet*. 372 (9634), pp. 224–233.
- Mehrian-Shai, R., Reichardt, J. K. V., Harris, C. C. and Toren, A. (2019) The gut–brain axis, paving the way to brain cancer. *Trends in Cancer*. 5 (4), pp. 200–207.
- Mennigen, R. and Bruewer, M. (2009) Effect of probiotics on intestinal barrier function. *Annals of the New York Academy of Sciences*. 1165 (1), pp. 183–189.
- Mercer, J. R., Yu, E., Figg, N., Cheng, K.-K., Prime, T. A., Griffin, J. L., *et al.* (2012) The mitochondria-targeted antioxidant MitoQ decreases features of the metabolic syndrome in ATM+/-/ ApoE-/- mice. *Free Radical Biology and Medicine*. 52 (5), pp. 841–849.
- Merched, A., Tollefson, K. and Chan, L. (2010) Beta2 integrins modulate the initiation and progression of atherosclerosis in low-density lipoprotein receptor knockout mice. *Cardiovascular Research*. 85 (4), pp. 853–63.

## REFERENCES

- Mestas, J. and Ley, K. (2008) Monocyte-endothelial cell interactions in the development of atherosclerosis. *Trends in Cardiovascular Medicine*. 18 (6), pp. 228–32.
- Meyer, A. L., Elmadfa, I., Herbacek, I. and Micksche, M. (2007) Probiotic, as well as conventional yogurt, can enhance the stimulated production of proinflammatory cytokines. *Journal of Human Nutrition and Dietetics*. 20 (6), pp. 590–8.
- Miao, X.-Y., Liu, H.-Z., Jin, M.-M., Sun, B.-R., Tian, H., Li, J., Li, N. and Yan, S.-T. (2019) A comparative meta-analysis of the efficacy of statin-ezetimibe co-therapy versus statin monotherapy in reducing cardiovascular and cerebrovascular adverse events in patients with type 2 diabetes mellitus. *European Review for Medical and Pharmacological Sciences*. 23 (5), pp. 2302–2310.
- Michael, D. R., Ashlin, T. G., Davies, C. S., Gallagher, H., Stoneman, T. W., Buckley, M. L. and Ramji, D. P. (2013) Differential regulation of macropinocytosis in macrophages by cytokines: implications for foam cell formation and atherosclerosis. *Cytokine*. 64 (1), pp. 357–61.
- Michael, D. R., Davies, T. S., Loxley, K. E., Allen, M. D., Good, M. A., Hughes, T. R. and Plummer, S. F. (2019) *In vitro* neuroprotective activities of two distinct probiotic consortia. *Beneficial Microbes*. 10 (4), pp. 437–447.
- Michael, D. R., Davies, T. S., Moss, J. W. E., Calvente, D. L., Ramji, D. P., Marchesi, J. R., Pechlivanis, A., Plummer, S. F. and Hughes, T. R. (2017) The anti-cholesterolaemic effect of a consortium of probiotics: An acute study in C57BL/6J mice. *Scientific Reports*. 7 (1), pp. 2883.
- Michael, D. R., Moss, J. W. E., Calvente, D. L., Garaiova, I., Plummer, S. F. and Ramji, D. P. (2016) *Lactobacillus plantarum* CUL66 can impact cholesterol homeostasis in Caco-2 enterocytes. *Beneficial Microbes*. 7 (3), pp. 443–51.
- Milenkovic, J., Milojkovic, M., Jevtovic Stoimenov, T., Djindjic, B. and Miljkovic, E. (2017) Mechanisms of plasminogen activator inhibitor 1 action in stromal remodeling and related diseases. *Biomedical Papers*. 161 (4), pp. 339–347.
- Million, M., Angelakis, E., Paul, M., Armougom, F., Leibovici, L. and Raoult, D. (2012) Comparative meta-analysis of the effect of *Lactobacillus* species on weight gain in humans and animals. *Microbial Pathogenesis*. 53 (2), pp. 100–108.

## REFERENCES

- Mizoguchi, T., Kasahara, K., Yamashita, T., Sasaki, N., Yodoi, K., Matsumoto, T., *et al.* (2017) Oral administration of the lactic acid bacterium *Pediococcus acidilactici* attenuates atherosclerosis in mice by inducing tolerogenic dendritic cells. *Heart and Vessels*. 32 (6), pp. 768–776.
- Moludi, J., Alizadeh, M., Lotfi Yagin, N., Pasdar, Y., Nachvak, S. M., Abdollahzad, H. and Sadeghpour Tabaei, A. (2018) New insights on atherosclerosis: A cross-talk between endocannabinoid systems with gut microbiota. *Journal of Cardiovascular and Thoracic Research*. 10 (3), pp. 129–137.
- Moore, K. J. and Tabas, I. (2011) Macrophages in the pathogenesis of atherosclerosis. *Cell*. 145 (3), pp. 341–55.
- Moss, J. (2018) *Anti-inflammatory actions of nutraceuticals : Novel emerging therapies for atherosclerosis ?* Cardiff University.
- Moss, J. W. E., Davies, T. S., Garaiova, I., Plummer, S. F., Michael, D. R. and Ramji, D. P. (2016) A unique combination of nutritionally active ingredients can prevent several key processes associated with atherosclerosis in vitro. *Plos One*. 11 (3), pp. e0151057.
- Moss, J. W. E. and Ramji, D. P. (2016) Nutraceutical therapies for atherosclerosis. *Nature Reviews. Cardiology*. 13 (9), pp. 513–32.
- Moss, J. W. and Ramji, D. P. (2015) Interferon- $\gamma$ : Promising therapeutic target in atherosclerosis. *World Journal of Experimental Medicine*. 5 (3), pp. 154–9.
- Mullard, A. (2014) GSK's darapladib failures dim hopes for anti-inflammatory heart drugs. *Nature Reviews Drug Discovery*. 13 (7), pp. 481–482.
- Mullard, A. (2018) Anti-inflammatory cardiovascular therapies take another hit. *Nature Reviews Drug Discovery*. 17 (12), pp. 853–853.
- Myung, S.-K., Myung, S.-K., Lee, Y. J., Seo, H. G. and Korean Meta-analysis Study Group (2012) Efficacy of omega-3 fatty acid supplements (eicosapentaenoic acid and docosahexaenoic acid) in the secondary prevention of cardiovascular disease. *Archives of Internal Medicine*. 172 (9), pp. 686.

## REFERENCES

- Nagenborg, J., Goossens, P., Biessen, E. A. L. and Donners, M. M. P. C. (2017) Heterogeneity of atherosclerotic plaque macrophage origin, phenotype and functions: Implications for treatment. *European Journal of Pharmacology*. 816, pp. 14–24.
- Nakagawa-Toyama, Y., Yamashita, S., Miyagawa, J., Nishida, M., Nozaki, S., Nagaretani, H., *et al.* (2001) Localization of CD36 and scavenger receptor class A in human coronary arteries — a possible difference in the contribution of both receptors to plaque formation. *Atherosclerosis*. 156 (2), pp. 297–305.
- Nanayakkara, N., Ranasinha, S., Gadowski, A. M., Davis, W. A., Flack, J. R., Wischer, N., Andrikopoulos, S. and Zoungas, S. (2018) Age-related differences in glycaemic control, cardiovascular disease risk factors and treatment in patients with type 2 diabetes: a cross-sectional study from the Australian National Diabetes Audit. *BMJ Open*. 8 (8), pp. e020677.
- Newby, A. C., George, S. J., Ismail, Y., Johnson, J. L., Sala-Newby, G. B. and Thomas, A. C. (2009) Vulnerable atherosclerotic plaque metalloproteinases and foam cell phenotypes. *Thrombosis and Haemostasis*. 101 (6), pp. 1006–11.
- Niemarkt, H. J., De Meij, T. G., van Ganzewinkel, C., de Boer, N. K. H., Andriessen, P., Hütten, M. C. and Kramer, B. W. (2019) Necrotizing enterocolitis, gut microbiota, and brain development: role of the brain-gut axis. *Neonatology*. 115 (4), pp. 423–431.
- Niwa, T., Wada, H., Ohashi, H., Iwamoto, N., Ohta, H., Kirii, H., Fujii, H., Saito, K. and Seishima, M. (2004) Interferon-gamma; Produced by bone marrow-derived cells attenuates atherosclerotic lesion formation in LDLR-deficient mice. *Journal of Atherosclerosis and Thrombosis*. 11 (2), pp. 79–87.
- Nozaki, S., Kashiwagi, H., Yamashita, S., Nakagawa, T., Kostner, B., Tomiyama, Y., *et al.* (1995) Reduced uptake of oxidized low density lipoproteins in monocyte-derived macrophages from CD36-deficient subjects. *Journal of Clinical Investigation*. 96 (4), pp. 1859–1865.
- Oesterle, A., Laufs, U. and Liao, J. K. (2017) Pleiotropic effects of statins on the cardiovascular system. *Circulation Research*. 120 (1), pp. 229–243.
- Ohta, H., Wada, H., Niwa, T., Kirii, H., Iwamoto, N., Fujii, H., Saito, K., Sekikawa, K. and Seishima, M. (2005) Disruption of tumor necrosis factor- $\alpha$  gene diminishes the development of

## REFERENCES

- atherosclerosis in ApoE-deficient mice. *Atherosclerosis*. 180 (1), pp. 11–17.
- Ohtani, N. and Kawada, N. (2019) Role of the gut-liver axis in liver inflammation, fibrosis, and cancer: a special focus on the gut microbiota relationship. *Hepatology Communications*. 3 (4), pp. 456–470.
- Okazaki, H., Igarashi, M., Nishi, M., Sekiya, M., Tajima, M., Takase, S., *et al.* (2008) Identification of neutral cholesterol ester hydrolase, a key enzyme removing cholesterol from macrophages. *Journal of Biological Chemistry*. 283 (48), pp. 33357–33364.
- Oppi, S., Lüscher, T. F. and Stein, S. (2019) Mouse models for atherosclerosis research-which is my line? *Frontiers in Cardiovascular Medicine*. 6, pp. 46.
- Owen, L., Reinders, M., Narramore, R., Marsh, A. M. R., Gar Lui, F., Baron, R., Plummer, S. and Corfe, B. M. (2014) A double blind, placebo controlled, randomised pilot trial examining the effects of probiotic administration on mood and cognitive function. *Proceedings of the Nutrition Society*. 73 (OCE1), pp. E29.
- Ozaki, E., Campbell, M. and Doyle, S. L. (2015) Targeting the NLRP3 inflammasome in chronic inflammatory diseases: current perspectives. *Journal of Inflammation Research*. 8, pp. 15–27.
- Pan, L.-L., Wu, Y., Wang, R.-Q., Chen, J.-W., Chen, J., Zhang, Y., *et al.* (2018) (-)-Epigallocatechin-3-gallate ameliorates atherosclerosis and modulates hepatic lipid metabolic gene expression in apolipoprotein e knockout mice: involvement of TTC39B. *Frontiers in Pharmacology*. 9, pp. 195.
- Pereira, D. I. A. and Gibson, G. R. (2002) Cholesterol assimilation by lactic acid bacteria and bifidobacteria isolated from the human gut. *Applied and Environmental Microbiology*. 68 (9), pp. 4689–93.
- Petruski-Ivleva, N., Viera, A. J., Shimbo, D., Muntner, P., Avery, C. L., Schneider, A. L. C., Couper, D. and Kucharska-Newton, A. (2016) Longitudinal patterns of change in systolic blood pressure and incidence of cardiovascular disease. *Hypertension*. 67 (6), pp. 1150–1156.
- Pinkosky, S. L., Newton, R. S., Day, E. A., Ford, R. J., Lhotak, S., Austin, R. C., *et al.* (2016) Liver-specific ATP-citrate lyase inhibition by bempedoic acid decreases LDL-C and attenuates

## REFERENCES

atherosclerosis. *Nature Communications*. 7 (1), pp. 13457.

Plüddemann, A., Neyen, C. and Gordon, S. (2007) Macrophage scavenger receptors and host-derived ligands. *Methods*. 43 (3), pp. 207–217.

Plummer, S. F., Garaiova, I., Sarvotham, T., Cottrell, S. L., Le Scouiller, S., Weaver, M. A., Tang, J., Dee, P. and Hunter, J. (2005) Effects of probiotics on the composition of the intestinal microbiota following antibiotic therapy. *International Journal of Antimicrobial Agents*. 26 (1), pp. 69–74.

Plummer, S., Madden, J. A. J., Garaiova, I., Sen, S., Dear, K. L. E., Tarry, S. A., Williams, C. F. and Hunter, J. O. (2013) Effects of probiotics on the caecal and faecal microbiota of Irritable Bowel Syndrome patients receiving antibiotics: a pilot study. *Short Communication*. pp. 183–6.

Plummer, S., Weaver, M. A., Harris, J. C., Dee, P. and Hunter, J. (2004) Clostridium difficile pilot study: effects of probiotic supplementation on the incidence of C. difficile diarrhoea. *International Microbiology*. 7 (1), pp. 59–62.

Preiss, D. and Baigent, C. (2017) Cardiovascular disease: PCSK9 inhibition: a new player in cholesterol-lowering therapies? *Nature Reviews Nephrology*. 13 (8), pp. 450–451.

Prescott, M. F., Sawyer, W. K., Von Linden-Reed, J., Jeune, M., Chou, M., Caplan, S. L. and Jeng, A. Y. (1999) Effect of matrix metalloproteinase inhibition on progression of atherosclerosis and aneurysm in LDL receptor-deficient mice overexpressing MMP-3, MMP-12, and MMP-13 and on restenosis in rats after balloon injury. *Annals of the New York Academy of Sciences*. 878, pp. 179–90.

Purroy, A., Roncal, C., Orbe, J., Meilhac, O., Belzunce, M., Zalba, G., *et al.* (2018) Matrix metalloproteinase-10 deficiency delays atherosclerosis progression and plaque calcification. *Atherosclerosis*. 278, pp. 124–134.

Qin, Z. (2012) The use of THP-1 cells as a model for mimicking the function and regulation of monocytes and macrophages in the vasculature. *Atherosclerosis*. 221 (1), pp. 2–11.

Qiu, L., Tao, X., Xiong, H., Yu, J. and Wei, H. (2018) Lactobacillus plantarum ZDY04 exhibits a strain-specific property of lowering TMAO via the modulation of gut microbiota in mice. *Food*

## REFERENCES

*and Function*. 9 (8), pp. 4299–4309.

Qiu, L., Yang, D., Tao, X., Yu, J., Xiong, H. and Wei, H. (2017) Enterobacter aerogenes ZDY01 attenuates choline-induced trimethylamine n-oxide levels by remodeling gut microbiota in mice. *Journal of Microbiology and Biotechnology*. 27 (8), pp. 1491–1499.

Rachmilewitz, D., Katakura, K., Karmeli, F., Hayashi, T., Reinus, C., Rudensky, B., *et al.* (2004) Toll-like receptor 9 signaling mediates the anti-inflammatory effects of probiotics in murine experimental colitis. *Gastroenterology*. 126 (2), pp. 520–8.

Rad, A. H., Abbasalizadeh, S., Vazifekhah, S., Abbasalizadeh, F., Hassanalilou, T., Bastani, P., *et al.* (2017) The future of diabetes management by healthy probiotic microorganisms. *Current Diabetes Reviews*. 13 (6), pp. 582–589.

Raghu, H., Lopus, C. M., Wang, Q., Wong, H. H., Lingampalli, N., Oliviero, F., *et al.* (2017) CCL2/CCR2, but not CCL5/CCR5, mediates monocyte recruitment, inflammation and cartilage destruction in osteoarthritis. *Annals of the Rheumatic Diseases*. 76 (5), pp. 914–922.

Rajkumar, H., Mahmood, N., Kumar, M., Varikuti, S. R., Challa, H. R. and Myakala, S. P. (2014) Effect of probiotic (VSL#3) and omega-3 on lipid profile, insulin sensitivity, inflammatory markers, and gut colonization in overweight adults: a randomized, controlled trial. *Mediators of Inflammation*. 2014, pp. 348959.

Ramji, D. P. and Davies, T. S. (2015) Cytokines in atherosclerosis: Key players in all stages of disease and promising therapeutic targets. *Cytokine and Growth Factor Reviews*. 26 (6), pp. 673–85.

Randolph, G. J. (2014) Mechanisms that regulate macrophage burden in atherosclerosis. *Circulation Research*. 114 (11), pp. 1757–71.

Rao, R. K. and Samak, G. (2013) Protection and restitution of gut barrier by probiotics: nutritional and clinical implications. *Current Nutrition and Food Science*. 9 (2), pp. 99–107.

Rao, X., Huang, X., Zhou, Z. and Lin, X. (2013) An improvement of the  $2^{-\Delta\Delta CT}$  method for quantitative real-time polymerase chain reaction data analysis. *Biostatistics, Bioinformatics and Biomathematics*. 3 (3), pp. 71–85.



## REFERENCES

- Razmpoosh, E., Javadi, A., Ejtahed, H. S., Mirmiran, P., Javadi, M. and Yousefinejad, A. (2019) The effect of probiotic supplementation on glycemic control and lipid profile in patients with type 2 diabetes: A randomized placebo controlled trial. *Diabetes and Metabolic Syndrome: Clinical Research & Reviews*. 13 (1), pp. 175–182.
- Recinos, A., Carr, B. K., Bartos, D. B., Boldogh, I., Carmical, J. R., Belalcazar, L. M. and Brasier, A. R. (2004) Liver gene expression associated with diet and lesion development in atherosclerosis-prone mice: induction of components of alternative complement pathway. *Physiological Genomics*. 19 (1), pp. 131–142.
- Rerksuppaphol, S. and Rerksuppaphol, L. (2015) A randomized double-blind controlled trial of lactobacillus acidophilus plus bifidobacterium bifidum versus placebo in patients with hypercholesterolemia. *Journal of Clinical and Diagnostic Research : JCDR*. 9 (3), pp. KC01-4.
- Rezaei, M., Sanagoo, A., Jouybari, L., Behnampoo, N. and Kavosi, A. (2017) The effect of probiotic yogurt on blood glucose and cardiovascular biomarkers in patients with type II diabetes: a randomized controlled trial. *Mashhad University of Medical Sciences*. 6 (4), pp. 26–35.
- Ricci, C. and Ferri, N. (2015) Naturally occurring PDGF receptor inhibitors with potential anti-atherosclerotic properties. *Vascular Pharmacology*. 70, pp. 1–7.
- Ridker, P. M., Everett, B. M., Pradhan, A., MacFadyen, J. G., Solomon, D. H., Zaharris, E., *et al.* (2019) Low-dose methotrexate for the prevention of atherosclerotic events. *New England Journal of Medicine*. 380 (8), pp. 752–762.
- Rizos, E. C., Ntzani, E. E., Bika, E., Kostapanos, M. S. and Elisaf, M. S. (2012) Association between omega-3 fatty acid supplementation and risk of major cardiovascular disease events. *JAMA*. 308 (10), pp. 1024.
- Robbins, C. S., Hilgendorf, I., Weber, G. F., Theurl, I., Iwamoto, Y., Figueiredo, J.-L., *et al.* (2013) Local proliferation dominates lesional macrophage accumulation in atherosclerosis. *Nature Medicine*. 19 (9), pp. 1166–1172.
- Roberts, J. D., Suckling, C. A., Peedle, G. Y., Murphy, J. A., Dawkins, T. G. and Roberts, M. G. (2016) An exploratory investigation of endotoxin levels in novice long distance triathletes, and

## REFERENCES

- the effects of a multi-strain probiotic/prebiotic, antioxidant intervention. *Nutrients*. 8 (11), pp. 733.
- Rohwedder, I., Montanez, E., Beckmann, K., Bengtsson, E., Dunér, P., Nilsson, J., Soehnlein, O. and Fässler, R. (2012) Plasma fibronectin deficiency impedes atherosclerosis progression and fibrous cap formation. *EMBO Molecular Medicine*. 4 (7), pp. 564–76.
- Rosen, E. D. and Spiegelman, B. M. (2000) Peroxisome proliferator-activated receptor gamma ligands and atherosclerosis: ending the heartache. *The Journal of Clinical Investigation*. 106 (5), pp. 629–31.
- Rouch, A., Vanucci-Bacqué, C., Bedos-Belval, F. and Baltas, M. (2015) Small molecules inhibitors of plasminogen activator inhibitor-1 – An overview. *European Journal of Medicinal Chemistry*. 92, pp. 619–636.
- Ruscica, M., Pavanello, C., Gandini, S., Macchi, C., Botta, M., Dall’Orto, D., *et al.* (2019) Nutraceutical approach for the management of cardiovascular risk – a combination containing the probiotic *Bifidobacterium longum* BB536 and red yeast rice extract: results from a randomized, double-blind, placebo-controlled study. *Nutrition Journal*. 18 (1), pp. 13.
- Sabico, S., Al-Mashharawi, A., Al-Daghri, N. M., Yakout, S., Alnaami, A. M., Alokail, M. S. and McTernan, P. G. (2017) Effects of a multi-strain probiotic supplement for 12 weeks in circulating endotoxin levels and cardiometabolic profiles of medication naïve T2DM patients: a randomized clinical trial. *Journal of Translational Medicine*. 15 (1), pp. 249.
- Saborowski, M., Dölle, M., Manns, M. P., Leitolf, H. and Zender, S. (2018) Lipid-lowering therapy with PCSK9-inhibitors in the management of cardiovascular high-risk patients: Effectiveness, therapy adherence and safety in a real world cohort. *Cardiology Journal*. 25 (1), pp. 32–41.
- Saikia, D., Manhar, A. K., Deka, B., Roy, R., Gupta, K., Namsa, N. D., Chattopadhyay, P., Doley, R. and Mandal, M. (2018) Hypocholesterolemic activity of indigenous probiotic isolate *Saccharomyces cerevisiae* ARDMC1 in a rat model. *Journal of Food and Drug Analysis*. 26 (1), pp. 154–162.
- Sampson, U. K., Fazio, S. and Linton, M. F. (2012) Residual cardiovascular risk despite optimal

## REFERENCES

LDL cholesterol reduction with statins: the evidence, etiology, and therapeutic challenges. *Current Atherosclerosis Reports*. 14 (1), pp. 1–10.

Sano, H., Sudo, T., Yokode, M., Murayama, T., Kataoka, H., Takakura, N., Nishikawa, S., Nishikawa, S. I. and Kita, T. (2001) Functional blockade of platelet-derived growth factor receptor-beta but not of receptor-alpha prevents vascular smooth muscle cell accumulation in fibrous cap lesions in apolipoprotein E-deficient mice. *Circulation*. 103 (24), pp. 2955–60.

Sansone, R., Rodriguez-Mateos, A., Heuel, J., Falk, D., Schuler, D., Wagstaff, R., *et al.* (2015) Cocoa flavanol intake improves endothelial function and Framingham Risk Score in healthy men and women: a randomised, controlled, double-masked trial: the Flaviola Health Study. *The British Journal of Nutrition*. 114 (8), pp. 1246–55.

Sarwar, N., Danesh, J., Eiriksdottir, G., Sigurdsson, G., Wareham, N., Bingham, S., Boekholdt, S. M., Khaw, K.-T. and Gudnason, V. (2007) Triglycerides and the risk of coronary heart disease: 10,158 incident cases among 262,525 participants in 29 Western prospective studies. *Circulation*. 115 (4), pp. 450–8.

Saso, L., Korkina, L. and Zarkovic, N. (2017) Modulation of oxidative stress: pharmaceutical and pharmacological aspects 2017. *Oxidative Medicine and Cellular Longevity*. 2017, pp. 1–2.

Schenkel, A. R., Mamdouh, Z. and Muller, W. A. (2004) Locomotion of monocytes on endothelium is a critical step during extravasation. *Nature Immunology*. 5 (4), pp. 393–400.

Schneiderman, J., Sawdey, M. S., Keeton, M. R., Bordin, G. M., Bernstein, E. F., Dilley, R. B. and Loskutoff, D. J. (1992) Increased type 1 plasminogen activator inhibitor gene expression in atherosclerotic human arteries. *Proceedings of the National Academy of Sciences of the United States of America*. 89 (15), pp. 6998–7002.

Schrijvers, D., Demeyer, G., Herman, A. and Martinet, W. (2007) Phagocytosis in atherosclerosis: Molecular mechanisms and implications for plaque progression and stability. *Cardiovascular Research*. 73 (3), pp. 470–480.

Schrijvers, D. M. (2005) Phagocytosis of apoptotic cells by macrophages is impaired in atherosclerosis. *Arteriosclerosis, Thrombosis, and Vascular Biology*. 25 (6), pp. 1256–1261.

## REFERENCES

- Sekiya, M., Osuga, J.-I., Nagashima, S., Ohshiro, T., Igarashi, M., Okazaki, H., *et al.* (2009) Ablation of neutral cholesterol ester hydrolase 1 accelerates atherosclerosis. *Cell Metabolism*. 10 (3), pp. 219–28.
- Sekiya, M., Osuga, J., Igarashi, M., Okazaki, H. and Ishibashi, S. (2011) The role of neutral cholesterol ester hydrolysis in macrophage foam cells. *Journal of Atherosclerosis and Thrombosis*. 18 (5), pp. 359–364.
- Serri, O., Li, L., Maingrette, F., Jaffry, N. and Renier, G. (2004) Enhanced lipoprotein lipase secretion and foam cell formation by macrophages of patients with growth hormone deficiency: possible contribution to increased risk of atherogenesis? *The Journal of Clinical Endocrinology and Metabolism*. 89 (2), pp. 979–985.
- Shah, M. M., Saio, M., Yamashita, H., Tanaka, H., Takami, T., Ezaki, T. and Inagaki, N. (2012) Lactobacillus acidophilus strain L-92 induces CD4(+)CD25(+)Foxp3(+) regulatory T cells and suppresses allergic contact dermatitis. *Biological & Pharmaceutical Bulletin*. 35 (4), pp. 612–6.
- Shaikh, S., Brittenden, J., Lahiri, R., Brown, P. A. J., Thies, F. and Wilson, H. M. (2012) Macrophage subtypes in symptomatic carotid artery and femoral artery plaques. *European Journal of Vascular and Endovascular Surgery*. 44 (5), pp. 491–497.
- Shapiro, M. D. and Fazio, S. (2017) Apolipoprotein B-containing lipoproteins and atherosclerotic cardiovascular disease. *F1000Research*. 6, pp. 134.
- Sharma, S., Puri, S. and Kurpad, A. V (2018) Potential of probiotics in hypercholesterolemia: a review of in vitro and in vivo findings. *Alternative Therapies in Health and Medicine*. 24 (2), pp. 36–43.
- Shimada, Y. J. and Cannon, C. P. (2015) PCSK9 (Proprotein convertase subtilisin/kexin type 9) inhibitors: past, present, and the future. *European Heart Journal*. 36 (36), pp. 2415–2424.
- Shimizu, M., Hashiguchi, M., Shiga, T., Tamura, H. and Mochizuki, M. (2015) Meta-analysis: effects of probiotic supplementation on lipid profiles in normal to mildly hypercholesterolemic individuals. *PLoS One*. 10 (10), pp. e0139795.
- Shin, S., Park, H.-B., Chang, H.-J., Arsanjani, R., Min, J. K., Kim, Y.-J., *et al.* (2017) Impact of

## REFERENCES

- intensive LDL cholesterol lowering on coronary artery atherosclerosis progression. *JACC: Cardiovascular Imaging*. 10 (4), pp. 437–446.
- Shireman, R. B., Muth, J. and Toth, J. P. (1988) [14C]Acetate incorporation by cultured normal, familial hypercholesterolemia and Down's syndrome fibroblasts. *Lipids and Lipid Metabolism*. 958 (3), pp. 352–360.
- Singh, K. and Rohatgi, A. (2018) Examining the paradox of high high-density lipoprotein and elevated cardiovascular risk. *Journal of Thoracic Disease*. 10 (1), pp. 109–112.
- Singh, S., Bhatia, R., Singh, A., Singh, P., Kaur, R., Khare, P., *et al.* (2018) Probiotic attributes and prevention of LPS-induced pro-inflammatory stress in RAW264.7 macrophages and human intestinal epithelial cell line (Caco-2) by newly isolated *Weissella cibaria* strains. *Food and Function*. 9 (2), pp. 1254–1264.
- Skochko, O. V and Kaidashev, I. P. (2017) Effect of pioglitazone on insulin resistance, progression of atherosclerosis and clinical course of coronary heart disease. *Wiadomosci Lekarskie*. 70 (5), pp. 881–890.
- Smelt, M. J., de Haan, B. J., Bron, P. A., van Swam, I., Meijerink, M., Wells, J. M., Faas, M. M. and de Vos, P. (2013) Probiotics can generate FoxP3 T-cell responses in the small intestine and simultaneously inducing CD4 and CD8 T cell activation in the large intestine. *PLoS One*. 8 (7), pp. e68952.
- Smits, H. H., Engering, A., van der Kleij, D., de Jong, E. C., Schipper, K., van Capel, T. M. M., *et al.* (2005) Selective probiotic bacteria induce IL-10–producing regulatory T cells in vitro by modulating dendritic cell function through dendritic cell–specific intercellular adhesion molecule 3–grabbing nonintegrin. *Journal of Allergy and Clinical Immunology*. 115 (6), pp. 1260–1267.
- Song, M., Park, S., Lee, H., Min, B., Jung, S., Park, S., Kim, E. and Oh, S. (2015) Effect of *Lactobacillus acidophilus* NS1 on plasma cholesterol levels in diet-induced obese mice. *Journal of Dairy Science*. 98 (3), pp. 1492–1501.
- Srivastava, R. A. K., Mistry, S. and Sharma, S. (2015) A novel anti-inflammatory natural product from *Sphaeranthus indicus* inhibits expression of VCAM1 and ICAM1, and slows atherosclerosis

## REFERENCES

- progression independent of lipid changes. *Nutrition & Metabolism*. 12 (1), pp. 20.
- Stancu, C. S., Sanda, G. M., Deleanu, M. and Sima, A. V. (2014) Probiotics determine hypolipidemic and antioxidant effects in hyperlipidemic hamsters. *Molecular Nutrition and Food Research*. 58 (3), pp. 559–568.
- States, J. C., Singh, A. V., Knudsen, T. B., Rouchka, E. C., Ngalame, N. O., Arteel, G. E., Piao, Y. and Ko, M. S. H. (2012) Prenatal arsenic exposure alters gene expression in the adult liver to a proinflammatory state contributing to accelerated atherosclerosis. *PLoS One*. 7 (6), pp. e38713.
- Steffen, Y., Vuillaume, G., Stolle, K., Roewer, K., Lietz, M., Schueller, J., Lebrun, S. and Wallerath, T. (2012) Cigarette smoke and LDL cooperate in reducing nitric oxide bioavailability in endothelial cells via effects on both eNOS and NADPH oxidase. *Nitric Oxide*. 27 (3), pp. 176–184.
- Štofilová, J., Langerholc, T., Botta, C., Treven, P., Gradišnik, L., Salaj, R., *et al.* (2017) Cytokine production in vitro and in rat model of colitis in response to *Lactobacillus plantarum* LS/07. *Biomedicine and Pharmacotherapy*. 94, pp. 1176–1185.
- Stroes, E. S., Thompson, P. D., Corsini, A., Vladutiu, G. D., Raal, F. J., Ray, K. K., *et al.* (2015) Statin-associated muscle symptoms: impact on statin therapy-European atherosclerosis society consensus panel statement on assessment, aetiology and management. *European Heart Journal*. 36 (17), pp. 1012–22.
- Sukhovshin, R. A., Toledano Furman, N. E., Tasciotti, E. and Trachtenberg, B. H. (2016) Local inhibition of macrophage and smooth muscle cell proliferation to suppress plaque progression. *Methodist DeBakey Cardiovascular Journal*. 12 (3), pp. 141–145.
- Sun, B., Boyanovsky, B. B., Connelly, M. A., Shridas, P., van der Westhuyzen, D. R. and Webb, N. R. (2007) Distinct mechanisms for OxLDL uptake and cellular trafficking by class B scavenger receptors CD36 and SR-BI. *Journal of Lipid Research*. 48 (12), pp. 2560–70.
- Sun, H.-J., Zhao, M.-X., Liu, T.-Y., Ren, X.-S., Chen, Q., Li, Y.-H., Kang, Y.-M. and Zhu, G.-Q. (2016) Salusin- $\beta$  induces foam cell formation and monocyte adhesion in human vascular smooth muscle cells via miR155/NOX2/NF $\kappa$ B pathway. *Scientific Reports*. 6, pp. 23596.

## REFERENCES

- Sun, J. and Buys, N. (2015) Effects of probiotics consumption on lowering lipids and CVD risk factors: A systematic review and meta-analysis of randomized controlled trials. *Annals of Medicine*. 47 (6), pp. 430–440.
- Sun, L., Li, E., Wang, F., Wang, T., Qin, Z., Niu, S. and Qiu, C. (2015) Quercetin increases macrophage cholesterol efflux to inhibit foam cell formation through activating PPAR $\gamma$ -ABCA1 pathway. *International Journal of Clinical and Experimental Pathology*. 8 (9), pp. 10854–60.
- Swanson, J. A. (1989) Phorbol esters stimulate macropinocytosis and solute flow through macrophages. *Journal of Cell Science*. 94 ( Pt 1), pp. 135–42.
- Sykes, M. (1990) Unusual T cell populations in adult murine bone marrow. Prevalence of CD3+CD4-CD8- and alpha beta TCR+NK1.1+ cells. *Journal of Immunology*. 145 (10), pp. 3209–15.
- Sykora, M. M. and Reschke, M. (2019) Immunophenotyping of tissue samples using multicolor flow cytometry. *Methods in Molecular Biology*. 1953, pp. 253–268.
- Tabas, I. (2009) Macrophage apoptosis in atherosclerosis: consequences on plaque progression and the role of endoplasmic reticulum stress. *Antioxidants and Redox Signaling*. 11 (9), pp. 2333–9.
- Tabas, I., Williams, K. J. and Borén, J. (2007) Subendothelial lipoprotein retention as the initiating process in atherosclerosis: update and therapeutic implications. *Circulation*. 116 (16), pp. 1832–44.
- Talayero, B. G. and Sacks, F. M. (2011) The role of triglycerides in atherosclerosis. *Current Cardiology Reports*. 13 (6), pp. 544–52.
- Tall, A. R., Yvan-Charvet, L., Terasaka, N., Pagler, T. and Wang, N. (2008) HDL, ABC transporters, and cholesterol efflux: implications for the treatment of atherosclerosis. *Cell Metabolism*. 7 (5), pp. 365–375.
- Tan, B., Xiao, H., Li, F., Zeng, L. and Yin, Y. (2015) The profiles of mitochondrial respiration and glycolysis using extracellular flux analysis in porcine enterocyte IPEC-J2. *Animal Nutrition*. 1 (3), pp. 239–243.

## REFERENCES

- Thomas, C. M., Hong, T., van Pijkeren, J. P., Hemarajata, P., Trinh, D. V., Hu, W., Britton, R. A., Kalkum, M. and Versalovic, J. (2012) Histamine derived from probiotic lactobacillus reuteri suppresses TNF via modulation of PKA and ERK signaling. *PLoS One*. 7 (2), pp. e31951.
- Tian, J., Hu, S., Sun, Y., Yu, H., Han, X., Cheng, W., *et al.* (2013) Vasa vasorum and plaque progression, and responses to atorvastatin in a rabbit model of atherosclerosis: contrast-enhanced ultrasound imaging and intravascular ultrasound study. *Heart*. 99 (1), pp. 48–54.
- Tontonoz, P., Nagy, L., Alvarez, J. G., Thomazy, V. A. and Evans, R. M. (1998) PPARgamma promotes monocyte/macrophage differentiation and uptake of oxidized LDL. *Cell*. 93 (2), pp. 241–52.
- Tosheska Trajkovska, K. and Topuzovska, S. (2017) High-density lipoprotein metabolism and reverse cholesterol transport: strategies for raising HDL cholesterol. *Anatolian Journal of Cardiology*. 18 (2), pp. 149–154.
- Tsai, C.-C., Lin, P.-P., Hsieh, Y.-M., Zhang, Z., Wu, H.-C. and Huang, C.-C. (2014) Cholesterol-lowering potentials of lactic acid bacteria based on bile-salt hydrolase activity and effect of potent strains on cholesterol metabolism in vitro and in vivo. *The Scientific World Journal*. 2014, pp. 690752.
- Tse, K., Tse, H., Sidney, J., Sette, A. and Ley, K. (2013) T cells in atherosclerosis. *International Immunology*. 25 (11), pp. 615–22.
- Ufnal, M., Zadlo, A. and Ostaszewski, R. (2015) TMAO: A small molecule of great expectations. *Nutrition*. 31 (11–12), pp. 1317–1323.
- Ukibe, K., Miyoshi, M. and Kadooka, Y. (2015) Administration of Lactobacillus gasseri SBT2055 suppresses macrophage infiltration into adipose tissue in diet-induced obese mice. *British Journal of Nutrition*. 114 (08), pp. 1180–1187.
- Upadhyya, S., Mooteri, S., Peckham, N. and Pai, R. G. (2004) Atherogenic effect of interleukin-2 and antiatherogenic effect of interleukin-2 antibody in apo-E-deficient mice. *Angiology*. 55 (3), pp. 289–294.
- Valanti, E.-K., Dalakoura-Karagkouni, K. and Sanoudou, D. (2018) Current and emerging



## REFERENCES

- reconstituted HDL-apoA-I and HDL-apoE approaches to treat atherosclerosis. *Journal of Personalized Medicine*. 8 (4).
- Valls, R.-M., Farràs, M., Suárez, M., Fernández-Castillejo, S., Fitó, M., Konstantinidou, V., *et al.* (2015) Effects of functional olive oil enriched with its own phenolic compounds on endothelial function in hypertensive patients. A randomised controlled trial. *Food Chemistry*. 167, pp. 30–35.
- Vassiliadis, E., Barascuk, N. and Karsdal, M. A. (2013) Atherofibrosis - a unique and common process of the disease pathogenesis of atherosclerosis and fibrosis - lessons for biomarker development. *American Journal of Translational Research*. 5 (1), pp. 1–14.
- Voloshyna, I., Littlefield, M. J. and Reiss, A. B. (2014) Atherosclerosis and interferon- $\gamma$ : New insights and therapeutic targets. *Trends in Cardiovascular Medicine*. 24 (1), pp. 45–51.
- Wakabayashi, T., Takahashi, M., Yamamuro, D., Karasawa, T., Takei, A., Takei, S., *et al.* (2018) Inflammasome activation aggravates cutaneous xanthomatosis and atherosclerosis in ACAT1 (Acyl-CoA Cholesterol Acyltransferase 1) deficiency in bone marrow. *Arteriosclerosis, Thrombosis, and Vascular Biology*. 38 (11), pp. 2576–2589.
- Walldius, G., Jungner, I., Holme, I., Aastveit, A. H., Kolar, W. and Steiner, E. (2001) High apolipoprotein B, low apolipoprotein A-I, and improvement in the prediction of fatal myocardial infarction (AMORIS study): a prospective study. *The Lancet*. 358 (9298), pp. 2026–2033.
- Wan, W. and Murphy, P. M. (2013) Regulation of atherogenesis by chemokines and chemokine receptors. *Archivum Immunologiae et Therapiae Experimentalis*. 61 (1), pp. 1.
- Wang, B., He, P.-P., Zeng, G.-F., Zhang, T. and Ou Yang, X.-P. (2017a) miR-467b regulates the cholesterol ester formation via targeting ACAT1 gene in RAW 264.7 macrophages. *Biochimie*. 132, pp. 38–44.
- Wang, C., Zhang, Y., Yang, Q., Yang, Y., Gu, Y., Wang, M. and Wu, K. (2007) A novel cultured tissue model of rat aorta: VSMC proliferation mechanism in relationship to atherosclerosis. *Experimental and Molecular Pathology*. 83 (3), pp. 453–458.

## REFERENCES

- Wang, J., Uryga, A. K., Reinhold, J., Figg, N., Baker, L., Finigan, A., *et al.* (2015a) Vascular smooth muscle cell senescence promotes atherosclerosis and features of plaque vulnerability. *Circulation*. 132 (20), pp. 1909–1919.
- Wang, J., Zhang, H., Chen, X., Chen, Y., Menghebilige and Bao, Q. (2012) Selection of potential probiotic lactobacilli for cholesterol-lowering properties and their effect on cholesterol metabolism in rats fed a high-lipid diet. *Journal of Dairy Science*. 95 (4), pp. 1645–54.
- Wang, L., Guo, M.-J., Gao, Q., Yang, J.-F., Yang, L., Pang, X.-L. and Jiang, X.-J. (2018) The effects of probiotics on total cholesterol: A meta-analysis of randomized controlled trials. *Medicine*. 97 (5), pp. e9679.
- Wang, P.-X., Ji, Y.-X., Zhang, X.-J., Zhao, L.-P., Yan, Z.-Z., Zhang, P., *et al.* (2017b) Targeting CASP8 and FADD-like apoptosis regulator ameliorates nonalcoholic steatohepatitis in mice and nonhuman primates. *Nature Medicine*. 23 (4), pp. 439–449.
- Wang, T.-M., Chen, K.-C., Hsu, P.-Y., Lin, H.-F., Wang, Y.-S., Chen, C.-Y., Liao, Y.-C. and Juo, S.-H. H. (2017c) microRNA let-7g suppresses PDGF-induced conversion of vascular smooth muscle cell into the synthetic phenotype. *Journal of Cellular and Molecular Medicine*. 21 (12), pp. 3592–3601.
- Wang, Y., Fu, W., Xie, F., Wang, Y., Chu, X., Wang, H., *et al.* (2010) Common polymorphisms in ITGA2, PON1 and THBS2 are associated with coronary atherosclerosis in a candidate gene association study of the Chinese Han population. *Journal of Human Genetics*. 55 (8), pp. 490–4.
- Wang, Y., Wang, G. Z., Rabinovitch, P. S. and Tabas, I. (2014) Macrophage mitochondrial oxidative stress promotes atherosclerosis and nuclear factor- $\kappa$ B-mediated inflammation in macrophages. *Circulation Research*. 114 (3), pp. 421–433.
- Wang, Y., Wang, W., Wang, N., Tall, A. R. and Tabas, I. (2017d) Mitochondrial oxidative stress promotes atherosclerosis and neutrophil extracellular traps in aged mice. *Arteriosclerosis, Thrombosis, and Vascular Biology*. 37 (8), pp. e99–e107.
- Wang, Z., Wang, G., Zhu, X., Geng, D. and Yang, H. (2015b) Interleukin-2 is upregulated in patients with a prolapsed lumbar intervertebral disc and modulates cell proliferation, apoptosis and extracellular matrix metabolism of human nucleus pulposus cells. *Experimental*

## REFERENCES

*and Therapeutic Medicine*. 10 (6), pp. 2437.

Wara, A. K., Croce, K., Foo, S., Sun, X., Icli, B., Tesmenitsky, Y., Esen, F., Rosenzweig, A. and Feinberg, M. W. (2011) Bone marrow-derived CMPs and GMPs represent highly functional proangiogenic cells: implications for ischemic cardiovascular disease. *Blood*. 118 (24), pp. 6461–4.

Weber, C., Fraemohs, L. and Dejana, E. (2007) The role of junctional adhesion molecules in vascular inflammation. *Nature Reviews Immunology*. 7 (6), pp. 467–477.

Weintraub, W. S. and Gidding, S. S. (2016) PCSK9 inhibitors: a technology worth paying for? *Pharmacoeconomics*. 34 (3), pp. 217–20.

Weng, X., Cheng, X., Wu, X., Xu, H., Fang, M. and Xu, Y. (2014) Sin3B mediates collagen type I gene repression by interferon gamma in vascular smooth muscle cells. *Biochemical and Biophysical Research Communications*. 447 (2), pp. 263–270.

Wepy, J. A., Galligan, J. J., Kingsley, P. J., Xu, S., Goodman, M. C., Tallman, K. A., Rouzer, C. A. and Marnett, L. J. (2019) Lysophospholipases cooperate to mediate lipid homeostasis and lysophospholipid signaling. *Journal of Lipid Research*. 60 (2), pp. 360–374.

Whayne, T. (2013) Problems and possible solutions for therapy with statins. *International Journal of Angiology*. 22 (02), pp. 075–082.

Whitman, S. C., Rateri, D. L., Szilvassy, S. J., Cornicelli, J. A. and Daugherty, A. (2002) Macrophage-specific expression of class A scavenger receptors in LDL receptor(-/-) mice decreases atherosclerosis and changes spleen morphology. *Journal of Lipid Research*. 43 (8), pp. 1201–8.

Whitman, S. C., Ravisankar, P., Elam, H. and Daugherty, A. (2000) Exogenous interferon- $\gamma$  enhances atherosclerosis in apolipoprotein E-/- mice. *The American Journal of Pathology*. 157 (6), pp. 1819–1824.

Williams, E. A., Stimpson, J., Wang, D., Plummer, S., Garaiova, I., Barker, M. E. and Corfe, B. M. (2009) Clinical trial: a multistrain probiotic preparation significantly reduces symptoms of irritable bowel syndrome in a double-blind placebo-controlled study. *Alimentary*

## REFERENCES

*Pharmacology and Therapeutics*. 29 (1), pp. 97–103.

Witztum, J. L. (2002) Splenic immunity and atherosclerosis: a glimpse into a novel paradigm? *The Journal of Clinical Investigation*. 109 (6), pp. 721–4.

Wong, N. D., Zhao, Y., Quek, R. G. W., Blumenthal, R. S., Budoff, M. J., Cushman, M., *et al.* (2017) Residual atherosclerotic cardiovascular disease risk in statin-treated adults: The multi-ethnic study of atherosclerosis. *Journal of Clinical Lipidology*. 11 (5), pp. 1223–1233.

World Health Organization (2018) Cardiovascular diseases (CVDs). Available from: [https://www.who.int/en/news-room/fact-sheets/detail/cardiovascular-diseases-\(cvds\)](https://www.who.int/en/news-room/fact-sheets/detail/cardiovascular-diseases-(cvds)) [Accessed 19 April 2019].

Xiao, N., Yin, M., Zhang, L., Qu, X., Du, H., Sun, X., *et al.* (2009) Tumor necrosis factor- $\alpha$  deficiency retards early fatty-streak lesion by influencing the expression of inflammatory factors in apoE-null mice. *Molecular Genetics and Metabolism*. 96 (4), pp. 239–244.

Xiong, W., Wang, X., Dai, D., Zhang, B., Lu, L. and Tao, R. (2017) The anti-inflammatory vasostatin-2 attenuates atherosclerosis in ApoE<sup>-/-</sup> mice and inhibits monocyte/macrophage recruitment. *Thrombosis and Haemostasis*. 117 (02), pp. 401–414.

Yamada, S., Senokuchi, T., Matsumura, T., Morita, Y., Ishii, N., Fukuda, K., *et al.* (2018) Inhibition of local macrophage growth ameliorates focal inflammation and suppresses atherosclerosis. *Arteriosclerosis, Thrombosis, and Vascular Biology*. 38 (5), pp. 994–1006.

Yamasaki, K., Yamashita, A., Zhao, Y., Shimizu, Y., Nishii, R., Kawai, K., *et al.* (2018) In vitro uptake and metabolism of [ <sup>14</sup> C]acetate in rabbit atherosclerotic arteries: biological basis for atherosclerosis imaging with [ <sup>11</sup> C]acetate. *Nuclear Medicine and Biology*. 56, pp. 21–25.

Yamazaki, H., Takahashi, M., Wakabayashi, T., Sakai, K., Yamamuro, D., Takei, A., *et al.* (2018) Loss of ACAT1 attenuates atherosclerosis aggravated by loss of NCEH1 in bone marrow-derived cells. *Journal of Atherosclerosis and Thrombosis*. pp. 44040.

Yancey, P. G., Bortnick, A. E., Kellner-Weibel, G., de la Llera-Moya, M., Phillips, M. C. and Rothblat, G. H. (2003) Importance of different pathways of cellular cholesterol efflux. *Arteriosclerosis, Thrombosis, and Vascular Biology*. 23 (5), pp. 712–719.

## REFERENCES

- Yao, W., Li, K. and Liao, K. (2009) Macropinocytosis contributes to the macrophage foam cell formation in RAW264.7 cells. *Acta Biochimica et Biophysica Sinica*. 41 (9), pp. 773–780.
- Yasuda, T., Grillot, D., Billheimer, J. T., Briand, F., Delerive, P., Huet, S. and Rader, D. J. (2010) Tissue-specific liver X receptor activation promotes macrophage reverse cholesterol transport in vivo. *Arteriosclerosis, Thrombosis, and Vascular Biology*. 30 (4), pp. 781–6.
- Ye, S. (2015) Putative targeting of matrix metalloproteinase-8 in atherosclerosis. *Pharmacology & Therapeutics*. 147, pp. 111–122.
- Yin, K., Liao, D. and Tang, C. (2010) ATP-binding membrane cassette transporter A1 (ABCA1): A possible link between inflammation and reverse cholesterol transport. *Molecular Medicine*. 16 (9–10), pp. 438–449.
- Yokoyama, M., Origasa, H., Matsuzaki, M., Matsuzawa, Y., Saito, Y., Ishikawa, Y., *et al.* (2007) Effects of eicosapentaenoic acid on major coronary events in hypercholesterolaemic patients (JELIS): a randomised open-label, blinded endpoint analysis. *The Lancet*. 369 (9567), pp. 1090–1098.
- Yoon, H., Ju, J., Lee, J., Park, H., Lee, J., Shin, H., Holzapfel, W., Park, K. and Do, M.-S. (2013) The probiotic *Lactobacillus rhamnosus* BFE5264 and *Lactobacillus plantarum* NR74 promote cholesterol efflux and suppress inflammation in THP-1 cells. *Journal of the Science of Food and Agriculture*. 93 (4), pp. 781–787.
- Zadelaar, S., Kleemann, R., Verschuren, L., de Vries-Van der Weij, J., van der Hoorn, J., Princen, H. M. and Kooistra, T. (2007) Mouse models for atherosclerosis and pharmaceutical modifiers. *Arteriosclerosis, Thrombosis, and Vascular Biology*. 27 (8), pp. 1706–1721.
- Zakiev, E. R., Sukhorukov, V. N., Melnichenko, A. A., Sobenin, I. A., Ivanova, E. A. and Orekhov, A. N. (2016) Lipid composition of circulating multiple-modified low density lipoprotein. *Lipids in Health and Disease*. 15 (1), pp. 134.
- Zernecke, A. (2017) CD98 promotes vascular smooth muscle cell accumulation in atherosclerosis to confer plaque stability. *Atherosclerosis*. 256, pp. 128–130.
- Zhang, C. (2009) MicroRNA-145 in vascular smooth muscle cell biology: A new therapeutic

## REFERENCES

target for vascular disease. *Cell Cycle*. 8 (21), pp. 3469–3473.

Zhou, R., Tardivel, A., Thorens, B., Choi, I. and Tschopp, J. (2010) Thioredoxin-interacting protein links oxidative stress to inflammasome activation. *Nature Immunology*. 11 (2), pp. 136–140.

Zou, T.-B., Zhu, S.-S., Luo, F., Li, W.-Q., Sun, X.-R. and Wu, H.-F. (2017) Effects of astaxanthin on reverse cholesterol transport and atherosclerosis in mice. *BioMed Research International*. 2017, pp. 1–6.